Life Cycle and Ultrasonic Based Non-Destructive Analysis of Recycled and Remanufactured Carbon Fibre Reinforced Plastic Composite

BY

DAVID ALEXANDER PETER PATERSON

A thesis submitted for the fulfilment of the requirement for the degree

ENGINEERING DOCTORATE

2018

Advanced Forming Research Centre,

Department of Design, Manufacture and Engineering Management

University of Strathclyde

Glasgow

United Kingdom

Abstract

Carbon fibre reinforced plastic (CFRP) is composite material with a wide variety of applications. Typically, the industries in which CFRP is predominately used are the aerospace, wind turbine, automotive and sports equipment industries, noting that CFRP is lighter than traditional materials while at the same time able to be used in critical safety applications (airline travel for instance.). With a backdrop of climate change, sustainability, a growing CFRP market, and with CFRP being a relatively expensive material to construct, much attention has been directed towards end-of-life (EOL) options for CFRP to avoid landfill, in particular, recycling and remanufacturing.

This thesis investigates two areas of recycled and remanufactured CFRP; a) an analysis of the terminology surrounding recycled and remanufactured CFRP and b) a non-destructive evaluation of recycled and remanufactured CFRP. In the case of the terminology surrounding CFRP, this thesis documents the importance of correct terminology, conducts a literature survey of current recycling and remanufacturing practices, identifies that remanufacturing is not occurring and indeed not possible, and that recycling terminology is in some cases not applicable. Further new terminology to describe products manufactured using fibres obtained via recycling is presented, this terminology being rf-CFRP.

Additionally, a novel tool focused upon identifying whether a product is recycled, remanufactured, reconditioned, repaired or re-used is also presented. The tool, which was endorsed by industry and academia via two round of independent stakeholder review, and compared to existing tools via literature survey, serves as a means for researchers, the public and industrialists to better articulate recovered EOL products.

Given the desire to re-use CFRP, it is imperative that the materials are evaluated in order to determine future applications. Thus, this thesis also documents the determination of the elastic constants of rf-CFRP via an immersion based ultrasonic wave velocity technique. A full derivation of the governing equation, the Christoffel equation, from first principles is presented, along with a relatively thorough literature review outlining the current way the technique is used on virgin CFRP (v-CFRP). The experimental section of thesis finds that for a stated experimental and manufacturing

process, ultrasound through transmission will in general provide a larger % difference between ultrasonic Young‟s modulus and mechanically derived Young‟s Modulus for rf-CFRP when compared to v-CFRP. It was also found that % difference values for one sample of rf-CFRP were in keeping with the results of virgin CFRP, along with a possible indication of transverse waves being more stable than longitudinal waves in rf-CFRP; both of which gives credence to the argument of further investigation in this area. Lastly, bespoke Matlab programs which return the wave velocity in terms of the elastic constants for solids, facilitate the determination of elastic constants from phase velocity data and which also may be used as future teaching aids are further presented.

Contents

List of Figures

-

-

-

-

List of Tables

-

-

List of Abbreviations

Acronym / Term	Meaning
a	Equilibrium position of particle element a
a‟	Displaced position of particle element a

b	Equilibrium position of particle b or position of displaced particle element a
b‟‟	Displaced position of particle element b
u	Vector describing particle element displacement
Δu	Change in vector describing particle element displacement when two neighbouring particles elements are compared to each other
$d\vec{u}$	Differential form of Δu
P	A position vector from an origin point to the equilibrium position of the particle element
ΔP	Change in position vector from origin for two neighbouring particle elements
Q	Displaced position vector (function of P and time) from origin
ΔQ	Change in displacement position vector from origin for two neighbouring particle elements
ºC	Degrees Celsius
$\Delta'(\vec{r},t)$	Deformation
$\nabla\cdot$	Divergence
ε_{ij}	Strain
$[\boldsymbol{\varepsilon}]$ Γ	Strain Tensor
	Christoffel Matrix
λ	wavelength
ρ	Density
$ijkl$	Subscript notation used with Stiffness, strain, stress and compliance
$\boldsymbol{\sigma}$	Couchy Stress Tensor
µm	Micro meters
ω	Angular frequency
ΔL	Extended Length minus Original Length
A	Area
ABS	Acrylonitrile Butadiene Styrene
AFRA	Aircraft Fleet Recycling Agency
AIP	American Institute of Physics
Al	Aluminium
ASTM	American Society of Testing Materials
AVK	Federation of Reinforced Plastics
BMP	Best Management Practices
C	Tensor of Elasticity
CC	Carbon composite

CF	Carbon fibre
CFR	Carbon fibre remanufacturing
CFRP	Carbon fibre reinforced plastic
CRESIM	Carbon Fibre Recycling
CRR	Centre for Remanufacturing and Reuse
D	Position vector from origin (Wave propagation)
DARPA	Defence Advanced Research Project Agency
e	Exponential Function
EEA	European Environmental Agency
ELV	End of Life Vehicles Directive
EOL	End of life
EU	European Union
ERN	European Remanufacturing Network
F	Force
f	Frequency
g cm^{-3}	Grams per cm cubed
GFRP	Glass Fibre Reinforced Plastic
GPa	Giga Pascal
HSSMI	High Speed Sustainable Manufacturing Institute
ICoR	International Conference on Remanufacturing
$\vec{k}$	Wave Vector
k	Wave Number
Kg	Kilograms
Kg m^{-3}	Kilograms per cubic meter
kWh	Kilowatt hours
L	Length
Lb	Pounds
Ln	Natural Logarithm
Lg	Logarithm
M	Meters
MHz	Megahertz
MRO	Maintenance Repair and Operations
ms^{-1}	Meters per Second
NDT/E	Non-Destructive Testing / Evaluation
Nm^{-2}	Newtons per metre squared
OECD	Organisation for Economic Co-operation and Development
OEM	Original equipment manufacturer
QNDE	Review of Progress of in Quantitative Non-Destructive Evaluation
PAMELA	Process for Advanced Management of End of Life Aircraft
PAN	Polyacrylonitrile
rf-CFRP / CFRP-rf	Reused Fibre Carbon Fibre Reinforced Plastic

$[\overrightarrow{T_n}]$	Cauchy Stress Tensor
TARMAC	Tarbes Advanced Recycling and Maintenance Aircraft Company
SIR	Scottish Institute of Remanufacture
SEM	Scanning Electron Microscope
$\vec{u}$	Displacement Vector
$[\boldsymbol{\nabla u}]$	Displacement Gradient Tensor
v	Phase Velocity
v-CF	Virgin Carbon Fibre
v-CFRP	Virgin Carbon Fibre Reinforced Plastic
VF	Virgin Fibre
WEEE	Waste Electrical and Electronic Equipment Directive
WF	Waste Framework

Re-Glossary

The following glossary identifies re-processes discussed within this thesis. The reprocesses presented are brief outlines of existing definitions found within literature (see chapter 3). A full discussion of these re-process is held off until chapter 3 with this glossary serving as a quick reference to allow for differentiation between the reprocesses.

Remanufacture

Remanufacture is the process of restoring a used product back to like new condition from the customer‟s perspective with the restored product also being issued with a warranty at least equal to the original. Remanufacture involves, cleaning, disassembly, component restoration or replacement, reassembly and testing.

Recondition

Reconditioning is the processes of restoring a used product back to a condition which approaches like new - a reconditioned product will not be of sufficient standard to be classed as good as new. Reconditioning processes restores or replaces major components that have failed or that are about to fail. Warranties issued with reconditioned products are generally of lesser standard that what is issued original.

Repair

Given a particular fault in a product, if a process is conducted to correct this fault, the product is said to have been repaired. Whereas remanufacturing restores the product back to original standard and recondition restores major failed components and components which are about to fail to a high quality standard, the repairing processes deals only with restoring failed components to a useable condition. The overall product is not in full general restored and any warranties issued with repaired products, in general cover only the repaired part.

Reuse

Reuse is the process of where products or component are used again for the same purpose once they have reached end-of-life

Recycle

Recycling is the process of where EOL components are transformed into a new state in physical-chemical sense. Unlike remanufacturing, reconditioning, repairing and reusing the integrity of the product is not maintained in the process of recycling - the embodied energy associated with manufacturing components from raw materials is lost in the recycling process. The output of a recycling process creates new raw materials which may be used to manufacture new products or components.

Acknowledgements

I would first and foremost like to offer my sincere thanks to my supervisors‟ Dr Ijomah and Dr Windmill. Your guidance and experience has been exceptional and considering one cannot obtain a doctorate without supervision, I‟m extremely grateful that you accepted me as your student. Without your help, guidance and experience I would not be writing these acknowledgments. I would also like to thank you again for giving me the opportunity to study at Tsinghua University, Beijing, while also providing funding to appear and present work at two international conferences.

I would also like to thank Dr Kao of the remanufacturing group and Mr Smillie from the Center for Ultrasonic Engineering. Dr Kao, your wisdom and experience in both recycling composite and manufacturing composite was greatly appreciated, and helped me a great deal. Mr Smillie, I cannot thank you enough for the time spent on the ultrasonic equipment in your lab. I realise both the availability of the equipment and your time was very limited and I‟m sincerely grateful for fitting me in and squeezing me in whenever you got free moment.

I will also like to thank everyone (too many to name) who has ever helped me by offering their time and assistance. Lastly, I would also like to thank Dr Evans from the Advanced Forming Research Centre for giving me the funds to purchase composite manufacturing equipment and to study for this degree in association with the centre.

To my mum dad and brother, what can I say other than thank you. Thanks for supporting me every step of the way during my university career thus far. Last but no means least I would like to pay tribute to my darling wife Helen. Helen, you picked me up when I was feeling stressed, you kept me motivated when I was feeling overwhelmed and provided a loving environment which allowed me to focus on this degree. Without your help and understanding completing this degree may not have been possible; in many ways this degree belongs just as much to you as it does to me.

Author’s declaration

I declare that this submission is entirely my own work

I declare that, except where fully referenced direct quotations have been included, no aspect of this submission has been copied from any other source

I declare that all works cited in this submission have been appropriately referenced

I understand that any act of academic dishonesty such as plagiarism or collusion may result in the non-award of my degree

Signed

Dated

Published Journal and Conference papers

Published Journal Articles

Paterson, D.A.P., Ijomah, W., Windmill, J., 2018a Elastic constant determination of unidirectional composite via ultrasonic bulk wave through transmission

measurements A review. Progress in materials Science. In Press:AAM https://doi.org/10.1016/j.pmatsci.2018.04.001

Paterson, D.A.P., Ijomah, W.L., Windmill, J.F.C., 2017. End-of-Life decision tool with emphasis on Remanufacturing. J. Clean. Prod. 148, 653–664. doi:10.1016/j.jclepro.2017.02.011

Paterson, D.A.P., Ijomah, W., Windmill, J., 2016. An analysis of end-of-life terminology in the carbon fiber reinforced plastic industry. Int. J. Sustain. Eng. 9, 130–140. doi:10.1080/19397038.2015.1136361

Published Conference Articles

Paterson, D.A.P., Ijomah, W., Windmill, J., Kao, C-C., Smilie, G., 2018. Ultrasonic Bulk Wave Measurements on Composites using Fibres from Recycled CFRP in: Review of Progress in Quantitative Non-Destructive Evaluation, AIP Conference Proceedings, vol 1949, 130010. DOI: 10.1063/1.5031605

Paterson, D.A.P., Ijomah, W., Windmill, J., 2015. Carbon fibre reinforced plastic EOL : protecting remanufacturing status and life cycle route analysis, in: International Conference on Remanufacturing. pp. 1753–1759. doi:http://strathprints.strath.ac.uk/53781/

Conferences and workshops attended

Review of Progress of in Quantitative Non-Destructive Evaluation (QNDE), Provo, Utah, July 17 – 20, 2017

Scottish Institute of Remanufacturing (SIR) Conference, Glasgow, March 7th, 2017

European Remanufacturing Network (ERN) Workshop, Glasgow, September 13th 2016

Company Visits

Autocraft Drive train solutions
Syston Lane, Belton
Grantham, Lincolnshire
NG32 2LY, United Kingdom

Mackie Transmission LTD
95 Causewayside Street
Tollcross, Glasgow
G32 8LT, United Kingdom

Cummings ReCon
2-10 Napier Pl,
Cumbernauld, Lanarkshire
G68 0BP, United Kingdom

Glasgow Computer Recycling
Anniesland Business Park,
Netherton Rd, Glasgow
G13 1EU, United Kingdom

Copyright permissions

Research published by the current author during the course of this degree, has been used extensively to construct this research. Chapter 1, chapter 3 and chapter 4 are constructed in part using work from (Paterson et al., 2016), chapter 5 was constructed in part using work from (Paterson et al., 2015) and (Paterson et al., 2017), chapter 7 constructed using work from (Paterson, et al., 2018a) and chapter 8 constructed in part using work from (Paterson et al., 2018).

Additionally, this thesis uses images taken from previously published papers by past and present researchers. Proper citations are given where diagrams, tables or images

are taken from the work by the present author or from the work of other researchers. The copyright permission given below;

Figure 3 - *Reprinted with permission from Paterson, D.A.P., Ijomah, W., Windmill, J., 2016. An analysis of end-of-life terminology in the carbon fiber reinforced plastic industry. Int. J. Sustain. Eng. 9, 130–140. doi:10.1080/19397038.2015.1136361*

Figure 4 - *Reprinted with permission from Paterson, D.A.P., Ijomah, W., Windmill, J., 2016. An analysis of end-of-life terminology in the carbon fiber reinforced plastic industry. Int. J. Sustain. Eng. 9, 130–140. doi:10.1080/19397038.2015.1136361*

Figure 10 - *Reprinted with permission from Paterson, D.A.P., Ijomah, W., Windmill, J., 2016. An analysis of end-of-life terminology in the carbon fiber reinforced plastic industry. Int. J. Sustain. Eng. 9, 130–140. doi:10.1080/19397038.2015.1136361*

Figure 11 - *Reprinted with permission from Ijomah, 2002, "A model-based definition of the generic remanufacturing business processes", Plymouth University, doi:10026.1/601*

Figure 12 - *Reprinted with permission from Paterson, D.A.P., Ijomah, W.L., Windmill, J.F.C., 2017. End-of-Life decision tool with emphasis on Remanufacturing. J. Clean. Prod. 148, 653–664. doi:10.1016/j.jclepro.2017.02.01, under creative commons Attribution License https://creativecommons.org/licenses/by/4.0/*

Figure 13 - *Reprinted with permission from Paterson, D.A.P., Ijomah, W.L., Windmill, J.F.C., 2017. End-of-Life decision tool with emphasis on Remanufacturing. J. Clean. Prod. 148, 653–664. doi:10.1016/j.jclepro.2017.02.01, under creative commons Attribution License https://creativecommons.org/licenses/by/4*

Figure 14 - *Reprinted with permission from Paterson, D.A.P., Ijomah, W.L., Windmill, J.F.C., 2017. End-of-Life decision tool with emphasis on Remanufacturing. J. Clean. Prod. 148, 653–664. doi:10.1016/j.jclepro.2017.02.01, under creative commons Attribution License https://creativecommons.org/licenses/by/4.0/*

Figure 15 - *Reprinted with permission from Paterson, D.A.P., Ijomah, W.L., Windmill, J.F.C., 2017. End-of-Life decision tool with emphasis on Remanufacturing. J. Clean. Prod. 148, 653–664. doi:10.1016/j.jclepro.2017.02.01, under creative commons Attribution License https://creativecommons.org/licenses/by/4.0/*

Figure 16 - *Reprinted with permission from Paterson, D.A.P., Ijomah, W.L., Windmill, J.F.C., 2017. End-of-Life decision tool with emphasis on Remanufacturing. J. Clean. Prod. 148, 653–664.*

doi:10.1016/j.jclepro.2017.02.01, under creative commons Attribution License https://creativecommons.org/licenses/by/4.0/

Figure 17 - *Reprinted with permission from Paterson, D.A.P., Ijomah, W.L., Windmill, J.F.C., 2017. End-of-Life decision tool with emphasis on Remanufacturing. J. Clean. Prod. 148, 653–664. doi:10.1016/j.jclepro.2017.02.01, under creative commons Attribution License https://creativecommons.org/licenses/by/4.0/*

Figure 26 - *Reprinted with permission from Zimmer JE, Cost JR. Determination of the elastic constants of a unidirectional fibre composite using ultrasonic velocity measurements. Acoust Soc Am; 47: 795–803.Copyright 1970, Acoustic Society of America*

Figure 27 - *Reprinted with permission from Zimmer JE, Cost JR. Determination of the elastic constants of a unidirectional fibre composite using ultrasonic velocity measurements. Acoust Soc Am; 47: 795–803.Copyright 1970, Acoustic Society of America*

Figure 28 - *Reprinted from Composites, Vol 1 / edition number 3, Markham, M. F., Measurement of the elastic constants of fibre composites by ultrasonics, Pages No 145-149., Copyright (1970), with permission from Elsevier*

Figure 29 - *Reprinted from Composites, Vol 1 / edition number 3, Markham, M. F., Measurement of the elastic constants of fibre composites by ultrasonics, Pages No 145-149., Copyright (1970), with permission from Elsevier*

Figure 30 - *Reprinted from Smith RE. Ultrasonic elastic constants of carbon fibres and their composites. J Appl Phys; 43: 2555–2561with the permission of AIP Publishing*

Figure 31 - *Reprinted from Smith RE. Ultrasonic elastic constants of carbon fibres and their composites. J Appl Phys; 43: 2555–2561with the permission of AIP Publishing*

Figure 32 - *Experimental Mechanics, Elastic moduli of transversely isotropic graphite fibres and their composites, 19, 1979, page 41-49, Kriz RD, Stinchcomb WW, With permission of Springer*

Figure 33 – *Review of Progress in Quantitative Nondestructive Evaluation, Chapter 6, Measurement of ultrasonic wavespeeds in off-axis directions of composite materials, Vol. 6A, 1987, page 1093–1101, Pearson LH, Murri WJ, Copyright* Springer Science+Business Media New York *US, With permission of Springer*

Figure 34 - *Review of Progress in Quantitative Nondestructive Evaluation, Chapter 8, Ultrasonic evaluation of in-plane and out-of-plane elastic properties of composite materials, Vol. 8, 1989, page 1489–1496, Rokhlin SI, Wang W, Copyright Springer Science+Business Media New York, With permission of Springer*

Figure 36 – *Reprinted from Composites part B: Engineering, Vol 66, Castellano, A; Foti, P; Fraddosio, A; Marzano, Salvatore; Piccioni, Mario Daniele; Mechanical characterization of CFRP composites by ultrasonic immersion tests: Experimental and numerical approaches, Pages 299-310, Copyright (2014), with permission from Elsevier*

Figure 37 – *Reprinted from Composites part B: Engineering, Vol 66, Castellano, A; Foti, P; Fraddosio, A; Marzano, Salvatore; Piccioni, Mario Daniele; Mechanical characterization of CFRP composites by ultrasonic immersion tests: Experimental and numerical approaches, Pages 299-310, Copyright (2014), with permission from Elsevier*

Figure 38 – *Reprinted from Composites part B: Engineering, Vol 66, Castellano, A; Foti, P; Fraddosio, A; Marzano, Salvatore; Piccioni, Mario Daniele; Mechanical characterization of CFRP composites by ultrasonic immersion tests: Experimental and numerical approaches, Pages 299-310, Copyright (2014), with permission from Elsevier*

Figure 40 *- Reprinted from Paterson, D.A.P., Ijomah, W., Windmill, J., Kao, C-C., Smilie, G., 2018. Ultrasonic Bulk Wave Measurements on Composites using Fibres from Recycled CFRP in: Review of Progress in Quantitative Non-Destructive Evaluation,* AIP Conference Proceedings, *vol 1949, 130010. DOI: 10.1063/1.5031605*

Figure 67 - *Reprinted with permission from Zimmer JE, Cost JR. Determination of the elastic constants of a unidirectional fibre composite using ultrasonic velocity measurements. Acoust Soc Am; 47: 795–803.Copyright 1970, Acoustic Society of America*

Figure 68 - *Reprinted with permission from Zimmer JE, Cost JR. Determination of the elastic constants of a unidirectional fibre composite using ultrasonic velocity measurements. Acoust Soc Am; 47: 795–803.Copyright 1970, Acoustic Society of America*

Figure 69 - *Reprinted from Composites, Vol 1 / edition number 3, Markham, M. F., Measurement of the elastic constants of fibre composites by ultrasonics, Pages No 145-149., Copyright (1970), with permission from Elsevier*

Figure 70 - *Reprinted from Composites, Vol 1 / edition number 3, Markham, M. F., Measurement of the elastic constants of fibre composites by ultrasonics, Pages No 145-149., Copyright (1970), with permission from Elsevier*

Figure 71 - *Reprinted from Composites, Vol 1 / edition number 3, Markham, M. F., Measurement of the elastic constants of fibre composites by ultrasonics, Pages No 145-149., Copyright (1970), with permission from Elsevier*

Figure 72 - *Reprinted from Smith RE. Ultrasonic elastic constants of carbon fibres and their composites. J Appl Phys; 43: 2555–2561with the permission of AIP Publishing*

Figure 73 - *Reprinted from Smith RE. Ultrasonic elastic constants of carbon fibres and their composites. J Appl Phys; 43: 2555–2561with the permission of AIP Publishing*

Figure 74 - *Reproduced with permission from Dean GD, Lockett FJ., Determination of the Mechanical Properties of Fibre Composites by Ultrasonic Techniques. Anal Test Methods High Modul Fibres Compoistes ASTM STP 521, Am Soc Test Mater; 326–346., Copyright ASTM International 100 Barr Harbor Drive, West Conshohocken, PA 19428*

Figure 76 - *Wilkinson SJ, Reynolds WN. The propagation of ultrasonic waves in carbon-fibrereinforced plastics. J Phys D Appl Phys; 7: 50–57, © IOP Publishing, Reproduced with permission. All rights reserved*

Figure 78 - *Wilkinson SJ, Reynolds WN. The propagation of ultrasonic waves in carbon-fibrereinforced plastics. J Phys D Appl Phys; 7: 50–57, © IOP Publishing, Reproduced with permission. All rights reserved*

Figure 79 - *Reprinted from Ultrasonics, Vol 16 / edition number 4, Reynolds WN, Wilkinson SJ The analysis of fibre-reinforced porous composite materials by the measurement of ultrasonic wave velocities, 159-163., Copyright (1978), with permission from Elsevier*

Figure 80 - *Reprinted from Ultrasonics, Vol 16 / edition number 4, Reynolds WN, Wilkinson SJ The analysis of fibre-reinforced porous composite materials by the measurement of ultrasonic wave velocities, 159-163., Copyright (1978), with permission from Elsevier*

Figure 81 - *Experimental Mechanics, Elastic moduli of transversely isotropic graphite fibres and their composites, 19, 1979, page 41-49, Kriz RD, Stinchcomb WW, With permission of Springer*
Figure 82 - *Experimental Mechanics, Elastic moduli of transversely isotropic graphite fibres and their composites, 19, 1979, page 41-49, Kriz RD, Stinchcomb WW, With permission of Springer*

Figure 83 - *Review of Progress in Quantitative Nondestructive Evaluation, Chapter 6, Measurement of ultrasonic wavespeeds in off-axis directions of composite materials, Vol. 6A, 1987, page 1093–1101, Pearson LH, Murri WJ, Copyright* Springer Science+Business Media New York *US, With permission of Springer*

Figure 84 - *Review of Progress in Quantitative Nondestructive Evaluation, Chapter 6, Measurement of ultrasonic wavespeeds in off-axis directions of composite materials, Vol. 6A, 1987, page 1093–1101, Pearson LH, Murri WJ, Copyright* Springer Science+Business Media New York *US, With permission of Springer*

Figure 85 - *Review of Progress in Quantitative Nondestructive Evaluation, Chapter 6, Measurement of ultrasonic wavespeeds in off-axis directions of composite materials, Vol. 6A, 1987, page 1093–*

1101, Pearson LH, Murri WJ, Copyright Springer Science+Business Media New York *US, With permission of Springer*

Figure 86 - *Review of Progress in Quantitative Nondestructive Evaluation, Chapter 8, Ultrasonic evaluation of in-plane and out-of-plane elastic properties of composite materials, Vol. 8, 1989, page 1489–1496, Rokhlin SI, Wang W, Copyright Springer Science+Business Media New York, With permission of Springer*

Figure 87 - *Review of Progress in Quantitative Nondestructive Evaluation, Chapter 8, Ultrasonic evaluation of in-plane and out-of-plane elastic properties of composite materials, Vol. 8, 1989, page 1489–1496, Rokhlin SI, Wang W, Copyright Springer Science+Business Media New York, With permission of Springer*

Figure 88 - *Review of Progress in Quantitative Nondestructive Evaluation, Chapter 8, Ultrasonic evaluation of in-plane and out-of-plane elastic properties of composite materials, Vol. 8, 1989, page 1489–1496, Rokhlin SI, Wang W, Copyright Springer Science+Business Media New York, With permission of Springer*

Figure 92 - *Reprinted from Composites part B: Engineering, Vol 66, Castellano, A; Foti, P; Fraddosio, A; Marzano, Salvatore; Piccioni, Mario Daniele; Mechanical characterization of CFRP composites by ultrasonic immersion tests: Experimental and numerical approaches, Pages 299-310, Copyright (2014), with permission from Elsevier*

Figure 93 - *Reprinted from Composites part B: Engineering, Vol 66, Castellano, A; Foti, P; Fraddosio, A; Marzano, Salvatore; Piccioni, Mario Daniele; Mechanical characterization of CFRP composites by ultrasonic immersion tests: Experimental and numerical approaches, Pages 299-310, Copyright (2014), with permission from Elsevier*

Figure 94 - *Reprinted from Composites part B: Engineering, Vol 66, Castellano, A; Foti, P; Fraddosio, A; Marzano, Salvatore; Piccioni, Mario Daniele; Mechanical characterization of CFRP composites by ultrasonic immersion tests: Experimental and numerical approaches, Pages 299-310, Copyright (2014), with permission from Elsevier*

Table 5 - *Reprinted with permission from Paterson, D.A.P., Ijomah, W., Windmill, J., 2016. An analysis of end-of-life terminology in the carbon fiber reinforced plastic industry. Int. J. Sustain. Eng. 9, 130–140. doi:10.1080/19397038.2015.1136361*

Table 12 - *Reprinted with permission from Paterson, D.A.P., Ijomah, W., Windmill, J., 2016. An analysis of end-of-life terminology in the carbon fiber reinforced plastic industry. Int. J. Sustain. Eng. 9, 130–140. doi:10.1080/19397038.2015.1136361*

Table 13 - *Reprinted with permission from Paterson, D.A.P., Ijomah, W.L., Windmill, J.F.C., 2017. End-of-Life decision tool with emphasis on Remanufacturing. J. Clean. Prod. 148, 653–664.*

doi:10.1016/j.jclepro.2017.02.01, under creative commons Attribution License https://creativecommons.org/licenses/by/4.0/

Table 14 - *Reprinted with permission from Paterson, D.A.P., Ijomah, W.L., Windmill, J.F.C., 2017. End-of-Life decision tool with emphasis on Remanufacturing. J. Clean. Prod. 148, 653–664. doi:10.1016/j.jclepro.2017.02.01, under creative commons Attribution License https://creativecommons.org/licenses/by/4.0/*

Table 15 - *Reprinted with permission from Paterson, D.A.P., Ijomah, W.L., Windmill, J.F.C., 2017. End-of-Life decision tool with emphasis on Remanufacturing. J. Clean. Prod. 148, 653–664. doi:10.1016/j.jclepro.2017.02.01, under creative commons Attribution License https://creativecommons.org/licenses/by/4.0/*

Table 16 - *Reprinted with permission from Paterson, D.A.P., Ijomah, W.L., Windmill, J.F.C., 2017. End-of-Life decision tool with emphasis on Remanufacturing. J. Clean. Prod. 148, 653–664. doi:10.1016/j.jclepro.2017.02.01, under creative commons Attribution License https://creativecommons.org/licenses/by/4.0/*

Table 17 - *Reprinted with permission from Paterson, D.A.P., Ijomah, W.L., Windmill, J.F.C., 2017. End-of-Life decision tool with emphasis on Remanufacturing. J. Clean. Prod. 148, 653–664. doi:10.1016/j.jclepro.2017.02.01, under creative commons Attribution License https://creativecommons.org/licenses/by/4.0/*

Table 18 - *Reprinted with permission from Paterson, D.A.P., Ijomah, W.L., Windmill, J.F.C., 2017. End-of-Life decision tool with emphasis on Remanufacturing. J. Clean. Prod. 148, 653–664. doi:10.1016/j.jclepro.2017.02.01, under creative commons Attribution License https://creativecommons.org/licenses/by/4.0/*

Table 19 - *Reprinted with permission from Paterson, D.A.P., Ijomah, W.L., Windmill, J.F.C., 2017. End-of-Life decision tool with emphasis on Remanufacturing. J. Clean. Prod. 148, 653–664. doi:10.1016/j.jclepro.2017.02.01, under creative commons Attribution License https://creativecommons.org/licenses/by/4.*

Table 55 - *Reprinted from Composites structures, Vol 67 / Edition number 1, Reddy, S. Siva Shashidhara, Reddy; Balasubramaniam, Krishnan; Krishnamurthy, C. V; Shankar, M; Ultrasonic goniometry immersion techniques for the measurement of elastic moduli, Pages 3-17., Copyright (2005), with permission from Elsevier*

Table 56 - *Reprinted from Composites structures, Vol 67 / Edition number 1, Reddy, S. Siva Shashidhara, Reddy; Balasubramaniam, Krishnan; Krishnamurthy, C. V; Shankar, M; Ultrasonic goniometry immersion techniques for the measurement of elastic moduli, Pages 3-17., Copyright (2005), with permission from Elsevier*

Chapter 1: Introduction

1.1 Introduction

The levels of municipal waste recorded between 1990 and 2007 by Organisation for Economic Co-operation and Development (OECD) countries rose almost year by year from approximately 537 million tonnes to 670 million tonnes; from 2007-2013 the levels have stayed at approximately within 3% of 2007 levels (OECD, 2015). To tackle waste generation head on, the European Union (EU) has issued and continually updates/revises multiple waste related directives and targets for its members. Notable waste related directives include the waste of electrical and electronic equipment (WEEE) directive (European Parliament and Council, 2012), the end of life vehicles (ELV) directive (European Parliament and Council, 2000a), the landfill directive (European Parliament and Council, 1999), the incineration of waste directive (European Parliament and Council, 2000b), the waste shipment regulation (European Parliament and Council, 2006) and the waste framework (WF)
(European Parliament and Council, 2008).

Alongside increasing waste regulations there is also increased demand for CFRP, by 2021 the global tonnage of CFRP is expected to have increased by approximately 210% from 2014 levels (Kraus and Kühnel, 2015). Coupled with growing demand, carbon fibre can be expensive to produce costing up to £10,000 per ton (Marsh, 2009). Further, although considered a complex waste type, the economic and environmental benefits (Howarth et al., 2014; Song et al., 2009; Suzuki and Takahashi, 2005; Witik et al., 2013) of recycling are such that CFRP EOL strategies to avoid landfill receives much attention.

Terminology that routinely appears within industry and academia in relation to the recycling practices includes recycled CFRP, recycled fibres, reclaimed fibres and remanufacture or re-manufacture. However, it is not been shown that the terms recycling and remanufacturing are applicable terms in this sector, thus an evaluation

of terminology in the EOL CFRP, including possible development of new tools which could ensure correct terminology, is required.

It is also the case that ultrasonic NDT/E techniques have been shown to be both robust and reliable strategies to determine not only the mechanical properties of virgin composite materials but also provide insight into others areas, including but not limited to void content, defect detection and symmetry class (Hosten, 2001; Rokhlin et al., 2011; Scott and Scala, 1982; Summerscales, 1990, 1987). However, no such large scale studies have taken place on what industry and academia refer to as remanufactured CFRP.

Thus, it can now be said that this research examines the industrial and academic efforts to recycle and remanufacture CFRP from a terminology standpoint and from a NDT/E standpoint.

1.2 Research questions

The core principal at the heart of this research is the product commonly referred to within industry and academia as recycled and remanufactured (re-manufactured) CFRP. It is also the case that research is conducted in relation to these products in two distinct areas. Thus, naturally two research questions, distinct from each other, arise. These are given as follows,

1. Are the products denominated as recycled CFRP and remanufactured (remanufactured) CFRP actually by definition, recycled and remanufactured CFRP? If not, why not? And is there a more accurate way of describing these products?

2. Ultrasonic velocity measurements, specifically, the through transmission technique, have long been used to determine the elastic constants of virgin CFRP. Products denominated as recycled and remanufactured CFRP are not v-CFRP; thus, are the standard ultrasonic through transmission measurements routinely used on v-CFRP applicable to recycled and remanufactured (if these are the correct terms) CFRP?

1.3 Deliverables of research

Based on the research questions, a number of deliverables are expected. The deliverables from this thesis are given below.

In relation to research question 1

- Literature survey outlining the practices and instances within industry where the terms recycling and remanufacturing are occurring in relation to CFRP
- Presentation of accepted definitions of recycled and remanufactured products from industry and academia
- Cross reference of established definitions with practices conducted by academia and industry to then form a decision as to whether the practices conducted are actually recycling and remanufacturing operations
- Identification of new terminology better positioned to denominate these products
- Identification whether CFRP is incapable of being remanufactured
- Creation of bespoke flow chart and question set to assist in future decision making process of labelling an EOL product which has received a re-process
  - Industrial and academic review of the flow chart and question set

In relation to research question 2

- Derivation of the Christoffel equation, an equation governing the relationship between wave velocity and elastic constants of a solid, from first principles
- Literature review on determination of elastic constants of v-CFRP highlighting the long established experimental arrangements and existing knowledge on the subject
- Determination of elastic constants of v-CFRP via an ultrasonic immersion based velocity measurement and via mechanical testing with comparison of result
- CFRP recycling and subsequent manufacturing operations to create the „remanufactured" CFRP.
- Determination of elastic constants of „remanufactured" CFRP via an ultrasonic immersion based velocity measurement and via mechanical testing with comparison of result

- Comparison, in terms of accuracy, between the v-CFRP and the „remanufactured" CFRP
- Bespoke Matlab programmes to serve both as a teaching aid in this research area and also to identify and present the findings recorded from experiment

1.4 Contributions to knowledge

The contributions to knowledge arising as a result of this research are as follows.

1. Cross examination of practices, in relation to CFRP, conducted within industry and academia currently labelled as recycling and remanufacturing with accepted definitions of recycling and remanufacturing.

2. Identification that CFRP remanufacturing terminology is used incorrectly, recycling terminology is used both correctly and in a somewhat liberal manner to describe products and processes created by academia and industry and that CFRP is not capable of being remanufactured.

3. Identification of new terminology which more accurately describes the products created by academia and industry, terminology which is in keeping with accepted definitions and also in accordance with existing EU directives.

4. Development and presentation of a novel EOL decision making tool which may be used to form a decision as to whether a product has been recycled, repaired, re-used, reconditioned or remanufactured and as means to quickly and efficiently determine remanufacturing synonyms.

5. Review documenting a chronological progression of findings and contributions to knowledge within literature concerning the immersion based ultrasonic through transmission determination of elastic constants of unidirectional v-CFRP, circa 1970-2014.

6. Determination that while applicable as a means to investigate elastic constants and Young"s modulus of „remanufactured" CFRP, for the manufacturing procedure and experimental arrangement outlined in this research, generally a lower % difference between ultrasound derived Young"s modulus and mechanical derived Young"s modulus is found for v-CFRP when compared to „remanufactured"- CFRP.

7. Development of bespoke Matlab programmes which both construct and executing the Christoffel equation, provide information on wave polarization and serve as a means to determine elastic constants.

Contributions to knowledge 1-7 are found to be original for various reasons. Looking at contribution 1, while there is an abundance of literature documenting, outlining, reviewing and documenting recycling and remanufacturing of CFRP, there is no analysis of these practices, from a terminological standpoint conducted within literature. Developing this, contribution 2 identifies for the first time in literature that that terminology is used incorrectly and liberally at present, and that CFRP is incapable of being remanufactured. Building on this on, contribution 3 presents new terminology to describe the products created by academia and industry - thus, the products created by industry and academia are able to be described more accurately moving forward.

Concerning contribution 4, it is the case that models and tools designed to demonstrate the difference between recycled, re-used, repaired, reconditioned and remanufactured products are present within literature. The tool presented in this research while similar, is distinct from existing tools in that, the decision as to whether a product is recycled, re-used, repaired, reconditioned or remanufactured is removed from the user. That is, the tool presented in this work informs the user directly as to the status of a product i.e. the user does not form their own decision, which is the case for existing tools. Looking at contribution 5, a literature review is presented. Existing reviews on the subject cover lots of literature and often have a wide scope; the review in this thesis substitutes scope for depth. That is, the scope of the review is limited to the extent where more depth, in terms of a papers contribution to knowledge, benefits, and drawbacks are able to be presented. Further, two information tables outlining some 40 contributions to knowledge are presented. Looking now at contribution 6, building on contribution 5, multiple studies within literature may be found which concern the elastic constant determination of v-CFRP via the ultrasonic through transmission technique. However, in terms of determining the elastic constants and Young‟s Modulus, of „recycled and remanufactured‟ CFRP, the majority of the literature originates from a destructive mechanical standpoint and no study to date examines the

applicability of employing existing ultrasonic through transmission technique on rf-CFRP in this regard.

Lastly, contribution 7 documents bespoke computer programmes. These programmes construct the Christoffel equation from first principles, document the velocity and polarization vector associated with propagating waves and provide a means to determine material elastic constants. These programmes may be used as both a teaching aid to understand the way in which the Christoffel equation is developed and executed, as a means to determine the wave velocity relationship polarization relationship in solids, and in experimental analysis when seeking to determine the elastic constants of solids.

1.5 Beneficiaries of research

The beneficiaries of this research are industrial, academic and governmental policy stakeholders, all of which are involved in the re-use of CFRP. The rationale for this view point, while discussed more in depth when the research contributions are presented individually, is briefly outlined below.

- Using the correct terminology to describe recovery strategies allows for
    1. Greater potential for effective research
    2. Improved dialogue between industry and academia
    3. Increased likelihood of gauging market more accurately
    4. Better compliance with new or existing legislation
    5. Increased awareness of remanufacturing within the field
    6. More accurate description of products created

- Novel tool, identifying and informing the user of which EOL operation conducted allows for
    1. More accurate description of products
    2. Quick test to identify remanufacturing and to identify remanufacturing synonyms such as „overhaul“ or „rebuild“
    3. Reduction of user error (removes final decision from user)
    4. Increased awareness of a remanufactured product (when used in conjunction with existing tools)

- Development of bespoke Matlab programmes and conducting experimental results on rf-CFRP allows for,
    1. The accuracy of „remanufactured“ CFRP Young“s modulus determination via ultrasound through transmission for the manufacturing and experimental procedure outlined, when compared to v-CFRP.
    2. Increased awareness in the ultrasonic research community of relatively new and novel products i.e. „remanufactured CFRP“
    3. Teaching aid for students via
        - Thorough derivation of Christoffel equation from first principles
        - Matlab programme outlining the relationship in solids between the elastic wave velocity and the elastic properties of the material
    4. Fully customizable Matlab programmes able to determine elastic solids of materials and document findings using these data sets

1.6 Structure of thesis

Given the two research questions this thesis is effectively split into two sections. Section 1, which covers chapters 3, 4, and 5, and section 2, which documents chapters 6, 7, 8. The breakdown of these chapters is given as follows.

Chapter 1

Chapter 1 provides an introduction to the research. The research questions are identified along with the deliverables of the thesis. The contributions to knowledge and the beneficiaries of the research are also presented in this chapter.

Chapter 2

Chapter 2 discusses the research methodology to collect the data set. The selection of ontology, epistemology and research method along with techniques is identified. Both research questions are discussed in terms of the methodology used in this chapter.

Chapter 3

This chapter provides the definitions of EOL terminology used within the research. That is, remanufacture, recycling, reconditioning, repairing and re-using are defined with the differences between each treatment clearly mapped out. Further, brief background knowledge on CFRP is also presented.

Chapter 4

This chapter identifies the market for CFRP products, the rationale as to why recycling and remanufacturing are conducted and provides a literature survey of the instances within industry and academia of where the term remanufacture and recycle both appear in terms of EOL CFRP treatment. Further, an analysis of whether the practices conducted by industry and academia are indeed remanufacturing and recycling, as directed by chapter 2, is also presented. Additionally, new terminology better suited to describing these products and justification as to the importance of correct EOL terminology in general sense is also presented.

Chapter 5

Chapter 5, concerns the presentation of a novel tool designed to allow for the correct terminology to be applied to a product, given the product has received a treatment which may be classed as recycling, remanufacturing, reconditioning, repairing or reusing. Existing tools which separate these terms are presented and discussed with a clear distinction between this research and the existing research identified.
Additionally, academic and industrial feedback on the tool is also presented.

Chapter 6

Having answered the first research question, attention is now drawn to the second research question. Looking forward to both a literature review, documentation of a bespoke Matlab programme and an experimental section of this thesis, chapter 6 presents an initial mathematical framework to allow for a smoother transition into these future chapters. That, is, the relationship between the elastic constants of a material and the velocity of an ultrasonic plane wave is presented from first principles.

Chapter 7

A contribution to knowledge of this thesis is a literature survey concerning the determination of elastic constants of v-CFRP via an ultrasonic immersion based through transmission technique. Seminal works dating back to circa 1970 and stretching onto 2014 are presented in chronological order and reviewed in their own merit. Further, two unique contributions to knowledge tables are also presented. These tables document some 40 contributions to knowledge during this research period. To ensure efficiency of the thesis, this chapter presents a condensed version of this literature review. The unabridged version is given in appendix 2.

Chapter 8

Chapter 8 presents the experimental section of this thesis. In this chapter v-CFRP is created with the elastic constants determined via ultrasonic through transmission.
The material Young‟s modulus is subsequently determined via mechanical testing and ultrasound through transmission. Additionally, v-CFRP is recycled with the reclaimed fibres being used to manufacture „remanufactured‟ CFRP. The elastic constants and Young‟s modulus figures are again obtained, similar to v-CFRP. An analysis in terms of accuracy between v-CFRP and rf-CFRP is discussed.

Chapter 9

Chapter 9 documents the conclusion of this thesis. A recap of the research undertaken, the findings documented and the contributions to knowledge arising from this thesis are outlined. Additionally, further work which builds on the research conducted within this thesis is also presented in this chapter.

Appendix 1

Chapter 6 documents a derivation of the Christoffel equation from first principles. This appendix documents additional mathematical verification of the concepts discussed in chapter 6, including execution of the Christoffel equation.

Appendix 2

The literature review presented in chapter 7 is an abridged version of a longer more in-depth review. This appendix documents the full length literature review.

Appendix 3

The experimental wave velocities from all CFRP samples are listed in this chapter in full.

Appendix 4

Appendix 4 provides bespoke Matlab programmes designed within the course of this research.

Appendix 5

Appendix 5 provides the force and displacement data experimentally recorded for all the CFRP samples.

Appendix 6

Appendix 6 presents a conference paper, presented at QNDE 2017. This conference paper is referenced in chapter 8 of this thesis. Table 1 presents an additional outline structure of this thesis with content and major research outcomes also presented.

Chapters	Content	Major Research Outcomes
Chapter 1: Introduction Overview of the research	*Identification goals, deliverables and beneficiaries along with contributions to knowledge*	*N/A*
Chapter 2: Research Design The manner in which research questions are investigated	*How I viewed the research and the methods taken to investigate research questions. Philosophical assumptions and research methods identified*	*Ontology, Epistemology, research method selected*
Chapter 3: Re-processes and CFRP Identification of re-based processes and outline of CFRP	*How were the re-based processes defined? What is CFRP?*	*Established definitions of reprocess taken from British National Standards and are in keeping with literature*
Chapter 4: CFRP Analysis of recycle and remanufacturing terminology in current CFRP re-use operations and proposal of new terminology	*What is the CFRP market and the drivers for end-of-life CFRP recovery? How does academia perform recycling and remanufacturing of CFRP and are these terms correct? How was new terminology selected?*	***Contribution to knowledge*** *Identification that remanufacturing is not occurring, CFRP is incapable of being remanufactured, recycling is not always the most accurate terminology and new terminology to describe products*
Chapter 5: Novel Tool Bespoke tool to ensure correct terminology	*What are existing methods for product classification? How does my tool differ from these? How did the tool receive endorsement?*	***Contribution to knowledge*** *Bespoke tool able to correctly classify products which have been subjected to a re-processes - endorsement by academic and industrial review*
Chapter 6: Christoffel Equation Derivation of formula pivotal to NDT of all solids	*How is ultrasonic wave velocity related to the elastic constants of solids?*	*Relationship between wave velocity and elasticity of a solid i.e. the relationship which allows for NDT to be conducted*
Chapter 7: Ultrasonic Literature Review of CFRP Existing knowledge on the determination of elastic constants of v-CFRP is presented	*What are the experimental methods of determining the elastic constants of CFRP ultrasonically?*	***Contribution to knowledge*** *Literature review documenting the elastic constant determination of uni-directional CFRP via ultrasonic through transmission*
Chapter 8: Experimental Analysis Determination of the elastic constants of v-CFRP and CFRP currently denominated as recycled or remanufactured CFRP	*What was the experimental arrangement? How were the elastic constants determined? What do the results mean?*	***Contribution to knowledge*** *Application of ultrasound through transmission as a means to determine elastic constants of products currently referred to as recycled or remanufactured CFRP*
Chapter 9: Conclusion Conclusion of thesis	*Research findings and contributions and future work?*	*Research summary and identification of future work*

Table 1 – Structure of this thesis with chapter content and major research outcomes

Chapter 2: Research Design

To obtain a reliable and robust data set in any research, an examination of the initial research question is essential. Essential in that, to understand the way and manner in which data should be collected, organized, analysed, and understood stems from the initial research questions themselves. For clarity, the research questions arising in this research are presented again.

1. Are the products denominated as recycled CFRP and remanufactured (remanufactured) CFRP actually by definition, recycled and remanufactured CFRP? If not, why not? And is there a more accurate way of describing these products?

2. Ultrasonic velocity measurements, specifically, the through transmission technique, have long been used to determine the elastic constants of virgin CFRP. Products denominated as recycled and remanufactured CFRP are not v-CFRP; thus, are the standard ultrasonic through transmission measurements routinely used on v-CFRP applicable to recycled and remanufactured (if these are the correct terms) CFRP?

As two different but related research areas are under examination within the thesis, the way in which data is retrieved, processed, evaluated, and analysed may change for each research question. As such, this chapter will provide discussion on potential aspects of research design, and then ultimately select the most appropriate methods for this research.

The potential aspects of research design, as outlined by Easterby-Smith (2012), which are key to obtaining a reliable, informative, meaningful data set, are ontology, epistemology, methodology, and methods and techniques. Such is the level of detail provided by Easterby-Smith (2012), this text is used extensively within this chapter. As such, an additional reference to Easterby-Smith (2012), is only provided when a direct quotation is used or when the authors findings are discussed.

2.1 Philosophical assumptions and hierarchical relationship

The areas of ontology, epistemology, research methodology, and methods and techniques, have a hierarchical relationship which is demonstrated by examination of Figure 1.

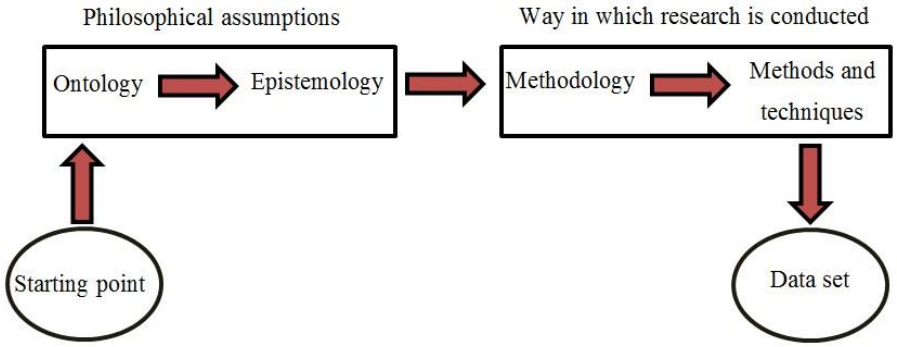

Figure 1 - Flowchart outlining the steps involved in obtaining a reliable and meaningful data set

Looking first at ontology and epistemology, to ensure that the data set obtained through research is both accurate and robust, it is important to begin from the correct starting point. That is, in agreement with the hierarchical relationship identified by Easterby-Smith (2012) and in Figure 1, prior to adopting various methods and techniques to actually collect and analyse the data, one must form decisions, whether sub conscious or conscious, regarding fundamental viewpoints of how one views the research. These fundamental viewpoints are commonly referred to as philosophical assumptions with the terminology ontology and epistemology being collective nouns for these areas.

2.2 Ontology

Ontology in a general sense is regarded as how does one consider the nature of existence to be or how one views the nature of reality. Within ontology, four key areas are prevalent; realism, internal realism, relativism, and nominalism, noting that the beliefs of realism and nominalism represent opposite ends of the spectrum, with

internal realism and relativism bridging the gap between these extremes. While researchers may adhere to more than one of these ontological belief structures, it is generally the case that researchers in the natural sciences adhere to realism whereas researchers in the field of social science adhering to nominalism. Each area is briefly discussed below.

2.2.1 Realism

Researchers who adhere to realism, i.e. realists, believe that when researching a given area a single truth exists. Further, the researchers cannot impact the truth governing the reality and merely observe the truth by virtue of the research conducted. The theories used to describe the truth are independent from what is being observed and so only the truth is considered valid, i.e. if the theory disagrees with the truth, the theory is incorrect, only the truth is correct. From a natural science point of view realism is highly suited, for example, when seeking the truth or reality as to why an apple falls from the tree, the truth or reality already existed prior to investigation and was external to the researcher i.e. gravity.

2.2.2 Internal realism

The view of the internal realist is not as extreme as that of the pure realist with internal realists, like realists, believing that a single truth or a single reality exists within the research area. However, unlike, realists, internal realists, believe that the truth or reality is never able to be directly measured and so evidence to deduce the truth or reality is only ever obtained from indirect observations, i.e. it is essentially impossible to obtain all the factual evidence surrounding this truth. Similar to realists, the theory associated with the truth is independent from the truth or reality.

For reinforcement of this concept, Easterby-Smith (2012), point to how the Heisenberg uncertainty principle puts forward the concept that the more accurate you can measure the position of a particle the less accurate you can measures its velocity, and vice versa.

2.2.3 Relativism

Unlike realism and internal realism, whose subscribers believe the truth or reality is out there waiting to be discovered, researchers who adhere to relativism subscribe to the concept that a single truth is not out there and that the given truth or reality is created by people themselves with Easterby-Smith (2012), pointing to the science of climate change to provide clarity on this. The authors state that in 1990 an intergovernmental panel on climate change put forward the notion that global warming, via CO_2 emissions from fossil fuels, was a serious threat to human civilization; however, their data showed global warming occurring 1000 years ago, which in turn led to another possible reality that global warming is not necessarily caused by CO_2 but instead may indeed be part of the earth‟s natural cycle of climate change. The key point in this belief structure is that the same evidence is available to all researchers but no absolute definitive conclusion may be drawn from a single piece of evidence. Thus, the agreement of reality or the truth of reality is formed through an agreement by the main protagonists and not through discovering a single truth.

2.2.4 Nominalism

The structure of nominalism is the opposite of realism. Adopters of nominalism believe that there is no single truth and that social reality or truth is developed through the language and behaviour of society itself. Exemplifying the nominalist belief system, Easterby-Smith (2012), highlights an nominalist view of a corporate profit obtained at the end of year. A nominalist would view this subject from perspective of

how profit figures are obtained by various operational decisions to maximise or minimise the overall profit.

Table 2 is given to reinforce the various ontologies and how they differ.

Ontology	Reality or truth	Evidence available
Realism	Single truth exists	Reality or truth already exists and can be found
Internal Realism	Single truth exists but obscure and determined indirectly	Reality or truth already exists but is not able to be found directly
Relativism	Multiple truths or realities exists	Many truths or reality exists and depends on the position of observer
Nominalism	No truth exists	No single truth or reality exits and so the truth or reality is a human construct.

Table 2 - Truth and evidence for the four types of ontology, adapted from (Easterby-Smith et al., 2012)

2.3 Epistemology

Epistemology concerns how one views the world or the way in which an observer (researcher) interacts with the natural world. The two dominant epistemologies are regarded as positivism and social constructionism (or social constructivism). Similar to realism and nominalism these belief structures occupy polar positions, however, Easterby-Smith (2012), point out that they have found no single philosopher who subscribes entirely to a epistemology, and that often times, researcher adhere mainly to one but cross over between the two.

2.3.1 Positivism and Social constructionism

The positivist belief structure focuses on the idea that the reality/truth/phenomenon exists externally from the observer and that an observer should be able to determine

its properties objectively, that is, without any personal beliefs from the observer impacting on the result. Easterby-Smith (2012), points out that the positivist application to the social science led, in part, to the creation of a new paradigm, social constructionism. Social constructionism is essentially the opposite of positivism, in that reality is not exterior and independent from the observer, and so in this belief structure the reality is formed by a construct of human interaction and behaviour. Unlike a positivist who would gather data objectively, a social scientist, adhering to social constructionism, would be more interested in understanding the importance of what subjects think and feel within the reality, thus better understanding the different experiences subjects have. Easterby-Smith (2012), document key criteria and defining characteristics between positivism and social constructionism, this is given as Table 3.

Differences between positivism and social constructionism								
	Observer	Human interests	Explanations	Research progresses through	Concepts	Units of analysis	Generalized through	Sampling requires
Positivism	Independent	Considered to be irrelevant	Causality	Hypothesis and deductive reasoning	Concepts must be defined so they can be studied	Should be simple	Statistical probabilities	Large random samples
Social Constructionism	Non independent (part of what is being observed)	The crux, i.e. what drives the science	A general understanding of the reality should be demonstrated	Meaningful data set which leads to ideas being developed	People of interests, stakeholders, should contribute thoughts	Can be very complex	Theoretical abstraction	Small specific samples

Table 3 - Differences between positivism and social constructionism, adapted from (Easterby-Smith et al., 2012)

2.4 Ontology and Epistemology Selection

Having reviewed both ontology and epistemology, it is appropriate at this point to form a decision regarding the philosophical belief structure this research subscribes to. This selection is reached at this point and prior to examination of research methodologies and methods and techniques given that the choice of ontology and epistemology dictate somewhat which methodology and methods one choses to use. Considering the first research question and choice of ontology; in this instance, realism, internal realism, and relativism have applicability. From a realist point of view the truth exists (remanufacturing and recycling are defined), and so research may be conducted to investigate whether the current products are recycled and remanufactured and the results directly measured. From an internal realist point of view, a single truth also exists but is somewhat obscure and so pinning down a clear definition of remanufacturing and recycling practices in every case is problematic leading to a decision being formed through indirect means. From the view point of relativism, many definitions of recycling and remanufacturing exist (which is indeed the case) and so the reality (definitions) depends upon the viewpoint of the observer. Note nominalism is not in general suitable in this instance as the basic assumption of a truth existing (practices are defined) is taken.

The decision taken in this research is to adopt realism; i.e. a single truth does indeed exist. A remanufacturing definition from literature is accepted as being absolutely correct with the view point of the observer not impacting upon the definitions and a decision as to whether the products have the correct denomination (i.e. recycled or remanufactured) is able to taken directly. Further, the practices conducted within academia and industry are also assumed to be absolute and so again the view point of the observer does not impact upon the reality and decisions again may be formed directly.

Looking now at the choice of epistemology, with the choice of realism highlighting that this research considers a single truth (definitions of practices are correct) the selection of positivism has been made. That is, the truth is not considered to change depending on the view point of the observer, the principle of causality is used when answering the research question, concepts are clearly defined allowing them to be studied and measured and answering the research question is aided by breaking down the truth (definitions) to their constituent parts.

Looking now at the second research question realism and positivism were again selected. Considering realism, a single truth that is able to be studied directly is assumed to exist, i.e. the velocity at which waves propagate through both isotropic materials and anisotropic materials are independent of the theories used to describe them, not dependent on the view point of the observer and is able to be measured directly. Considering the selection of positivism; the observer is not part of what is being observed, human interests are not part of the equation, causality is demonstrated, hypothesis and deductions are used to help answer research question and clear boundaries/concepts/limitations are defined with the results being fairly simple and accurate.

Selecting realism and positivism as philosophical assumptions as part of the research design to investigate both research questions, this research carries a more quantitative aspect than a qualitative one. Ijomah 2002 expands on this topic when she states that the quantitative paradigm adheres to the notion that by using logical reasoning and proven rules then new knowledge obtained objectively will be produced, whereas for qualitative research the observer is actively involved in the reality and new knowledge is formed through in part incorporating stakeholder analysis. Thus the findings of this thesis can be considered to stemming from a point of universal accessible truth and be quantitative in nature.

2.5 Research methodologies

Easterby-Smith (2012) identify three research methodologies which are well suited to those who subscribe to positivism; experimental, quasi-experimental and survey research. These three methodologies are now discussed.

2.5.1 Experimental and quasi-experimental

From a realist positivist point of view, the concept of an experiment is to discover the already existing truth and so, naturally experimentation may take many different forms. Easterby-Smith (2012) identify what they call classic experimentation, a method which dominates the natural sciences and is repeatable by others. Classic

experimentation involves observing both an experimental group and a control and what effects external input have on the experimental group when compared to the control group. Demonstrating this Easterby-Smith (2012) identify a classic fertilizer experiment - to identify the effects of a new fertilizer, an experimental group (one part of a field) would receive the new fertilizer and a control group (second part of a field) would not receive the new fertilizer. In this type of arrangement, the investigator conditions both the experimental and control group themselves to be identical, save for the changes recorded in the experimental group, Also, classic scientific experiments, such as measuring the amount of sound absorbed by a material or measuring how long it takes for a queue to be processed, which may not appear to have experimental and control groups fall under this type of research methodology.

In quasi-experimental analysis, the investigator has less control over the experimental and control groups in that these groups deviate from being fully matched, save for the changes to the experimental group. The reason quasiexperimental methods were developed was that in some circumstances, (mainly behavioural) experimental investigation was not sufficient. Consider the example given by Easterby-Smith (2012); within a business setting, there could a desire to investigate a highflier development scheme, however, the investigator cannot simply assign managers at random to the scheme (experimental group) and control group as the managers would themselves be aware of what is happening, and so influence the results by say performance related behaviour. In this instance, a classic form of quasi-experimental approach is to get the mangers to perform identical tests and then to conduct post interview and pre interview analysis of the managers who joined the scheme and for managers who didn‟t. The key aspect for quasi-experimental is the different control groups and so it is hard to make a solid conclusion of the impact that the given change (in this case, the highflier course) had on the experimental group owing to non-identical experimental and control groups.

2.5.2 Survey

The survey method leads to the investigator becoming detached, and so this method is naturally suited to positivism, i.e. data is able to be obtained objectively and independently. From a realist point of view, the truth is out there and exists, and so using large sample surveys can lead to the truth being obtained, even though multiple variables exists which all have an impact upon the truth. Typically three type of survey

exist, factual, inferential and exploratory; factual surveys typically consist of market research or opinion polls, inferential surveys are concerned with establishing a relationship between a concept (hypothesis) and a set of variables and exploratory surveys set out to establish a concept or a hypothesis. Easterby-Smith (2012), provide further discussion on these three types. As with all research care should be taken when forming a conclusion from surveys and so question type and the amount of questions are key aspects of survey design.

2.6 Research methodology selection

Looking at the first research question, from an experimental point of view, owing to a realist positivist approach, an experiment could be designed to empirically prove whether or not the products currently denominated as recycled and remanufactured CFRP are actually by definition recycled and remanufactured CFRP and equally further state if new terminology is more suitable. From a quasi-experimental point of view, the case for this approach is more difficult to state; owing to the fact that little to no human behavioural element is required to be investigated. Lastly, from a survey point of view, it is indeed feasible to seek the truth by constructing and sending out various surveys, which could take the form of opinion polls, to various stakeholders involved in the CFRP re-use industry.

Given that this research stems from a philosophical standpoint of realism and positivism, the experimental method was selected.

Looking now at the second research question, the experimental approach has direct applicability and has also been selected as the methodology of choice. That is, direct, observer independent, objective detection of elastic waves through CFRP is sought. Judging that the research question is framed by way of a comparison, the experimental group in this instance could be considered as the products currently denominated as recycled and remanufactured CFRP and the control group could be considered as virgin CFRP. The experiments considered in this instance are not reliant on human behaviour and so quasi-methods are not in general applicable, and surveys will not in general sense allow for discussion on the research question.

2.7 Methods and techniques

Having now demonstrated that experimentation is the chosen research methodology to provide meaningful insight on both research questions, it is appropriate to discuss the methods and techniques used to obtain the data set. At this point only a generic outline of the experimental method used is discussed with the relevant chapters providing additional findings on the experimental arrangements.

The investigation of both research questions is by experiment and follows the classic experimental approach of the natural sciences, the scientific method. The scientific method, (Anderson, 1983; Carey, 2011; Kothari, 2004; Marder, 2011; Rajendra Kumar, 2008) is a framework for how to form a meaningful and robust conclusion from the experiments conducted.

The first process in the scientific method is to ask a question, i.e. the research question. There follows some background research and a hypothesis. The hypothesis stems from the research question and the background research is essentially a guess as to the outcome of an experiment. Given At this point, an experiment is conducted and if the hypothesis aligns with the experimental result then the hypothesis is correct. If the hypothesis does not align with the experimental findings then the hypothesis is incorrect and another one has to be constructed. This process continues until hypothesis aligns with experimental findings. Figure 2 outlines the steps involved in the scientific method.

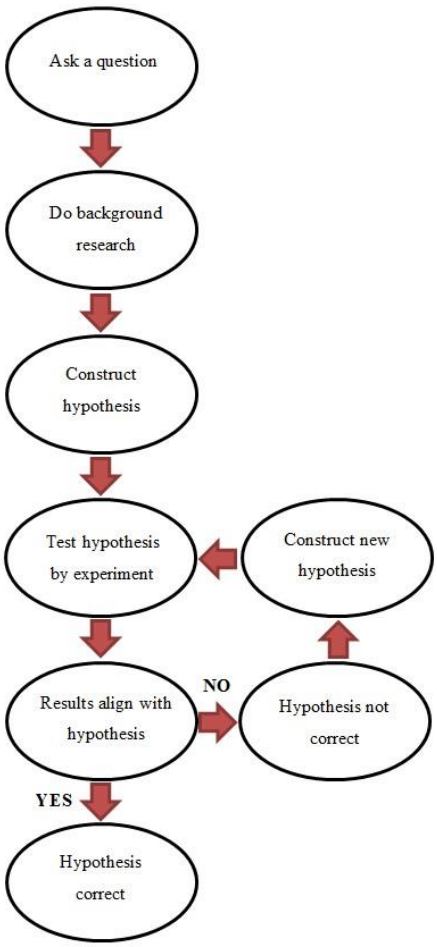

Figure 2 – outlining the steps involved in the scientific method

2.8 Research design for bespoke tool

Through investigation in research question 1, another contribution to knowledge, a novel EOL tool for correct product classification was developed. Thus, it is appropriate to outline the research design associated with this additional contribution to knowledge.

The bespoke tool presented in chapter 5 is focused upon identifying which reprocess has been applied to an end-of-life product and so again the ontology selection was realism – an appropriate choice considering the definitions are regarded as a single truth. The epistemology selection was again in keeping with research questions 1 and 2 in that positivism was selected (the truth does not change via view point of observer). The research methodology and methods in this instance was not in general the experimental approach or scientific method and was more aligned to the survey

approach. In this instance, a tool was designed from a realist positivist view point and then it was subjected to two rounds of academic and industrial feedback to obtain endorsement of the tool. Similar to research question 1 and 2, the experimental arrangement (in this case the endorsement process) is presented in more detail in the relevant chapter.

2.8 Conclusion

Within this chapter, thesis research design has been outlined. The ontological selection to help answer both research questions was realism - this thesis believes that the truth is out there, able to be determined and is independent from the researcher searching for it. The epistemology selection for both research questions was positivism - theories are not in general being generated they are more akin to being tested, facts and deductive logic are used to confirm or deny hypothesis, human interests are irrelevant and again the observer is independent of what is being studied. Additionally the methodology for both research questions was experimentation - concepts are clearly defined, the truth already exists, able to be determined independently from observer, hypotheses are able to be made and the primary role is to test theories, not primarily create them.

Further, the generic model of experimental design i.e. the scientific method, was also presented, with further identification that chapter 4 and chapter 8 outline the way in which the data set to answer the first research question and second research questions were obtained.

Additionally, this chapter also identified that the bespoke tool in chapter 5, also stemmed from a view point of realism and positivism. However, the experimental approach was not taken and a method more aligned to survey, a endorsement by review method, was used to endorse the authors‟ findings. Similar to chapters 4 and 8, chapter 5 was identified as providing additional clarity on the review method approach taken.

Moving forward, chapter 3 presents the relevant definitions of product treatments used within this research.

Chapter 3: Definition of terminology and CFRP

3.1 EOL terminology

Within this research, common product recovery strategies (recovered in the sense that they do not go to landfill) such as recycle, remanufacture, recondition, repair and re-use are thought of as being distinct from one another. This is a distinction not always made within literature, with Table 4 providing examples from literature.

Authors	Industrial Sector	EOL terminology	Notes
(Go et al., 2011)	Electrical and Electronic	Remanufacture, reconditioning, re-use,	Re-use defined as using EOL product directly, with remanufacturing adhering in general terms to the definition used in this work. Also, in this instance the authors are not clear on the subtle differences between recondition and remanufacture and almost lump both together.

(Ke et al., 2011)	Automotive	Remanufacture, recycle, reconditioning	The definition of remanufacture as in general in keeping with the definition used in this research, however, the authors do not in general identify recycle and recondition as a separate process from remanufacture. That is, remanufactured products are stated as containing reconditioned parts and remanufacture is also considered a recycling process.
(Gao et al., 2010)	Industrial engineering	Remanufacture, repair, re-use	Remanufacture is described in a tenuous way and do not acknowledge the accepted standard that the performance of the product should be at least equal to as new condition. Thus, no clear separation between terms is apparent.
(Pigosso et al., 2010)	Aerospace	Remanufacture, refurbishment, reuse, recycle, overhaul	A general description of remanufacturing, in line with the definition used in this research is documented in this instance. The use of overhaul to describe remanufacturing is also discussed. However, the authors do not clearly separate refurbishing from remanufacturing. That is, remanufacture products are said to containing refurbished parts within this text. It is also the case, that reuse is defined as reusing directly and recycle is defined as with the definitions presented in this work.
(Zuidwijk and Krikke, 2008)	Production engineering (Eco design methods)	Remanufacture and recycle	The authors in this instance cite EU directives to state what is meant by recycling. It is also the case that remanufacturing is also defined tenuously as, "the recovery of components and products into „as good as new" condition"

Table 4 - Identifies some of the different ways in which EOL terms are discussed within literature. Adapted from (Paterson et al., 2016)

It will also be shown in the course of this research that remanufacturing is routinely classed as a subset of recycling in the CFRP re-use industry. Looking now at the practices and definitions presented in this work, these definitions are formed from various sources within literature, (Gray and Charter, 2007; Ijomah, 2002; Ijomah et al., 2007, 2005, 2004; King et al., 2006; Parker, 2010). Critically however, all definitions of practices presented in this work are in keeping with the standards adopted by the British Government (BS 8887-2, 2009). The British Standard definition was selected for various reasons, 1) the definition is the official definition as adopted by British Government, 2) the research was conducted at the University of Strathclyde, Glasgow, United Kingdom and 3) the BSI agrees for the large part with wider remanufacturing definitions offered by powerful institutions, such as the United States Government – Federal repair cost savings act of 2015 (Federal Act, 2015) and with the European Union Action Plan for the Circular Economy (European Action Plan, 2015).

Looking now at the definitions of practices in keeping with (BS 8887-2, 2009) standards, noting that BSI definitions are not quoted directly, using the references cited, including the BSI, the definitions of terminology are better able to be discussed

and explained more thoroughly. Note additionally, with a belief structure adhering to realism, these definitions of practices are thus taken as absolute.

3.1.1 Remanufacture

A definition from literature is given as,

> *„remanufacturing is the only end of life process where used products are brought at least to Original Equipment Manufacturer (OEM) performance specification from the customer"s perspective and at the same time, are given warranties that are equal to those of equivalent new products"* (Ijomah, 2002)

Digging deeper into what constitutes remanufactured product, the product must have a core, which can be disassembled. The constituent parts of the core are then cleaned, examined, and tested. Each part is either replaced with a part, which meets the original product performance specification, or is restored to a condition at least meeting the original specification of the product. The disassembled product is then tested, and then reassembled and tested again. Once successfully remanufactured, the product is issued with a warranty equal or better than the original product. The processes involved in remanufacturing (BS 8887-2, 2009; Ijomah, 2002; Ijomah et al., 2007; King et al., 2006; Nasr and Thurston, 2006; Paterson et al., 2017, 2016; Sundin, 2004; Sundin et al., 2009) are given in Figure 3

Note also, the concept of core. The term product and core is sometimes used interchangeably, for instance, Sundin (2004) and Wei (2014) define the product as a core. This work states the product has to have a core, in that the core can be thought of as resulting from various parts or components undergoing a modular manufacturing assembly process, such that the resulting product (now a core) is able to be disassembled. Note further, in order to undergo a remanufacturing process, the core should be an assembly of various parts or components. That is, if only a single non-assembled item in isolation was restored back to as new condition, this would be classed as product or component restoration only. Remanufacturing is a process which involves component restoration, but is applicable to assembled products.

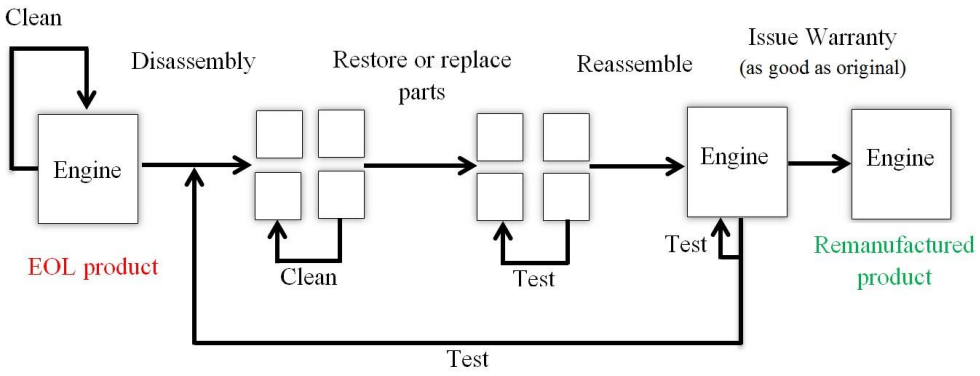

Figure 3 – Standard remanufacturing process. *Reprinted with permission from Paterson, D.A.P., Ijomah, W., Windmill, J., 2016. An analysis of end-of-life terminology in the carbon fiber reinforced plastic industry. Int. J. Sustain. Eng. 9, 130–140. doi:10.1080/19397038.2015.1136361*

The remanufacturing definitions offered in the aforementioned American Federal cost savings act of 2015 (Federal Act, 2015) and in the European Union Action Plan for the Circular Economy (European Action Plan, 2015) are given below.

The federal repair cost savings act defines a remanufactured vehicle component as,

"vehicle component (including an engine, transmission, alternator, starter, turbocharger, steering, or suspension component) that has been returned to same-asnew, or better, condition and performance by a standardized industrial process that
incorporates technical specifications (including engineering, quality, and testing standards) to yield fully warranted products"

The European Union Action Plan for a circular economy describes remanufacturing as

"A series of manufacturing steps acting on an end-of-life part or product in order to return it to like-new or better performance, with corresponding warranty"

The close relationship to the accepted definition used in this research is able to be observed.

3.1.2 Recondition

Reconditioning is a similar process to remanufacturing. There are however, subtle differences which relate to the amount of labour effort and product performance.

Similar to remanufacturing, reconditioning involves taking a product and restoring / replacing all components parts which have failed or are on the verge of failure. In reconditioning, the product is returned to a condition which may be regarded as an acceptable standard – generally parts are not returned to the original specification. Further, any warranties issued for reconditioned products are typically less than a warranty given to a virgin product or indeed a remanufactured product. In terms of labour content recondition involves less work than remanufacture, in terms of performance quality a reconditioned product is lower than a remanufactured product. Further reading may be found from (BS 8887-2, 2009; Ijomah, 2002; King et al., 2006).

3.1.3 Repair

Considering a product, such as motor vehicle, it can be said that over time various parts of the product may degrade or cease working all together. Repairing a product, concerns only the correction of a specific fault, and not does provide a restoration of the product in a global sense, the same way in which remanufacture or to a less extent recondition does. That is, for a given a fault within a product, if an operation has been conducted to correct that fault only, then product is said to have been repaired. In terms of product quality, almost certainly all repaired products are not restored to the original performance standard and any guarantee issued to the product, will in general only cover the corrected fault. Repairing a product requires less work than both recondition and remanufacture and the quality of the product is less than recondition and remanufacture.

Reinforcing the difference in labour content and product performance between a remanufactured, reconditioned and repaired product, Table 5 is presented.

Level of effort	Level of labour involved	Quality of warranty given	Product performance
Greatest	Remanufacture	Remanufacture	Remanufacture
Neither greatest or least	Recondition	Recondition	Recondition
Least	Repair	Repair	Repair

Table 5 – Documenting the difference between strategies in terms of labour, performance and warranty *Reprinted with permission from Paterson, D.A.P., Ijomah, W., Windmill, J., 2016. An analysis of end-of-life terminology in the carbon fiber reinforced plastic industry. Int. J. Sustain.*

3.1.4 Re-use

Re-using a product is the process of taking the EOL product and using it again for the same purpose. Product re-use may also be used in a generic way and act as a collective noun for the EOL strategies, however, to alleviate confusion this usage is general not taken within this thesis.

Noting that re-use is defined in the (BS 8887-2, 2009) is in accordance with the 2003 version of the WEEE directive, (European Parliament and Council, 2003). The modern WEEE directive, (European Parliament and Council, 2012) defines reuse in accordance with the WF directive, (European Parliament and Council, 2008) and noting that the definition of re-use in WF directive (European Parliament and Council, 2008), is consistent with the definition in the 2003 WEEE directive, (European Parliament and Council, 2003), then moving forward the term re-use may be defined from either (BS 8887-2, 2009) or (European Parliament and Council,
2008) and can be cited directly as

„re-use" means any operation by which products or components that are not waste are used again for the same purpose for which they were conceived;

Note additionally, that (European Parliament and Council, 2003) defines waste in accordance with (Council of The European Communities, 1975). However, similar to the last argument, the 2008 WF directive, (European Parliament and Council, 2008), is in keeping with the 1975, (Council of The European Communities, 1975) definition of waste and so the (European Parliament and Council, 2008) definition of waste is used within this research; Noting that waste may be thought of as a product or substance which the owner intends to, or is required to, discard.

3.1.5 Recycle

Recycling may be thought of as processing waste materials in a physical-chemical sense into materials which may be used again either for the same purpose or for a different purpose. A key aspect of recycling, and what sets recycling aside from repair, re-use, recondition and remanufacture is the structure of the original EOL product has been lost. That is, emergy - the amount of energy expired to create the product from raw materials, is lost. During the recycled process materials are returned to raw material format and may be used again to manufacture new products.

Similar to re-use, (BS 8887-2, 2009) defines recycling in accordance with the 2003 version of the WEEE directive, (European Parliament and Council, 2003) and with the updated 2012 WEEE directive, (European Parliament and Council, 2012). Also, the 2008 WF directive, (European Parliament and Council, 2008), defines recycling in accordance with the 2003 WEEE directive, (European Parliament and Council, 2003), and so recycling as defined in this research is in keeping with (BS 8887-2, 2009), (European Parliament and Council, 2012) and with, (European Parliament and Council, 2008). Note that for (European Parliament and Council, 2012) and (BS 8887-2, 2009) a process excluded from recycling is identified as being the incineration of waste with energy recovery or the energy recovery through the controlled combustion of waste.

Figure 4 outlines the recycling life cycle option for EOL products, which is similar to a collective EOL life cycle diagram found within the (BS 8887-2, 2009).

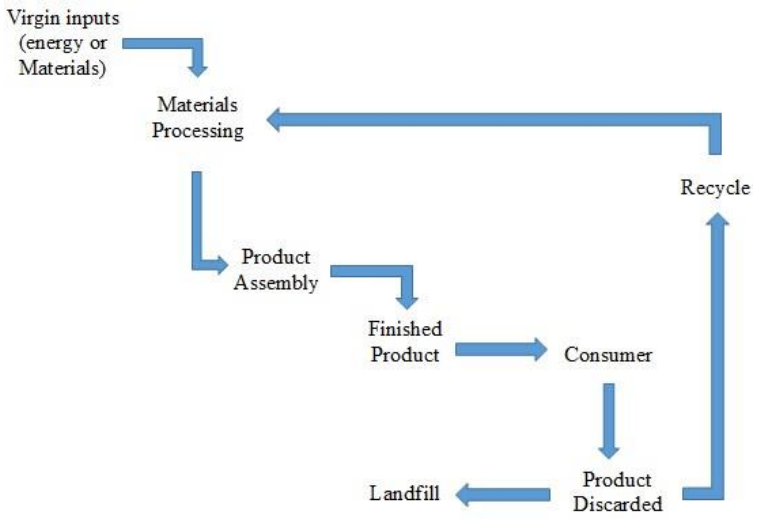

Figure 4 _ Recycle life cycle option, *Reprinted with permission from Paterson, D.A.P., Ijomah, W., Windmill, J., 2016. An analysis of end-of-life terminology in the carbon fiber reinforced plastic industry. Int. J. Sustain. Eng. 9, 130_140. doi:10.1080/19397038.2015.1136361*

Key definitions of EOL strategies discussed in this thesis have now been identified and explained. Moving forward, these practices are discussed freely without acknowledgement or excessive reference to this chapter. Note however, licence is taken to discuss additional processes, practices or strategies should the need arise. Moving forward the general concept behind composite materials is presented.

3.1.6 Additional Terminology

Additional terminology can also be found within the existing literature, which includes recovery, repurpose, and refurbish.

Recovery

Recovery can be thought of as a collective noun for the re-process discussed thus far. In terms of (BS 8887-2, 2009) and EU directives such as the WF directive, recovery is any operation where waste is transformed into a useful material which may be used to replace other materials or components. Given the broad usage of recovery, for example all re-process may be classed as recovery, recovery is used generically within this thesis. Explicit recovery terminology from EU directives is developed in chapter 4, when seeking to identify more accurate terminology for products manufactured by industry and academia.

Repurpose

Repurpose is effectively re-use with the subtle distinction of re-purposed end-of-life components or products being used in a different role than they were original designed for. For the purposes of this thesis, the subtle distinction between repurpose and re-use is overlooked.

Refurbish

In terms of (BS 8887-2, 2009), no distinction is made between refurbish and recondition. This thesis favours recondition terminology.

3.2 Carbon Fibre Reinforced Plastic (CFRP)

Prior to examining the market for CFRP products and the terminology surrounding CFRP, carbon fibre and CFRP itself are first briefly discussed.

3.2.1 Carbon fibres

Carbon fibres manufactured as a result of taking a pre-cursor, typically Polyacrylonitrile (PAN), but also pitch, and subjecting it to a manufacturing process designed to both extract elements and strengthen the carbon structure of the precursor. Morgan (2005) outline the typical stages involved in the carbon fibre production process.

The first stage in the manufacturing process is to perform oxidization. At this stage, to stabilize the PAN subject to carbonization, the PAN is subject to oxidation via a series of controlled heat treatments. The density of the PAN fibre will increase at this point. Next the PAN fibre is subject to carbonization. Carbonization is the process of extracting elements such as water (H_2O), carbon dioxide (CO_2), ammonia (NH_3), and sodium (Na). Carbonization, which can consist of both low and high temperature, is again performed via a series of complicated heat treatments and also by using Nitrogen (N_2) to help remove unwanted elements.

The next optional stage, to ensure a high modulus fibre, is performed via a process of graphitization. Graphitization is again a heat process designed to improve the crystallite orientation of the fibres. Moving on, the fibres are given a surface treatment. This treatment which may encourage matrix bonding is performed in a variety of ways,

with a typical approach being an electrolytic process – the output of which results in adding some oxygen atoms to the surface of the fibres. Finally the fibres may be dipped in a sizing solution to encourage fibre alignment, matrix adhesion and fibre protection. Figure 5 is given to reinforce the carbon fibre manufacturing process.

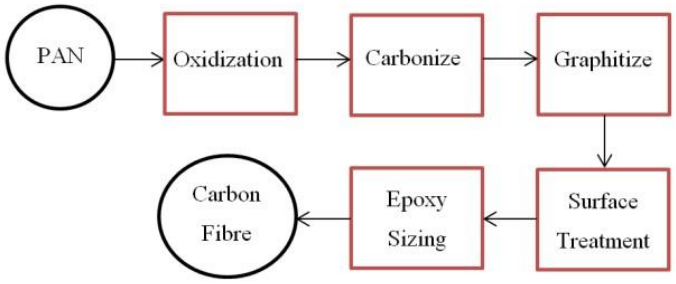

Figure 5 – Simplified Carbon fibre manufacturing process from precursor

3.2.1 Carbon fibre reinforced plastic

CFRP is a composite product of carbon fibres which reinforced with, typically, thermoset and thermoplastic resins, such as Polyester, Epoxide, Polyamide, Polycarbonate, Epoxy Vinyl Ester and Polyetheretherketone (Morgan, 2005). The principal behind CFRP is that a matrix element (the thermoset or thermoplastic resin) is used to provide a rigid structure for the carbon fibres. Both matrix and element work together to produce a composite material, which offers premium qualities and significant strength to weight ratio.

Further, as with the varying matrix elements which can be used to determine the epoxy resin, by exploiting the direction of the fibres there are a variety of different ways in which CFRP can be designed, in terms of fibre architecture. For instance, CFRP may be designed to be quasi-isotropic, unidirectional, cross ply etc. This thesis investigates CFRP which is unidirectional in nature and to a lesser extent CFRP which is quasi-isotropic in nature. As such Figure 6 a) and b) are given to reinforce the concept of unidirectional and quasi-isotropic CFRP.

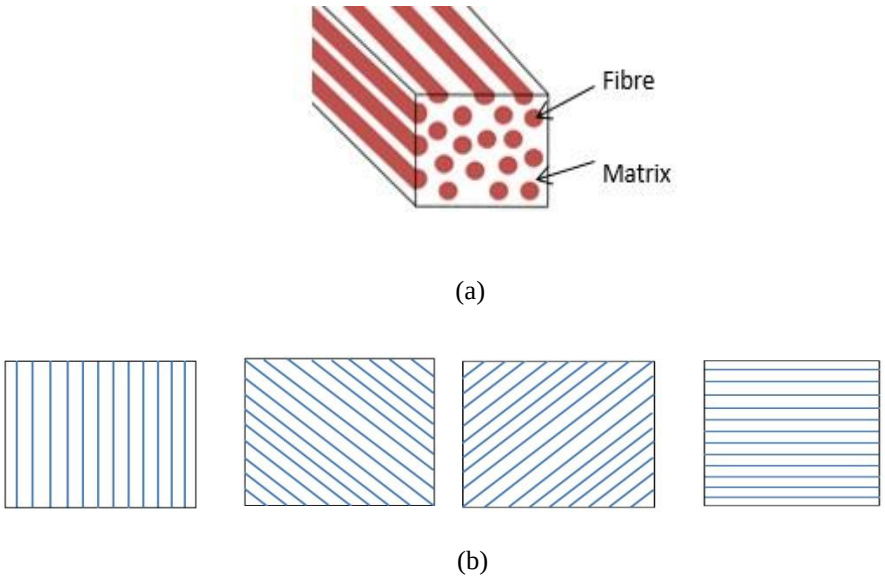

Figure 6 –Hypothetical Layers of carbon fibre at 0, -45, 45 and 90 degrees. For a layup of [0,-45,45,90]s these layers are layered [0,-45,45,90,90,45,-45,0]

It is also of merit to mention that in the direction of the fibres, higher strength and stiffness are obtained when compared to directions transverse to fibre direction. Thus, the selection of fibre architecture is often dictated by the load the CFRP will be subjected to, hence, a wide variety of various fibre architectures are commonly used. Further still, fibre architectures also adhere to various symmetry classes. The CFRP under investigation in this thesis, i.e. unidirectional and quasi-isotropic, adhere to hexagonal symmetry (or in some cases orthotropic symmetry) and isotropic symmetry.

Chapter 4: Analysis of terminology in regards to EOL CFRP

4.1 CFRP market and why the desire to recycle and remanufacture

4.1.1 CFRP market

A particularly good source for information on the global and regional size of the composite market is the annual composites market report, commissioned by the Federation of Reinforced Plastics (AVK) and Carbon Composites e.V. (CCeV). The section of the report of most interest in this thesis is the market study conducted on CFRP by CCeV, which henceforth, is referenced as, Kraus and Kuhnel (2015). Prior to the findings, a brief history on CCeV is presented. CCeV is a collection of research institutions and companies (which at the time of review had 272 members) involved in the product, manufacture, distribution and sales of fibre composites. Kraus and Kuhnel (2015) additionally point out that approximately 63% (by consumption) of the 2014 global production of carbon fibre originated from, the SGL group – the carbon company, Toray, TohoTenax, Cytec and Hexal; all of which are members of CCeV.

Looking now at the CF and CFRP market, key information relating to the size of the global market in both global financial terms and tonnage terms can be established (Kraus and Kühnel, 2015). In 2014, the market tonnage of CF increased to 200% of 2009 levels with the demand further expected to rise with the 2021 global tonnage expected to increase by approximately 120% of 2014 levels. Noting that the global turn over for CF achieved in 2014 was recorded as approximately 1.98 billion US dollars. Regarding CFRP, the market tonnage of CFRP increased to approximately 200% of 2009 levels in 2014 with an expected increase of 110% than 2014 levels in 2021. Note that the CFRP revenue in 2014 was 10.6 billion US dollars. This information is presented as Tables 6 and 7.

CF global demand (in tonnes)	
2009	27,000
2010	33,000
2011	39,000
2012	44,000
2013	47,000
2014	53,000
2015 (estimated)	58,000
2016 (estimated)	65,000

2021 (estimated)	116,000

Table 6 – Global demand (tonnes) for CF between the years 2009 and 2021

CFRP global demand (in tonnes)	
2009	41,000
2010	51,000
2011	59,000
2012	66,000
2013	72,000
2014	83,000
2015 (estimated)	91,000
2016 (estimated)	101,000
2021 (estimated)	175,000

Table 7 - Global demand (tonnes) for CFRP between the years 2009 and 2021

Looking now, at additional information relating to specific industries. The four largest markets for CF per tonnage are Aerospace and defence, automotive, wind turbines and sports and leisure. These market are also the largest in terms of specific turnover. Tables 8 and 9 provide tonnage and turnover figures respectively for CF.

Industry CF demand (in tonnes) for 2014		Market share
Aerospace and Defence	15,400	29%
Automotive	8,500	16%
Wind Turbines	7,400	14%
Sport and Leisure	6,400	12%
Moulding and Compound	5,800	11%
Pressure Vessels	2,700	5%
Civil Engineering	2,300	4%
Marine	800	2%
Others	3,700	7%

Table 8 – Industry specific demand for CF in tonnes during 2014

CF Industry specific turnover (US millions Dollars) for 2014		Market share
Aerospace and Defence	950.4	48%
Automotive	217.8	11%
Wind Turbines	205.9	10%
Sport and Leisure	170.3	9%
Moulding and Compound	142.6	7%
Pressure Vessels	79.2	4%
Civil Engineering	75.2	4%
Marine	19.8	1%
Others	118.8	6%

Table 9 - Industry specific turnover for CF in US million dollars during 2014

Kraus and Kuhnel (2015) also provide insight onto the industry specific demand and market for carbon composites (CC) in general. This information is presented as Table 10 and Table 11.

Industry CC demand (in tonnes) for 2014		Market share
Aerospace and Defence	32,200	31%
Automotive	21,800	21%
Wind Turbines	13,200	14%
Sport and Leisure	13,200	12%
Civil Engineering	5,000	11%
Marine	1,400	5%
Others	18,500	4%

Table 10 – Industry specific demand for CC in tonnes during 2014

CC Industry specific turnover (US billion Dollars) for 2014		Market share
Aerospace and Defence	10.2	62%
Automotive	1.9	11%
Wind Turbines	1.3	8%
Sport and Leisure	1.2	7%
Civil Engineering	0.4	2%
Marine	0.1	1%
Others	1.5	9%

Table 11 - Industry specific turnover for CF in US million dollars during 2014

The main industries involved in the manufacture of CF and CFRP have been identified. Key findings in relation to the global turnover of CF and CC alongside industry specific turnover for CF and CC have also been identified. Additionally, the manufacture of CF and CFRP has been shown to rise each year from 2009 and global forecast figures for both CF and CFRP production (in terms of tonnage) have been presented.

With the manufacture of CF, CFRP and CC having shown to be increasing year on year, it is appropriate to now examine additional rationale as to why CFRP is considered for recycle and remanufacture.

4.1.2 Why recycle and remanufacture CFRP

A principal reason supporting the need to recycle and remanufacture CFRP is the cost associated with manufacturing new CF when compared to the cost of obtaining CF through the recycling process. Boeing, (Carberry, 2008), who have developed the 787 Dreamliner (which is around 50% composite material), state that the energy required to create v-CF ranges from 25-75 Kwh/lb at a cost of 15-30 US dollars/lb while the energy required to produce CF through recycling consumes 1.3-4.5 kWh/lb at a cost of 8-12 US dollars/lb. Thus, potential savings of approximately 82% - 98% in terms of energy and approximately 50% – 70% in terms of cost may be made. It is also the case that owing to superior composite strength to weight ratio, aviation fuel efficiency is increased (Lewis, 2014). Additional information on Boeing, and equally the Airbus, recycling programmes is documented in section 3.3. Further research on the environmental / energy consumption analysis concerning reusing CF and CFRP, and CF and CFRP in general may be found within literature (Howarth et al., 2014; Song et al., 2009; Suzuki and Takahashi, 2005; Witik et al., 2013).

It is also the case that with the growing demand for CF and CFRP, and composite in general, there follows an accumulation of waste materials, McConnell (2010) states that in 2010 the USA and Europe were producing around 3000 tonnes of CFRP scrap each year. As stated previously, to tackle this form of waste, and waste in general (OECD countries recorded around 670 million tonnes annually during the period 2007 – 2003 (OECD, 2015)), the EU has passed various waste related directives that can impact on carbon fibre and CFRP, in a variety of ways. Examining this, consider the WF directive, (European Parliament and Council, 2008), article 4 point 1, which states a hierarchal system for dealing with waste to ensure an optimum environmental outcome, the hierarchy given is given as 1) prevention, 2) preparing for re-use, 3) recycling, 4) other recover and lastly 5) disposal. Note however, the WF directive allows member states to possibly deviate from the said hierarchy to accommodate a better environmental solution. The ELV directive (European Parliament and Council, 2000a), is also designed to tackle waste - noting the estimated 7-8 million tonnes of EOL vehicles scrap generated within the EU each year (EU, 2017). Article 7 point 2(b) of the directive states that as of 2015, recovery and re-use of EOL vehicles should reach 95% by vehicle and year and that re-use and recycling should meet at least 85% per vehicle and year.

Other directives include the WEEE directive (European Parliament and Council, 2012). The WEEE directive aims to divert and separate WEEE from other waste streams and provide quotas on collection rates; For example, article 7 point 1 states that from 2019 onward, the minimum amount of WEEE collected shall be either 65% of the average weight of the amount of electrical and electronic equipment that has been placed onto the market in the 3 years that proceeded the given year of collection or be 85% of the amount of WEEE generated within the territory of the member state. The incineration of waste directive (European Parliament and Council, 2000b), the waste shipment regulation directive (European Parliament and Council, 2006) and the integrated pollution and control directive (European Parliament And The Council, 2008) also impact composite and CFRP at various stages of their life cycle. For this research, the main directives affecting the recycling of composite can be said to be the WF directive, the ELV directive and the

WEEE directive.

Economic, environmental and legislative rationale as to why research focusing on the recycling and remanufacture of CF and CFRP having now been documented, prior to examining the industrial and academic efforts to recycle and remanufacture CF and CFRP, it is appropriate at this stage to analyse the importance of the using the correct terminology to describe processes carried out.

4.2 The importance of correct terminology

It may be argued that a regular incorrect application of EOL terminology has the potential to allow confusion to creep into the mind of researchers and consumers. This confusion may not appear to be significant when discussing consumables, but if the product has an impact on one‟s life then confusion can lead to dangerous territory. For example, if we consider a pair of shoes and apply a EOL process such as repair, recondition or remanufacture; one could argue that even if doubt existed over the quality of shoes (see Table 5 which equates typical product performance to EOL process) it may not be considered a deal breaker for the customer. However, would the same customer be so eager to embark on a long distance car journey using tyres, seatbelts, airbags, engines etc. that may be operating at a level beneath full capability? This situation highlights a real danger of an incorrect application of EOL terminology; if recondition or remanufacture are used to describe repaired or recycled products the

belief that remanufactured or reconditioned products are at the same level of quality as repaired or recycled products could begin to take root.

Furthermore, incorrect EOL terminology reduces the potential for effective research (difficulty in collecting appropriate research samples, information and information source) and dialogue within the industry as well as between the industry and key stakeholders (e.g. customers).

Looking specifically now at the importance of remanufacture, it is a generally considered principle that the public does not fully embrace remanufactured products as it does new products with (Abbey et al., 2015, 2014; Hamzaoui-Essoussi and Linton, 2014; Watson, 2009) presenting discussion on this. Reasons such as price, brand quality and potential prior ownership all play a role in consumer decision making in relation purchasing a remanufactured product. Further, these reasons tend to be complex, for example, the concept of a remanufactured product being cheaper in price than a new product may cause one customer to purchase it, but another to assume the quality is less than a new model and refrain from purchasing the remanufactured product. In addition, the rationale to purchase remanufactured goods can change from one product to the next or from one location to the next. Further, Hazen (2012) found that ambiguity in the definition/description of the remanufacturing process can influence the decision regarding the quality of a remanufactured product.

If the benefits of remanufacture are taken into account, benefits which include increased energy savings, increased employment opportunities, failure information fed back to manufactures and cheaper supply of products (Giuntini and Gaudette, 2003; Lund and Hauser, 2010), then getting the public to engage with remanufactured goods is obviously desirable. Hence, in the case of remanufacture, applying the term correctly should a) allow for an increase in remanufacturing, b) allow for a decrease in confusion, c) help reinforce the concept that the quality of a remanufactured product is always at least equal to the original and d) enable consistency in standards and quality thus increasing the difficulty for unscrupulous practitioners to pass off substandard products as genuine remanufactured products. There is also a potential legislative need to properly define remanufacture; a report produced by the High Speed Sustainable Manufacturing Institute (HSSMI), the Carbon Trust, the Centre for Remanufacturing and Reuse (CRR) and the Knowledge Transfer Network, (Smith-Gillespie et al., 2015), investigated the opportunities and challenges to remanufacturing in the UK and found that current legislation and taxation was not geared towards encouraging organizations to remanufacture. As such, it can be said

that any potential future incentives to encourage remanufacturing could only be available to organizations that actually perform true remanufacturing. It is also the case that an incorrect/ambiguous definition can lead to difficulties in gauging the industry; Lund and Hauser (2010) state that when the American remanufacturing industry was gauged in a previous paper, (Lund, 1996) its size was dramatically over estimated. This over estimation was caused by relying on information from membership lists of trade associations, where high numbers of members were only conducting remanufacturing by a very liberal definition - the definition to describe remanufacture did not separate remanufacture from recondition and so reconditioners were counted alongside remanufactures. It was also the case that the directors of these trade associations provided too high an estimate of remanufactures in their sector but outside of their membership.

Staying with the theme of misrepresenting the true remanufacturing industry and looking specifically at CFRP, in their examination of the environmental benefits of CFRP recycling against incineration and landfilling Witik (2013) advised that future work associated with the remanufacturing of CFRP should provide data on energy requirements, the resources used, waste produced and the emissions generated. If the incorrect EOL terminology is used (for example remanufacture) the environmental benefits associated with a particular strategy, could actually be environmental benefits associated with another EOL strategy. Looking now at the importance of defining recycle and other EOL terms correctly, justification can be found in the fact that terms such as recycle, re-use, reuse, recovery, waste etc., are routinely discussed in directives and legislation. It has already been noted that in the WF directive article 4 point 1) provides the waste hierarchy, which should be adopted by member states when dealing with waste, noting again that recycle, re-use and disposal occur throughout and that the same argument can be made looking again at the ELV directive. Thus, it is readily apparent that using terminology such as re-use, recovery, recycle and disposal correctly would allow companies or organizations to better comply with both existing and any new directives issued.

Additionally, if consulted to take part in discussions to create new directives or the national legislation that arise from these directives, applying EOL terminology correctly allows organizations to represent their practices and viewpoints more accurately. To exemplify this consider Witik (2013), who state that the WF waste hierarchy is only to be considered a good rule of thumb when dealing with CFRP. If a future strategy for CFRP waste management was conceived, noting that at present

CFRP does not have a specific directive but instead is regarded generally as waste or vehicle component, then a proper definition of terminology is called for, thus strengthening the case that practices, terminology and products are required to be defined correctly.

Having now documented the CF and CFRP market, identified the economic, environmental and legislative reasons for remanufacturing and recycling along with putting forward the importance and benefit of correct terminology, i.e. decreasing remanufacturing ambiguity, increasing remanufacturing awareness, better compliance with existing and new legislation, promoting more accurate data sets and dialogue within the industry the industrial and academic efforts to recycle and remanufacture CFRP are presented.

4.3 Industrial and academic efforts to recycle and remanufacture

Within academia much literature, including wide ranging literature reviews, concerning operations denoted as recycling and remanufacturing of CFRP, and composite in general – in particular glass composite, are able be found (Asmatulu et al., 2013; Goodship, 2010; Meredith et al., 2012; Morin et al., 2012; Oliveux et al., 2015; Perry et al., 2012; Pickering, 2006; Pimenta and Pinho, 2012, 2011; Rybicka et al., 2014; Shi et al., 2012a, 2012b; Snudden et al., 2014; Yang et al., 2012). As this research does not aim to provide an in depth market analysis (although industry engagement will be discussed), or discuss the pros and cons of the various recycling processes found in industry or indeed the pros and cons of the products arising from these processes, there was little merit in repeating the work already conducted by the researchers outlined above, thus, attention may be turned to the available literature for this information.

A more practical option, geared towards answering the first research question, is to review the literature with the intention of identifying the practices which are denoted in these works are recycling and remanufacturing, with the view of ultimately then reviewing these practices against the definitions presented in chapter 2.

Considering first recycling operations, within the literature identified, it is the case that in general two different types of recycling, which are quite distinct from each other, are able to be observed. The first type of recycling is classed as mechanical

recycling, with the second form of recycling being classed as fibre reclamation. Furthermore within the header of fibre reclamation, generally two distinction strategies are also observed, heat treatment and chemical treatment.

Looking first at mechanical recycling, mechanical recycling involves taking CFRP and performing techniques such as grinding, crushing and milling. Once the CFRP is crushed, milled and ground, the segregation of the fibres and the resin can take place. Noting here that owing to structure of the fibres and possible inclusion of trace elements of resin, after mechanical recycling the amount of pure carbon materials produced may be not be as high as the original fibres. Typical applications for mechanical recycled CFRP include use as filler or for resin reinforcement in new composites. Figure 7 is presented to provide, as best can be, a general mechanical recycling process.

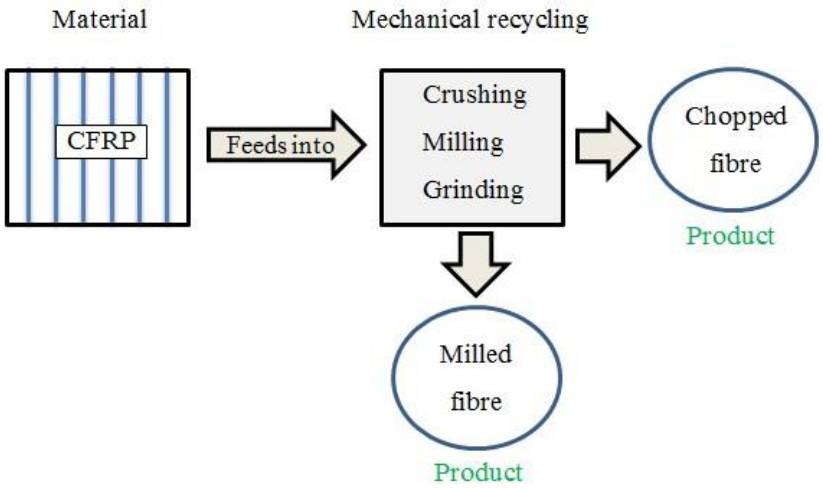

Figure 7 - Mechanical recycling of carbon fibre

An important point able to be made concerning mechanical recycling is that mechanical recycling does not allow in general, considering the severity of the recycling process, for the original VF part of the CFRP to be reclaimed in its original form; thus future mechanical tests have to be conducted on the composite level. Note that the composite mechanical behaviour using fibres obtained through mechanical recycling is in general complex, that is, the fibre fragments produced through mechanical recycling suffer from significant fibre breakage and a random fibre arrangement. (Ogi et al., 2007; Okayasu et al., 2013; Oliveux et al., 2015) document

the process of taking crushed CFRP and mixed this with acrylonitrile butadiene styrene (ABS) resin to create new CFRP.

Further, to give an idea of the scale of the crushing, milling and grinding, Ogi (2007) crush 3.4 x 0.4mm^2 pieces of virgin CFRP with the resulting average fibre length resulting from this process is around 200 µm, which is significantly smaller than the original fibres which measure the length of the surface of the sample, Pickering (2006) also identify that particles of 50 µm are able to be produced. Alongside random fibre arrangement and fibre length, fibre volume may also play a role in the composite properties. That is, implanting chopped and powered fibres that include trace elements of resin, with new resin, will in general record a lower volume of fibre content than the original. Attention may be turned to Pimenta and Pinho

(2011) for discussion on this.

Looking now at fibre reclamation, unlike mechanical recycling, this seeks to recover the fibres from CFRP by means of thermal and chemical processes - these processes seek to destroy the matrix (noting that energy or molecules from the matrix can potentially be recovered). Within literature a number of options have been outlined that can facilitate fibre reclamation, namely pyrolysis, oxidation in a fluidised bed and chemical recycling – noting that pyrolysis and oxidation in a fluidised bed may be regarded as heat treatment.

Looking first at pyrolysis, pyrolysis involves subjecting the CFRP to heat, Meyer (2009) documented temperatures of 700^{o}C, 900^{o}C, 1100^{o}C and 1300^{o}C, sometimes in the absence of oxygen. During the pyrolysis the matrix element breaks down and leaving the typically, non-combustible fibres and fillers to emerge from the process, (Pickering, 2006). Further, depending on the particular pyrolysis process, i.e. combination of temperature and length of time under that temperature, the sophistication of the process and aspects such as laboratory and commercial pyrolysis processes, the resulting fibres and fillers which emerge from the pyrolysis process do so with a complex mixture of properties (Pimenta and Pinho, 2012). Additionally, during the pyrolysis process, a solid carbon product, char, is generated and may also be attached to the fibres. It is also the case that during the pyrolysis process, potential also exists to reuse expelled gases to help further power the same pyrolysis process. A simplified example of the pyrolysis process is given in Figure 8.

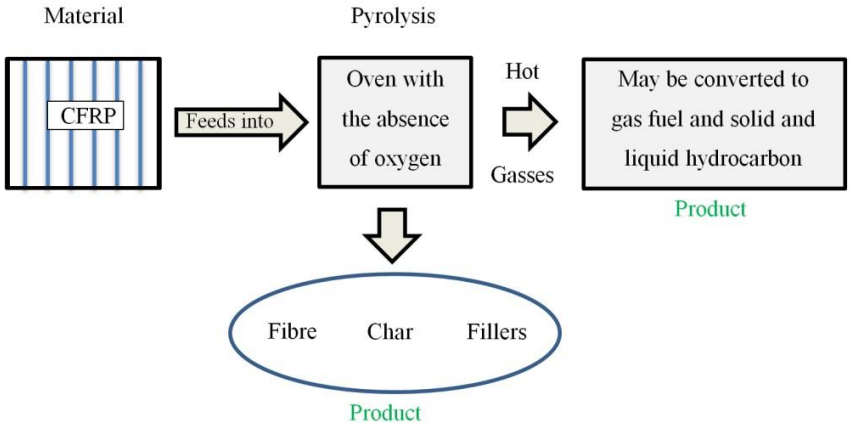

Figure 8 – Simplified pyrolysis process for CFRP

Moving forward, the second fibre reclamation technique and also the second thermal technique, is the oxidation in a fluidised bed approach. Spearheaded by the researchers at the University of Nottingham, the oxidation in the fluidised bed approach takes CFRP scrap (around 25 mm in size) and lays it on a bed of silica sand, which is itself on a metal mesh. The bed is subjected to hot steam (around 450550 °C) and so becomes fluidised. During this process, CFRP, and equally glass composite, begins to decompose in that the polymer matrix volatises from the composite so the fibres and fillers are separated from polymer (Pickering, 2006).

Subsequently, the fibres and oxidised molecules are carried in the airflow with a cyclone used to separate the fibres from the airflow. Similar to pyrolysis the energy of the matrix is recoverable - the resin is fully oxidised in an afterburner to allow for this. The received fibres emerge with a generally fluffy form with a mean length of 6-8 mm with very little surface contamination (Pickering, 2006). A simplified version of the oxidation in a fluidised bed approach is given in Figure 9.

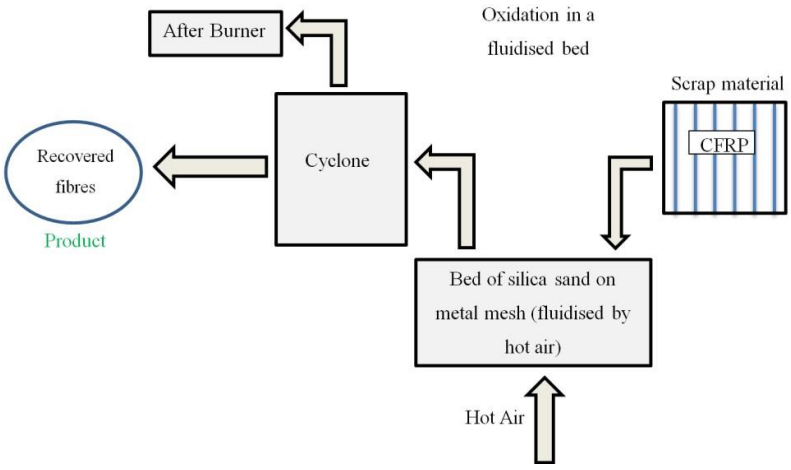

Figure 9 – Oxidation in a fluidised bed

An additional fibre reclamation process discussed with literature, which does not fall under mechanical recycling or thermal based recycling, is chemical recycling. Chemical treatment is the general name for the process of exposing a composite to a reactive medium, such as supercritical fluids or catalytic solutions, generally under low temperature conditions (<350 °C). The chemical recycling process causes monomers, which are the building blocks of polymers to form groups known as oligomers, noting that the creation of these oligomers leads to the separation of matrix and fibres, allowing the fibres to be collected. Many chemicals solutions exist which can facilitate chemical recycling and it is also the case that the energy from the matrix is also recoverable using chemical recycling. Attention may be drawn to literature already cited in section 4.3 for further reading.

The three main composite recycling processes discussed in literature have now been documented, i.e. the mechanical recycling process, the thermal recycling process and the chemical recycling process. Additionally, two collective nouns for these processes were also put forward, i.e. mechanical based recycling and fibre reclamation based recycling. Note further, outside of mechanical based and fibre reclamation based recycling, terminology also appears in literature as a way to re-use (almost directly) CFRP. Asmatulu (2013) state that an approach labelled as „direct structural composite recycling" is where large EOL composite products are cut into smaller size sections, which can be used directly in smaller composite components. Prior to discussing industrial attempts to recycle and remanufacture composite, the instances of where academia use the terminology remanufacture or remanufacture is presented.

(Morin et al., 2012; Oliveux et al., 2017, 2015; Perry et al., 2012; Pimenta and Pinho, 2012, 2011, Shi et al., 2014, 2012a; Tian et al., 2017) all discuss using recycled carbon fibres (noting that recycled almost exclusively means fibre reclamation and not mechanically recycled CFRP) to generate new CFRP or as described in literature to re-manufacture CFRP. That is, reclaimed fibres are reimpregnated with new resin to re-manufacture new CFRP. Take Shi (2012a) for instance, who state when discussing fibres emerging from a recycling processes, "*It is possible to recycle fibre from FRP, and to remanufacture them into high-value RFRP for reuse"* (noting that FRP and R-FRP were previously defined in the particular paper as fibre reinforced plastic and recycled-fibre reinforced plastic. It is also often the case within the literature that remanufacture is labelled as a subset of recycling in that the remanufacturing process is part of the recycling process. For example, Pimenta and Pinho (2012) state that that

the process of reimpregnating reclaimed fibres with resin (dubbed composite remanufacture) is the second phase of the fibre reclamation stage (or recycling stage). Additionally, the term remanufacture has also been used within literature to describe the process of taking waste CFRP and performing splitting, hot and cold forming to mould the scrap CFRP into new shapes, with up to 50% of original mechanical properties maintained (Adams et al., 2014). Figure 10 presents a block diagram of the generic re-manufacturing process outlined within literature.

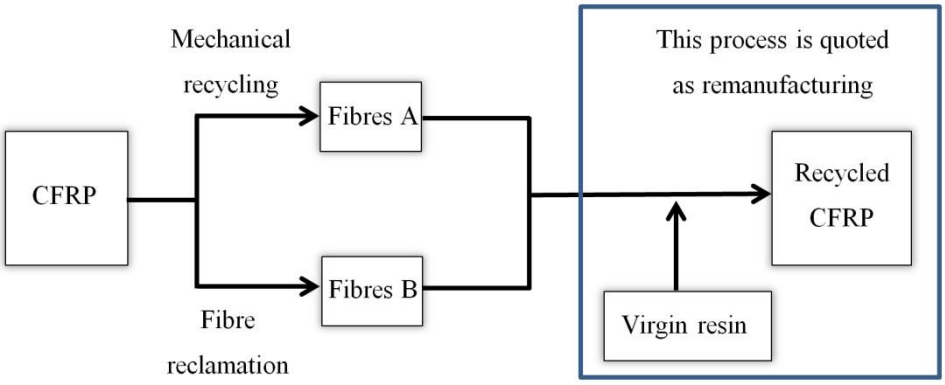

Figure 10 – CFRP remanufacturing process described within literature *Reprinted with permission from Paterson, D.A.P., Ijomah, W., Windmill, J., 2016. An analysis of end-of-life terminology in the carbon fiber reinforced plastic industry. Int. J. Sustain. Eng. 9, 130–140. doi:10.1080/19397038.2015.1136361*

Having now documented the academic strategies to recycle composite materials and identified the process of re impregnating fibres obtained via recycling, i.e. what academia refers to as the remanufacturing process, it is now appropriate to examine industrial efforts in this regard.

Looking first at AdTech International Incorporated, „Carbon Fibre Remanufacturing™“ (http://carbonfibreremanufacturing.com/) (CFR) – noting that AdTech International Incorporated date back to 1997 and have a raison d'etre of developing efficient solutions to the problem of excess material that is generated by industry and commerce. CFR state that they are a global leader in carbon fibre remanufacturing and were established to develop extensive recycling programmes for high-grade carbon fibre, carbon fibre that is currently in service across manufacturers of composites and aerospace companies globally.

CFR obtain the excess or scrap carbon fibres, including fibre from tow that has fallen off tubes at some stage, which are generated as part of the manufacturing process and once obtained, these fibres become designated as reclaimed fibres. CFR then perform

applications such as „detangling, milling and cutting" of these fibres, thus allowing them to be used again for industry specific applications. The fibres, now called remanufactured carbon fibres, are stated to have retained their virgin properties, are available at discount prices and have the ability to be used in construction of CFRP.

Interestingly the term recycle is also used by CFR; it is used when describing the overarching operation of what they perform, for example, a particular recycling programme offered by CFR includes providing remanufacture of carbon fibres. Particulars of CFR include a recycling capability of 130,000 lbs per month, 3 industrial scale warehouses (one at 60,000 square feet and two at 100,000 square feet) a 300,000 lbs per month detangling capacity, an overall precision cutting capacity of 280,000 lbs per month and a 60,000+ lbs per month yarn manufacturing capacity.

The second example is ELG Carbon Fibre limited, (http://www.elgcf.com/), noting here that the initial incarnation of the company dates back to 2003, and that they are similar to CFR in that they also seek to collect carbon fibre deemed as industry waste or scrap. ELG state that they are the world"s first commercial sized carbon fibre recycling plant and in 2015 they managed to recycle and reclaim over 1000 tonnes (of 2,200,000 lbs) of carbon fibre from dry fibre (similar to CFR), cured and uncured pre-preg and laminate materials.

On reception of scrap, or EOL carbon-composite, ELG state that the material is recycled into a new varied product line, which includes both milled fibre and chopped fibre. The recycling process stated by ELG, is effectively the pyrolysis thermal treatment discussed previously, that is, the collected EOL or waste composite is collected, shredded, put through pyrolysis and then chopped. Unlike CFR, ELG do not state that recycled carbon fibre approaches the qualities of the virgin counterparts.

Another example is Adherent Technologies Inc. (http://www.adherenttech.com/). Adherent, who clients include the likes of NASA, IBM, the United States, Army, Navy Air force and Defence Advanced Research Projects Agency (DARPA), Lockheed Martin, Honeywell, Raytheon, develop technologies to help solve demanding commercial material problems; one of these interests being the recycling of composite materials. Two key technologies put forward by Adherent are the Vacuum Cracking Process and the Wet Chemical Breakdown, noting that the Vacuum Cracking Process is effectively pyrolysis treatment previously discussed and the Wet Chemical Breakdown being a variety of chemical recycling previously discussed.

Looking now at the recycling programmes that Boeing and Airbus, the two largest aerospace companies in the world, are involved in. These recycling programmes are the Aircraft Fleet Recycling Association (AFRA) and the Process for Advanced Management of End of Life Aircraft (PAMELA) respectively.

Attention is first drawn to AFRA.

AFRA, (http://www.afraassociation.org/index.cfm) who were founded in 2006, are a global leader within the aircraft recycling industry and have approximately 70 members with years of aircraft recycling knowledge between them. Their members includes the likes of Adherent Technologies, Boeing, Bombardier, ELG, Embraer, KLM UK engineering, Rolls Royce, the University of Nottingham and many more. Through the grouping together of like-minded organizations, AFRA is able to offer accreditation in the areas of both aircraft disassembly and aircraft recycling. The AFRA Best Management Practices (BMP) guide is used to provide details of best practice for both disassembly and recycling, and thus is a way of helping companies to be best positioned to become accredited by AFRA. In relation to composite the BMP are for the recycler to separate materials, such as metals and carbon fibres, in-to a grade fine enough that using such materials as feed stock for a manufacturing process is possible.

With AFRA quoting approximately 12,000 aircraft are expected to be retired over the next two decades, environmental opportunities associated with EOL composites are able to be found. Carberry (2008) put forward that the 2 million pounds of carbon fibre scrap that was expected to be produced in 2014, from commercial jet manufacturing would be able to, if recovered and used in exchange for virgin fibre, provide energy savings to power 175,000 typical homes per annum. Looking now at the Airbus PAMELA programme, Airbus state that in 2005 they became the first aircraft manufacture to voluntarily launch a programme designed to tackle and solve issues that are associated with aircraft reaching permanent retirement. Supported by the European commission on launch, the PAMELA programme outlines best strategy on dealing with retired aircraft, the process governs storage, decommission, disassembly, dismantling and finally the recycling of materials along with proper management of waste that may be deemed as being potentially hazardous. Since the conception of PAMELA, Airbus subsequently expanded on the initial PAMELA programme and along with SITA France (a subsidiary of Suez Environment), Snecma (a subsidiary of the Safran

Group) and Equip‟aero Industrie formed a joint venture, the „Tarbes Advanced

Recycling and Maintenance Aircraft Company (TARMAC) Aerosave‟ (http://www.tarmacaerosave.aero/index.php?lang=en).

TARMAC Aerosave state that they are Europe‟s largest aircraft storage company (250 aircraft capability) and are a leading force in Europe within the field of storage, maintenance and recycling of aircraft in environmentally friendly manner. TARMAC Aerosave have expanded on the PAMELA programme and quote figures of recycling processes recovering 90% of the total weight of the aircraft.

Besides the TARMAC Aerosave programme, Airbus is also in collaboration with CFK-Valley Stade Recycling GmbH & Co KG, (http://www.cfk-recycling.com/index.php?id=57), with CFK-Valley performing fibre reclamation through pyrolysis for dry scrap CFRP, pre-preg CFRP and EOL CFRP products. Similar to the Boeing, Airbus also examines their carbon footprint when constructing new aircraft, and has partly done so in a somewhat strange but entirely relevant way using biological based research. Two locations on their Hamburg site (one location being in proximity of a paint shop with the other being in proximity of the runway used to cater for test flights of new jets) have bee hive colonies. The quality of the honey extracted from these colonies (Airbus quote that more than 600 jars of honey are produced each year) are representative of the environmental damage to the soil air and water over the 12 square kilometre area where the bees collect their pollen and nectar needed to produce the honey.

Other industrial efforts included the Cannon group‟s, in collaboration with EU, Carbon Fibre Recycling through Special Impregnation (CRESIM) programme (http://www.life-cresim.com/), this EU funded pilot project investigated CFRP recycling and applications for recycled CFRP. Additionally, Fraunhofer (www.fraunhofer.de/en.html), who are a large application-oriented research organization based in Europe have an Institute for Manufacturing Technology and Advanced Materials, which offers a remanufacturing course spanning 40 hours (approximately 1 week) and gives instructions on how to repair carbon fibre reinforced plastics.

Note also, further information on industrial recycle and remanufacture may be found from the composite recycling and remanufacturing literature previously cited and also from Heil (2011) who presents a similar analysis of the market.

Having now examined the academic and industrial attempts to recycle and remanufacture composite material, along with having also defined the terms recycled and remanufactured it is now appropriate to examine whether industry and academia are actually conducting recycling and remanufacturing as defined in this research. Table 12, presents a recap of terminology identified in this section.

Term / Theme	Operation
Mechanical recycling of CFRP	Crushing, grinding and milling of CFRP
Fibre reclamation-based recycling of CFRP	Removal of matrix via heat or chemical treatment, leaving the fibres largely intact
Re-manufacture	Implanting reclaimed or crushed fibres with new resin
Recycled CFRP	Name for the product created by conducting mechanical recycling or fibre reclamation and then impregnating fibres with new resin
Remanufactured fibres	Name given by CFR to virgin fibres, obtained as scrap or from excess via manufacturing processes, which have been detangled, milled and cut to create a usable product
Remanufacturing course	Name given by Fraunhofer to a CFRP repairing course offered
Remanufacturing subset of recycling	The remanufacture process is routinely thought of as a subset of the recycling process

Table 12 - Summary of the descriptions associated with recycling and remanufacturing terminology in the CFRP industry *Reprinted with permission from Paterson, D.A.P., Ijomah, W., Windmill, J., 2016. An analysis of end-of-life terminology in the carbon fiber reinforced plastic industry. Int. J. Sustain. Eng. 9, 130–140. doi:10.1080/19397038.2015.1136361*

4.4 Analysis of recycling and remanufacturing terminology

Having completed background research in relation to the first research question, in keeping with the scientific method outlined in Figure 2, a suitable hypothesis is able to be put forward.

„Industry and academia are not remanufacturing, recycling is occurring and that given the desire to ultimately obtain fibres largely unharmed from EOL CFRP, recycled CFRP and recycled fibres are liberal ways to describe the products created by industry and academia.“

In order to conduct a critique the processes conducted by industry and academia in relation to remanufacturing and recycling, and to incidentally identify if the position

taken by the author is correct, an analysis is required. The way this is performed in this thesis is to put forward key aspects and product characteristics of true remanufacturing and recycling processes, as defined in chapter 3, with a direct comparison to the practices and process conducted on EOL CFRP hitherto discussed.

4.4.1 Analysis of Remanufacture

4.4.1.1 Have standard remanufacturing protocols been followed?

No evidence from the literature or industry has been recorded documenting a standard remanufacturing process in which CFRP would undergo disassembly, component cleaning, replacement, rebuilding or restoration to as new standard, reassembly and testing.

Figure 3 and figure 10 also highlight the lack of remanufacturing protocols involved in the manufacture of non-virgin CFRP. Figure 10 shows clearly that remanufacturing is thought of as reclaimed fibres being impregnated with virgin resin, noting that impregnation can be obtained in various ways, including injection moulding, compression, vacuum assisted resin transfusion and resin film transfusion, (Feraboli et al., 2012; Oliveux et al., 2015; Pimenta and Pinho, 2012). Figure 3 demonstrates the standard remanufacturing protocols and it is evident that CFRP remanufacturing does not follow these protocols.

4.4.1.2 Is quality equal (or better) to that of original?

It is generally the case within literature (Adams et al., 2014; Oliveux et al., 2015; Pimenta and Pinho, 2012, 2011) that the mechanical performance of CFRP (created by remanufacturing) is stated as being inferior to that of virgin CFRP. In some instances, properties can approach virgin-like properties, but issues such as fibre adhesion, fibre degradation and breakages and non-ideal recycling processes account for various degrees of complex mechanical degradation.

Looking at carbon fibres in isolation, CFR state that their remanufactured carbon fibres retain their virgin-like properties. However in this instance, CFR are reclaiming and sorting fibre that is manufacturing waste or scrap, i.e. fibre that has not yet been used. If the fibre has not been used or processed, it is by definition not possible to remanufacture these fibres. CFR sort/detangle/cut reclaimed fibres and call them remanufactured. This is not remanufacturing.

4.4.1.3 Is remanufactured CFRP issued with a warranty equal to that of the original?

No evidence exists within academia or industry that warranties equal to that originally supplied are issued with remanufactured CFRP. In the case of CFR, if the fibres have not been used they cannot have been issued with a warranty ergo, the warranty given (if any) to the "remanufactured" fibres is the first warranty issued for this product.

4.4.1.4 Is remanufactured discussed as an individual EOL process?

Within industry and academia remanufacturing is routinely regarded as part of the recycling process (see figure 10). CFRP that has been created through remanufacturing is typically called recycled CFRP, which given the accepted understanding of remanufacturing is a nonsensical concept. Remanufacturing and recycle are separate EOL strategies and while, it may be possible to recycle parts of a remanufactured product (discarded parts for example), remanufacture is not considered part of recycling processes.

4.4.1.5 Decision

Based on the four key factors identified, a decision on whether remanufacturing terminology, is appropriate to describe the products manufactured by industry and academia is given.

In relation to remanufacturing protocols, it was shown that industry and academia do not conduct these practices. Remanufacturing in this sector is thought of implanting reclaimed fibres with virgin resin. Further, no evidence supports the notion that CFRP which has undergone „remanufacturing" is being returned to as new condition and issued with an as new warranty. Lastly, it was also shown that remanufacturing is thought of a subset of recycling in this sector. Thus, it can be stated clearly that industry and academia are not remanufacturing CFRP.

However, it is also the case that no evidence exists to suggest that remanufacturing terminology is deliberately being used incorrectly given that CFRP „remanufacturing" and „remanufactured CFRP" bears little resemblance to genuine remanufacturing and remanufactured products. A reasonable conclusion would be that some CFRP based researchers in academia and practitioners within industry may simply be unaware of the concept of a true remanufactured product.

4.4.2 Analysis of Recycling

The literature, including this text, has shown that in general, recycling of CFRP is grouped into two groups, Group 1 mechanical recycling and Group 2 fibre reclamation. These two groups will be evaluated separately from each other in the forthcoming text.

4.4.2.1 Mechanical recycling

Figure 4 demonstrates that the recycling of discarded products results in the creation of material/energy that may be used in exchange for virgin materials when manufacturing new products. Additionally, it has been stated that emergy is lost when performing recycling and it is this fundamental concept that allows the term mechanical recycling to be used in the context of CFRP.

The fibres and resin that were originally part of the virgin CFRP are no longer in the same form, they have been crushed, milled and ground into a form which can then be used to create a new product; the new product being in part used material (crushed fibres) and in part new product (for example, impregnated with new resin). The

composite emergy has been completely lost during this process, allowing mechanical recycling to be regarded as a legitimate form of recycling with no issues arising.

4.4.2.2 Fibre reclamation

Recycling processes associated with fibre reclamation are slightly more complicated to analyse owing to the fact that fibre reclamation is itself considered a recycling process by industry and academia, and that the creation of new products from reclaimed fibres is considered recycled CFRP. Both fibre reclamation and recycled CFRP are examined with the former evaluated first.

Considering a discarded material or product that is recycled, the emergy is lost leaving only the pre-processed materials or energy from these materials. The strategy within industry and academia to reclaim fibres, deemed as a recycling process, is to extract fibres from discarded CFRP with as little damage or change to the fibres as possible, thus, two areas are worthy of consideration in this instance, 1) are the fibre reclamation processes recycling operations and 2) is the term recycled fibres acceptable to describe the fibres reclaimed through chemical or heat treatment? Looking first at point 1) the fibre reclamation process such as heat and chemical treatment have been shown to dissolve the matrix leaving the fibres, in various degrees of state. It has also been shown that the energy of the matrix is recoverable and in some instances, may power the fibre reclamation process itself. Thus, an argument can be put forward that the emergy of the composite has been destroyed, noting that Song (2009) stated that autoclave moulding alone can account for an estimated 29.1 MJ/kg additional energy to be expired, and so through both heat and chemical processes the composite (overall) has been recycled and so physiochemical properties of the EOL product have been altered and thus leaving the fibres to be reclaimed and used again.

Looking now at point 2) „is the term recycled fibres appropriate to describe the resulting fibres reclaimed through chemical or heat treatment.“ Given that the strategy within industry and academia is to reclaim the fibres with as minimum possible damage done to the fibres, a contradiction between the terms recycled and emergy begins arise in this instance. That is, composite recycling is focused upon recycling the bonded structure of fibres and matrix but critically leaving the fibres in a pre-bonded condition and able to be directly used again and so the emergy associated with the fibres alone is largely kept. While at present the reclaimed fibres are not in general

in the same condition as virgin pre-bonded fibres, for instance reclaimed fibres lose their sizing and may suffer from pitting, the reclaimed fibres are largely in the same condition when compared to pre-processed fibers, noting the energy required to produce virgin fibres 183–286 MJ/kg (Song et al., 2009). Taking this into consideration along with the future desire to improve the composite recycling process such that fibres are completely unharmed in composite recycling, in the opinion of the author recycled fibres is not in general accurate terminology to describe fibres reclaimed from composite recycling. Further, recycled fibres terminology may also imply that existing fibres have been recycled with new fibres manufactured using these materials.

An additional argument can be developed by examining EU directives and guidance. The WF directive, (European Parliament and Council 2008), defines the terms recycling as,

"any operation by which waste materials are reprocessed into products, materials or substances whether for the original or other purposes. It includes the reprocessing of organic material but does not include energy recovery and the reprocessing into materials that are to be used as fuels or for backfilling operations"

To characterize all the operations of recycling would be virtually impossible, and as definitions are often general descriptions of practices, the potential exists for different interpretations. To assist with such problems, the EU has also issued additional guidance, (European Commission, 2012). In this guidance the practice of recycling is expanded upon,

"only the reprocessing of waste into products, materials or substances can be accepted as recycling. Processing of waste which still results in a waste which subsequently undergoes other waste recovery steps would not be considered recycling, but pre-treatment prior to further recovery"

As such, if mechanical, heat and chemical treatments are regarded as legitimate forms of recycling CFRP (which literature, including this thesis, subscribes to) then the resulting fibres that are created from recycling cannot be considered waste. If fibres are not considered waste, they cannot therefore be recycled in this context (recycling operations can only be conducted on waste).

Moving away from fibre reclamation, the usage of the term recycled CFRP as a means to describe CFRP created using reclaimed fibres is examined. It has already been shown that the process of recycling a composite can result in reclaimed fibres, which by definition can also be called the „composite recyclate" – recyclate being the product arising from the recycling process. As such, the term „recycled CFRP" can be taken to mean either, reclaimed fibres or „CFRP recyclate".

Taking this into consideration then using the terminology recycled CFRP to describe CFRP manufactured using reclaimed fibres and virgin resin is best avoided. Strictly speaking these products could be referred to as CFRP manufactured using virgin resin and a) recycled CFRP, b) reclaimed fibres or c) CFRP recyclate.

Even if recycled CFRP is taken in a general sense to mean CFRP created using recycled fibres, this thesis has identified that recycling terminology (in relation to fibres) is generally not applicable and so again the terminology recycled CFRP should be avoided.

4.4.2.3 Decision

This text has shown that in terms of mechanical recycling, the term recycle is correctly applied with no issues arising. However, reclaimed fibres are not recycled fibres and should not be regarded as such. The final issue of creating CFRP from reclaimed fibres and labelling it, recycled CFRP is a more complex issue. While the practices involved in fibre reclamation such as pyrolysis and chemical treatments are recycling operations, new products created from reclaimed fibre are not in general recycled products and so the term recycled CFRP should be avoided. It has been shown that within industry and academia, in relation to CFRP, no evidence of remanufacturing exists, and that in the case of recycle, the term should in general not be applied to reclaimed fibres or products created from reclaimed fibres. It is now appropriate to propose new terminology to better describe the products created denominated as recycled CFRP, or for that matter, in a general sense as recycled composite.

4.5 Proposal of New Terminology

To identify new terminology to describe CFRP constructed from reclaimed fibres, attention may be turned to the major EU directives such as the ELV directive, WF directive and WEE directive, all of which can affect the CFRP lifecycle. The idea being that should these new materials be subject to regulations moving forward by utilizing pre-existing terminology from the EU, then these new products will have a grounding in already established terminology. Given that recycling and remanufacturing have been shown as not applicable to describe CFRP manufactured using fibres from CFRP recycling, potential terminology which can be found from WF directive (European Parliament and Council 2008), is re-use, recovery and preparing for re-use. These are defined respectively,

"„re-use" means any operation by which products or components that are not waste are used again for the same purpose for which they were conceived;"

"„recovery" means any operation the principal result of which is waste serving a useful purpose by replacing other materials which would otherwise have been used to fulfil a particular function, or waste being prepared to fulfil that function, in the plant or in the wider economy. Annex II sets out a non-exhaustive list of recovery operations;"

"„preparing for re-use" means checking, cleaning or repairing recovery operations, by which products or components of products that have become waste are prepared so that they can be re-used without any other pre-processing."

Examining these terms, preparing for re-use terminology can be dismissed. This is because the manufacturing processes of impregnating fibres obtained via recycling (i.e. the recycled CFRP or CFRP recyclate) with virgin resin is only very loosely and tenuously reflects the definition given above.

Moving onto recovery. The EU consider recovery to be the opposite of disposal and so any operation which diverts products or components away from disposal, including recycling, can generally be as considered a recovery operation. Given the broad scope of recovery, adopting recovery terminology to describe products manufactured using recycled CFRP does little to clarify that these products are manufactured using ideally pristine fibres obtained via recycling.

Additionally, CFRP recyclate is not considered as waste and so adopting recovery and preparing for re-use operations to describe products manufactured using the recyclate

could perhaps infer that the established recycling processes of heat treatment or chemical treatment result in waste being produced.

Examining now re-use. Re-use states that products or components that are not waste are used again for the same purpose for which they were conceived. Further, the EU issued guidance in addition to the WF directive, stating that some repairing may be carried out (in this case, a sizing operation for example), while still regarding the product as re-used.

… Re-use is a means of waste prevention; it is not a waste management operation. For example, if a person takes over a material, e.g. piece of clothing, directly from the current owner with the intention of re-using (even if some repairing is necessary) it for the same purpose, this comprises evidence that the material is not a waste.
(European Commission 2012)

With CFRP recyclate being used again to manufacture new composite, given how reuse terminology is understood a degree of applicability can be seen. Further weight is added to adopting re-use terminology in replacement for the liberal usage of recycling or remanufacturing terminology given the ultimate goal of CFRP recycling is to extract the fibres while incurring no damage (the breakage of CFRP into smaller manageable sizes is still anticipated however). Thus, CFRP manufactured using virgin resin and fibres obtained via recycling is more accurately described as re-used fibre CFRP (rf-CFRP) or CFRP from re-used fibres (CFRP-rf).

Re-use terminology is also understood in a similar way in the WEEE directive (European Parliament and Council 2012), given that this directive defines re-use in accordance with the WF directive (repeated again for clarity).

„re-use" means any operation by which products or components that are not waste are used again for the same purpose for which they were conceived."

Re-use is also defined in the ELV directive, (European Parliament and Council 2000a). This definition is given below,

"any operation by which components of end-of life vehicles are used for the same purpose for which they were conceived"

Re-use terminology is again understood in the same way as both the WF directive and the WEEE directive, in that re-use is again regarded as using components again for the

same purpose. Note however, given the focus the ELV directive places on waste in that every ELV is regarded as waste, re-use in this directive applies to waste. This is however not a huge concern given that once recycling occurs, the fibres or CFRP recyclate is no longer subjected to the directive. The important aspect here is that re-use terminology is generally understood in a similar way to both the WF and the WEEE directive in addition to being more applicable than recovery and preparing for re-use operations. Additionally, in terms of the BSI (BS 8887-2, 2009), the term re-use is in agreement WEEE directive, or WF directive and so rf-CFRP, is again applicable terminology.

It should also be noted that the re-use fibre terminology is generally not applicable when describing CFRP made from mechanically recycled CFRP. This is because there is a significant loss of the structural integrity of the fibres since mechanical recycling crushes, chops and mills the fibres into far smaller pieces, and in some cases into a powder. Thus, by adopting rf-CFRP a distinction between mechanical recycling and fibre reclamation is created.

Another benefit from adopting this terminology is that any potential confusion and ambiguity over the concept/definition of recycled CFRP may be reduced, therefore a potential barrier to a successful implantation of a future CRFP EU directive (should the EU create one) would be eliminated. For instance, without being involved in industry and its research, one would struggle to state that recycled CFRP may be created by recycling a CFRP composite structure in such a way as to acquire as best can be (in terms of the amount of damage) the pre-bonded carbon fibres and then impregnating these reclaimed fibres with a new matrix element. Whereas describing CFRP as rf-CFRP implies that the CFRP is of course CFRP with re-used fibres.

Further, adopting the method of examining EU directives to classify CFRP manufactured using reclaimed fibres as rf-CFRP also serves to build on the work carried out by Glavic and Lukman (2007). In their review of sustainability terms and definitions, reuse is quoted as,

"Reuse means using waste as a raw material in a different process without any structural changes."

This definition of reuse is taken by the authors from the European Environmental Agency (EEA) glossary and it is directly in conflict with the definitions given in this thesis. Re-use is generally not regarded as taking waste and reusing it in a different

process, it is regarded as taking products that generally not waste reusing them for the same application (as defined by the WF directive). Examining a fresh definition from the EEA glossary, reuse is quoted as

"Material reuse without any structural changes in materials"

Although the modern definition of reuse eliminates the notion of products being waste prior to reuse and the insistence of reusing the material in a different process, this definition is still problematic owing to the insistence of no structural change. It has already been shown that under the WF directive, even if something is repaired (which is by definition a structural change), it can still be regarded as product re-use. Hence, it may be the case that (a) re-use is defined separately from reuse (re-use is not included in glossary) or (b) the glossary comprises only approximate definitions. Taking (a) and (b) into account, it can be stated that when conducting further sustainability studies it is advised that applicable directives/legislation should be consulted given that subtle differences in terminology may be apparent.

To identify appropriate terminology to describe CFRP manufactured using fibres obtained via recycling, major EU directives such as the WF, WEEE and ELV directive were examined. Re-use terminology, was shown to be applicable terminology to describe these products. A final area requiring discussion prior to concluding this chapter is an analysis of whether CFRP, or composite, in general is able to be truly remanufactured.

4.6 Can CFRP be Remanufactured?

Remanufacture as defined in chapter 3, is not occurring within the field of composite EOL strategy. It is appropriate therefore to investigate whether composite is actually able to be remanufactured. Given that at a minimum remanufacturing requires a core which can be disassembled, restored or replaced, and reassembled, understanding these factors is crucial to understanding if CFRP can be remanufactured.

This research does not consider CFRP as having a core or being a core. Specifically, the constituents of the CFRP act together to create a unified material which components can be created from, and which is part of a larger assembly (or core). CFRP is not un-similar to an alloy material in this regard, in that various materials are used to create a unified material which may be used to manufacture new products used

as part of a larger assembled unit (or core). With the absence of a core, CFRP is not able to be remanufactured; it is a single material not able to be disassembled and then reassembled.

If the combination of fibres and matrix was hypothetically regarded as a core of assembled products, CFRP is still incapable of being disassembled with the view to replacing or restoring core components to as new condition. The goal of academia and industry is to obtain the fibres in pre-assembled condition only; there is no mechanism to restore the fibres on a fibre level to at least new condition. The goal of fibre reclamation is to obtain fibres with no damage caused to them by disassembly (recycling) only.

Further, if one thought of the fibres as a core or the matrix as a core then the answer that CFRP is not remanufacturable is still returned. Both the fibres and matrix are incapable of being disassembled, restored to as new condition and successfully reassembled and so cannot be remanufactured.

It can be stated that CFRP cannot be remanufactured, however as alluded to earlier a core which uses CFRP to some degree could be remanufactured. This adds an element of confusion. To alleviate confusion an example of aircraft remanufacture is given. Given that an aircraft is a large assembled unit comprising many different parts it could be regarded as a core (comprising multiple smaller cores). It is possible to remanufacture the aircraft or various sections of the aircraft. In this instance, any composite panels would be replaced as part of wider remanufacturing processes being conducted on the core (the core is being remanufactured with the CFRP being replaced as part of a remanufacturing process).

4.7 Conclusion

This chapter has investigated the industrial and academic practices to of CFRP recycling and remanufacturing. It has been shown that while CFRP is capable of being recycled, terminology such as recycled CFRP, recycled fibres and remanufactured (or re-manufactured) are not in general applicable terms to describe products created using fibres obtained from for use in this sector. Evidence for this viewpoint was found by analysing industrial and academic practices in relation to remanufacturing and recycling definitions. It was found that no evidence exists of remanufacturing taking

place, that reclaimed fibres are not the same as recycled fibres, and the term recycled CFRP is an ambiguous way of describing CFRP created from reclaimed fibres.

Having shown that terms such as remanufacture and recycled CFRP are to be avoided, new terminology to describe CFRP created from reclaimed fibres was further presented. The new terminology was given as re-used fibre CFRP (rf-CFRP) or CFRP from re-used fibres (CFRP-rf). This new terminology agrees largely with how re-use is defined within EU directives, with (BS 8887-2, 2009) and is a more accurate way to describe reclaimed fibre-based CFRP. It was also been shown that rf-CFRP is not applicable for CFRP created from crushed, milled and ground fibres and so an additional benefit of the new terminology was identified. That is, a clear separation between crushed, milled and ground fibre-based CFRP products and fibre reclamation-based CFRP is created (at present, recycled CFRP may be used to describe CFRP from crushed, milled and chopped fibre-based CFRP as well as reclaimed fibre-based CFRP).

In addition to conducting for the first time in literature a review into to the specific practices from an EOL terminology point of view, through identifying correct terminology remanufacturing awareness in this sector is increased, potential blocks to gauging the CFRP recycling and remanufacturing industry are removed, companies/organizations now have a specific reference text allowing them to help create new directives, and help ensure compliance with existing EU directives. Additionally, an analysis of the remanufacturability of CFRP has also been presented, with a finding that CFRP is incapable of being remanufactured. Lastly, this chapter also documented that when discussing specific sustainability terminology within literature, it may be best practice to define these terms in the context of directives/legislation. Thus, it was advised that future studies into sustainability concepts/products/practices should take into account that possible existing directives/legislation may exist in which the same term is defined differently (with differences being potentially subtle) in separate directives.

Chapter 5: EOL decision tool to assist in correct product classification and designation

5.1 Why a decision tool

In the last chapter it was identified that researchers and companies involved in CF and CFRP re-use are on occasion using terminology that is not strictly correct and truly reflective of their practices. A natural thought arises as to what could be done to assist researchers and companies to designate their products and processes more accurately. Section 4.2 highlights that correct product designation helps to reduce the likelihood of incorrectly gauging the market place, helps companies and stakeholders better comply with existing and potentially new legislation, increases the potential for effective research and seeks to reduce confusion between various EOL terminologies in general.

To this end, a strategy to allow for the correct designation of products, in terms of recycle, remanufacture, recondition, repair and re-use, is presented within this chapter. This strategy comes via a combination of an interactive flow chart and a series of short questions, each with yes/no answers - noting the path of the flow chart is mapped out according to the particular point at which a yes or no answer is given. The novelty in this tool, and which separates it from existing tools, is that through allowing an interactive based approach, most independent thought is removed from the user, and thus the tool informs the user of the correct classification, and not the other way round, i.e. the user does not make their own decision, the tool does it for them.

5.2 Existing methods for product classification

Generally two clear methodologies, which are very often presented in conjunction with each other, are used to describe and understand the difference between EOL operations.

The first strategy to convey the differences between recycle, remanufacture, recondition, repair and re-use is to outline within literature (including this current research) the standardized definitions of these practices. This strategy is almost ubiquitous for obvious reasons and is by far the most favourable method found within literature; attention may be drawn to chapter 3 for references in this regard. An additional method of denoting the differences between these practices, leading towards the contribution to knowledge and novelty of this work, is through the use of tools. Noting that unlike the strategy of defining practices within literature, existing tools which identify the differences between EOL processes do not contain any formal written definition of the EOL processes.

Looking at the first tool within literature, Ijomah (2002) presents a hierarchy based tool with remanufacturing sitting atop of reconditioning, and recondition sitting atop repairing. Ijomah (2002) used the tool to highlight the difference between a remanufactured product, a reconditioned product and a repaired product, in terms of amount of the amount of labour content involved, the quality of warranties issued and the overall performance of the product. This tool is presented as Figure 11, with Table 13 highlighting various authors who have used this tool, or a variant of this tool, and the rationale as to why they used the tool.

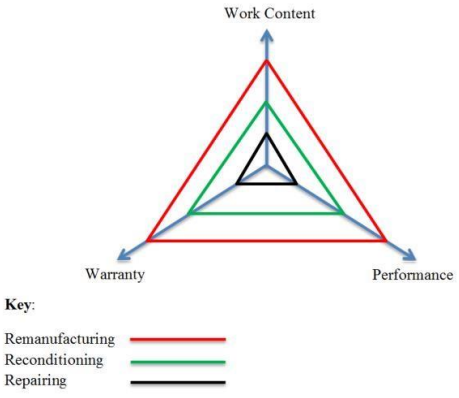

considering work content, warranty and overall performance**Figure 11** - Highlighting the difference in content of remanufacturing reconditioning and repa *Reproduced with permission from Ijomah,* ir when

2002, "A model-based definition of the generic remanufacturing business processes", Plymouth University, doi:10026.1/601

Focus of literature	How tool was used	Tool documented within literature
To determine a robust definition of remanufacturing	To emphasis the differences between remanufacturing, reconditioning and repairing, in terms of labour content, warranty and product performance.	(Ijomah, 2002)
To highlight alternative strategies for EOL waste	See (Ijomah, 2002)	(King et al., 2006)
The role of remanufacturing in economic and ecological growth	See (Ijomah, 2002)	(Ijomah, 2009)
A case study to explore how some Swedish companies currently incorporate product/service systems into their products, and identify new ways which they could do so, with an additional focus on remanufacturing.	See (Ijomah, 2002)	(Sundin et al., 2009)
To discuss remanufacturing and problems facing remanufacturing	See (Ijomah, 2002)	(Gurler, 2011)
To identify remanufacturing and typical remanufacturing processes	See (Ijomah, 2002)	(Matsumoto and Ijomah, 2013)
To investigate terminology surrounding CFRP recovery operations	See (Ijomah, 2002)	(Paterson et al., 2016)

Table 13 - Literature, and focus of that literature, which documents the use of EOL tool presented in figure 11. *Reprinted with permission from Paterson, D.A.P., Ijomah, W.L., Windmill, J.F.C., 2017. End-of-Life decision tool with emphasis on Remanufacturing. J. Clean. Prod. 148, 653–664. doi:10.1016/j.jclepro.2017.02.01, under creative commons Attribution License https://creativecommons.org/licenses/by/4.0/*

As seen from Table 13, the way in which the tool was initially used by Ijomah (2002), i.e. to highlight the differences in terms of labour, performance and warranty, is still the same way the tool is used today, even with subsequent literature having a different focus in each case. The tool is clearly effective in reinforcing subtle differences between remanufacture, recondition and repair, however it is indeed the case that the tool does not inform the user as to whether a product is remanufactured, reconditioned, repaired. The user would have to digest the available literature (including using the tool outlined above) and still have to form a decision themselves as to the correct status of a product. Note however, the process of allowing the user to independently form a decision allows the scenario in which a user could make an incorrect decision to arise.

An additional tool focused on highlighting the differences, from a cradle to grave standpoint, between recycle, remanufacture, recondition, repair and re-use is also found within literature. The structure the second tool takes is that of a sequential block diagram of a cradle to grave production process with recycle, remanufacture, possibly recondition, repair and re-use options are then fed back into the block diagram from the product disposal stage. A typical demonstration of this tool is given as Figure 12.

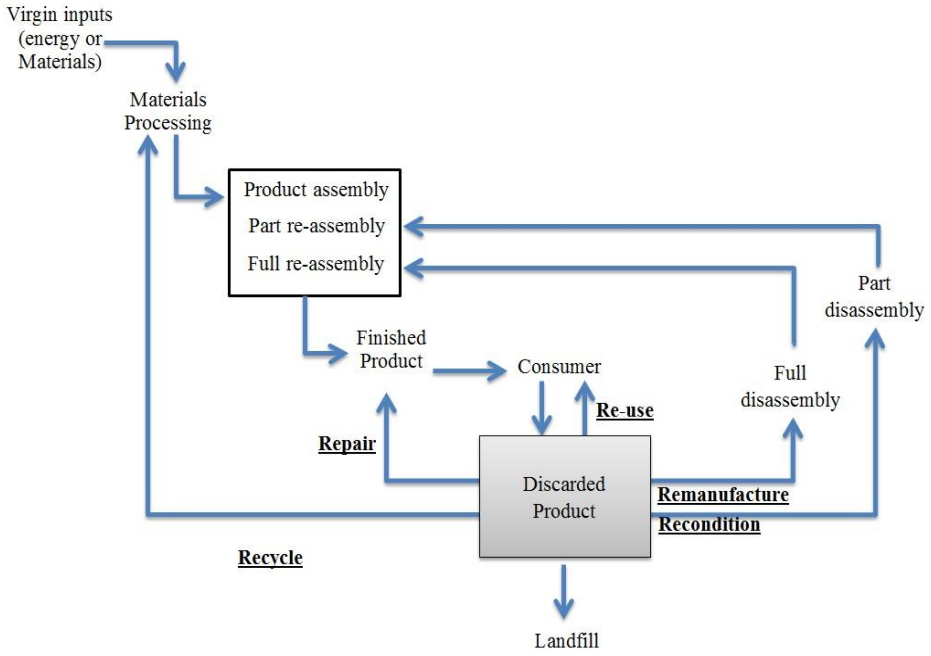

Figure 12 - Product cradle to grave tool highlighting end of life processes, adapted from (King et al., 2006) and (Paterson et al., 2016). *Reprinted with permission from Paterson, D.A.P., Ijomah, W.L., Windmill, J.F.C., 2017. End-of-Life decision tool with emphasis on Remanufacturing. J. Clean. Prod. 148, 653–664. doi:10.1016/j.jclepro.2017.02.01, under creative commons Attribution License https://creativecommons.org/licenses/by/4.0/*

Similar to Table 13, Table 14 presents literature which uses the tool, documents how the tool was used and the focus of the literature.

Focus of literature	How tool was used	Tool documented within literature

To identify and discuss remanufacturing, the processes of remanufacturing and benefits of remanufacturing	To present hierarchy of expected economic value associated with recycle, remanufacture, repair and re-use, in the context of the a cradle to grave production process	(Lund, 1985)
Effect of fastening and joining mechanisms on remanufacture	To demonstrate the strategies available for products to avoid landfill, in the context of a cradle to grave production process	(Shu and Flowers, 1995)
Product design that impacts on remanufacturing	See (Shu and Flowers, 1995)	(Shu and Flowers, 1999)
To highlight that a key enabler to sustainable growth is to close the loop on the manufacture to landfill production cycle	See (Shu and Flowers, 1995)	(Nasr and Thurston, 2006)
To determine the views of remanufacturing academics on various issues relating to remanufacturing	See (Shu and Flowers, 1995)	(King and Barker, 2007)
Environmental benefits of remanufacturing	See (Shu and Flowers, 1995)	(King and Gu, 2010)
Analysis of reverse logistics for electronic goods in Malaysia with a focus on business performance in terms of EOL recovery strategies	To highlight the reverse logistics processes, in the context of a cradle to grave product production process	(Khor and Udin, 2012)
Development of a conceptual design framework which incorporates EOL thinking	To demonstrate a conceptual framework for a more sustainable form of aircraft design	(Ribeiro and Gomes, 2014)
Design for multiple life cycles	To highlight the consideration of material flow during cradle to cradle design process	(Go et al., 2015)

Table 14 - Literature, and focus of that literature, which documents the use of EOL tool presented in figure 12. *Reprinted with permission from Paterson, D.A.P., Ijomah, W.L., Windmill, J.F.C., 2017. End-of-Life decision tool with emphasis on Remanufacturing. J. Clean. Prod. 148, 653–664. doi:10.1016/j.jclepro.2017.02.01, under creative commons Attribution License https://creativecommons.org/licenses/by/4.0/*

Note however, in this instance, not all authors incorporate recondition into the tool, that is, (Go et al., 2015; Lund, 1985; Nasr and Thurston, 2006; Ribeiro and Gomes, 2014; Shu and Flowers, 1999, 1995) do not incorporate recondition, whereas, (Khor and Udin, 2012; King et al., 2006; King and Barker, 2007; King and Gu, 2010) incorporate recondition. Similar to Table 13, it can be said that Table 14 documents that the tool presented in Figure 12 is used within literature in generally the same way. That is, Figure 12 is used to highlight the differences in EOL recovery strategies with reference to a cradle to grave production process. Further, similar to Figure 11, no definitive answer as to whether a product has been remanufactured, reconditioned,

repaired, re-used or recycled, is provided and therefore, the user must again form a decision themselves as to the status of a product.

At this point it can be said that the tools in both Figure 11 and Figure 12 have been used in different ways; Figure 11 has been used to highlight the differences between reconditioning, remanufacturing, and repairing, with respect to labour content, level of warranty, and product performance. Figure 12, on the other hand, has been used to understand at which point recycling, remanufacture, recondition, repair and re-use is implemented in the context of a cradle to grave production process. It is therefore the case that both tools do not explicitly state or determine if a product has been recycled, remanufactured, reconditioned, repaired or re-used. That is, to determine the correct status of a product, the user must consult both definitions and tools, and then use their own judgement. The tool presented in this chapter fills this gap in knowledge and for the first time within literature, a tool which accurately determines whether a product has been recycled, remanufactured, reconditioned, repaired or re-used is presented.

5.3 Research Methodology

The development process for the new bespoke tool is now discussed, with Figure 13 documenting the approach taken. Following this, an explanation of stages A, B and C is given. The strongest focus is placed upon section C, the tool development phase.

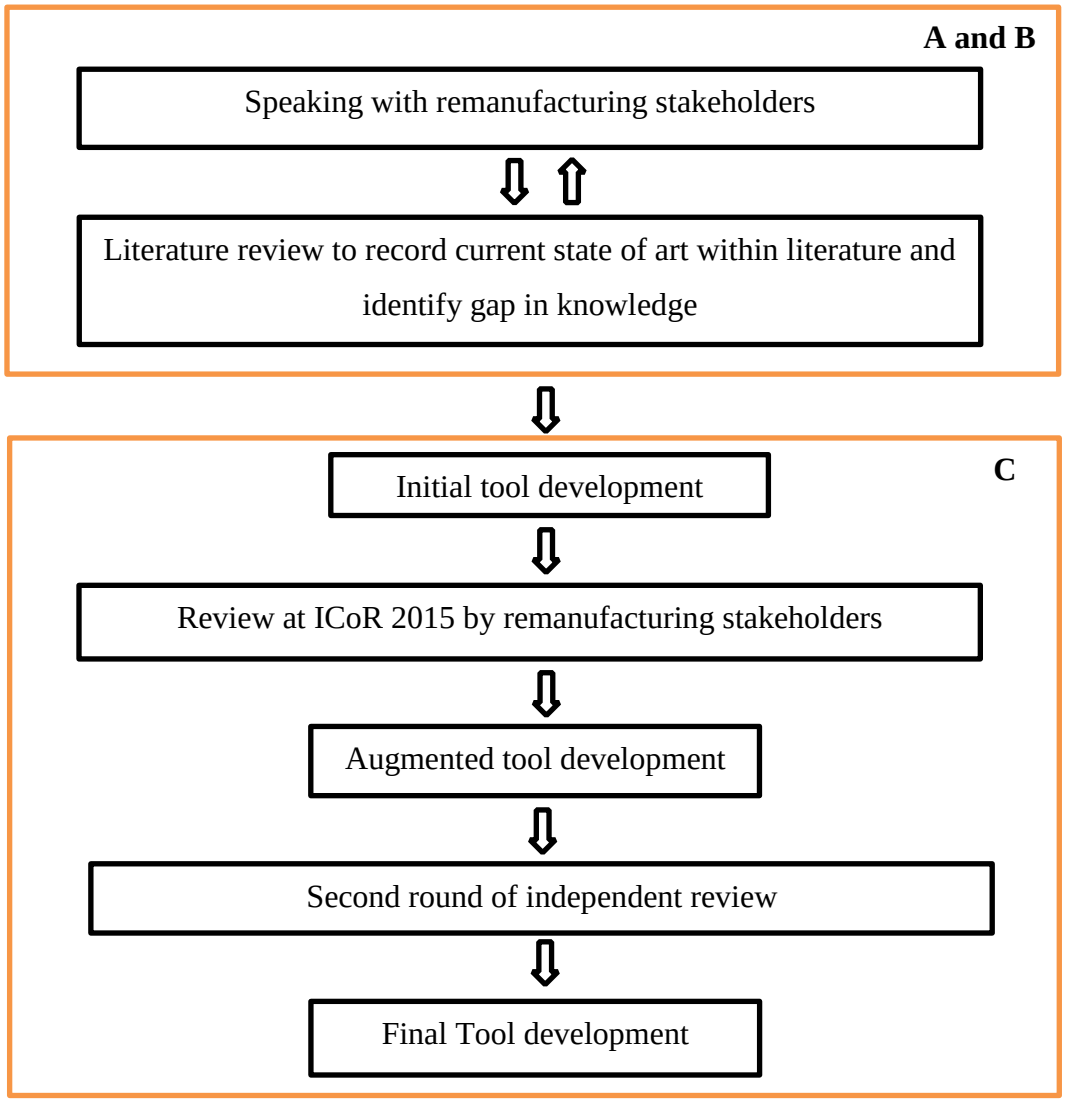

Figure 13 – Graphical depiction of the methodology adopted in this research. *Reprinted with permission from Paterson, D.A.P., Ijomah, W.L., Windmill, J.F.C., 2017. End-of-Life decision tool with emphasis on Remanufacturing. J. Clean. Prod. 148, 653–664. doi:10.1016/j.jclepro.2017.02.01, under creative commons Attribution License https://creativecommons.org/licenses/by/4.0/*

Section A and B

A: This section involved speaking with / visiting industrialists and academics, to find out how identification of used products status / classification was undertaken.

- Companies visited – Mackie Automatic Transmissions Ltd, Autocraft Drivetrain Solutions
- Scottish institute of remanufacture events

B: Literature review to record state of the art and thus identify any gap in knowledge.

- Identification that to correctly identify the status of a secondary market product, one is often required to form their own decision by using existing definitions or via existing tools.
- Gap identified – lack of a method that can be used to easily identify secondary market products that is easy and inexpensive and does not require the user to have advanced knowledge of the differences between the various processes

Note that consultation with industrialists and academics occurred both prior to and during the literature survey, hence, the two way arrows documented in Figure 13.

Section C

Initial tool development

Based on the information taken from the literature, a prototype tool to determine if a product has been recycled, remanufactured, reconditioned, repaired or re-used was developed.

Given that the tool should be simple to use, and be distinct from existing tools, the question of how to design the tool to incorporate the definitions of reprocesses in an efficient way posed an interesting challenge. The strategy adopted in this thesis was to incorporate an interactive element by way of a flow chart and questions (with yes / no answers), while also recognizing that remanufacture involved the most labour content. Specifically, the user answers questions with yes or no and progresses through the flow chart ultimately arriving at the status of the product which has received a re-process; all achieved critically without the user having any knowledge of the definitions of these practices.

Also, with a remanufactured product involving the most effort in terms of labour and having the best product warranty status, by detailing the processes involved in remanufacturing as documented by Ijomah (2002), then all product recovery options should also be therefore be identified, with the additional benefit being that the essential characteristics of a remanufactured product are also able to be presented

The initial tool, presented at ICoR 2015, (Paterson et al., 2015), is given in Figure 14 and Table 15.

Question No	Question
1	Is emergy (energy expired to create product from raw materials) retained from original EOL product?
2	Does the product have a core?
3	Is core capable of being disassembled?
4	Has the core been disassembled?

5	Is warranty of product equal to or better than the original?
6	Have all core components been cleaned, inspected, replaced / repaired to original standard and had its core reassembled such that the product is in like new condition?
7	Have all major broken components and components on the verge of failure been replaced or repaired?
8	Has the product been restored to an acceptable level in any significant way (and core reassembled if applicable)?

Table 15 - Original question set presented at ICoR 2015. *Reprinted with permission from Paterson, D.A.P., Ijomah, W.L., Windmill, J.F.C., 2017. End-of-Life decision tool with emphasis on Remanufacturing. J. Clean. Prod. 148, 653–664. doi:10.1016/j.jclepro.2017.02.01, under creative commons Attribution License https://creativecommons.org/licenses/by/4.0*

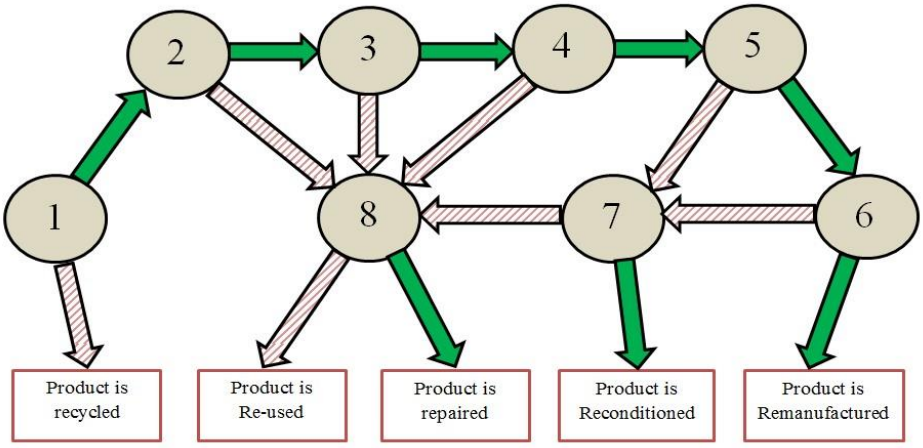

Figure 14 – Original flow chart presented at ICoR 2015. *Reprinted with permission from Paterson, D.A.P., Ijomah, W.L., Windmill, J.F.C., 2017. End-of-Life decision tool with emphasis on Remanufacturing. J. Clean. Prod. 148, 653–664. doi:10.1016/j.jclepro.2017.02.01, under creative commons Attribution License https://creativecommons.org/licenses/by/4.0/*

The principal behind the tool is that the user would start at position 1, answer yes or no to question 1, and then progress through the flow chart and question set accordingly - noting that each question only has a yes or no answer. In terms of Figure 14, a yes answer is denoted as a green arrow and a no answer is denoted as a red (dashed) arrow.

Review at ICoR 2015 by remanufacturing stakeholders

The prototype tool was presented at the ICoR 2015. This venue was chosen for the initial review of the tool as an international conference on remanufacturing would allow for many members of the wider remanufacturing and sustainability community to be directly exposed to the tool and thus allow the authors to gauge the general response to the tool. Further, the delegate list at this conference was composed of academics and operational remanufacturers from various countries and backgrounds

and so feedback obtained from such a rich environment would of great benefit to the development of the tool.

As part of the initial review, verbal feedback was obtained from three conference delegates, each from different vocations. Table 16 documents both the position and relevancy of each reviewer along with the observations and concerns raised.

Reviewer	Position	Relevance to subject matter	Observations from Reviewers
A	Academic from G-SCOP laboratory within the University of Grenoble France, whose research interests including remanufacturing and sustainability.	Expert in the field of remanufacturing and sustainability. Academic is not based in the United Kingdom.	No direct mention of product being returned to better than new quality and that this issue was only implied.
B	Representative of an American company directly involved in the remanufacture of hydraulic components.	American operational remanufacturer of hydraulic components. Representative is not based in the United Kingdom.	In some instances, remanufacturers in America are on occasion unaware of the quality of the original product. Thus by insisting that the product should be returned to like new condition then the scope of the research may be limited to areas outside America.
C	Representative from a company involved in large construction programme devised in association with the British Government.	Significantly large manufacturing based construction programme which has its own sustainability policy.	Emergy, while the correct term, it is an unusual term from a public perspective and thus the public may struggle to understand its meaning.

Table 16 - Identifying the position and relevancy of reviewers involved in the first review stage of this research. *Reprinted with permission from Paterson, D.A.P., Ijomah, W.L., Windmill, J.F.C., 2017. End-of-Life decision tool with emphasis on Remanufacturing. J. Clean. Prod. 148, 653–664. doi:10.1016/j.jclepro.2017.02.01, under creative commons Attribution License https://creativecommons.org/licenses/by/4.0/*

Augmented tool development

The academic and industrial feedback obtained at ICoR 2015 is now discussed. Taking into account this constructive feedback, changes required to the question set and flow chart, resulting in an augmented tool, are also highlighted.

In relation to comment from reviewer A (ICoR 2015)

This point was taken on board. A decision was taken to rewrite question 6. Question 6 was rewritten as,

„Have all core components been cleaned, inspected, replaced / repaired to original standard and had its core reassembled such that the product is in like new condition or better?"

In relation to comment from reviewer B (ICoR 2015)

In relation to point 2, it was felt that no changes would be made prior to an investigation into what is currently classed as a remanufactured product within the United States. That is, working definitions of remanufacturing products were consulted prior to altering the flow chart and question set. To this end, two useful sources which documented existing working definitions of a remanufacturing product from an American perspective were consulted. The first sourced definition was from the aforementioned American Federal Repair Cost Savings Act of 2015 (Federal act 2015) and the second source definition of remanufacturing was from the Remanufacturing Industries Council
(RIC, 2015).

Looking first at the federal repair cost saving act of 2015, (noting that this act was signed into law on the 10/07/2015) a remanufactured vehicle component is defined as,

"vehicle component (including an engine, transmission, alternator, starter, turbocharger, steering, or suspension component) that has been returned to same-asnew, or better, condition and performance by a standardized industrial process that
incorporates technical specifications (including engineering, quality, and testing standards) to yield fully warranted products"

Looking now at the Remanufacturing Industries Council, which is an American National Standards Institute (ANSI) accredited standards developer, and whose members compose remanufacturers such as Caterpillar and Xerox, the current remanufacturing definition put forward by them is given as,

"Remanufacturing is a comprehensive and rigorous industrial process by which a previously sold, worn, or non-functional product or component is returned to a "like-new" or "better-than-new" condition and warranted in performance level and quality

It can be seen that both definitions state clearly that a remanufactured product must be returned to original equipment specification or better. Thus the point raised at ICoR i.e. „determining if a product has been returned to like new condition is sometimes impossible", may be correct from certain members of the delegation point of view it bears no relation on how a remanufactured product should be defined. That is, official legislation and an ANSI accredited standards developer, the RIC, have both shown that American remanufactured products are required to be returned to at least as new condition.

However, it is the case that the documented definitions for American products are slightly out of sync with the British standard definition (BS 8887-2, 2009), when it comes to the concept of a warranty. The British standard stipulates remanufactured products should have a warranty that is at least equal to the original, whereas the Federal Repair Act states that remanufactured products should be fully warranted and RIC state that remanufactured products should be warranted in performance level and quality.

Taking both the issue of like new condition and quality of warranty into account, to allow for the range of this tool to cover American remanufacture, the decision was made to alter question 5 of the question set. It should be noted however, this alteration is for warranty purposes only, i.e. the like new condition issue raised at ICoR 2015 has been shown not to affect the flow chart of question set scope.

Question 5, was rewritten, with the inclusion of the following text,

For British remanufacture - Is warranty of product equal to or better than the original?

For American remanufacture - Is the product fully warranted?

In relation to comment from reviewer C (ICoR 2015)

This point was taken on board in this instance. As such, the view was taken to provide an altogether more comprehensive explanation of what emergy is. To facilitate this, question 1 is rewritten as,

„Is emergy (see N.B.) retained from original EOL product?"

With, the N.B being included under question 8 and containing the explanation of what emergy is, which is given as,

„To create a product of out raw materials then various processes/actions have to be performed. These various processes and actions all require (to some degree) energy to be expired. The total amount of energy expired in creating a product is known as emergy or embodied energy. When recycling a product, the product is returned to raw materials and so this emergy is lost and therefore new energy must be expired to create a new product from the raw materials.'

As a result of the initial review, it was found that no changes were required for either the flow chart or to the order of questions. However, to incorporate the observations raised by stakeholders, i.e. Table 16, questions 1, 5 and 6 were required to be updated. The updated tool, known as the augmented tool, is now shown as Table 17 and Figure 15.

Question No	Question
1	Is emergy (see N.B.) retained from original EOL product?
2	Does the product have a core?
3	Is core capable of being disassembled?
4	Has the core been disassembled?
5	For British remanufacture - Is warranty of product equal to or better than the original? For American remanufacture - Is the product fully warranted?
6	Have all core components been cleaned, inspected, replaced / repaired to original standard and had its core reassembled such that the product is in like new condition or better?
7	Have all major broken components and components on the verge of failure been replaced or repaired?
8	Has the product been restored to an acceptable level in any significant way (and core reassembled if applicable)?
N.B. To create a product of out raw materials then various processes/actions have to be performed. These various processes and actions all require (to some degree) energy to be consumed. The total amount of energy expired in creating a product is known as emergy or embodied energy. When recycling a product, the product is returned to raw materials and so this emergy is lost and therefore new energy must be expired to create a new product from the raw materials.	

Table 17 – Updated question set incorporating stakeholder feedback. *Reprinted with permission from Paterson, D.A.P., Ijomah, W.L., Windmill, J.F.C., 2017. End-of-Life decision tool with emphasis on Remanufacturing. J. Clean. Prod. 148, 653–664. doi:10.1016/j.jclepro.2017.02.01, under creative commons Attribution License https://creativecommons.org/licenses/by/4.0/*

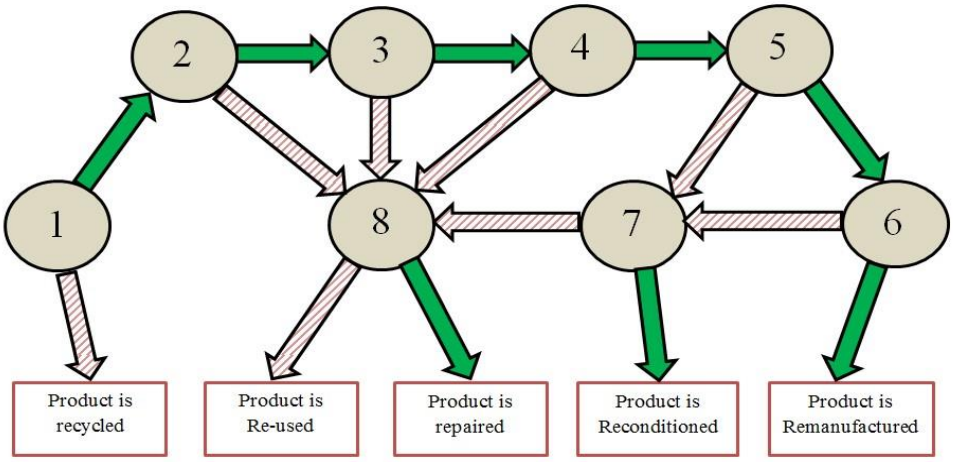

Figure 15 - Original flow chart from ICoR 2015. No changes were required after first review stage - included again for completeness. *Reprinted with permission from Paterson, D.A.P., Ijomah, W.L., Windmill, J.F.C., 2017. End -of-Life decision tool with emphasis on Remanufacturing. J. Clean. Prod. 148, 653–664. doi:10.1016/j.jclepro.2017.02.01, under creative commons Attribution License https://creativecommons.org/licenses/by/4.0/*

Second round of independent review

The augmented tool was then subject to another round of independent review. In this instance, the tool was reviewed by representatives from research institutions who are engaged with industrial bodies. With both academic and industrial affiliations it was envisaged that feedback obtained from these reviewers would be well grounded from both an academic and industrial standpoint. In this instance, the reviewers provided independent written reviews of the augmented tool. Table 18 documents both the position and relevancy of the reviewer along with the observations and concerns raised.

Reviewer	Position	Relevance to subject matter	Observations from Reviewers
A	Representative from a Government sponsored remanufacturing institution	The remanufacturing body has a focus on developing the remanufacturing industry within Scotland	Clarity required on whether all emergy or just some of emergy should remain
			It may be the case that not everyone is aware of the concept of a core, and so clarity on the difference between a product and a core, in this context, is required
B	Representative of a national manufacturing research institution	Institution involved in cutting edge manufacturing processes and bridging the goals between industry and academia	Clarity required on question 2 as it was felt that all products would contain a core if they are returned as a whole. Further, it was also felt that the way the question was written could imply products were being returned in parts or in component form. If this was the intention, the question should be written to reflect this.

			Clarity required on question 6, as the way in which it is written would be perhaps too ambiguous for manufacturers to answer. The way in which the question is written possibly implies that the remanufacturing steps should mirror the manufacturing steps and that the focus should be on a remanufactured product being at least as good as original standard.
			The term „significant way" in question 8 was possible vague
			The word expire is not applicable in this context
			Possible merge the question set and flow chart into one tool to improve usability

Table 18 - Identifying the position and relevancy of reviewers involved in the review stage of the augmented tool development. *Reprinted with permission from Paterson, D.A.P., Ijomah, W.L., Windmill, J.F.C., 2017. End-of-Life decision tool with emphasis on Remanufacturing. J. Clean. Prod. 148, 653–664. doi:10.1016/j.jclepro.2017.02.01, under creative commons Attribution License https://creativecommons.org/licenses/by/4.0/*

Final tool development

The concerns raised in the second review stage were taken into consideration and a final version of the tool, and contribution to knowledge of this chapter, was developed. Discussion of the points highlighted through review and any changes made to the augmented tool are given is now presented.

In relation to the first concern from reviewer A (independent review)

Depending on the complexity of the product undergoing an EOL process the term emergy can be a difficult concept to tie down. For example, in reviewing the practices of CFRP recycling, Paterson et al (2016) stated that even though a composite recycling process produced fibres with some emergy loss, this was not sufficient to denote these products as being classically recycled. Thus, the point is taken on board with a statement that small losses of emergy are in general ok included in the question set and also with the assumption that in almost all cases the decision as to whether a product has been recycled is a fairly simple one to make.

Question 1 is rewritten as,

„Is the vast majority of the emergy (see N.B) from the original EOL product remaining?"

In relation to the second concern from reviewer A and the first concern from reviewer B (independent review)

Concerns surrounding the concept of a core were raised by both Review A and Review B. The rationale behind question 2 was to ensure that no single component items slipped through the net such as, say a single piece of metal for instance. However, as both reviewers expressed interest in question 2 both points are taken on board in this instance and changes were made to the original question. Question 2 was rewritten as follows,

„Is the product constructed through a manufacturing assembly process involving different parts (such products typically denoted as cores)? Noting that items constructed from a single piece of material, for example some hardware tools, do not have to be assembled and thus are not classed as cores in this instance".

The rewritten question addresses both reviewers concerns. In terms of reviewer A, any confusion over the terms product and core have now been removed by identifying that cores are products which have to be assembled using different parts. In terms of reviewer B, the reason to why the question was asked becomes apparent, i.e. to remove the possibility of products which are not in general able to be described as a cores, i.e. a stand-alone plant pot or a simple spanner or mug for instance, from slipping through to the later stages.

In relation to second concern from reviewer B (independent review)

The point is taken on board and the question rewritten to accommodate the concern that was raised. Question 6 was rewritten as,

„Have all the core components been inspected and subsequently rebuilt or replaced and been reassembled and tested such that the overall product and core components are at a standard equalling that of like new condition or better?"

The question now focuses less on specific remanufacturing process such as cleaning and more on ensuring the global remanufacturing characteristic of „like new" performance.

In relation to third concern from reviewer B (independent review)

The review suggested that the term significant was a vague term to use in this instance. The review comment is noted, rational, reasonable and totally understandable; however the decision taken in this instance is that the term „significant" should remain in the question set. The reason that the term „significant" remains in the question set is that there is in general a grey area between repair and re-use. For instance, after the publication of the WF directive (European Parliament and Council, 2008), additional guidance on this directive was also issued, (European Commission, 2012). When describing re-use, point 1.4.3 of this guidance allows for

"some repairing" to be conducted on a re-used product. Thus, the term „significant" while not crystal clear, owing to the already existing grey area, does allow for at least some distinction between a re-used product and a repaired product.

In relation to fourth concern from reviewer B (independent review)

The review"s point is taken on board in this instance. The wording was changed from "expired" to "consumed".

In relation to fifth concern of reviewer B (independent review)

The review"s point was taken on board. Both the question set and flow are indeed able to be merged into one document.

5.4 Final tool

After two rounds of stakeholder review, a bespoke tool to determine if a product is recycled, remanufactured, reconditioned, re-used or repaired was developed. This is given as Table 19 and Figure 16 – with an alternative version of the final tool, which merges Table 19 and Figure 16 together, given as Figure 17. The validity of the tool has been ensured by the robustness of research design which included thorough analysis by stakeholders on two separate occasions. The tool stood up well to both

rounds of review in that only the wording of some of the questions was altered and so the original interactive flow chart and order of the questions was not changed during both rounds of the review process. It is also the case that no suggestion that the flow chart or question order should be changed occurred during the review process, thus strengthening the case that no definitions of processes were violated using this tool.

Question No	Question
1	Is the vast majority of emergy (see N.B.) retained from original EOL product?
2	Is the product constructed through a manufacturing assembly process involving different parts (such products typically denoted as cores)? Noting that items constructed from a single piece of material, for example some hardware tools, do not have to be assembled and thus are not classed as cores in this instance.
3	Is core capable of being disassembled?
4	Has the core been disassembled?
5	For British remanufacture - Is warranty of product equal to or better than the original? For American remanufacture - Is the product fully warranted?
6	Have all the core components been inspected and subsequently rebuilt or replaced and been reassembled and tested such that the overall product and core components are at a standard equalling that of like new condition or better?
7	Have all major broken components and components on the verge of failure been replaced or repaired?
8	Has the product been restored to an acceptable level in any significant way (and core reassembled if applicable)?
N.B. To create a product of out raw materials then various processes/actions have to be performed. These various processes and actions all require (to some degree) energy to be consumed. The total amount of energy consumed in creating a product is known as emergy or embodied energy. When recycling a product, the product is returned to raw materials and so this emergy is lost and therefore new energy must be consumed to create a new product from the raw materials.	

Table 19 - Final version of the question set. *Reprinted with permission from Paterson, D.A.P., Ijomah, W.L., Windmill, J.F.C., 2017. End-of-Life decision tool with emphasis on Remanufacturing. J. Clean. Prod. 148, 653–664. doi:10.1016/j.jclepro.2017.02.01, under creative commons Attribution License https://creativecommons.org/licenses/by/4.0/*

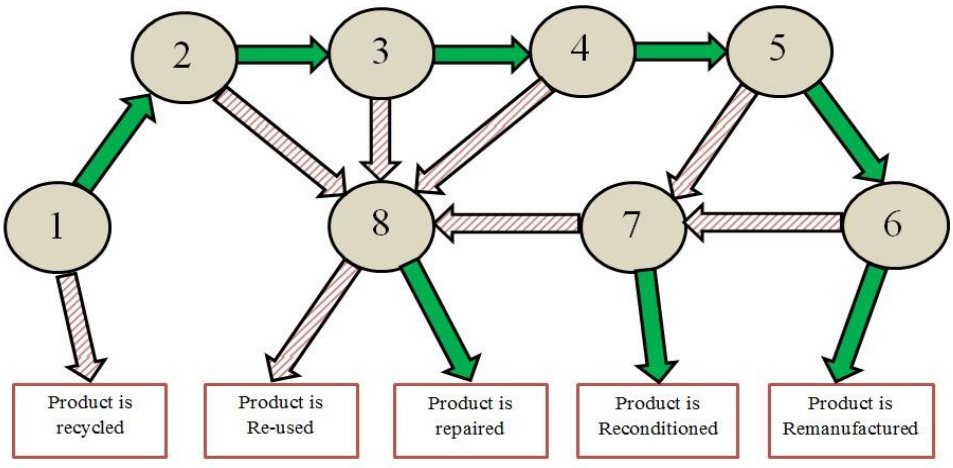

Figure 16 - Final version of the flow chart, which is unchanged from original design.
Reprinted with permission from Paterson, D.A.P., Ijomah, W.L., Windmill, J.F.C., 2017. End-of-Life decision tool with emphasis on Remanufacturing. J. Clean. Prod. 148, 653–664. doi:10.1016/j.jclepro.2017.02.01, under creative commons Attribution License https://creativecommons.org/licenses/by/4.0/

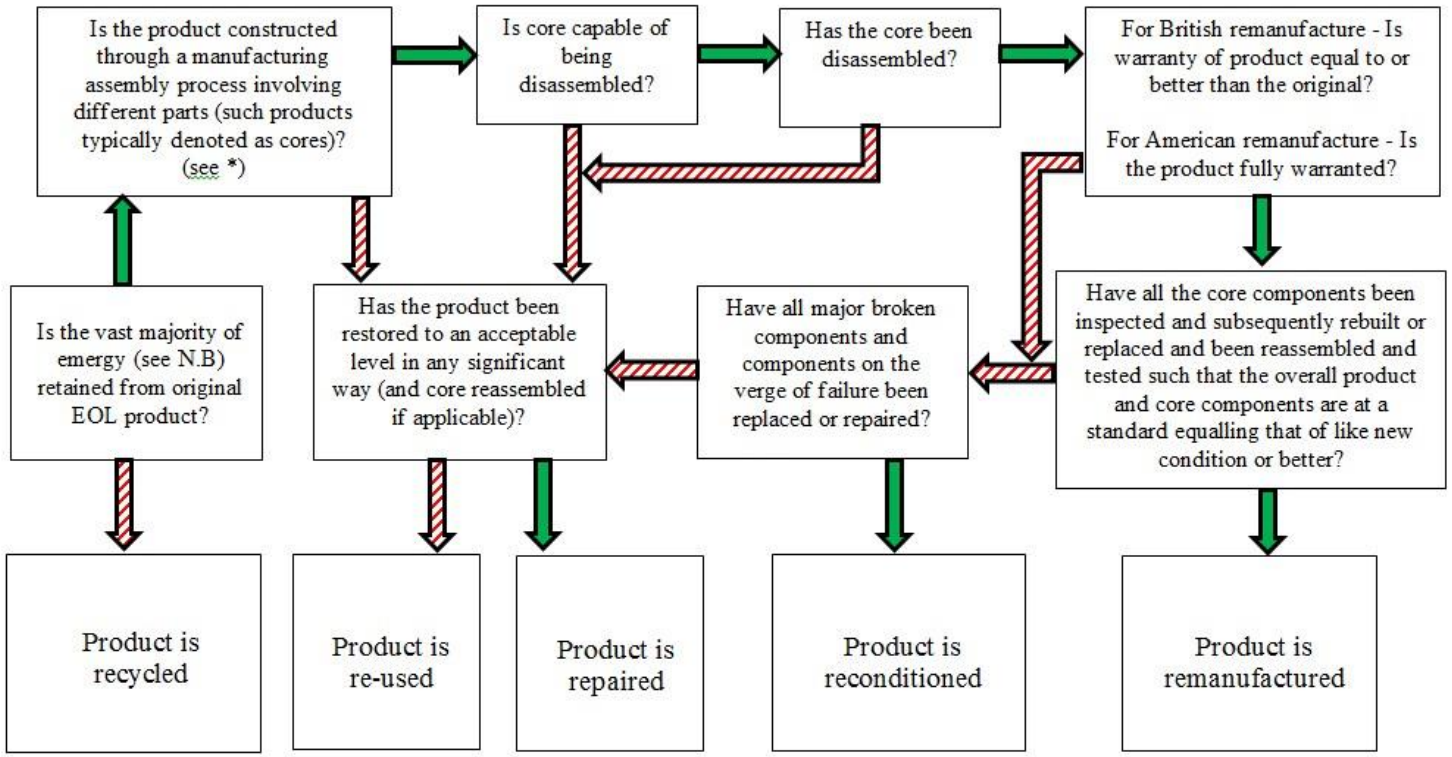

* Noting that items constructed from a single piece of material, for example some hardware tools, do not have to be assembled and thus are not classed as cores in this instance.

N.B. To create a product of out raw materials then various processes/actions have to be performed. These various processes and actions all require (to some degree) energy to be consumed. The total amount of energy consumed in creating a product is known as emergy or embodied energy. When recycling a product, the product is returned to raw materials and so this emergy is lost and therefore new energy must be consumed to create a new product from the raw materials

Yes ⇧ No ⇧

Figure 17 – Combined flow chart and question set**.** *Reprinted with permission from Paterson, D.A.P., Ijomah, W.L., Windmill, J.F.C., 2017.*

5.6 Discussion

As previously stated, the general method to determine if a product has been recycled, remanufactured, reconditioned, repaired or re-used is to interpret the existing definitions of these processes and, possibly with the help of existing tools, come to a conclusion by oneself as to the status of the product. This strategy however, allows for the possibility of confusion, which can lead to errors when forming a decision as to the status of a product. The tool presented in this chapter seeks to eliminate any potential confusion and thus allows one to quickly and efficiently determine if a product is recycled, re-used, repaired, reconditioned, or remanufactured. Also, considering the negative role that ambiguity in the remanufacturing process can have, also included in this tool is a full definition of a remanufactured product. Put simply, this system allows for clear identification of what type of EOL treatment a product has received without having intimate knowledge of the subtle differences between EOL treatments. For example, to determine if a product is recycled, the system presented in this work only requires one question to be asked, namely, „Is the vast majority of emergy retained from original product?“ That is, investigating whether emergy has been retained or not gets to the heart of recycling (in that emergy has been lost) and so a quick determination of a recycled, or not recycled, product is made. Noting that this system allows for identification of a recycled product without entering into any discussion regarding the particular processes involved in recycling. Further, the concept of a core is also used to determine quickly if a product can be reconditioned or remanufactured, for example, question 2 inquires whether the product has a core, if the answer is no, then immediately reconditioned and remanufactured are eliminated and product must be at this point, re-used or repaired.

Considering now re-use and repair, the ruling out either of these two treatments is not possible in the proposed system. Why? Consider the following; examining the definitions of EOL treatments a case could be made that significant cross over between remanufacture, recondition, repair and re-use exists, which, if left unchecked, has the potential to greatly increase confusion levels and possibly overcomplicate the flow chart. For instance, while it is true that a reconditioned or remanufactured product requires a product core, it is not true that a product with a core is always required to be reconditioned or remanufactured, i.e. products with cores can still be repaired or just re-used. This aspect forces the flow chart to have a degree of flexibility such that,

even though a product has a core, the core cannot be used to eliminate repair or re-use. Thus, after navigating question 1, owing to the cross over between definitions of practices, from any stage in the flow chart there is always a path back to question 8. For instance, even though a product has a core and even though the core may have been disassembled and reassembled, the product at hand may still fall under repair or re-use.

The cross over between remanufacture, recondition, repair and re-use leads to the realisation that singling out individual product characteristics that a product must have to be called re-used, repaired, reconditioned or remanufactured is fraught with difficulty. However, the system presented in this chapter manages to do so. It does so by virtue of asking leading questions and using the definition of remanufacture to eliminate potential recovery treatments leaving the only probable answer remaining as the recovery treatment performed. Thus, the issue highlighted with existing methods, i.e. the user must always form their own opinion as to whether a product has been recycled, repaired, re-used, reconditioned or remanufactured, has been removed; the new system presented here informs the user directly.

5.6.1 Scope of the tool

It is important to point out that the system devised in this chapter does not present a deep understanding of the various operational requirements and processes involved in successfully recycling, remanufacturing reconditioning, repairing and re-using products – this analysis has been previously conducted in the many works cited thus far. For instance, the system presented here omits the fact that in order to successfully and continually remanufacture, a company/organization would require a steady supply of cores and that the product should fail from a functionality standpoint and not from a dissipative standpoint.

Specifically, the system presented in this work is not designed to be used by companies or individuals to form a decision as to whether they should begin remanufacturing processes or if a product should be remanufactured, a review of decision making tools is readily found within literature (Goodall et al., 2014). The goal of the tool is to allow for a decision to be made as to which type of product treatment has been given, not as a tool to determine which recovery is best suited to

an organization‟s needs. Thus, by limiting the scope of the tool to one in which an identification of product status is the main focus, a simple and easy to use tool was developed.

5.6.2 Advantages and tool applications

Both definitions of practices and existing tools were shown as legitimate ways to better understand product recovery and material recovery in terms of recycle, remanufacture, recondition, repair and re-use. However, it was been shown that these existing mechanisms do not explicitly identify a recycled, remanufactured, reconditioned, repaired or re-used product. The novel tool in this chapter builds on existing knowledge and for the first time within literature, a method to determine both quickly and accurately whether a product has been recycled, remanufactured, reconditioned, repaired or re-used was presented.

Further, the tool presented in this chapter is able to determine the correct product status in situations in which the user has little or no knowledge of EOL recovery (i.e. no knowledge of recycle, remanufactured, recondition, repair or re-use) and thus has direct applicability to various researchers and the general public. Building on this theme, it is appropriate to return momentarily to the first research question of this thesis. Using the tool developed in this chapter, researchers who hitherto labelled their products as remanufactured would quickly find out, by virtue of the question 1 alone, that remanufacturing is not the correct term, and also identify recycling as the correct term for thermal, chemical and mechanical treatments. An important distinction when you consider that with global composite consumption is growing year on year, chapter 4, (Kraus and Kühnel, 2015), if left unchecked, an impression of a composite remanufacturing industry could be established. Using the tool to find terminology to describe, what researchers currently refer to as re-manufactured CFRP or recycled CFRP, is more problematic owing to the fact this product has not received a recovery operation, i.e. the product is purely manufactured – there is no „re‟ element.

However, it is true that the findings from chapter 4 indicating that reclaimed fibres from chemical and thermal recycling are more realistically classed as re-used as opposed to recycled, would be returned if the fibres are viewed independently of the composite. That is, after recycling and subsequent impregnation with new matrix element, these fibres retain large amounts of emergy when compared to virgin manufacture, and so the first question of the tool would receive a positive answer. The

second question which investigates presence of a core would result in a negative answer, and with question 8 also resulting in a negative response, the answer of reused is returned. Thus, for an operational recycler of CFRP with no knowledge of the subtle differences in recovery strategies, this tool serves as an aid to better articulate their final product, and importantly, the term remanufacture is avoided.

Similar to this concept, a key barrier to the successful implementation of remanufacturing in the UK in terms of consumer engagement is through the false labelling of „remanufactured" products, (Spelman and Sheerman, 2014). Thus, given that the definitions of remanufacturing used as a basis to develop this tool, are in keeping with literature, for example, (BS 8887-2, 2009), the tool presented in this work may be used as a quick, reliable and robust test to determine the correct status of secondary market products by both consumers and stakeholders involved in EOL recovery.

Further, the tool identified in this work may also be used along with existing methods as an effective mechanism to help gauge the wider remanufacturing industry. That is, owing to the simple design and execution of the tool, the tool may be sent to companies involved in EOL recovery processes. In this way, a quick test of the products that are being produced by the company would be enough information for a researcher to determine if the company can be called a remanufacturer. This is of particular interest in cases in which remanufacturers use different terminology to describe remanufacturing. For instance, if the term „overhaul" is being used in the aerospace industry to describe remanufacturing operations, (Gray and Charter, 2007), then by using this tool it would quickly and effortlessly become apparent to both the company and the researcher that overhaul and remanufacture can describe the same process.

Additionally, the literature identified in tables 13 and 14, noting that each work has a different research focus, has been shown to use existing tools to develop the concept of remanufacturing or to highlight the different recovery strategies in terms of a cradle to grave production process. Thus, these researchers now have an additional tool to assist them in reinforcing the concept of a remanufactured product, while also allowing the reader to interactively determine the difference between a recycled, remanufactured, reconditioned, repaired and re-used product.

Further, and focusing on the characteristics of a remanufactured product, an additional benefit from the proposed tool is that only the essential characteristics of a remanufactured product are presented. Expanding on this point, attention may be

drawn to a list outlining the general characteristics that a remanufactured product should have, (Andreu, 1995). This list is outlined below.

1. The product has a core that can be the basis of the restored product. A core is the used equipment to be remanufactured.
2. The product is one which fails functionally rather than by dissolution or dissipation.
3. The core is capable of being disassembled and of being restored to original specification.
4. The recoverable value added in the core is high relative to both its market value and its original cost.
5. The product is one that is factory built rather than field assembled.
6. A continuous supply of cores is available.
7. The product technology is stable.
8. The process technology is stable.

Note that since its original publication, this list has either been replicated or cited directly by various authors as a way to identify the characteristics of a remanufactured product, (Barquet et al., 2013; Go et al., 2015; Ijomah et al., 2007; Linder and Williander, 2015; Matsumoto and Ijomah, 2013; Sundin et al., 2009; Winkler, 2010).

Evaluating this list, it is the authors‟ opinion that only points 1), 2) and 3) are truly indicative of a remanufactured product. That is, a remanufactured product must by definition meet the first three points only. From the authors‟ perspective the remaining points are not considered essential for a product to be remanufactured and are only included in the list for reasons stemming from an economic standpoint.

Consider point 4) which focuses upon the economic value of the core. This point has no bearing on whether a product can be remanufactured – it only has a bearing of whether or not it would be economical advantageous to remanufacture. Consider point 5), again this finding has no bearing on whether a product can be remanufactured and owing to evolving technology and processes it may not be required at all even from an economic standpoint. Points 6), 7) and 8) again are not relevant when considering if a product can be remanufactured - they are only generally relevant when forming a decision on the economic advantages of a remanufacturing operation.

Thus the case is made that points 4-8) are best described as criteria that one would expect from a product that has been remanufactured from an economical/industrial view point. The tool presented in this chapter states a remanufactured product‟s characteristics in isolation of whether it should or should not be remanufactured, and from the characteristics that one would generally expect from an economically driven remanufactured product, a quality that the list by

Andreu (1995) fails to do.

Removing the economically driven element from the list provided by Andreu, allows a less complicated list of the characteristics associated with a remanufactured product to be expressed. That is, another output from this tool is that a list of only essential product characteristics, characteristics that are not debatable, can be presented within literature. Unlike the current list by Andreu, the new list gets to the basis of a remanufactured product directly and may be used as a more realistic and fundamental checklist to both reinforce the concept of a remanufactured product and also to identify a remanufactured product.

For clarity, the essential qualities of a remanufactured product as outlined in the question set and flow chart are expressed, similar to that by Andreu, in a list. This list is given below as points 1-5.

Essential Characteristics of a Remanufactured product

1. Product emergy is retained
2. The product has a core
3. The core is capable of being disassembled and reassembled
4. The product has a warranty equal or better than original
5. All core components have been replaced or restored to their original standard.

5.7 Conclusion

This chapter has documented a bespoke tool designed to assist in the decision making process as to whether a product has been recycled, re-used, repaired, reconditioned or remanufactured. Existing tools within literature have been identified and discussed with the novelty of the tool presented in this chapter identified. That is, it was shown that existing methods to determine the status of a product require the user to interpret tools or read definitions in order to make a decision. The tool presented in this work effectively removes this decision making process from the user (the tool tells them, i.e. they don‟t in general form their own decision).

Along with helping to strengthen the definition of a remanufactured product, the tool has also been highlighted as having applicability in other industries such as public perception or in the aerospace industry as a check for a remanufacturing synonym

such as overhaul. Further, by allowing the tool to be focused on what type of EOL treatment a product has received and not which type the product should receive, it was possible to deconstruct a widely used list of remanufacturing product characteristics into a list of only the essentially characteristics of a remanufactured product. That is, supply of cores, stable process and product technology, factory assembly and recovery value associated with the core were shown to be characteristics of a product remanufactured from an economical point of view, i.e. they are not essential for a product to be classed as remanufactured. Further, attention was turned back to the first research question in that the tool returned a correct answer of recycled to describe industry and academic based thermal, chemical and mechanical treatment for EOL CFRP, while also highlighting that remanufacturing is not the correct terminology to describe composite made from reclaimed fibres, i.e. what this research describes as rf-CFRP. Additionally it was further highlighted that if reclaimed fibres were put through the tool in isolation of the matrix element, they would be classed as re-used, which is in keeping with the findings from chapter 4.

Additionally, the tool presented in this chapter was crafted from two rounds of review from both industry and academia. An initial tool presented at ICoR 2015 was endorsed with discussion, and subsequent changes documented. The amended tool was then subject to an additional round of review which resulted in the final tool and question set. It is of merit to note that during the review process only the questions were altered, the original flow chart and ordering of questions survived two rounds of cross examination, thus no errors in product classification were recorded in the review process.

Having now documented a conclusion to the first research question, and presented an additional contribution to knowledge, by way of this chapter, attention is now drawn to the second research question.

Chapter 6: Acoustic wave velocity and elastic constant relationship in solids

At this stage the recycling and „remanufacturing" processes conducted by industry and academia have been investigated. In addition to documenting these processes it has been shown that „remanufacturing" terminology is being used incorrectly and that recycling terminology is used correctly and in a liberal way. New terminology has also been presented to better describe these materials. Additionally, the problems associated with incorrect terminology have also been identified and discussed. Given the on-going research by industry and academia to recycle and reuse vCFRP, an awareness of product qualities is of clear importance; i.e. only through an awareness of material properties can rf-CFRP begin to find new applications. It is therefore appropriate to investigate the material properties of rf-CFRP. The second research question outlines the scope of this investigation, given again as below for completeness,

Ultrasonic velocity measurements, specifically, the through transmission technique, have long been used to determine the elastic constants of virgin CFRP. Products denominated as recycled and remanufactured CFRP are not v-CFRP; thus, are the standard ultrasonic through transmission measurements routinely used on v-CFRP applicable to recycled and remanufactured (if these are the correct terms) CFRP?

Prior to this analysis additional groundwork is required; specifically, a) a supporting argument for investigating the elastic constants, b) the rationale for adopting NDT and the choice of NDT (ultrasound), c) a derivation of wave velocity and elastic constants relationship and d) a relevant literature review. In this chapter, a), b) and c) are discussed with the literature review given separately in chapter 7.

6.1 Elastic constants, NDT and Ultrasound Through Transmission

6.1.1 Elastic Constants

When seeking to evaluate rf-CFRP, various materials properties may be determined, for instance electrical properties, radioactive properties, mechanical properties, thermal properties etc. Given practical constraints of this thesis, coupled with CFRP (and composite in general), often being selected for superior mechanical performance over existing materials, for example strength to weight ratio, the decision was taken to investigate mechanical properties.

The term mechanical properties is in itself however broad and covers various properties including Young‟s modulus, bulk modulus, toughness, rigidity, hardness, Poisson‟s ratio and ultimate tensile strength. Further, given that very often composite materials experience some form of loading when in practical application, the elastic properties of the materials are hugely important. In the elastic region, a material which has undergone deformation (see section 6.2.1) will return to its original state once the loading (or external force) has been removed, i.e. no permanent deformation, rupture or fracture will occur in the elastic region. It is also the case that within the elastic region various mechanical properties can at a fundamental level be explained as a function of the material elastic constants. Thus determining the elastic constants of a material allows for various mechanical properties of materials in the elastic region to be derived, for example, Young‟s modulus, bulk modulus, shear modulus, Poisson‟s ratio, toughness etc.

6.1.2 NDT/E

With a decision taken to investigate the elastic constants, and therefore elastic properties of the rf-CFRP, it is appropriate to discuss why the choice of NDT is appropriate.

Within literature the general method to examine the elastic properties of rfCFRP is via mechanical based tensile, compression and shear testing. It is true that some non-destructive testing is utilized in the examination of rf-CFRP, but not as means to

determine the elastic constants of the composite; consider Pimenta and Pinho (2012) and Pimenta (2010) who examined mechanical properties of rf-CFRP and v-CFRP. The authors use mechanical testing based on ASTM standards (ASTM D 3039/D 3039M–14, 2014; ASTM D 3518/D 3518M–94, 2008; ASTM D 5379/D 5379M–05, 2008) as a means to evaluate the mechanical properties. The nondestructive testing element used by (Pimenta and Pinho, 2012) and (Pimenta et al., 2010) was both optical microscope analysis and SEM analysis and was used to determine aspects such as fibre breakage, thickness and recycling phenomenon like fibres bunching together.

The focus on using mechanical testing to examine the elastic properties of rfCFRP, while also using non-destructive methods to examine areas such as surface fracture, residual resin and fibre content is also recorded and cited in many of the works documented thus far, (Adams et al., 2014; Heil, 2011; Ogi et al., 2007; Okayasu et al., 2013; Oliveux et al., 2015; Shi et al., 2012a). Note that in the case of Adams et al, the authors adopt standard mechanical testing but also adopt a nondestructive vibration test.

Given the strong focus on mechanical testing at the expense of NDT to determine the mechanical and elastic properties of rf-CFRP, rationale for exploring NDT is apparent. In addition the benefits of NDT are also key drivers and provide further research justification.

A typical NDT benefit is practicality. NDT measurements can often be conducted on in-situ components which can provide reduced down time by avoiding delay caused by large scale disassembly. Further, when conducting testing in a laboratory setting NDT can again offer more practicality than mechanical based testing. Thermography and ultrasonic NDT can for example be performed on a small laboratory desk whereas mechanical testing requires larger laboratories able to provide easy installation and house large scale equipment. NDT can also provide financial savings. For example, the extensometer (which is only a small part of much larger mechanical testing arrangement) used as part of this research was priced around £35,000, whereas the ultrasonic transducers used were only in the 100‟s of pounds. Further, giving the ability to conduct in-situ measurements, potential faults or areas requiring attention are highlighted before they cause a system failure and thus costly unscheduled system downtime is avoided. Further still, mechanical testing can also require particular shaped components which require therefore some degree of destructive machining. Lastly, NDT is also non-destructive and so has an advantage over some forms of mechanical testing which are destructive.

Having now highlighted that literature focuses on mechanical testing to determine various elastic properties of rf-CFRP along with highlighting the benefits of NDT over mechanical testing, research justification for conducting NDT has been shown. Attention is now turned to the rationale for ultrasonic analysis.

6.1.3 Ultrasound Through Transmission

Various types of NDT have application to composite materials, for instance ultrasound, acoustic emission, thermography, eddy current analysis, and radiography (X-Ray). Recent composite NDT reviews, (Gholizadeh, 2016; Ibrahim, 2014; Jolly et al., 2015), discuss these various strategies further. The choice of ultrasound was selected for this thesis, specifically the choice of ultrasound through transmission.

The choice of ultrasound through transmission was selected principally because the technique exploits a fundamental relationship between acoustic wave velocity and the elastic constants of a solid; this relationship is not exploited directly using other NDT techniques. Consider for instance, ultrasound pulse echo, ultrasound imaging (arrays, scanning acoustic microscope etc.) eddy current analysis, thermography, acoustic emission and radiography. These techniques are most often applied to identify and characterise surface and internal defects, delaminations and voids; the elastic constants are only able to be indirectly inferred having knowledge of the defect. The goal of these many NDT approaches is focused upon defect detection. Note however that while the elastic constants are not returned, mechanical properties can still be determined; thermography for instance can be used in conjunction with on-going mechanical loading to accurately estimate composite properties such as fatigue limits (Vergani et al., 2014). Further, ultrasound through transmission is a long established technology with regards to v-CFRP. A literature review in chapter 7 presents around 45 years of literature and highlights some 40 different contributions to knowledge during this period. With ultrasound through transmission having well documented application to v-CFRP, adopting the same NDT approach to rf-CFRP will return results clearly of interest to the CFRP NDT research community. There is also a lack of literature, (see chapter 7) into the use of ultrasound through transmission to determine the elastic constants of rf-CFRP, thus further justification for adopting this approach is provided.

Additionally ultrasound is a practical and safe technology requiring minimal safety conditions and so is ideal for operations in multiple environments by multiple researchers. Consider for example the health and safety concerns which have an impact on the efficiency and location of where radiography is able to be conducted. Finally, in addition to the justification provided thus far, given that this research was conducted in cooperation with the Centre for Ultrasonic Engineering (which included access to staff members and equipment), ultrasound was a natural choice.

6.2 Acoustic wave velocity and elastic constant relationship in solids

Having opted for the ultrasound through transmission technique as the desired approach to determine the elastic constants of rf-CFRP (noting the elastic constants allow the mechanical properties of solids in the elastic region to be determined), the fundamental relationship between wave velocity and elastic constants is presented. The relationship is presented as the Christoffel equation which is an incredibly powerful equation and houses a lot of information. Thus, prior to a literature review and experimental analysis, a derivation of the Christoffel equation from first principles is outlined. The Christoffel equation derivation is relatively complex and so to keep this thesis manageable, parts of the derivation are placed into an appendix. Performing a relatively in depth derivation allows, for a) a standalone chapter able to accessed independently of this thesis and b) the literature review and experimental analysis to be far more accessible owing to the thorough ground work involved in laying the fundamental principles.

The Christoffel equation, both in terms of derivation and execution, is dependent on aspects such as deformation, strain, stress, the compliance and stiffness matrices (the constitutive equation), divergence of stress and the equation of motion. Thus, for a complete examination of the Christoffel equation it is the case that all these areas are to some degree required to be discussed.

Much literature exists concerning the fundamentals of acoustic wave propagation,(Auld, 1990; Musgrave, 1954a; Prosser, 1987; Rokhlin et al., 2011; Rose, 2014). In this chapter, the development and presentation of the Christoffel equation follows the pattern of derivation as outlined previously by Auld (1990) with additional information bolstering the subject matter also utilized - information drawn from other

sources and derivations referenced to in literature but not traditionally shown with literature.

Further areas found in literature such as coordinate transforms are not required in this thesis or in the Christoffel derivation and so are not included in this chapter. This chapter does not cover the whole gambit of acoustic wave phenomenon and is instead strongly focused on only the essential areas required to allow for the wave velocity to be expressed in terms of the elastic constants of materials.

6.2.1 Deformation

Acoustic waves propagating within a solid arise from the interplay between deformation and elastic restoring forces (stress). Thus, to provide a mathematical framework to understand wave propagation, both deformation and stress are required to be understood. Deformation is considered first.

In acoustic wave propagation within solids, it is common practice to denote the material as a continuum, that is, the structure and oscillations of atoms at the atomic level is in general not considered, i.e. the material is treated as a series of small particle elements (composed of groups of atoms) which are connected in a continuous way. Thus, deformation in this context may be put forward as;

When particles (small volume elements) are displaced from their equilibrium positions in such a way that a relative displacement between two neighbouring particles occurs, deformation is said to have occurred.

This definition may also be considered graphically, which if done so allows for a mathematical definition of deformation to be derived. Consider Figure 18.

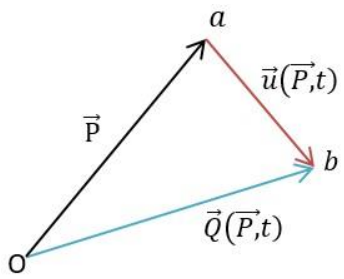

Figure 18 - Graphical representation of a particle displacement. Particle originally at position a, is moved to position b. Adapted from (Auld, 1990)

Figure 18 documents a particle (small volume element) at equilibrium position, position a, being moved to new position, position b. A position vector from an origin point to the equilibrium position of the particle is given by vector **P** (note that arrow notation and bold face notation used interchangeably). The displaced particle is at position „b" and given by the displaced position vector **Q** which is a vector function of **P** and time, t. The vector **u**, which is function of **P** and t, may therefore be considered as a measure of particle displacement from equilibrium. Vector **u,** the displacement vector, through vector addition, may be defined as equation 1,

$$\vec{u}(\vec{P},t) = \vec{Q}(\vec{P},t) - \vec{P} \qquad (1)$$

Deformation is however only apparent when relative displacement has occurred. This concept is outlined in Figure 19.

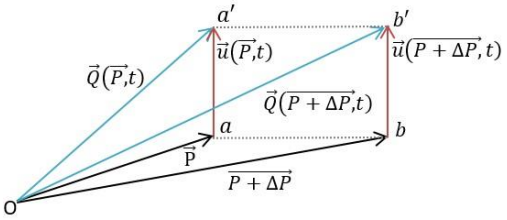

Figure 19 – Relative displacement between two neighbouring particles. In this instance there is no relative displacement after movement to new location, a" and b". Adapted from(Auld, 1990)

Figure 19 documents the resultant displacement between two particles, displaced from their equilibrium positions by the same amount. That is, at equilibrium positions, a and b, the particles undergo a displacement such that the resulting location of these particles is a" and b". Although a clear difference in position vector from origin to particle a and particle b can be observed, i.e. they differ by a change in

P, ΔP, the displacement vector for the relative particles is unchanged and not equal to zero, i.e.

$$\vec{u}(\vec{P},t) = \vec{u}(\overrightarrow{P+\Delta P},t) \neq 0$$

That is, the relative displacement between the displaced particles is unchanged and so no deformation is recorded. Thus, as the displacement vector does not equal zero when no deformation is present, the displacement vector in isolation is not sufficient to define deformation.

As deformation is defined as the relative displacement, from equilibrium position, between two particles, it is natural to consider a variable which describes the relative displacement between particles after displacement from equilibrium. That is, a

variable which describes the small change in **u** arising from a small change in **P** is required, i.e. Δ**u**,

$$\overrightarrow{\Delta u} = \vec{Q}\left(\overrightarrow{P + \Delta P}, t\right) - \left(\overrightarrow{P + \Delta P}\right) - \left(\vec{Q}\left(\vec{P}, t\right) - \vec{P}\right) \qquad (2)$$

As Δ**P** tends to zero, and at constant time, equation 2 may be considered in differential form, that is

$$d\vec{u}\left(\vec{P}, t\right) = \frac{d\vec{u}}{d\vec{P}} d\vec{P} \qquad (3)$$

Expanding equation (3) to reflect that the vector variable **P** is a function of 3 variables, x, y and z, gives equation (4)

$$d\vec{u}\left(\vec{P}, t\right) = \frac{\partial \vec{u}\left(\vec{P}, t\right)}{\partial P_x} dP_x + \frac{\partial \vec{u}\left(\vec{P}, t\right)}{\partial P_y} dP_y + \frac{\partial \vec{u}\left(\vec{P}, t\right)}{\partial P_z} dP_z \qquad (4)$$

Note however that vector variable **u** is a function of 3 variables, x, y and z, that is,

$$\vec{u}\left(\vec{P}, t\right) = \hat{x} u_x\left(\vec{P}, t\right) + \hat{y} u_y\left(\vec{P}, t\right) + \hat{z} u_z\left(\vec{P}, t\right) \qquad (5)$$

And so equation (4) may be expanded to reflect this, this expansion given as equation (6)

$$\begin{aligned} d\vec{u}\left(\vec{P}, t\right) = {} & \hat{x}\left(\frac{\partial u_x\left(\vec{P}, t\right)}{\partial P_x} dP_x + \frac{\partial u_x\left(\vec{P}, t\right)}{\partial P_y} dP_y + \frac{\partial u_x\left(\vec{P}, t\right)}{\partial P_z} dP_z\right) \\ & + \hat{y}\left(\frac{\partial u_y\left(\vec{P}, t\right)}{\partial P_x} dP_x + \frac{\partial u_y\left(\vec{P}, t\right)}{\partial P_y} dP_y + \frac{\partial u_y\left(\vec{P}, t\right)}{\partial P_z} dP_z\right) \\ & + \hat{z}\left(\frac{\partial u_z\left(\vec{P}, t\right)}{\partial P_x} dP_x + \frac{\partial u_z\left(\vec{P}, t\right)}{\partial P_y} dP_y + \frac{\partial u_z\left(\vec{P}, t\right)}{\partial P_z} dP_z\right) \end{aligned} \qquad (6)$$

It is now apparent that given a change in **P**, and assuming the change in **P** is known, then d**u,** the small change in **u** between two particles displaced from equilibrium positions given a change of **P**, is now able to be realised. It is also true that displacement as documented in Figure 19, displacement known as rigid translation (sliding the whole medium from one position to another) results in a value of 0 for d**u**. Thus, a d**u** value other than 0 will always arise when a medium has been deformed.

While d**u** will never be 0 for a deformed medium, it is not true that a d**u** value other than 0 will always describe a deformed medium. A medium may be manipulated via a rotation such that d**u** will not be equal to zero, but still not deformed. Figure 20 demonstrates this point.

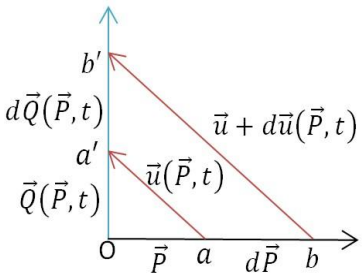

Figure 20 – Documents rotation of 90 degrees so that particles a and b are now located at positions a‟ and b‟

Figure 20 demonstrates that owing to a rotation of 90 degrees the displacement between particles „a‟ and „b‟ is the same as before rotation but the relative particle displacement, d**u,** is not equal to zero - a non-zero d**u** is not sufficient to determine if deformation has occurred. Using both Figure 19 and Figure 20, a value which does remain zero in both cases is able to be expressed. Consider the dotted lines in Figure 19 to equal d**Q**(**P**,t) and d**P** such that,

$$\vec{Q}\left(\overrightarrow{P+\Delta P},t\right) = \vec{Q}\left(\vec{P},t\right) + d\vec{Q}\left(\vec{P},t\right) \text{ and } \overrightarrow{P+\Delta P} = \vec{P} + d\vec{P} \qquad (7)$$

With d**Q**(**P**,t) being the infinitesimal change in **Q** arising from the infinitesimal change in **P** and d**P** being the infinitesimal change in **P**. Using these relations, it can be seen that the equation (8) will equal zero in both cases.

$$\Delta\left(\vec{P},t\right) = dQ\left(\vec{P},t\right) - dP \qquad (8)$$

Equation (8) is used to mathematically define deformation, i.e. all non-zero outputs from equation (8) are indicative of deformation. Further, performing a subtraction of two vectors with equal magnitude but pointing in different directions will not return a zero vector thus, both quantities are defined as scalar values. Further still, as identified by Auld (1990), equation (9) will also equal 0 in both cases, and is more helpful formula (in terms of eventual further manipulation). Thus equation (9) is the measure of deformation used within this thesis.

$$\Delta'\left(\vec{P},t\right) = dQ^2\left(\vec{P},t\right) - dP^2 \qquad (9)$$

After multiplying out equation (9) and rearranging terms, the global measure of deformation is able to be expressed as equation (10). The derivation of equation (10) from equation (9) is given in section 4.1 of appendix 1.

$$\Delta'\left(\vec{P},t\right) = dQ^2\left(\vec{P},t\right) - dP^2 = 2\varepsilon_{ij}\left(\vec{P},t\right)dP_i dP_j \qquad (10)$$

With,

$$\varepsilon_{ij}(\vec{P},t) = \frac{1}{2}\left(\frac{\partial u_i(\vec{P},t)}{\partial P_j} + \frac{\partial u_j(\vec{P},t)}{\partial P_i} + \frac{\partial u_k(\vec{P},t)}{\partial P_i}\frac{\partial u_k(\vec{P},t)}{\partial P_j}\right) \qquad (11)$$

$$for\ i,j,k = x,y,z$$

Noting the convention within academia is to perform a summation over any repeated subscripts which appear solely on the right hand side of the equation.

6.2.2 Strain and linearized theory for small particle displacement

With reference to (Brinson and Brinson, 2008; Chaves, 2013; Tuttle, 2015) the concept of strain is introduced. Strain, at a given point, or point strain, may be normal or shear; normal strain being a dimension alteration of the medium (the ratio of the change in length over reference length) and shear strain the reduction in angle between two sets of orthogonal axis after deformation.

Further, equation (11) is the mathematical definition of both normal strain and shear strain. For instance, normal point strain in the x-direction is determined by setting both the i and j elements of equation (11) to x and performing summation over k. This gives,

$$\varepsilon_{xx} = \frac{1}{2}\left(\frac{\partial u_x(\vec{P},t)}{\partial P_x} + \frac{\partial u_x(\vec{P},t)}{\partial P_x} + \left(\frac{\partial u_x(\vec{P},t)}{\partial P_x}\right)^2 + \left(\frac{\partial u_x(\vec{P},t)}{\partial P_y}\right)^2 + \left(\frac{\partial u_x(\vec{P},t)}{\partial P_z}\right)^2\right)$$

However, for very small particle deviations, as is common with acoustic wave propagation the squared terms may be dropped and the x direction normal point strain can be expressed by equation (12).

$$\varepsilon_{xx} = \frac{\partial u_x}{\partial P_x} \qquad (12)$$

A similar argument holds for the y and z normal point strains, i.e.

$$\varepsilon_{yy} = \frac{\partial u_y}{\partial P_y} \quad \varepsilon_{zz} = \frac{\partial u_z}{\partial P_z} \quad (13)$$

In terms of shear strain a similar argument holds

$$\varepsilon_{xy} = \varepsilon_{yx} = \frac{1}{2}\left(\frac{\partial u_x}{\partial P_y} + \frac{\partial u_y}{\partial P_x}\right)$$

$$\varepsilon_{xz} = \varepsilon_{zx} = \frac{1}{2}\left(\frac{\partial u_x}{\partial P_z} + \frac{\partial u_z}{\partial P_x}\right)$$

$$\varepsilon_{yz} = \varepsilon_{zy} = \frac{1}{2}\left(\frac{\partial u_y}{\partial P_z} + \frac{\partial u_z}{\partial P_y}\right) \qquad (14)$$

Under the same argument that led to equation (12) for very small particle displacements, linearized theory holds such that vector **P** is approximately equal to **Q** (see Figure 19), and so equation (10) may be rewritten as equation (15) and equation (11) may be rewritten as equation (16); **P** vector is replaced by vector of denomination **r**.

$$\Delta'(\vec{r}, t) = 2\varepsilon_{ij}(\vec{r}, t) dr_i dr_j \qquad (15)$$

$$\varepsilon_{ij}(\vec{r}, t) = \frac{1}{2}\left(\frac{\partial u_i(\vec{r}, t)}{\partial r_j} + \frac{\partial u_j(\vec{r}, t)}{\partial r_i}\right) \qquad (16)$$

Notice the dropping of the squared terms also in equation (16). Note additionally, strain elements are able to be expressed compactly as a tensor. This relationship is given below as equation (17) - noting that a tensor quantity is always given in bold in this thesis. A derivation of shear and normal strains are given in section 2.0 of appendix 1.

$$[\boldsymbol{\varepsilon}] = \begin{bmatrix} \frac{\partial u_x}{\partial r_x} & \frac{1}{2}\left(\frac{\partial u_x}{\partial r_y} + \frac{\partial u_y}{\partial r_x}\right) & \frac{1}{2}\left(\frac{\partial u_x}{\partial r_z} + \frac{\partial u_z}{\partial r_x}\right) \\ \frac{1}{2}\left(\frac{\partial u_x}{\partial r_y} + \frac{\partial u_y}{\partial r_x}\right) & \frac{\partial u_y}{\partial r_y} & \frac{1}{2}\left(\frac{\partial u_y}{\partial r_z} + \frac{\partial u_z}{\partial r_y}\right) \\ \frac{1}{2}\left(\frac{\partial u_x}{\partial r_z} + \frac{\partial u_z}{\partial r_x}\right) & \frac{1}{2}\left(\frac{\partial u_y}{\partial r_z} + \frac{\partial u_z}{\partial r_y}\right) & \frac{\partial u_z}{\partial r_z} \end{bmatrix} = \begin{bmatrix} \varepsilon_{xx} & \varepsilon_{xy} & \varepsilon_{xz} \\ \varepsilon_{xy} & \varepsilon_{yy} & \varepsilon_{yz} \\ \varepsilon_{xz} & \varepsilon_{yz} & \varepsilon_{zz} \end{bmatrix} \qquad (17)$$

6.2.3 Strain and particle displacement gradient relationship

Looking ahead to section 6.3, which derives the Christoffel equation, it is appropriate at this stage to identify a relationship between the particle displacement and strain. Looking at equation (6),

$$d\vec{u}(\vec{P},t) = \begin{aligned} &\hat{x}\left(\frac{\partial u_x(\vec{P},t)}{\partial P_x}dP_x + \frac{\partial u_x(\vec{P},t)}{\partial P_y}dP_y + \frac{\partial u_x(\vec{P},t)}{\partial P_z}dP_z\right) \\ &+\hat{y}\left(\frac{\partial u_y(\vec{P},t)}{\partial P_x}dP_x + \frac{\partial u_y(\vec{P},t)}{\partial P_y}dP_y + \frac{\partial u_y(\vec{P},t)}{\partial P_z}dP_z\right) \\ &+\hat{z}\left(\frac{\partial u_z(\vec{P},t)}{\partial P_x}dP_x + \frac{\partial u_z(\vec{P},t)}{\partial P_y}dP_y + \frac{\partial u_z(\vec{P},t)}{\partial P_z}dP_z\right) \end{aligned} \qquad (6)$$

Equation (6) describes the small changes in **u,** d**u**, that arise when small changes in **P** occur. Noting linearized theory where **P** becomes **r,** rewriting equation (6) in a compact scalar form, equation (17) is given.

$$\begin{bmatrix} du_x(\vec{r},t) \\ du_y(\vec{r},t) \\ du_z(\vec{r},t) \end{bmatrix} = \begin{bmatrix} \frac{\partial u_x(\vec{r},t)}{\partial r_x} & \frac{\partial u_x(\vec{r},t)}{\partial r_y} & \frac{\partial u_x(\vec{r},t)}{\partial r_z} \\ \frac{\partial u_x(\vec{r},t)}{\partial r_y} & \frac{\partial u_y(\vec{r},t)}{\partial r_y} & \frac{\partial u_y(\vec{r},t)}{\partial r_z} \\ \frac{\partial u_x(\vec{r},t)}{\partial r_z} & \frac{\partial u_y(\vec{r},t)}{\partial r_z} & \frac{\partial u_z(\vec{r},t)}{\partial r_z} \end{bmatrix} \begin{bmatrix} dr_x \\ dr_y \\ dr_z \end{bmatrix} \qquad (17)$$

As with academic convention, the matrix with the partial derivatives, which is actually a tensor of rank 2, may be defined as the displacement gradient tensor, whose elements and overall tensor may be given by,

$$[\boldsymbol{\nabla u}] \text{ with } \nabla u_{ij} = \frac{\partial u_i(\vec{r},t)}{\partial r_j} \qquad (18)$$

It can now be noted that upon dividing the displacement gradient tensor into both symmetric and anti-symmetric parts, as in equation (19)

$$[\boldsymbol{\nabla u}] = \frac{1}{2}([\boldsymbol{\nabla u}] + [\boldsymbol{\nabla u}]^T) + \frac{1}{2}([\boldsymbol{\nabla u}] - [\boldsymbol{\nabla u}]^T) \qquad (19)$$

Then the strain tensor $[\boldsymbol{\varepsilon}]$, may be thought of the symmetric part with the antisymmetric part equating to a rotation of the solid medium. That is,

$$[\boldsymbol{\varepsilon}] = \frac{1}{2}([\boldsymbol{\nabla u}] + [\boldsymbol{\nabla u}]^T) \qquad (20)$$

6.2.4 Stress

The next fundamental topic requiring discussion is stress. Within academia, stress is most commonly understood using infinitesimal volume elements, such as infinitesimal small cubes and infinitesimal small tetrahedrons, as tools to develop the

resulting argument. The approach taken in this thesis is consistent with this approach and as outlined by (Auld, 1990; Chaves, 2013; Cleland, 2003; Gopalakrishnan et al., 2011; Irgens, 2008).

Stress in its simplest form may be thought of as the resulting forces that arise when a solid body has undergone deformation. More specifically, stress may be thought of as the internal „restoring forces" that oppose the external deformation forces. Stress ultimately aims to restore the body to equilibrium as the external forces try to deform the body, noting that both restoring forces and deformation forces may be regarded as traction forces, in this case force per unit area, (Auld, 1990).

To provide a mathematical framework for this phenomenon, consider initially a small cube subjected to a deformation force at its boundaries. If an infinitesimal cube is extracted from this small cube, the elastic restoring forces (stresses) fighting against the deformation are able to be realised, this infinitesimal cube is given as Figure 21.

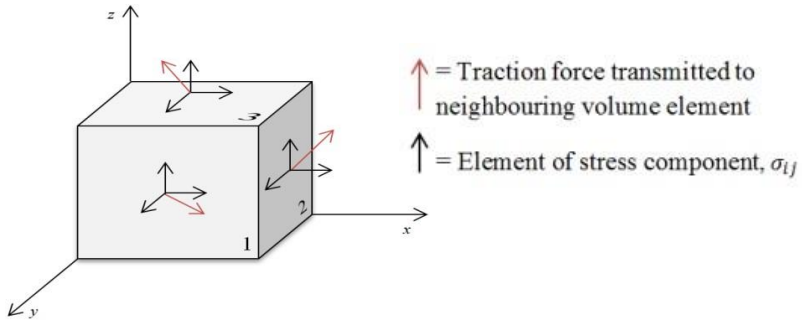

Figure 21 – Infinitesimal cube subject to a traction force and therefore showing stress and resulting traction force transmitted to neighbouring particle

It can be seen that elastic restoring forces, stated from now on as traction forces, are acting upon an additional infinitesimal volume element not shown and faces 1, 2 and 3 normal to coordinate directions, x y and z. Further, it can be stated that the traction force is comprised of 3 stress components, in this case, an x component, a y component and a z component.

The three stress components on a given face may be defined using equation (21),

$$\sigma_{ij} \qquad (21)$$

$$for\ i,j = x,y,z$$

Noting here that the ith component of stress may be thought of as the force direction and the jth component of stress may be thought of as the direction to which the surface

is facing or the direction to which a normal vector to a surface faces, i.e. in Figure 21, σ_{xy} is x component of stress acting on the y facing surface.

Additionally the total stress that each face undergoes may be represented compactly, and is known as the Cauchy stress tensor, given as equation (22),

$$\boldsymbol{\sigma} = \begin{bmatrix} \sigma_{xx} & \sigma_{xy} & \sigma_{xz} \\ \sigma_{yx} & \sigma_{yy} & \sigma_{yz} \\ \sigma_{zx} & \sigma_{zy} & \sigma_{zz} \end{bmatrix} \qquad (22)$$

Equations (23-25) may now be presented to document the traction forces impacting upon surfaces, which in this case are normal to coordinate axes, x, y and z,

$$\overrightarrow{T_x} = \sigma_{xx}\hat{x} + \sigma_{xy}\hat{x} + \sigma_{xz}\hat{x} \quad (23)$$

$$\overrightarrow{T_y} = \sigma_{yx}\hat{y} + \sigma_{yy}\hat{y} + \sigma_{yz}\hat{y} \quad (24)$$

$$\overrightarrow{T_z} = \sigma_{zx}\hat{z} + \sigma_{zy}\hat{z} + \sigma_{zz}\hat{z} \quad (25)$$

Noting that the traction forces that a particular surface is subjected to may be given as equations (26-28),

$$\overrightarrow{T_x} = \sigma_{xx}\hat{x} + \sigma_{yx}\hat{y} + \sigma_{zx}\hat{z} \quad (26)$$

$$\overrightarrow{T_y} = \sigma_{xy}\hat{x} + \sigma_{yy}\hat{y} + \sigma_{zy}\hat{z} \quad (27)$$

$$\overrightarrow{T_z} = \sigma_{xz}\hat{x} + \sigma_{yz}\hat{y} + \sigma_{zz}\hat{z} \quad (28)$$

As both sets of equations define two different vectors but use the same notation to describe these vectors, to avoid confusion going forward $\overrightarrow{T_i}$(where i may be x, y or z) applies only to equations (26-28) for the remained of this thesis unless otherwise stated.

Equations (26 – 28) only describe traction forces impacting on surfaces which perfectly face the x, y and z direction. It is more realistic to use the fundamental form of the traction force stress relationship to deal with surfaces whose surface normal is combination of x, y and z directions. Figure 22 is given to exemplify such a surface.

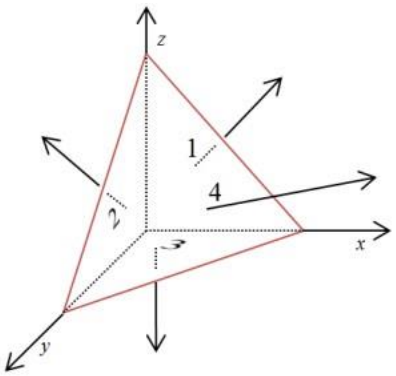

Figure 22 – Tetrahedron, with sides 1, 2, 3 and 4 having on outward traction force impacting on a neighbouring volume element (not shown in figure). The outward normal of side 4 has x, y and z dependence.

The general form of stress impacting upon a surface, which has a normal facing the n direction, is given by equation (29), noting the Cauchy stress tensor incorporating 9 terms.

$$\begin{bmatrix} T_{xn} \\ T_{yn} \\ T_{zn} \end{bmatrix} = \begin{bmatrix} \sigma_{xx} & \sigma_{xy} & \sigma_{xz} \\ \sigma_{yx} & \sigma_{yy} & \sigma_{yz} \\ \sigma_{zx} & \sigma_{zy} & \sigma_{zz} \end{bmatrix} \begin{bmatrix} n_x \\ n_y \\ n_z \end{bmatrix} \quad (29)$$

And so,

$$\left[\overrightarrow{T_n}\right] = [\boldsymbol{\sigma}][\hat{n}] \quad or \quad \overrightarrow{T_n} = \boldsymbol{\sigma} \cdot \hat{n} \quad (30)$$

Where,

$$\overrightarrow{T_n} = \overrightarrow{T_{xn}} + \overrightarrow{T_{yn}} + \overrightarrow{T_{zn}} \qquad (31)$$

Noting that x, y and z unit vectors symbols are omitted and that under the assumption of linearized theory (very small particle deviations) the Cauchy stress tensor is also symmetric in that $\sigma_{ij} = \sigma_{ji}$. A more detailed derivation of the general form of the stress equations is given in section 3.0 of appendix 1.

6.2.5 Relating stress to strain - constitutive relations

Having now documented a deformation, strain and stress, the constitutive relations, which are a set of equations which relate these variables, are now presented.

In the linear elastic region, this region being classed as one in which a deformed solid will return to equilibrium when the deformation is removed from the solid, Hooke"s law identifies that strain may be considered to be linearly proportional to stress, and vice-versa. As outlined by (Auld, 1990; Bunsell and Renard, 2005; Chaves, 2013; Rokhlin et al., 2011; Rose, 2014; Royer and Dieulesaint, 2000), the relationship between stress and strain is given by equation (31).

$$\begin{bmatrix} \sigma_{xx} \\ \sigma_{yy} \\ \sigma_{zz} \\ \sigma_{yz} = \sigma_{zy} \\ \sigma_{xz} = \sigma_{zx} \\ \sigma_{xy} = \sigma_{yx} \end{bmatrix} = \begin{bmatrix} C_{xxxx} & C_{xxyy} & C_{xxzz} & C_{xxyz} & C_{xxxz} & C_{xxxy} \\ C_{xxyy} & C_{yyyy} & C_{yyzz} & C_{yyyz} & C_{yyxz} & C_{yyxy} \\ C_{xxzz} & C_{yyzz} & C_{zzzz} & C_{zzyz} & C_{zzxz} & C_{zzxy} \\ C_{xxyz} & C_{yyyz} & C_{zzyz} & C_{yzyz} & C_{yzxz} & C_{yzxy} \\ C_{xxxz} & C_{yyxz} & C_{zzxz} & C_{yzxz} & C_{xzxz} & C_{xzxy} \\ C_{xxxy} & C_{yyxy} & C_{zzxy} & C_{yzxy} & C_{xzxy} & C_{xyxy} \end{bmatrix} \begin{bmatrix} \varepsilon_{xx} \\ \varepsilon_{yy} \\ \varepsilon_{zz} \\ \varepsilon_{yz} = \varepsilon_{zy} \\ \varepsilon_{xz} = \varepsilon_{zx} \\ \varepsilon_{xy} = \varepsilon_{yx} \end{bmatrix} \quad (31)$$

Expressing compactly, the stress elements from equation 31 are given as,

$$\sigma_{ij} = C_{ijkl}\varepsilon_{kl} \qquad (32)$$

$$for\ i, j, k, l = x, y, z$$

Noting that C_{ijkl} is the tensor of elasticity, tensor of stiffness or the stiffness tensor - the elastic properties of a solid are expressed by the values attributed to the elasticity tensor elements. Notice from equation (31) that some terms are repeated within the stiffness tensor; this is due to a symmetrical relationship within the stiffness tensor.

A more detailed examination of the symmetrical relationships is presented in section 4.0 of appendix 1.

The inverse of the stiffness tensor is known as the compliance tensor and relates the strain to stress, and is general speaking a measure of how compliant, or how subjectable to deformation, a solid body is. This is given as equation (33)

$$\varepsilon_{ij} = S_{ijkl}\sigma_{kl} \qquad (33)$$

$$for\ i, j, k, l = x, y, z$$

As this thesis concerns the elastic constants of a material, the tensor of stiffness is from this point almost exclusively discussed with the compliance tensor not generally discussed further.

6.2.6 Stress and particle displacement relation

The penultimate area requiring discussion is the relationship between stress and particle displacement. Whereas strain and particle displacement are related through equation (20), the relationship between stress and particle displacement are expressed through the dynamical equations of motion; the translational equation of motion and the rotational equation of motion. This thesis will only consider the translational equation of motion (from this point on to referred to as the dynamical equation of motion), with the dynamics of rotation being negligible for linearized theoretical assumptions (small deformations).

For a solid body of arbitrary volume, the forces acting on an infinitesimal volume element or particle, ΔV, may be thought of as being body forces acting on the volume and traction forces acting on the surface. At static equilibrium there is no resulting vector of force, and so the summation of body and surfaces forces when $\Delta V \rightarrow 0$ may be expressed as an integral, given here as equation (34),

$$\iint \boldsymbol{\sigma} \cdot \hat{n}\, dS + \iiint \vec{F}\, dV = 0 \qquad (34)$$

Incorporating a dynamic case (i.e. not static equilibrium), the particle is subjected to a force, which using Newton‟s second law allows equation (34) to be updated to equation (35)

$$\iint \boldsymbol{\sigma} \cdot \hat{n}\, dS + \iiint \vec{F}\, dV = \iiint \rho \frac{\partial^2 \vec{u}}{\partial^2 t} dV \quad (35)$$

Transforming the surface integral to a volume integral is done through the divergence theorem, i.e.

$$\iint \vec{F} \cdot \hat{n}\, dS = \iiint \nabla \cdot \vec{F}\, dV$$

Further, given that the original volume element was arbitrary, the integrals may be removed (in that the integrand defines forces acting upon an arbitrary volume element). Thus, equation (35) may be expressed as equation (36).

$$\nabla \cdot \boldsymbol{\sigma} = \rho \frac{\partial^2 \vec{u}}{\partial^2 t} - \vec{F} \quad (36)$$

Thus, for a vibrating medium the second derivative of particle displacement with respect to time, i.e., the acceleration of particle when it deviates from equilibrium, multiplied by the density and minus any possible body forces that may exist is equal to the divergence of the stress. For clarity the divergence of the stress is given as equation (37),

$$\nabla \cdot \boldsymbol{\sigma} = \hat{\mathrm{x}}\left(\left(\frac{\partial \sigma xx}{\partial x}\right)+\left(\frac{\partial \sigma xy}{\partial y}\right)+\left(\frac{\partial \sigma xz}{\partial z}\right)\right)+\hat{\mathrm{y}}\left(\left(\frac{\partial \sigma yx}{\partial x}\right)+\left(\frac{\partial \sigma yy}{\partial y}\right)+\left(\frac{\partial \sigma yz}{\partial z}\right)\right)$$

$$+\hat{z}\left(\left(\frac{\partial \sigma zx}{\partial x}\right)+\left(\frac{\partial \sigma zy}{\partial y}\right)+\left(\frac{\partial \sigma zz}{\partial z}\right)\right) \quad (37)$$

6.2.7 Wave propagation and notational conventions

The final element prior to introducing the Christoffel equation is to discuss plane wave propagation and notational convention.

6.2.7.1 Abbreviated subscript notation for stress strain and elasticity

Up to this point full subscript notation has been used. However, the convention with academia is to use abbreviated notation.

Table 20 documents full notation and abbreviated notation for stress and strain.

Full subscript notation	Stress abbreviated subscript notation	Strain abbreviated subscript notation	General relation	
			i, j	I, J
$(\sigma \text{ or } \varepsilon)_{xx}$	σ_1	ε_1	xx	1
$(\sigma \text{ or } \varepsilon)_{yy}$	σ_2	ε_2	yy	2
$(\sigma \text{ or } \varepsilon)_{zz}$	σ_3	ε_3	zz	3
$(\sigma \text{ or } \varepsilon)_{yz=zy}$	σ_4	$^1/_2\,\varepsilon_4$	$yz = zy$	4
$(\sigma \text{ or } \varepsilon)_{xz=zx}$	σ_5	$^1/_2\,\varepsilon_5$	$xz = zx$	5
$(\sigma \text{ or } \varepsilon)_{xy=yx}$	σ_6	$^1/\ \varepsilon_6$	$xz = zx$	6

Table 20 - Relationship between full subscript notation and abbreviated subscript notation for the stress and strain tensors along with the general relationship. Note that the abbreviated subscript notation in the general case is given by capital letters.

Noting that the ½ is introduced in the case of the strain tensor owing to the fact that the abbreviated subscript notation is defined for engineering strain and not tensor strain, hence the introduction of the factor of 1/2.

Elasticity may also be denominated using abbreviated notation as outlined in Table 20. The relationship between stress and strain, equation (32) and (33), may be rewritten as equations (38) and (39).

$$\sigma_I = C_{IJ}\varepsilon_J \qquad (38)$$

$$\varepsilon_I = S_{IJ}\sigma_J \qquad (39)$$

$$for\ I,J = 1,2,3,4,5,6$$

And so equation (31) may be rewritten as equation (40)

$$\begin{bmatrix}\sigma_1\\ \sigma_2\\ \sigma_3\\ \sigma_4\\ \sigma_5\\ \sigma_6\end{bmatrix} = \begin{bmatrix}C_{11} & C_{12} & C_{13} & C_{14} & C_{15} & C_{16}\\ C_{12} & C_{22} & C_{23} & C_{24} & C_{25} & C_{26}\\ C_{13} & C_{23} & C_{33} & C_{34} & C_{35} & C_{36}\\ C_{14} & C_{24} & C_{34} & C_{44} & C_{45} & C_{46}\\ C_{15} & C_{25} & C_{35} & C_{45} & C_{55} & C_{56}\\ C_{16} & C_{26} & C_{36} & C_{46} & C_{56} & C_{66}\end{bmatrix}\begin{bmatrix}\varepsilon_1\\ \varepsilon_2\\ \varepsilon_3\\ \varepsilon_4\\ \varepsilon_5\\ \varepsilon_6\end{bmatrix} \qquad (40)$$

Which in more compact notation is given by,

$$[\boldsymbol{\sigma}] = [\boldsymbol{C}] : [\boldsymbol{\varepsilon}]$$

$$[\boldsymbol{\varepsilon}] = [\boldsymbol{S}] : [\boldsymbol{\sigma}]$$

6.2.7.2 Wave propagation notation

Plane wave propagation is assumed to be understood by the reader; therefore, as with academic convention, equation (41) is given to describe a positive travelling plane wave (left to right) propagation in the x, y, and z direction.

$$e^{i(k_x x + k_y y + k_z z - wt)} = e^{i(\vec{k}\cdot\vec{D} - wt)} = e^{i\left(\left(k(\hat{k})\right)\cdot\vec{D} - wt\right)} \qquad (41)$$

Where **D** is a position vector from the origin with x, y and z directions, w is the angular frequency, k is the wave number, **k** is the wave vector and t is time elapsed. Further discussion on plane wave propagation, including how equation (41) is derived, is given in section 5.0 of appendix 1 and also from (Kinsler et al., 1982; Pain, 2005).

A final remake on wave propagation is made regarding polarization and propagation direction. When plane waves propagate throughout a solid they do so in a given direction, for instance, the x, y, or z direction (or a combination of these directions). The direction in which the particles oscillate around their equilibrium position (described hence forth as polarization direction) does not always have to coincide with the direction of propagation however. Two typical ubiquitous planes waves are the transverse (or shear) and longitudinal wave forms. Figure 23 documents the polarization and propagation directions for these standard types of waves.

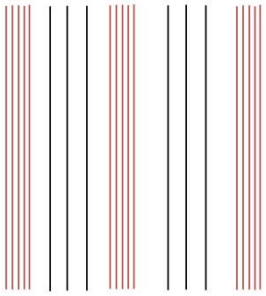

Longitudinal wave

Polarization direction horizontal

Propagation direction horizontal

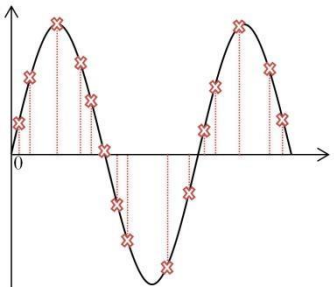

Transverse (shear) wave

Polarization direction vertical

Propagation direction horizontal

Figure 23 – Documenting the propagation direction and polarization direction of shear waves and longitudinal waves. The x"s in the shear wave examples all initially lie on the horizontal axes and are displaced by varying $_0$ amounts at 90 to the propagation direction. Longitudinal waves are polarized in the same direction as wave propagation with the figure showing a bird"s eye view of particles (straight lines) being close and far away from each other.

Figure 23 demonstrates the two most common types of plane waves. Shear waves are always polarized at 90° to propagation direction with longitudinal waves being polarized always in the same direction as wave propagation, i.e. 0°. Both transverse and longitudinal waves may be propagated through a solid.

Additionally, another type of wave, whose polarization is a combination of both longitudinal and transverse, may be propagated through a solid; these waves are denoted as being either quasi-longitudinal or quasi-transverse waves. Noting that most often, the polarization will be more transverse than longitudinal or be more longitudinal than transverse hence the use of the prefixes.

6.3 Christoffel equation

Having provided the necessary background information, the Christoffel equation is now formalised.

6.3.1 General form of Christoffel equation

In general terms the Christoffel equation may be thought of as follows,

For a plane wave propagating through a solid in a given direction, the Christoffel equation defines a relationship between the given waves", wavenumber, angular frequency, elastic constants and the density of the medium. Thus, upon realising that,

$$\frac{w}{k} = v$$

then the velocity of the propagating wave is able to be related to the elastic constants and density of the solid; that is for a known velocity and density, the elastic constants are able to be determined. The Christoffel equation is now expressed mathematically. As previously expressed, equation (36) states that the divergence of the stress is equal to the acceleration of particle displacement multiplied by the density while subtracting any potential body forces, i.e. the equation of motion,

$$\nabla \cdot \boldsymbol{\sigma} = \rho \frac{\partial^2 \vec{u}}{\partial^2 t} - \vec{F} \quad (36)$$

This equation may be rewritten noting that the acceleration of particle displacement vector may be regarded as the first partial derivative of the velocity of the particle displacement vector, given as equation (42),

$$\nabla \cdot \boldsymbol{\sigma} = \rho \frac{\partial \vec{v}}{\partial t} - \vec{F} \qquad (42)$$

Further, equation (20) denotes that the symmetric part of the displacement gradient tensor is equal to the strain, that is,

$$[\boldsymbol{\varepsilon}] = \frac{1}{2}([\boldsymbol{\nabla u}] + [\boldsymbol{\nabla u}]^T) \qquad (20)$$

Noting a notational change of,

$$[\boldsymbol{\nabla_s u}] = [\boldsymbol{\varepsilon}]$$

Then similar to the previous argument, converting displacement to velocity gives,

$$[\boldsymbol{\nabla_s v}] = \left[\frac{\partial \boldsymbol{\varepsilon}}{\partial \mathrm{t}}\right] \qquad (43)$$

Additionally, equation (43) may itself be rewritten to incorporate the compliance tensor from equation (39), that is,

$$[\boldsymbol{\nabla_s v}] = \left[\frac{\partial \boldsymbol{\varepsilon}}{\partial \mathrm{t}}\right] = [\boldsymbol{S}] : \frac{\partial \boldsymbol{\sigma}}{\partial \mathrm{t}} \qquad (44)$$

Obtaining now an equation for the velocity in terms of wave parameters only, i.e. eliminating the stress field from (42), equation (42) is first differentiated with respect to time, given as equation (45),

$$\nabla \cdot \frac{\partial \boldsymbol{\sigma}}{\partial t} = \rho \frac{\partial^2 \vec{v}}{\partial^2 t} - \frac{\partial \vec{F}}{\partial t} \qquad (45)$$

Equation (44) is now multiplied by the stiffness (which is the same as dividing by the compliance) giving,

$$[\boldsymbol{C}] : [\boldsymbol{\nabla_s v}] = \frac{\partial \boldsymbol{\sigma}}{\partial \mathrm{t}} \qquad (46)$$

Substituting equation (46) into equation (45) allows for equation (47) to express velocity independent of stress tensor (directly).

$$\nabla \cdot [\boldsymbol{C}] : [\boldsymbol{\nabla_s v}] = \rho \frac{\partial^2 \vec{v}}{\partial^2 t} - \frac{\partial \vec{F}}{\partial t} \qquad (47)$$

Tidying equation (47), consider first the divergence of stress expressed in abbreviated subscript notation,

$$\nabla \cdot \boldsymbol{\sigma} = \hat{\mathrm{x}}\left(\left(\frac{\partial \sigma_1}{\partial x}\right) + \left(\frac{\partial \sigma_6}{\partial y}\right) + \left(\frac{\partial \sigma_5}{\partial z}\right)\right) + \hat{y}\left(\left(\frac{\partial \sigma_6}{\partial x}\right) + \left(\frac{\partial \sigma_2}{\partial y}\right) + \left(\frac{\partial \sigma_4}{\partial z}\right)\right)$$

$$+ \hat{z}\left(\left(\frac{\partial \sigma_5}{\partial x}\right) + \left(\frac{\partial \sigma_4}{\partial y}\right) + \left(\frac{\partial \sigma_3}{\partial z}\right)\right)$$

Which expressed in matrix notation gives

$$\nabla \cdot \boldsymbol{\sigma} = \nabla_{iK} T_K = \begin{bmatrix} \partial/\partial x & 0 & 0 & 0 & \partial/\partial z & \partial/\partial y \\ 0 & \partial/\partial y & 0 & \partial/\partial z & 0 & \partial/\partial x \\ 0 & 0 & \partial/\partial z & \partial/\partial y & \partial/\partial x & 0 \end{bmatrix} \begin{bmatrix} \sigma_1 \\ \sigma_2 \\ \sigma_3 \\ \sigma_4 \\ \sigma_5 \\ \sigma_6 \end{bmatrix}$$

And so $\nabla \cdot$ is given by,

$$\nabla \cdot = \nabla_{iK} = \begin{bmatrix} \partial/\partial x & 0 & 0 & 0 & \partial/\partial z & \partial/\partial y \\ 0 & \partial/\partial y & 0 & \partial/\partial z & 0 & \partial/\partial x \\ 0 & 0 & \partial/\partial z & \partial/\partial y & \partial/\partial x & 0 \end{bmatrix} \quad (48)$$

Additionally, the transpose of the matrix representation of the divergence operator can be thought of as the symmetrical gradient operator ∇_s, that is,

$$[\boldsymbol{\varepsilon}] = [\boldsymbol{\nabla_s u}] \rightarrow \begin{bmatrix} \varepsilon_1 \\ \varepsilon_2 \\ \varepsilon_3 \\ \varepsilon_4 \\ \varepsilon_5 \\ \varepsilon_6 \end{bmatrix} = \begin{bmatrix} \partial/\partial x & 0 & 0 \\ 0 & \partial/\partial y & 0 \\ 0 & 0 & \partial/\partial z \\ 0 & \partial/\partial z & \partial/\partial y \\ \partial/\partial z & 0 & \partial/\partial x \\ \partial/\partial y & \partial/\partial x & 0 \end{bmatrix} \begin{bmatrix} u_x \\ u_y \\ u_z \end{bmatrix} \rightarrow \varepsilon_I = \nabla_{Lj} uj$$

and so,

$$\nabla_s = \nabla_{Lj} = \begin{bmatrix} \partial/\partial x & 0 & 0 \\ 0 & \partial/\partial y & 0 \\ 0 & 0 & \partial/\partial z \\ 0 & \partial/\partial z & \partial/\partial y \\ \partial/\partial z & 0 & \partial/\partial x \\ \partial/\partial y & \partial/\partial x & 0 \end{bmatrix} \quad (49)$$

Substituting equation (48) and (49) then equation (47) is rewritten as

$$\begin{bmatrix} \partial/\partial x & 0 & 0 & 0 & \partial/\partial z & \partial/\partial y \\ 0 & \partial/\partial y & 0 & \partial/\partial z & 0 & \partial/\partial x \\ 0 & 0 & \partial/\partial z & \partial/\partial y & \partial/\partial x & 0 \end{bmatrix} [\boldsymbol{C}] \begin{bmatrix} \partial/\partial x & 0 & 0 \\ 0 & \partial/\partial y & 0 \\ 0 & 0 & \partial/\partial z \\ 0 & \partial/\partial z & \partial/\partial y \\ \partial/\partial z & 0 & \partial/\partial x \\ \partial/\partial y & \partial/\partial x & 0 \end{bmatrix} [\vec{v}] = \rho \frac{\partial^2 \vec{v}}{\partial^2 t} - \frac{\partial \vec{F}}{\partial t} \quad (50)$$

This expression may be further simplified by assuming the **u** will be a plane wave, i.e.

$$\vec{\mathrm{u}} = e^{i\left(\left(k(\hat{k})\right)\cdot\vec{D} - wt\right)} \quad (51)$$

Noting that **v** is the derivative of (51) with respect to time. Assuming plane wave propagation, all future derivatives with respect to x, y and z will to some degree be proportional to equation (51), i.e.

$$\frac{\partial e^{i\left(\left(k(\hat{k})\right)\cdot\vec{D} - wt\right)}}{\partial x} = ikk_x e^{i\left(\left(k(\hat{k})\right)\cdot\vec{D} - wt\right)}$$

noting that kxin this instance refers to the x element of$\hat{k}$, and not to the x element of$\vec{k}$. Using this proportionality equations (48) and (49), the divergence and symmetrical operators, may be replaced using scalar quantities expressed as equations (52) and (53).

$$\begin{bmatrix} \partial/\partial x & 0 & 0 \\ 0 & \partial/\partial y & 0 \\ 0 & 0 & \partial/\partial z \\ 0 & \partial/\partial z & \partial/\partial y \\ \partial/\partial z & 0 & \partial/\partial x \\ \partial/\partial y & \partial/\partial x & 0 \end{bmatrix} \rightarrow ik \begin{bmatrix} k_x & 0 & 0 \\ 0 & k_y & 0 \\ 0 & 0 & k_x \\ 0 & k_z & k_y \\ k_z & 0 & k_x \\ k_y & k_x & 0 \end{bmatrix} \quad (52)$$

$$\begin{bmatrix} \partial/\partial x & 0 & 0 & 0 & \partial/\partial z & \partial/\partial y \\ 0 & \partial/\partial y & 0 & \partial/\partial z & 0 & \partial/\partial x \\ 0 & 0 & \partial/\partial z & \partial/\partial y & \partial/\partial x & 0 \end{bmatrix} \rightarrow ik \begin{bmatrix} k_x & 0 & 0 & 0 & k_z & k_y \\ 0 & k_y & 0 & k_z & 0 & k_x \\ 0 & 0 & k_z & k_y & k_x & 0 \end{bmatrix} \quad (53)$$

Substituting into equation (51) gives equation (54).

$$i^2k^2 \begin{bmatrix} k_x & 0 & 0 & 0 & k_z & k_y \\ 0 & k_y & 0 & k_z & 0 & k_x \\ 0 & 0 & k_z & k_y & k_x & 0 \end{bmatrix} [\boldsymbol{C}] \begin{bmatrix} k_x & 0 & 0 \\ 0 & k_y & 0 \\ 0 & 0 & k_x \\ 0 & k_z & k_y \\ k_z & 0 & k_x \\ k_y & k_x & 0 \end{bmatrix} [\vec{v}] = \rho \frac{\partial^2 \vec{v}}{\partial^2 t} - \frac{\partial \vec{F}}{\partial t} \qquad (54)$$

Additionally upon assuming body forces are negligible and differentiating the right hand side, i.e.

$$\vec{v} = -iwe^{i\left(\left(k(\hat{k})\right)\cdot\vec{D}-wt\right)}$$

$$\frac{\partial^2 \vec{v}}{\partial^2 t} = i^3(-w)(-w)(-w)e^{i\left(\left(k(\hat{k})\right)\cdot\vec{D}-wt\right)} = i^2w^2(i*-w)e^{i\left(\left(k(\hat{k})\right)\cdot\vec{D}-wt\right)} = i^2\mathrm{w}^2\vec{v}$$

then equation (54) may be written as,

$$k\,[\Gamma][v\,]\,\rho w\,[v\,] \quad (\,)$$

Noting the cancellation of i^2 from both sides, in subscript notation equation (55) is written as,

$$k\,\Gamma_{ij}v_j\,\rho w\,v_i \quad (\,)$$

With,

$$\Gamma_{ij} \quad * \quad \begin{matrix} & k_x & & & k_z & k_y \\ & k_y & & k_z & & k_x + [\boldsymbol{C}] \\ & & k_z & k_y & k_x & \end{matrix} \quad \begin{matrix} k_x & & \\ & k_y & \\ & & k_x \\ & k_z & k_y \\ k_z & & k_x \\ [k_y & k_x &] \end{matrix} \quad k_{iK} C_{KL} k_{Lj} \quad (\quad)$$

The Christoffel equation and the Christoffel matrix are now presented. Equation (55) or (56) is the Christoffel equation and equation (57) is the Christoffel matrix (noting that matrix takes on various forms depending on the class of symmetry the given solid belongs to).

6.3.2 Christoffel matrix for an isotropic and anisotropic solids

For particle displacement impacting on a hypothetical surface defined in a coordinate system, a solid, which has a boundary in alignment with this surface, may or may not respond in the same way when the solid is rotated i.e. the particle displacement is impacting on a different surface of the solid. Specifically solids may be regarded as having various types of symmetry with each class having a set number of independent elastic constants.

A completely anisotropic material will have 21 independent elastic constants while a completely isotropic material will only have 2 independent elastic constants, noting that various other symmetrical classes lie in between these two extreme cases. The symmetrical classes are not proven in this thesis but may be found from most all works on elasticity theory previously cited.

Given that the isotropic and anisotropic are the most simple and most complicated forms of the Christoffel matrix, which the other types of symmetry class falling between these classes, both are presented for reference. The isotropic case and anisotropic case are given equations (58) and (59) respectively.

$$[\;] \quad [\quad \begin{matrix} & (\quad) & (\quad) & & (\quad) \\ (\quad) & & & (\quad) & (\quad) \\ (\quad) & & (\quad) & & & (\quad) \end{matrix} \quad]\,(\quad)$$

$$[\Gamma] = \begin{bmatrix} \Gamma_{xx}' & \Gamma_{xy}' & \Gamma_{xz}' \\ \Gamma_{xy}' & \Gamma_{yy}' & \Gamma_{yz}' \\ \Gamma_{xz}' & \Gamma_{yz}' & \Gamma_{zz}' \end{bmatrix} \qquad (59)$$

$$\Gamma_{xx}' = C_{11}k_x^{\,2} + C_{66}k_y^{\,2} + C_{55}k_z^{\,2} + 2C_{56}k_yk_z + 2C_{15}k_zk_x + 2C_{16}k_xk_y$$

$$\Gamma_{yy}' = C_{66}k_x^{\,2} + C_{22}k_y^{\,2} + C_{44}k_z^{\,2} + 2C_{24}k_yk_z + 2C_{46}k_zk_x + 2C_{26}k_xk_y$$

$$\Gamma_{zz}' = C_{55}k_x^{\,2} + C_{44}k_y^{\,2} + C_{33}k_z^{\,2} + 2C_{34}k_yk_z + 2C_{35}k_zk_x + 2C_{45}k_xk_y$$

$$\Gamma_{xy}' = C_{16}k_x^{\,2} + C_{26}k_y^{\,2} + C_{45}k_z^{\,2} + (C_{46} + C_{25})k_yk_z + (C_{14} + C_{56})k_zk_x + (C_{12} + C_{66})k_xk_y$$

$$\Gamma_{xz}' = C_{16}k_x^{\,2} + C_{26}k_y^{\,2} + C_{45}k_z^{\,2} + (C_{45} + C_{36})k_yk_z + (C_{13} + C_{55})k_zk_x + (C_{14} + C_{56})k_xk_y$$

The process of deriving these Christoffel matrices is outlined in section 6.0 of appendix 1.

6.3.3 Executing the Christoffel equation

Having now performed a relatively thorough derivation of the Christoffel equation, the final part of this chapter deals with an example of the equation execution, for both an isotropic case and an anisotropic case.

In the isotropic case, a wave is considered to be propagating in the x direction. In this direction 3 typical waves will propagate, a longitudinal wave, and two transverse waves, polarised 90° from each other. Execution of the Christoffel equation returns the following phase velocities.

$$velocity\ of\ longitudinal\ wave\ in\ x\ direction = v_x = \sqrt{\frac{C_{11}}{\rho}} \qquad (60)$$

$$velocity\ of\ shear\ wave\ polarized\ in\ y\ direction = v_y = \sqrt{\frac{C_{44}}{\rho}} \qquad (61)$$

$$velocity\ of\ shear\ wave\ polarized\ in\ z\ direction = v_z = \sqrt{\frac{C_{44}}{\rho}} \qquad (62)$$

Note that given that every direction has equal properties in an isotropic case, the wave phase velocities will also be the same in any direction.

Considering now an anisotropic case, given that chapter 7 and chapter 8 examine almost exclusively uni-directional materials, the symmetry class of transverse isotropy is selected. For a wave travelling in the [1, 1, 0] direction (given the direction of fibres as the z direction (the 0 part of the vector), the following phase velocities and polarizations will be returned.

Velocity and resulting Polarization table			
Velocity	Vector	Dot product with direction $(1 \quad 1 \quad 0)$	Wave type
$\sqrt{\qquad\qquad}$	$(-1 \quad 1 \quad 0)$	0	Transverse wave
$v = \sqrt{\frac{C_{44}}{\rho}},$	$(0 \quad 0 \quad 1)$	0	Transverse wave
$\sqrt{\qquad\qquad\qquad}$	$(1 \quad 1 \quad 0)$	2	Longitudinal wave

Table 21 – plane wave velocities and associated polarization directions for a plane wave propagation in the [1, 1, 0] direction

A more detailed analysis on how the Christoffel equation is executed in the case of both isotropic and anisotropic symmetry classes can be found in section 7 of appendix 1.

6.4 Conclusion

The experimental section of this thesis is concerned with the applicability of the immersion based through transmission technique (which may be used to determine the elastic constants of material) when applied to CFRP constructed from re-used fibres. A key theoretical component critical to achieving this aim, is the relationship between plane wave velocity and the elastic constants; with this relationship being expressed by solving the Christoffel equation.

Through discussion of various aspects such deformation, strain, particle displacement, stress, the relationship between stress to strain, the tensor of elasticity and stiffness and wave propagation this chapter derived the Christoffel equation from first principles. Additional mathematical verification (including how to execute the Christoffel equation) which serves to reinforce the knowledge presented in this chapter was also highlighted as making up appendix 1. Future use the Christoffel equation within this thesis will be routine and this chapter will therefore allow the experimental section of this thesis to focus largely on the findings and less so upon the theoretical basis for these measurements.

Moving forward and prior to conducting experimental analysis, a literature review concerning the immersion based ultrasonic through transmission technique on rf-CFRP and v-CFRP is presented.

Chapter 7: Elastic constant determination of CFRP via the ultrasonic immersion based through transmission technique: A review

7.1 Introduction

Having now presented the fundamental relationship between acoustic wave velocities and the elastic constants of a solid, prior to investigating the second research question, a literature review of the area is presented. A literature survey concerning the focus of the question has proven to be elusive; suggesting that little research is occurring in this area. Data bases such as Web of Science (WoS), Science Direct (SD),

and the search engine Google Scholar (GS), have returned little literature in this area. For instance, searching for key words such as “CFRP, Ultrasonic” on WoS returned some 491 results, but when these results were refined to include the term recycling only 1 suitable paper was returned, that is, (Shi et al., 2014). Broadening the search criteria to include the terms “Composite, Ultrasound” returned over 3000 hits and when using the refining function to include recycling, 27 hits were returned, of these only one suitable paper was found, (Feraboli et al., 2012). Similar searches including key words such as

“Elastic Constants, Composite, CFRP, Carbon Composite, Ultrasound, Ultrasonic, NDT and Non-Destructive Testing” along with examining which papers cited the suitable papers recorded, generally failed to return further applicable papers, with an exception being (Meftah et al., 2017). This result is not entirely surprising given that the CFRP recycling papers encountered thus far, have almost solely documented mechanical form of testing to determine the elastic properties. Of the applicable papers that were found, on closer examination, it can be said that they do not explicitly investigate the second research question, this is because the way in which ultrasound was used does not return the elastic constants.

Shi (2014) perform ultrasonic pulse echo testing, a process known as “C-Scan” which uses acoustic attenuation measurements to produce images of the inspect area, on rf-CFRP and v-CFRP; the aim here being to assess the differences recorded after impact damage testing. Feraboli (2012) also uses a C-Scan in the same manner, while also using standard mechanical testing to determine the young‟s modulus. Meftah (2017) moved a step further and adopted a through transmission technique, velocity measurements were undertaken to investigate fibre orientation of rf-CFRP manufactured via injection of mechanically recycled short random fibres. Again the Young‟s modulus is not investigated.

In relation to the second research question, the papers give a strong indication that standard velocity measurements to determine the elastic constants will be applicable, given that use of velocity measurement in the three works. However, the existing work fails to use ultrasound through transmission to identify the young‟s modulus and instead relies on existing mechanical testing.

While the elastic constants of rf-CFRP have not been recorded via ultrasound through transmission within the available literature, the elastic constants of v-CFRP have long been recorded using this technique. To better understand the existing work on v-

CFRP, with a view to investigating the second research question, a literature review documenting many seminal works in this field is now presented. Given that CFRP can be constructed in hundreds of different architectures, a choice was made to focus on a single architecture for this thesis, uni-directional CFRP. Starting from initial conception of the immersion through transmission technique and moving chronologically forward, pertinent papers are reviewed in order with each paper building upon the last. Additionally, unique contributions to knowledge tables are also presented, and so for the first time within literature, major contributions to knowledge in this area are recorded and documented in simple and efficient manner, via two bespoke information tables. Further, the experimental section of this thesis is chapter 8, and to build all the knowledge prior to this chapter, experimental arrangements needed to determine the elastic constants are clearly mapped out in this chapter.

7.2 Review Methodology

The review presented in section 7.4 is an abridged version of a longer review which is found in appendix 2. The longer review discusses the same content as presented in this chapter, but goes in to substantial more depth. The longer review is approximately 26,000 words and to ensure efficiency in this thesis, a shorter abridged version is given in the main body.

The longer review in appendix 2 is a contribution to knowledge from this research in that seminal papers are reviewed in chronological order with the experimental findings, experimental technique and benefits and drawbacks all discussed. In terms of what is presented in this chapter, there is obvious cross over with appendix 2, however, this chapter leans toward reporting the results and avoids a critique of individual publications and refrains from more in-depth discussion. The boundaries of the review are given as Table 22.

Boundaries on the literature reviewed	Examples of research areas falling outside boundaries (excluded research areas)
Bulk waves (waves treated as acting in an infinite medium)	Lamb waves, Rayleigh waves, guided waves
Uni-directional composite (with where possible polymer matrix)	Cross ply composite, multidirectional laminates, thick composites, woven composites
Carbon fibre or graphite fibre (where possible)	Kevlar or Boron based fibres

Non gas coupled ultrasound through transmission (velocity based measurement)	Wave attenuation measurements, pulse echo techniques, point source point receiver technique, A-scans, B-scans, C-scans, Air coupled ultrasound, transmission – reflection coefficients
Elastic constant determination (mechanical properties) through experiment	Defect detection, porosity, fibre content, attenuation factor, theoretical modelling based on composite properties, mechanical tests, viscoelastic properties

Table 22 - Identifies the boundaries and scope of the literature review

Note that on occasion, one or more of the excluded research areas is discussed in the literature review. The rationale for discussing areas outside of the scope is made apparent from the context at that point.

The literature selected for this review was journal articles, conference papers and book publications. This literature was identified in part by searching through databases and also by reviewing the references cited in almost all published journal articles. Lastly, book reviews such as (Hosten, 2001; Rokhlin et al., 2011; Summerscales, 1990) also helped to identify further relevant literature.

Additionally, novel information tables which outline various contributions to knowledge from the authors in this review are also presented. Owing to the large amount of findings documented more than one table exists, i.e. findings are not all contained within the one table. Table 25 documents the 1970‟s - 1980‟s, with Table 26 documenting the 1980‟s – modern era. This decision has two clear benefits 1) findings are able to be presented in a more manageable format and 2) a quick way to access the contributions from both time periods is presented. The second point of merit is that not all information presented in the literature review is documented within the tables, that is, tables 25 and 26 are not meant to be used as a substitute for the literature reviewed. Thus, the tables present only a recap of the contributions to knowledge from a respective publication. A third point of merit building on both points 1 and 2 is that not all findings from the literature review are documented within the tables. For instance, Table 26 does not acknowledge whether publications from the period 1980 onward determined the full set of elastic constants. Table 25 demonstrates that determining elastic constants is achievable and so including this information in Table 26 was considered to be of no merit.

7.3 Phase and Group Velocity

Prior to the literature survey, a distinction between phase velocity and group velocity is made. Wave propagation having been described in chapter 6, did not in general discuss the subtle distinction between group velocity and phase velocity, this distinction is now discussed.

For a traveling plane wave (waves in which wavelength and frequency do not alter) the wave may be classed as having constant phase. That is, from a given phase reference point, say 90° the phase of the wave will travel through a complete cycle of 360° (one wavelength) through space and time and then return to the same reference point. The speed at which this process occurs is called the phase velocity of a wave. Note also that points of equal phase occurring in space and time are known as wave fronts. Figure 24 is given to reinforce the phase concept.

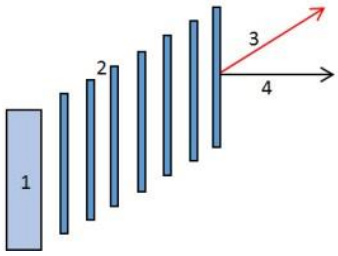

Legend

1 = Transducer

2 = Wave front

3 = Direction of group velocity

4 = Direction of phase velocity

Figure 24 – Depiction of a plane wave. The points a, b and c are at equal phase with respect to each other as the wave propagates through space and time. In this example, the wave front could be stated as point a, point b and point c etc. The speed at which the wave leaves point a and reaches point b, or leaves point b and reaches point c is known as the phase velocity.

Group velocity is the variation of a given wave‟s envelope or amplitude as it propagates through space and time. More specially, in some circumstances, various frequencies which can comprise an ultrasonic pulse may begin to travel at different velocities and so the direction of wave propagation, as measured via wave envelope may begin to deviate away from the direction of phase velocity and in the direction of what is known as group velocity. A representation of the group velocity effect is given in Figure 25.

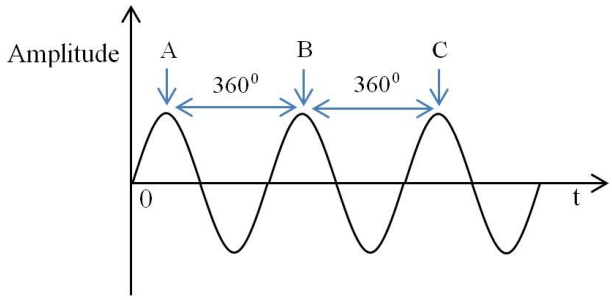

Figure 25 - The group velocity effect is shown. Path 4 is the direction of phase velocity, while path 3 is the direction of group velocity. Notice that group velocity causes the direction with respect to the transducer to deviate away from a normal - adapted from (Auld, 1990).

The distinction between phase and group velocity is an important one considering that that the Christoffel equation outlined in chapter 6, which relates velocity to the elastic constants, uses the phase velocity and not the group velocity.

A final point before the moving on to the literature review can be made concerning axis selection. When describing the axis selection for unidirectional composite in the forthcoming literature, the choice to assign the fibre axis as 1, 2, 3 or x, y or z, is made by individual authors. As such, these often change from publication to publication. This is of interest because, the choice of axis bears on the denomination of elastic constant. That is, depending on how authors geometrically view a material, the denomination of an elastic constant may alter from publication to publication, for example, C_{11} in one publication may refer to C_{33} in another publication. Confusion is limited however as the elastic constants in relation to the material parameters can of course not change but their denomination (or name) often does.

7.4 Literature review

One of the earliest recorded events of where ultrasonic wave velocity measurements are used to determine all the elastic constants of a fibre composite was by (Zimmer and Cost (1970). The material under investigation was uni-direction glass composite, which the authors point out, was modelled by hexagonal symmetry. The system employed by Zimmer and Cost is demonstrated in Figure 26

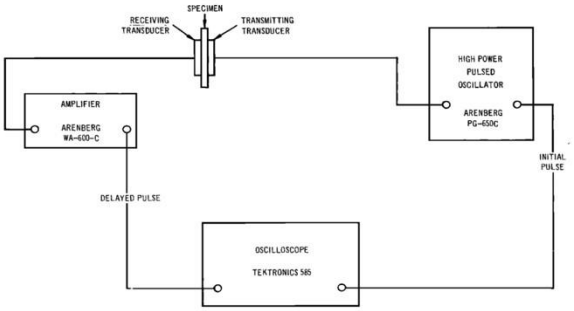

Figure 26 - Pulsed through transmission set up used by (Zimmer and Cost, 1970). *Reprinted with permission from Zimmer JE, Cost JR. Determination of the elastic constants of a unidirectional fibre composite using ultrasonic velocity measurements. Acoust Soc Am; 47: 795–803.Copyright 1970, Acoustic Society of America*

In this arrangement, the test piece is placed between two transducers and the length of time taken for a pulse to leave one transducer and arrive at the second transducer was recorded. Given that five elastic constants are required for hexagonal symmetry (otherwise known as transverse isotropy), similar to theory in chapter 6 the authors propagated various waves, at a frequency of 5MHz, in various directions (with reference to fibre direction).

To determine C_{33} and C_{11} the authors propagated longitudinal waves at 0° degrees and 90° to fibre direction with transverse waves propagated at 90° to fibre direction and polarized both in the plane and orthogonal to the plane containing fibre direction used to determine C_{44} and C_{66} (noting that C_{66} is not independent but instead relies on C_{33} and C_{23}). The final elastic constant, C_{12} was determined through propagating a longitudinal or transverse wave at 45° to fibre direction. This process resulted in quasi-wave propagation - noting that separate pieces of material were required to perform these tests.

The authors documented results from theoretical models (outside the scope of this review) and found close agreement with the theoretical values and ultrasonically measured values. In relation to elastic constant error, which resulted from a 2.5% and 1% error in velocity and density measurements, the elastic constants accuracy varied.

These results are recorded in Table 23.

Elastic constant	Experimental error (%)
C_{11}	6%
C_{12}	100%
C_{23}	15%

C_{33}	6%
C_{44}	6%

Table 23 - The elastic constants and associated experimental error derived from using ultrasonic velocity measurements on Scotchply 1002 (Glass fibre composite) adapted from (Zimmer and Cost, 1970)

Additionally, the authors also investigated shear wave dispersion effects and demonstrated changes in predicted and theoretical velocity when propagating waves from 0º to 90º. They demonstrated that when the angle of propagation to fibre reaches 45º, dispersion effects are approximately 30% (noting that C_{12} is determined using wave propagating at 45º) and subsequently decreases afterwards. These results are documented in Figure 27.

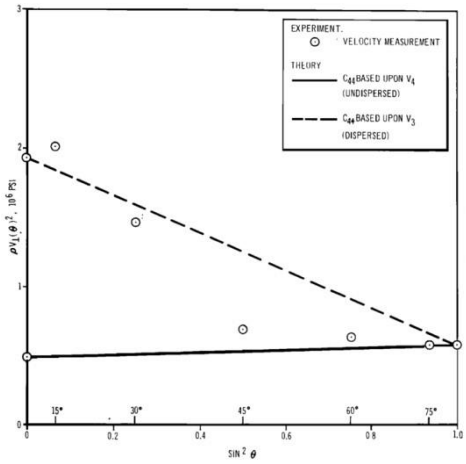

Figure 27 - Dispersion effects recorded by Zimmer and Cost when propagating shear waves polarized at right angles to the fibre. At angles of propagation to fibre direction of less than 45

(excluding 0o) noticeable dispersion was recorded. *Reprinted with permission from Zimmer JE, Cost JR. Determination of the elastic constants of a unidirectional fibre composite using ultrasonic velocity measurements. Acoust Soc Am; 47: 795–803.Copyright 1970, Acoustic Society of America*

Developed at approximately the same time was an alternative system by Markham (1970). Unlike the approach used by Zimmer and Cost, which required multiple test pieces, Markham presented a system in which the elastic constants of a transversely isotropic carbon fibre epoxy composite were able to be determined from a single test piece.

The same principle of wave velocity was used by Markham, with the sample positioned on a two-axis rotatable turntable, with transducers and samples immersed in water. Through Snell‟s laws, incident longitudinal waves were able to propagate through the sample in various directions, while also generating transverse waves in

various directions. The apparatus used by Markham is documented in Figure 28 with Figure 29 documenting a simplified version of the rotatable turntable system.

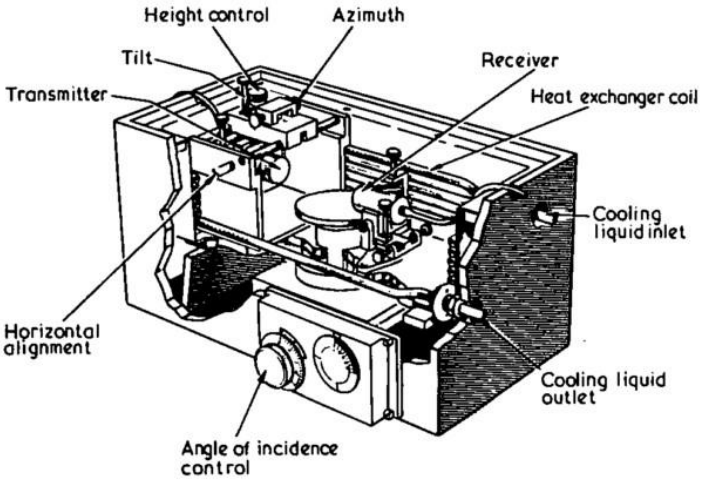

Figure 28 - General representation of the immersion based through transmission system. *Reprinted from Composites, Vol 1 / edition number 3, Markham, M. F., Measurement of the elastic constants of fibre composites by ultrasonics, Pages No 145-149., Copyright (1970), with permission from Elsevier*

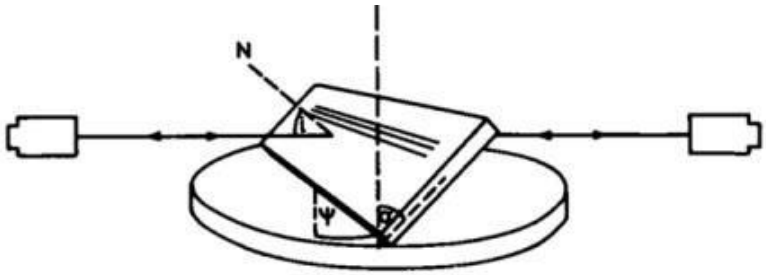

Figure 29 - General representation of transducer placement and of the rotatable turntable. *Reprinted from Composites, Vol 1 / edition number 3, Markham, M. F., Measurement of the elastic constants of fibre composites by ultrasonics, Pages No 145-149., Copyright (1970), with permission from Elsevier*

The transducer frequency was 1.25 - 5 MHz with an ultrasonic pulse of 1 μs and repetition rate of 1 kHz selected along with a digital delay timing system, accurate to $\pm 1x10^{-9}\ ns$, to record time of flight measurements between transmitter and receiver (both with and without a sample in between). Similar to (Zimmer and Cost, 1970), the nature of the waves required in this study were a) two longitudinal waves propagating along fibre direction axis and a direction perpendicular to this axis, b) two different transverse waves propagating perpendicular to the fibre axis and c) a longitudinal or transverse wave propagating at 45º to fibre axis with polarization in the plane of the fibre.

Both Zimmer and Cost (1970) and Markham (1970), demonstrate the applicability of the pulse based transmission approach in determining the elastic constants of unidirectional CFRP with the techniques still used today. Thus it can be stated that the progression within literature is described by refinements of these techniques.

Expansion on the previous works was by Smith (1972), who used the pulse transmission technique to investigate transverse isotropic fibre reinforced plastic (documenting both carbon fibre and graphite fibre based samples). The system used was essentially the Markham method, with two additional transducers present to trigger the oscilloscope just prior to the signal via sample path. The configuration is used by Smith alongside a representation of waves propagating through CFRP is shown as Figure 30 (a) and (b).

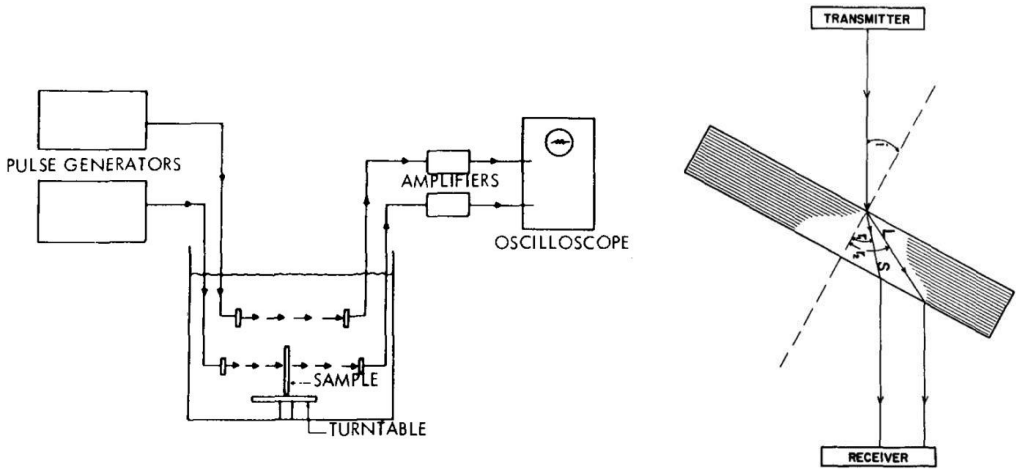

Figure 30 – Figure (a) documents the experimental arrangement as used by Smith, figure (b) documents the mode conversion process allowing both a longitudinal and shear wave to propagate through the sample when incident waves strike the surface at oblique angles.
Reprinted from Smith RE. Ultrasonic elastic constants of carbon fibres and their composites. J Appl Phys; 43: 2555–2561with the permission of AIP Publishing

The turntable rotates on an axis allowing for angle of incidence to be varied by a resolution of 0.1º. The frequency of operation was again 5 MHz and unlike previous work a higher frequency transducer was chosen to combat fringe or resonant effects - the transmitting transducer was ¾" in diameter and the receiving transducer was 10 MHz and ½" in diameter.

As with previous work, the elastic constants C_{11}, C_{33}, C_{66}, C_{44}, and C_{13} were all determined via propagating longitudinal and transverse waves and exploiting

Snell‟s laws. Additionally, Smith also investigated the impact elastic constants have on composite parameters, via conducting experiments on some 13 different samples. Key summarized findings recorded by Smith are presented in Table 24. Further, Smith confirmed the observations from (Zimmer and Cost, 1970), that C_{44} obtained from propagating a transverse wave at 90º to the fibre direction allows for better agreement between the experimental and the theoretical. Smith‟s experimental and theoretical result for an equation for C'_{55} (a variable presented in the text), is given as Figure 31

Key Findings (Composite level)	
Accuracy of result	C_{11}, C_{33}, C_{44} and C_{66} recorded as ±3%, C_{13} recorded as ±20%
Impact of fibre Young‟s modulus	C_{11}, C_{33} and C_{66} dependent on Young‟s modulus. C_{13} and C_{44} independent of fibre modulus but varied with fibre type for graphite fibres and were unclear for carbon fibres.
Impact of shear strength (used to evaluate fibre-matrix bond)	Constants do not greatly depend on shear strength
Differences between constants of graphite fibres and carbon fibres*	C_{11} and C_{66} differ greatly for graphite and carbon fibres. Carbon fibres being 10‟s of percent higher than graphite counterparts
*When elastic constants normalised to the same fibre loading, the difference between elastic constants was found to be as a result of the difference in properties of fibres and not through loading effects	

Table 24 - Key findings on the composite level, adapted from results by (Smith, 1972)

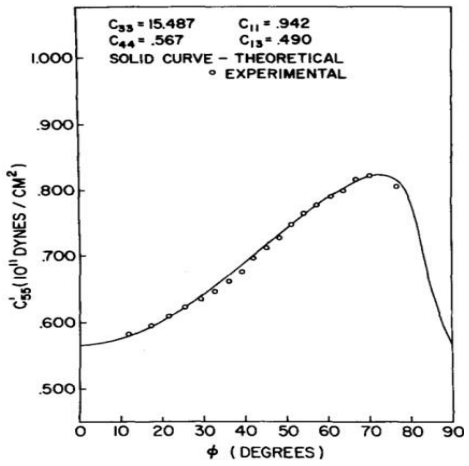

Figure 31 – Documenting the findings from Smith that a close relationship to the $_0$ theoretical is recorded using the Cdirection. Note that the variable C'_{44} value obtained from propagating a transverse wave at 90_{55} used by Smith was dependent C_{11}, C_{13}, C_{33} and C to fibre $_{44}$.

The mid 1970‟s also recorded additional publications from various authors who used both the Zimmer and Cost approach and the Markham technique to investigate other carbon fibre composites properties. For instance areas such as specimen homogeneity, specimen symmetry, degree of fibre misorientation, viscoelastic properties, off-axis shear and longitudinal wave propagation, theoretical analysis, composite fibre volume and composite porosity were studied (Dean and Lockett, 1973; Reynolds and Wilkinson, 1978; Wilkinson and Reynolds, 1974). Reviews of these works can be found in the longer review in appendix 2, with contributions to knowledge found in Table 25.

An additional paper from the 1970‟s is (Kriz and Stinchcomb, 1979). Alongside validating theoretical predictions made by Hashin (1972) using in part wave velocity data obtained from the Zimmer and Cost approach, the authors also investigated group velocity effects, hitherto largely not discussed in literature. Note that Kriz and Stinchcomb did not discover group velocity effects in general; when working on aluminium based composites, Gieske and Allred (1974), identified that the Markham method was using group velocity and not phase velocity. However, Kriz and Stinchcomb recorded these effects on carbon fibre based composites.

Kriz and Stinchcomb put forward the argument that potential exists for transversely isotropic material to cause wave energy to deviate from the wave normal to the extent where the receiving transducer would have to be moved in order to accurately record the wave and to avoid receiving a wave resulting from potential material reflections - the group velocity effect. Using an existing equation set from previous work by the author‟s, Kriz and Stinchcomb calculated the wave energy deviation for wave propagation at 45° to the fibre direction. The results are demonstrated in Figure 32.

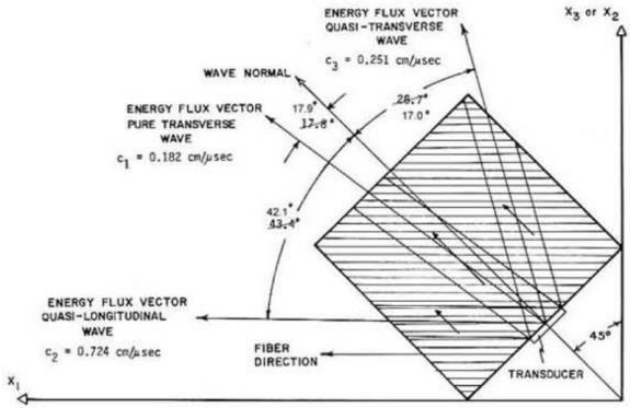

Figure 32 – Group velocity effect for three different types of wave propagating at 45° to fibre axis. Direction of pure transverse records an angle deviation of 17.9° from wave normal. Direction of quasi-transverse wave records angle deviation of 17° from wave normal. Direction of quasi-longitudinal wave records angle deviation of 42.1° from wave normal. *Experimental Mechanics, Elastic moduli of transversely isotropic graphite fibres and their composites, 19, 1979, page 41-49, Kriz RD, Stinchcomb WW, With permission of Springer*

Moving forward and prior to examining the double through transmission technique, it is appropriate to briefly discuss the pulse – echo approach (which is essentially a variation of through transmission).

Pulse echo is typically used to determine defects or flaws within a material but can also be used to determine the elastic constants. In regards to defect detection, pulse echo can be thought of as the following. A wave propagates through a given material and encounters a void which is large compared to the wavelength of wave, the dramatic change in acoustic impedance between the material and void causes a wave to be reflected to the surface. A time of flight measurement is then taken to gauge the depth of the void.

In regard elastic constant determination, pulse echo can at times be considered the same as through transmission. That is, if the wavelength is large, compared to any potential voids, but small compared to the specimen geometry, then the propagating wave will treat the material as a continuum (ignore the void) and the back wall of the specimen will reflect some of the wave back to the original transducer. A time of flight measurement can be taken and so the wave velocity may be determined. From a physics standpoint this process is really no different to the through transmission approach; owing to aspects such as waves traveling through the specimen twice, it is not generally classed as through transmission however. Evidence of where the pulse

echo technique has been used to measure the velocity in composite can be found in a report commissioned by the National Aeronautics and Space Administration (NASA), by Prosser (1987). Prosser demonstrated the applicability of the pulse echo techniques to unidirectional graphite composite when he sought to determine the elastic constants of a composite used in a previous publication, (Kriz and Stinchcomb, 1979). Using a pulse overlap system – essentially the comparison of successive back wall reflections to determine the time difference and subsequently the wave velocity – Prosser demonstrated that the elastic constants of a unidirectional graphite composite (T300/5208) could be determined. As with (Zimmer and Cost, 1970), to obtain the desired velocities, multiple samples were required to allow for propagation at varying angles to fibre axis. Prosser compares the elastic constants determined through pulse echo with those of Kriz and Stinchcomb and found in general good agreement. Additional reading can be found from (Graciet and Hosten, 1994) who present similar analysis when they adopt pulse echo and Fourier analysis to determine attenuation, wave speed, thickness and density simultaneously.

Moving back to literature concerning the through transmission technique, Pearson and Murri (1987), built on (Kriz and Stinchcomb, 1979) and further investigated the issue of the group velocity vector deviating from the phase velocity vector within an anisotropic medium. For unidirectional graphite composite exhibiting orthotropic symmetry and the assumption that the 1 direction is the fibre direction, Pearson and Murri created multiple samples exhibiting varying degrees of angle between fibre axis and surface. Using the Zimmer and Cost approach and the Markham method the authors propagated both longitudinal waves and transverse waves in the 1-2 and 1-3 planes. Figure 33 illustrates both the samples and the group velocity effect.

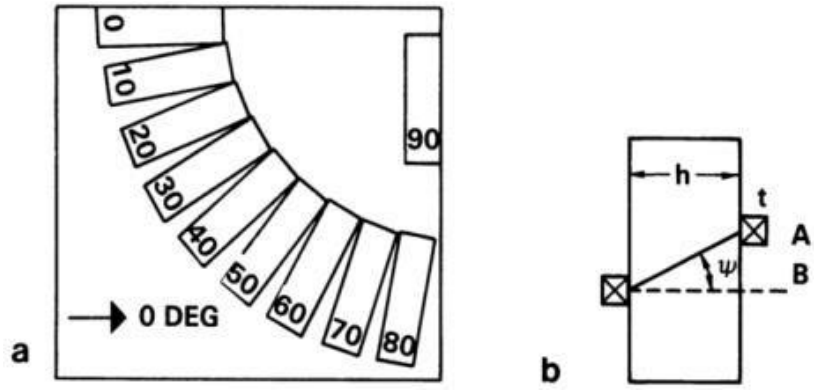

Figure 33 – Figure (a) documents various samples with degrees being reference to the fibre axis, figure (b) documents transducer placement and group velocity effect; transducer is moved to position A from position B, to compensate for group velocity effect as given by angle Ψ. *Review of Progress in*

The authors found that the only difference recorded between the group velocity and

 The authors documented angle deviation caused by the group velocity effect for both longitudinal and transverse waves in specific directions in both planes and recorded mathematical relationships between group velocity and phase velocity.

Building on this work and the general concept of increasing the accuracy of determining the elastic constants, two publications, (Rokhlin and Wang, 1989a, 1989b), introduced what is known as the double through transmission technique. The double through transmission technique is essentially the through transmission technique with an arguably slight combination of the pulse echo technique and is used today in many publications and so is considered a very important technique.

The experimental apparatus from Rokhlin and Wang (1989a) is shown in Figure 34.

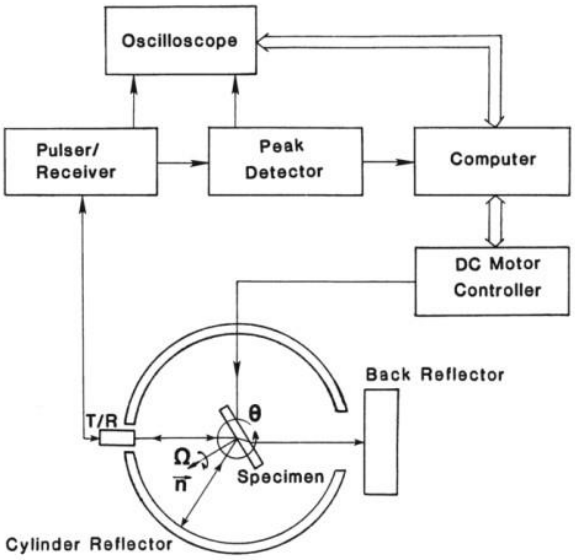

Figure 34 – Experimental apparatus of the double through transmission technique. A single transducer operates as both transmitter and receiver, both surface reflections and through transmission signals are able to be measured and note that the sample, transducer, cylinder and reflector are immersed in water (accurate ^{0} to temp – 0.1). *Review of Progress in Quantitative Nondestructive Evaluation, Chapter 8, Ultrasonic evaluation of in-plane and out-of-plane elastic properties of composite materials, Vol. 8, 1989, page 1489–1496, Rokhlin SI, Wang W, Copyright Springer Science+Business Media New York, With permission of Springer*

The double through transmission system takes into account the group velocity effect via the back reflector reflecting the ultrasonic beam in the same direction as it travelled originally, thus solving the problem of where to place the receiving transducer. Further information is found in the extended literature review given as appendix 2.

Using this technique, the authors conducted the same measurements as conducted by preceding authors to determine the phase velocity - noting that the group velocity was used instead of phase velocity which the authors effectively calculate in the same way as was previously outlined by Pearson and Murri (1987). Additionally, the authors similar to Pearson and Murri, employed a least squares fit procedure to determine the full set of elastic constants for uni-directional CFRP – noting the goal was to minimise the difference of the sum of squared experimental and theoretical velocities.

Building on this work, Rokhlin and Wang (1992) documented more thoroughly the relationship between the group velocity and phase velocity and also identified that phase velocity is required for elastic constant determination. Further, similar to Pearson and Murri, the authors also documented a least squares algorithm that allows for the elastic constant to be determined with a good degree of accuracy, even in the face of up to 5% scatter in the phase velocity results.

Moving forward an upgrade to the double through transmission technique was recorded by (Chu and Rokhlin, 1994a, 1994b, 1992) via a slight variation of the original technique; with the upgraded technique being known as the self-reference model (SRM). The novelty in this technique was via investigating increases in velocity measurement accuracy by using a reference velocity which incorporates the original sample. The distinction between the SRM and the standard approach is given in Figure 35.

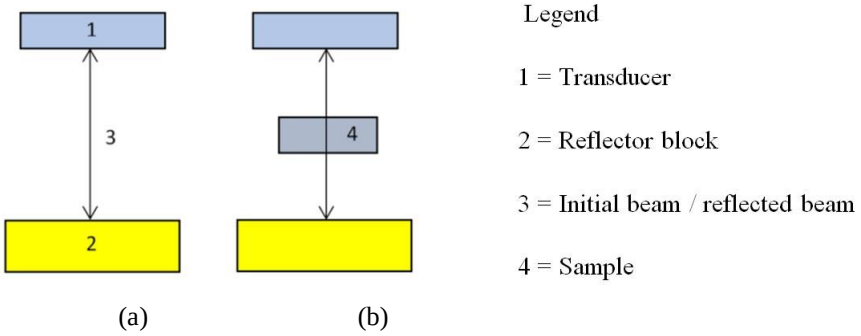

Figure 35 – Documenting the distinction between the standard double through transmission method and the SRM. Fig a) documents that the acoustic reference signal (water coupling medium not shown) measurement is made without the sample, fig b) documents for the SRM that acoustic reference measurement is made with sample at normal incidence.

Comparing the two systems in Figure 35, the authors found that maximum error owing to parallelism was recorded at normal incidence for the double through transmission system with error decreasing with increasing refraction. For the SRM, the opposite relationship was recorded, the most accurate results were obtained at normal incidence with slight increases in error being recorded as the refraction angle increased.

Expanding on the previous works was by Chu (1994) and Chu and Rokhlin (1994c) who sought to investigate the determination of elastic constants of unidirectional materials using limited velocity data in both the symmetry and nonsymmetry planes along with investigating which angles of propagation are best for determining specific elastic constants. Taking these works in conjunction with previous literature, (Chu and Rokhlin, 1994a, 1994b, 1992; Pearson and Murri, 1987; Rokhlin and Wang, 1992, 1989a, 1989b), who demonstrated that group velocity is able to be related to the phase velocity when conducting the Zimmer and cost approach, the Markham method and the double through transmission approach, it can be stated that circa 1994 the methods to determine the elastic constants of unidirectional composite materials were strongly established within literature.

In addition to the Zimmer and Cost approach, the Markham method and the double through transmission approach, other techniques are available. Through the 1990‟s investigations into how to relate phase velocity to group velocity measurements within CFRP was a field on-going research. As such, additional indirect relationships between the group velocity and elastic constants along with reconstruction algorithms may be found in literature (Arist gui and Baste, 1997; Balasubramaniam and Rao, 1998; Castagnede et al., 1989; Degtyar and Rokhlin, 1997; Deschamps and Bescond, 1995; Every and Sachse, 1992, 1990; K. Y. Kim et al., 1995; Kim, 1994; Kwang Yul Kim et al., 1995; Seiner and Landa, 2004).

Additionally, circa late 1980‟s – late 1990‟s various works, including significant contributions from a Bordeaux group led by Professor Bernard Hosten, investigated the viscoelastic properties of unidirectional composite materials, (Baudouin and Hosten, 1997, 1996; Cawley and Hosten, 1997; M Deschamps and Hosten, 1992; M. Deschamps and Hosten, 1992; Hosten, 1991; Hosten et al., 1987;
Hosten and Baudouin, 1995; Hosten and Castaings, 1993a, 1993b; Roux, 1990), via the techniques outlined in this review. Investigating viscoelastic properties of composites,

while interesting in its own merit and with literature documenting analysis of reflection and transmission coefficient amplitudes along with general attenuation measurements to investigate these properties, it is the case that viscoelastic properties are outside the scope of this review. However, acknowledgement is given to the fact that determining the viscoelastic properties requires the real elastic constants to be determined.

Through transmission via airborne ultrasound was also prevalent during this period. However, given that additional problems such as large impedance mismatch, extreme wave refraction, wave coupling, and the fact that the physics of wave propagation doesn‟t change once the waves are propagating through the medium, even with the double through transmission system having been documented in this field, (Hosten et al., 1996), it was felt that airborne ultrasound is best suited to an independent review. A recent literature review by Professor Chimenti of Iowa State University, (Chimenti, 2014), identifies both pertinent literature and gives particular focus to the many seminal works conducted as part of the French group led by

Professor Hosten at Bordeaux University.

Moving back to the immersion based approach, given that the experimental theory has been firmly established, Lavrentyev and Rokhlin (1997) sought to improve the technique by investigating accuracy of phase velocity measurements. Lavrentyev and Rokhlin (1997) identified that a longitudinal evanescent wave, created when the first critical angle is exceed can cause wave phase shift and so documented a slight adjustment to the mathematical relationship between phase velocity and elastic constants, as previously outlined by Chu and Rokhlin (1994a). Note that the accuracy increases recorded by the authors was found to be less than 1% with Wang (2003) further finding that phase error for a small amount of angles is not sufficient to account for a drastic change in elastic constants when using the least squares algorithm over a large data set (multiple angles of incidence). In 2005, a study seeking to compare results of elastic constant determination of uni-directional fibre via the double through transmission system and the standard Markham method was documented (Reddy et al., 2005). The authors found that the double through transmission system performed better than the Markham technique, however this was limited to glass epoxy uni-directional fibre in this study. Turning attention now to diffraction effects, (Adamowski et al., 2010, 2009, 2008, 2007), expanded on a previous publication by Wang (2003). Unlike Wang (2003) who conducted only a simulation of the diffraction effects, the authors conducted physical experiments.

Employing various transducers at various frequency, Adamowski found that diffraction effects can cause errors of around 1% in phase velocity measurements (Adamowski et al., 2010, 2009, 2008, 2007). Also, the diffraction decreased with increasing frequency when employing the through transmission technique. Countering these effects the authors suggest adopting an 80mm diameter polyvinylidene fluoride (PVDF) receiver, which caused negligible effects of phase velocity measurements. Noting that (Adamowski et al., 2009, 2008, 2007) documented these effects on aluminium, however (Adamowski et al., 2010) incorporate CFRP into similar studies and found similar results as previously outlined.

Concluding this review is Castellano (2014). At this point some 45 years of literature documenting bulk ultrasonic wave through transmission (in one form or another) of unidirectional composite has provided much information. Thus, Castellano document not a new experimental approach designed to increase the accuracy of measurement but instead document a bespoke computer programme to handle an existing measurement technique.

Using the double through transmission approach (Rokhlin and Wang, 1989a, 1989b), the authors determined the full five elastic constants of transversely isotropic CFRP. It should be mentioned that the authors designed their own apparatus in this instance, that is, the system allowed for both the Markham method and the double through transmission approach to be used. Figure 36 documents the custom mechanical grip allowing for both systems to be used.

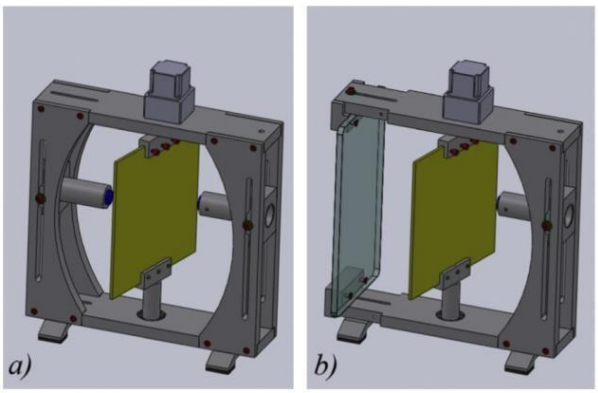

Figure 36 – Equipment used by (Castellano et al., 2014) that allows for both the Markham

method fig (a) and the do*from Composites part B: Engineering, Vol 66,* uble through transmission method fig (b) to be used. *Castellano, A; Foti, P; Fraddosio, A; Reprinted*

Marzano, Salvatore; Piccioni, Mario Daniele; Mechanical characterization of CFRP composites by ultrasonic immersion tests: Experimental and numerical approaches, Pages 299-310, Copyright (2014), with permission from Elsevier

The main novelty herein was the use of bespoke LabVIEW software. The software, deployed on a commercial PC, was used to control the oscilloscope, the rotation of stepper motor and the acquisition and reprocessing of experimental data to allow for a fully automated experimental process.

Figure 37 documents the graphic interface developed by the authors.

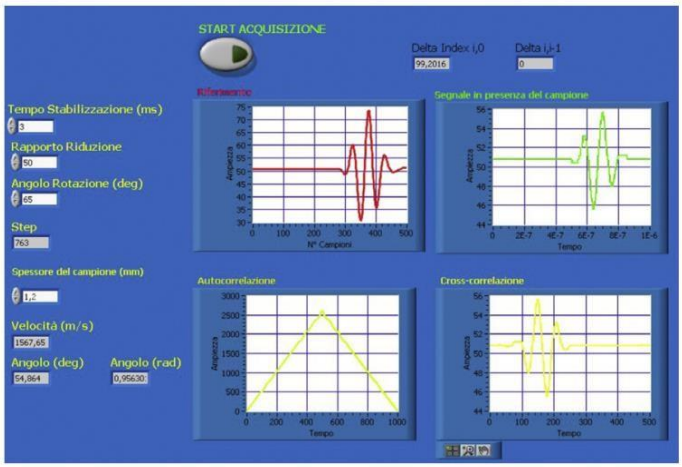

Figure 37 – Graphical interface as used by the (Castellano et al., 2014). *Reprinted from Composites part B: Engineering, Vol 66, Castellano, A; Foti, P; Fraddosio, A; Marzano, Salvatore; Piccioni, Mario Daniele; Mechanical characterization of CFRP composites by ultrasonic immersion tests: Experimental and numerical approaches, Pages 299-310, Copyright (2014), with permission from Elsevier*

Such is the precision of the bespoke experimental arrangement, through Snell‟s laws the three the three waves which propagate in both the isotropic and anisotropic plane were clearly observable. Figure 38, is given to demonstrate the results obtainable.

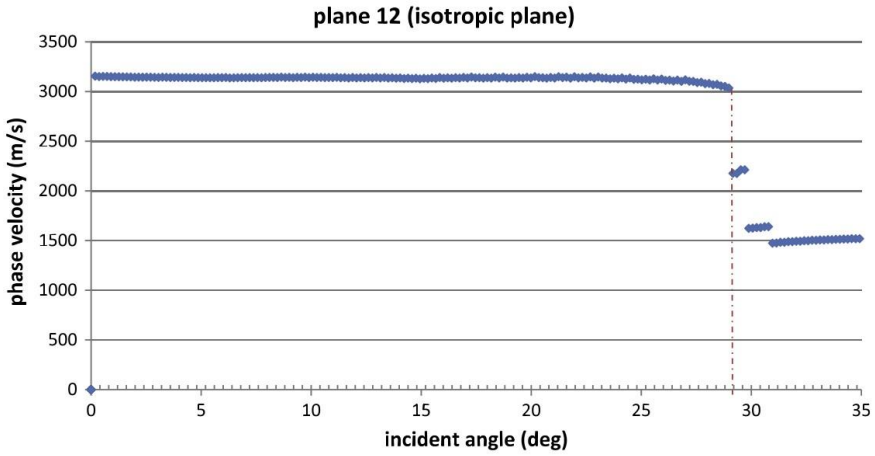

Figure 38 – The longitudinal, fast transverse and slow transverse waves recorded in the isotropic plane. Data between the longitudinal wave and the fast transverse wave is thought to be experimental error. *Reprinted from Composites part B: Engineering, Vol 66, Castellano, A; Foti, P; Fraddosio, A; Marzano, Salvatore; Piccioni, Mario Daniele; Mechanical characterization of CFRP composites by ultrasonic immersion tests: Experimental and numerical approaches, Pages 299-310, Copyright (2014), with permission from Elsevier*

7.5. Information Tables

This summarized literature review, (full version is given as appendix 2) has identified some 45 years of literature concerning the determination of elastic constants by ultrasonic through transmission. Accordingly, two unique information tables identifying contributions to knowledge during this period are given in this review. Notable findings documented within literature within the period 1970 – 1980 are documented in Table 25 and notable findings for the period 1980 – present day are documented in Table 26

Key Findings:1970 – 1980	Authors
Standard transmitting frequency used in measurements is 5 MHz but some authors also reported lower frequency at around 1 MHz	All
Sample specimen is limited to ensure body wave behaviour (in general thickness kept above two wavelengths and wavelength kept above fibre diameter).	All
When propagating in fibre direction, if pulse width equal to sample width, data on mode changing in inconclusive	(Dean and Lockett, 1973)
Unidirectional composite causes the wave energy direction to skew at angle, θ, from the phase wave front normal when waves strike surface obliquely	(Kriz and Stinchcomb, 1979)
Velocity able to be measured using direct contact through transmission technique	(Kriz and Stinchcomb, 1979; Reynolds and Wilkinson, 1978; Wilkinson and Reynolds, 1974; Zimmer and Cost, 1970)
Velocity able to be measured via immersing transducers in water and rotating sample and using through transmission technique	(Dean, 1971; Dean and Lockett, 1973; Markham, 1970; Reynolds and Wilkinson, 1978; Smith, 1972; Wilkinson and Reynolds, 1974)
Velocity able to measured using prism technique	(Dean, 1971; Dean and Lockett, 1973; Markham, 1970; Reynolds and Wilkinson, 1978; Wilkinson and Reynolds, 1974)
All elastic constants determined	(Dean and Lockett, 1973; Kriz and Stinchcomb, 1979; Markham, 1970; Reynolds and Wilkinson, 1978; Smith, 1972; Wilkinson and Reynolds, 1974; Zimmer and Cost, 1970)
Composite Young‟s Modulus (at varying angles to fibre axis) can be determined from velocity measurements	(Dean, 1971; Dean and Lockett, 1973; Zimmer and Cost, 1970)
C_{44} changes value depending whether the fibre axis is perpendicular or parallel to wave direction	(Dean, 1971; Dean and Lockett, 1973; Kriz and Stinchcomb, 1979; Markham, 1970; Smith, 1972; Zimmer and Cost, 1970)
Theoretical predictions for stiffness are in general in close agreement with experiment when propagating shear waves polarised in plane of the fibre from 0^o - 90^o in CFRP (using C_{44} measured perpendicular to fibre axis)	(Reynolds and Wilkinson, 1978; Smith, 1972; Wilkinson and Reynolds, 1974)

When propagating longitudinal waves for angles greater than 0º and less than 90º to the fibre direction in CFRP (in the plane of the fibre), the experimental values for stiffness do not follow the expect theoretical curve, thus, through attenuation, refraction and reflection (a pseudo-L wave is actually being propagated throughout the sample)	(Reynolds and Wilkinson, 1978; Wilkinson and Reynolds, 1974)
Theoretical predictions for stiffness are in general closer to experimental values when angle of propagation direction to fibre axis is >65º when propagating shear waves polarized perpendicular to plane of the fibre from 0º - 90º in glass composite or CFRP	(Wilkinson and Reynolds, 1974; Zimmer and Cost, 1970)
Theoretical predictions for stiffness are not in as good agreement with experiment to those of shear waves when propagating longitudinal waves from 0º - 90º in glass composite	(Zimmer and Cost, 1970),
The elastic constants determined through ultrasound velocity technique may be used with theoretical predictions to calculate individual fibre properties	(Kriz and Stinchcomb, 1979; Reynolds and Wilkinson, 1978; Smith, 1972)
Composite elastic constants $C_{11,}$ C_{33} and C_{66} are dependent on the fibre Young‟s modulus, while C_{13} and C_{44} are independent of fibre modulus but vary with fibre type (graphite fibres) and have a slightly unclear relationship in carbon fibres. Also, elastic constants do not greatly depend on shear strength of composite	(Smith, 1972)
Average elastic constants of disorientated CFRP (in one plane only) can be calculated	(Dean, 1971)
Velocity in fibre direction is not greatly impacted by void content and only a small dependency on type of resin used	(Dean, 1971; Reynolds and Wilkinson, 1978)
Velocity perpendicular to fibres dependent on both void content and type of fibre concentration	(Dean, 1971; Reynolds and Wilkinson, 1978)
Elastic constant determination through velocity measurements may be used to determine degree of porosity and fibre content	(Reynolds and Wilkinson, 1978)

Table 25 - Key findings from the literature reviewed 1970-1980. Findings demonstrate the ultrasonic velocity measurements are a legitimate and able practice to determine the elastic constants of transversely isotropic CFRP and what the constants are dependent upon. Findings also indicate the applicability of ultrasonic velocity measurements to gauge the porosity, fibre concentration and degree of disorientation of transversely isotropic CFRP.

Key Findings from 1980 – 2014	Authors
Establishment of group velocity relationship to phase velocity using time of flight data	All
Identification of possible error arising from incorrect placement of receiving transducers in Markham Method	(Pearson and Murri, 1987; Rokhlin and Wang, 1992, 1989a)
Group velocity effects cause different degrees of deviation for different wave types	(Castellano et al., 2014; Pearson and Murri, 1987; Rokhlin and Wang, 1992, 1989a)
A least squares minimization technique used (wholly or in part) to determine the set of elastic constants	(Adamowski et al., 2010, 2009, 2008, 2007; Castellano et al., 2014; Chu et al., 1994; Chu and Rokhlin, 1994c; Lavrentyev and Rokhlin, 1997; Pearson and Murri, 1987; Reddy et al., 2005; Rokhlin and Wang, 1992, 1989a; Wang et al., 2003)
Investigated robustness of least squares algorithm in relation to the choice of initial guess of elastic constant and noise inserted onto phase velocity measurements	(Chu et al., 1994; Chu and Rokhlin, 1994c; Rokhlin and Wang, 1992)
Identification that when using least squares algorithm for limited velocity data on orthotropic unidirectional graphite composite that ideally longitudinal waves should cover the region 0- 45º (or above) and transverse waves should cover the region 35 - 75º (or above) to the fibre axis	(Chu and Rokhlin, 1994c)
Double through transmission method used to determine phase velocity / elastic constants	(Castellano et al., 2014; Reddy et al., 2005; Rokhlin and Wang, 1992, 1989a)
Orientation of the principal axis of symmetry determined using the Markham method	(Castagnede et al., 1990)
15 MHz transducer used in double through transmission arrangement	(Rokhlin and Wang, 1992)
Self-reference method used to determine phase velocity / elastic constants	(Chu et al., 1994; Chu and Rokhlin, 1994a, 1994c; Lavrentyev and Rokhlin, 1997; Wang et al., 2003)

Identification of optimum refraction angles for determination of two elastic constants in non-symmetry planes of unidirectional orthotropic graphite composite	(Chu et al., 1994)
Identification, including subsequent compensation measures, that at certain angles of incidence a resultant phase shift can cause erroneous phase velocity measurements	(Lavrentyev and Rokhlin, 1997; Wang et al., 2003)
Diffraction effects cause a reduction in amplitude while having little effect on phase velocity measurements for refraction angles out with critical angle regions on unidirectional graphite fibre composite	(Wang et al., 2003)
Double through transmission verified as producing more precise and repeatable results than Markham method with more inaccuracy being recorded as the thickness of samples grew (transducers fixed)	(Reddy et al., 2005)
Demonstrated that as frequency increased diffraction effects decreased and dispersion effects increased for an aluminium plate and employed a PVDF receiver to reduce possible diffraction effects and measured elastic constants of unidirectional graphite fibre composite	(Adamowski et al., 2010, 2009, 2008, 2007)
Demonstrated that bespoke PC software, created on LabVIEW, was able to facilitate automated double through transmission based experiments	(Castellano et al., 2014)
Double through transmission system encounters maximum error due to parallelism effects at normal incidence and decreases as angle of refraction increases with the self-reference method having a contrasting relationship for phase velocity measurements in unidirectional graphite fibre composite	(Chu and Rokhlin, 1994a)
Identification of the optimum wave refraction angles, within a plane of symmetry, for determination of seven out of nine elastic constants in a weakly anisotropic composite (orthotropic unidirectional graphite composite)	(Chu and Rokhlin, 1994c)
Identification that for a strongly anisotropic composite (orthotropic unidirectional graphite composite) the sensitivity of elastic constants is not dependently only the refraction angle (i.e. phase velocity is not dependent on angle of refraction only)	(Chu and Rokhlin, 1994c)
Identification that for orthotropic materials that determination of seven, out of nine, elastic constants from symmetry planes and the remaining two, out of nine, from non-symmetry planes will result in more accurate values than would determination of all constants from non-symmetry planes	(Chu et al., 1994)

Table 26 - Key findings from the literature reviewed 1980-2014. Findings demonstrate the double through transmission is used extensively along with elastic constant reconstruction algorithms. These findings also indicate the optimum way to determine constants from orthotropic material along with methods to increase accuracy of results

7.6 Conclusion

This chapter has documented a summarized version of a relative large literature review (see appendix 2) which charts the progression of how the elastic constants of unidirectional composite were experimentally determined using ultrasonic bulk wave velocity measurements from circa 1970 – 2015. Additionally, the findings presented in this chapter outline which experimental techniques are used by which authors and also document the most accurate technique of modern times, the double through transmission technique. Additionally, two bespoke information tables outlining contributions to knowledge over some 45 years on knowledge were also provided. It was also recorded that little to no literature documents the determination of elastic constants of rf-CFRP via an immersion based ultrasonic through transmission technique. With over 45 years of recorded knowledge and experimentation conducted on uni-directional v-CFRP, this chapter has given insight into the type of research that has yet to be conducted on rf-CFRP. Considering that the various types of composite recycling i.e. thermal, mechanical, chemical, can result in different levels of fibres in terms of structure and performance, future rf-CFRP ultrasonic through transmission research areas are able to be readily identified. For instance, areas such as elastic constant determination, critical angle measurements, phase shifts, group velocity effects, robustness of reconstruction algorithms in terms of scatter and plane of determination, etc. are all potential areas for future investigation. Looking forward to chapter 8, with the second research question in mind, the applicability of using ultrasonic through transmission to investigate elastic constants of rf-CFRP is presented.

Chapter 8: Analysis of ultrasonic through transmission applied to rf-CFRP

Having now documented the relationship between ultrasonic wave velocity and elastic constants of a solid along with a literature review of the through transmission technique on uni-directional CFRP, it is appropriate now to perform the experimental part of this

thesis. Having already outlined the necessary information this chapter seeks to investigate the second research question using already established knowledge.

8.1 Experimental Methodology

Figure 39 is given to demonstrate the experimental methodology used in this research.

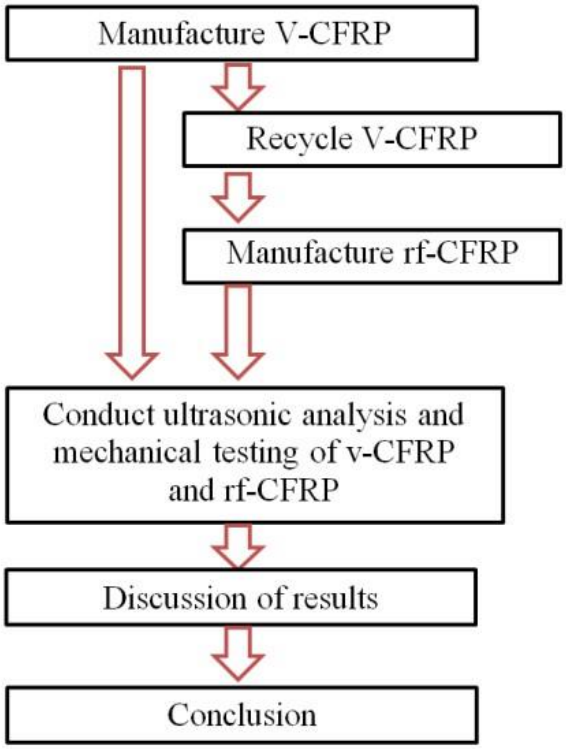

Figure 39 – Experimental methodology for ultrasonic analysis of both v-CFRP and rf-CFRP

8.2 Manufacture of v-CFRP and rf-CFRP

Unidirectional Pyrofil TR50S 15K carbon fibre along with EL2 epoxy resin and slow hardener were purchased from easy composites (www.easycomposites.co.uk). The fibre was manually excised into sections of 0.4m by 0.2m, with 16 of these sections stacked vertically to form a 16 layer unidirectional stack. At this point the 16 layer stack was placed onto a workstation coated in resin release agent. A vacuum assisted resin transfusion system, again purchased from easy composites, was then used to impregnate the uni-directional stack with mixed epoxy and slow hardener solution; note that the epoxy resin and hardener was mixed at a ratio of 100:30, as per

manufacturing guidelines and degassed prior to impregnation. Note that a 16 layers composite was upper limit of what could be manufactured. The vacuum assisted resin transfusion system relies on a vacuum and suction to impregnate the carbon fibre with matrix. The vacuum was not sufficiently powerful enough to produce fully impregnated composite when the number of layers was greater 16.

Once fully impregnated, the suction was removed and the sample was left in situ (with the vacuum maintained) as per manufacturing instruction for 48 hours to cure at room temperature.

Manufacture of rf-CFRP first required v-CFRP to be recycled. A pyrolysis process, (Meyer et al., 2009; Oliveux et al., 2015; Pickering, 2006; Pimenta and Pinho, 2012, 2011; Shi et al., 2012b), was performed. A standard Carbolite oven was preheated for approximately 1 hour until the figure of 600°C was reached. At this stage, v-CFRP samples were placed in the oven and allowed to dwell for 45 minutes. After this time period, the samples were removed and were allowed to cool in the ambient air.

The time period and temperature were chosen in accordance with (Meyer et al., 2009). The authors documented that at 600 °C, epoxy would have gone through a full pyrolysis process (complete oxidation) and that carbon fibre does not suffer oxidation at this temperature - note these results document only the epoxy resin and carbon fibres in isolation. The authors also identify that for pyrolysis of CFRP at 600 °C, oxidization of the carbon fibres will increase with increased dwelling times and so striking a balance to fully remove the resin and leave the fibres largely intact, a time period of 45 minutes was selected. This process was identical to that conducted in, (Paterson et al., 2018). This paper is included as appendix 6, with some findings discussed in section 8.4.

Once suitably cooled the fibre stack was then, similar to v-CFRP, subject to vacuum assisted resin transfusion. Given that the recycling process returns fibres more fragile than v-CFRP it is not possible to stack reclaimed fibres on top of each other. In this work, the reclaimed fibre stack was placed carefully onto a workstation coated in resin release agent. Once impregnated via vacuum assisted resin transfusion the samples were again similar to v-CFRP left in situ with a maintained vacuum for 48 hours.

Table 27 and 28 outline the manufactured samples of both v-CFRP and rfCFRP. 9 samples of v-CFRP and rf-CFRP were manufactured each (18 samples in total). Both v-CFRP and rf-CFRP samples 1-4 were used for ultrasound through transmission with v-CFRP and rf-CFRP samples 5-9 used for mechanical testing. Note that to

manufacture precise rectangles and squares an OMAX 115 water jet cutter was utilized.

Sample		Dimensions			Density
No.	Shape	Width (mm)	Length (mm)	Thickness (mm)	Kg/m^3
v-CFRP 1	Square	50	50	1.91	1340.3
v-CFRP 2	Square	50	50	1.94	1319.6
v-CFRP 3	Square	50	50	2.15	1293.0
v-CFRP 4	Square	50	50	2.13	1295.7
v-CFRP 5	Rectangle	15	250	1.75	N/A
v-CFRP 6	Rectangle	15	250	1.79	N/A
v-CFRP 7	Rectangle	15	250	1.83	N/A
v-CFRP 8	Rectangle	15	250	1.76	N/A
v-CFRP 9	Rectangle	15	250	1.82	N/A

Table 27 – Dimensions of CFRP samples, excised from larger sections of material.

Sample	Shape	Dimensions			Density (Kg/m^3)
		Width (mm)	Length (mm)	Thickness (mm)	
rf-CFRP 1	Square	50	50	1.43	1332.8
rf-CFRP 2	Square	50	50	1.25	1442.3
rf-CFRP 3	Square	50	50	1.29	1406.3
rf-CFRP 4	Square	50	50	1.33	1373.5
rf-CFRP 5	Rectangle	15	220	1.64	N/A
rf-CFRP 6	Rectangle	15	220	1.43	N/A
rf-CFRP 7	Rectangle	15	220	1.71	N/A
rf-CFRP 8	Rectangle	15	220	1.53	N/A
rf-CFRP 9	Rectangle	15	220	1.42	N/A

Table 28 – Dimensions of rf-CFRP, excised from larger sections of v-CFRP material.

Density was calculated using mass, density, volume relationship. The volume was established by through a geometrical volume relationship of a cuboid being depth x width x length. Measurements of v-CFRP and rf-CFRP dimensions were taken in mm using digital calipers accurate to 2 decimal places. The weight was calculated in grams using digital scales accurate to 3 decimal places.

8.3 Ultrasonic and Mechanical testing

Ultrasonic testing and mechanical testing of both v-CFRP and rf-CFRP is now discussed. V-CFRP is considered firstly.

8.3.1 v-CFRP ultrasonic analysis

The experimental arrangement used to determine the elastic constants of the v-CFRP was the Markham method, (Markham, 1970; Reddy et al., 2005; Smith, 1972). As a frame of reference, the fibre direction of all CFRP samples was chosen as the 3 direction with the through the sample direction chosen as 1 direction and the 2 direction fell therefore at 90 degrees to both the 1 and 3 directions. Figure 40 documents the experimental apparatus used in this thesis.

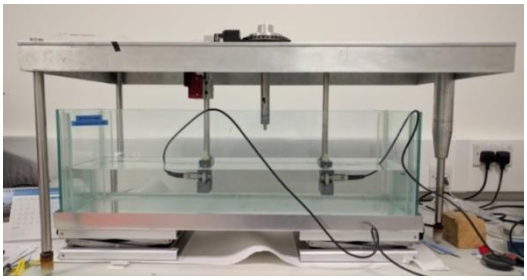

(a)

(b)

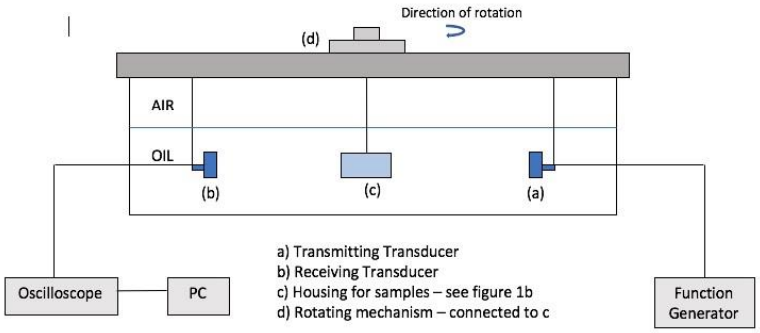

(c)

Figure 40- Figure (a) shows both the emitting and receiving transducers, immersed in a body of oil. Figure (b) shows the mechanical rotation device, controlled mechanically from above, upon which the samples were placed. In this research, the samples were not circular and were housed across the slots

and not housed within the slots. Figure (c) is a diagrammatical representation of the ultrasonic system presented in Figure (a) and (b).

Experimental procedure was as follows. First, sample v-CFRP 1 was loaded onto the apparatus shown in Figure 40 (b). This apparatus was then loaded into place directly between both the emitting and receiving transducer as documented in Figure 40 (a). The sample was housed in the setup such that the 3 axis (fibre direction) was at 90^0 vertical to the transducer face normal and so an incident wave would propagate through the 1-2 plane.

Starting from incident an angle of 0^0 the sample was rotated clockwise around the 3 axis until the signal was no longer able to be detected at the receiver – noting that transverse waves were created by virtue of Snell‟s Laws. During this clockwise rotation, the wave signals at various angles of incidence were recorded and thus both longitudinal and transverse wave velocities were able to be determined. To ensure accuracy of both the sound path and sample alignment between transducers the rotary equipment used had an angular resolution of 0.01° over 360°; the rotatory mechanism was provided by Time and Precision Industries, Hampshire, UK. Further, to ensure accurate measurement of the transit time and therefore the velocity taken to propagate through the samples, a cross correlation technique, in accordance with existing literature, (Trogé et al., 2016), was used. Determination of wave velocity was performed using MATLAB, noting that to account for any small changes in temperature a new reference velocity was taken each time a new sample was investigated.

At the point where no signal was detected the sample was removed and rotated 90 ^{o} ^{o} clockwise so that the 3 direction (fibre direction) was at 90 horizontal to the transducer face normal (waves now propagating through the 1-3 plane). A similar procedure as with the 1-2 plane was performed. Figure 41 documents the fibre axis to coordinate system relationship in addition to hypothetical waves propagating through the 1-2 plane as seen from a top down view.

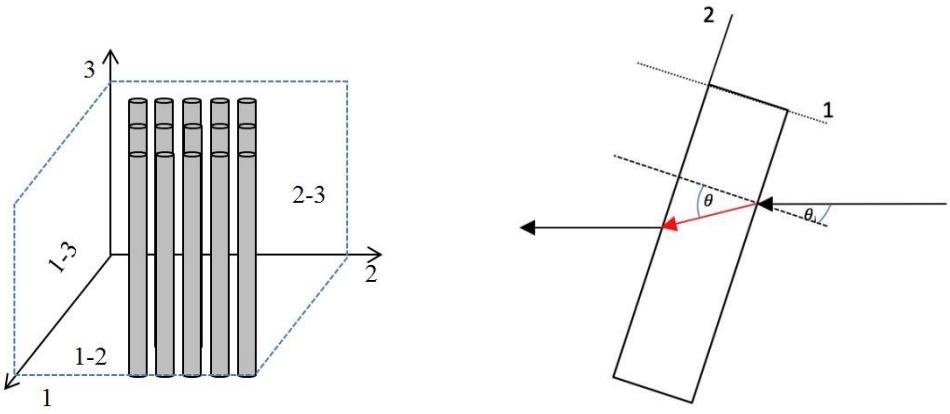

(a) (b)

Figure 41 _ Figure (a) documents the fibre direction to coordinate axis relationship. Figure (b) documents a top down view of a wave propagating in the 1-2 plane, θ is the refracted wave, θ_i is the incident angle (note the 3 axis is pointing out of the page in Figure b)

Additional experimental parameters are recorded in Table 29.

Transducer frequency	Coupling medium	Distance between transducers
2.25 MHz	Perfluoropolyether oil – PFPE	289.5mm

Table 29 – Additional experimental parameters

The parameters in Table 29 were not chosen exclusively for this research. The experimental set up as given in Figure 40 was in constant operational use by researchers within the Centre for Ultrasonic Engineering (CUE) at the University of Strathclyde.

As such the separation distance of 289.5 mm was already established prior to this research, but can however be justified. Given the desire to obtain plane wave propagation (plane wave propagation is required for the Christoffel equation), the system was established to facilitate using a variety of transducers while ensuring that the sample is kept in the far field of the ultrasonic beam. Locating the sample in the far field of the ultrasonic beam allows plane wave propagation to be approximated (Trogé et al., 2016).

Regarding the choice of oil as a couplant; a successful couplant should ensure no large signal attenuation while at the same time allowing for transverse waves to be

propagated (via Snell‟s laws) successfully through the sample. The choice of oil in this case achieves both factors. Again oil was not chosen specifically (the default couplant used within the CUE department is oil) but given that oil does not hinder any measurements of ultrasonic waves under investigation then decision was made to progress with the oil couplant.

Lastly, the transducers used in this instance were two Panametrics A304s‟ with a centre frequency of 2.25 MHz and a diameter of 1”. Within literature, frequencies of 1 MHz to 5 MHz have been selected to investigate the elastic constants of uni-directional v-CFRP. The 2.25 MHz selected for this thesis was within this range. Further, the wavelength of the wave meets the condition that it should be larger than the fibre diameter. Additionally, the transducers were excited via the function generator (see figure 40) to output a single cycle at centre frequency of 2.25 MHz with a pulse repetition rate of 6.67 ms thus ensuring that acoustic waves are detected by the receiving transducer before a new wave is transmitted from the emitting transducer. Further, with the choice of oil as a couplant the frequency of 2.25 MHz was a suitable choice in that the signals were sufficiently clear (i.e. they were not significantly attenuated such that signals were able to easily determined and analysed).

Each v-CFRP and rf-CFRP sample was measured using this experimental arrangement with appendix 3 documenting all wave velocities recorded for the both the v-CFRP and rf-CFRP samples.

Examining now the v-CFRP samples, the average wave velocities and the standard deviation for 1-2 and 1-3 planes are given in Table 30 and 31, with Figures 42 (a) and (b) documenting the average wave velocity against incident angle. These averages and standard deviations are obtained from the velocities recorded for the four v-CFRP samples listed as v-CFRP 1, 2, 3 and 4 in table 27.

Sample v-CFRP Average Plane 1-2		
Incident Angle	Velocity m/s	Wave type
0	2185.9 ± 51.34	L
3	2167.3 ± 48.16	L
6	2161.5 ± 59.80	L
9	2182.2 ± 59.25	L
12	2263.9 ± 49.72	L
14	2378.2 ± 39.75	L
15	2352.5 ± 98.52	L
16	1124.4 ± 19.02	T
17	1128.5 ± 16.02	T
18	1143.6 ± 15.40	T

19	1153.6 ± 15.27	T
20	1162.5 ± 13.48	T
21	1163.6 ± 11.36	T
24	1164.2 ± 9.82	T
27	1148.0 ± 12.06	T
30	1127.9 ± 14.36	T
33	1117.6 ± 19.31	T
36	1088.6 ± 23.32	T
38	1057.1 ± 15.95	T
Longitudinal wave not observed approximately >15º Transverse wave not observed approximately >39/40º		

Table 30 – Average ultrasonic velocity with respect to incident angle in the 1-2 plane for average v-CFRP sample

Sample v-CFRP Average Plane 1-3		
Incident Angle	Velocity m/s	Wave type
0	2270.5 ± 36.49	L
2	2274.1 ± 49.39	L
3	2267.9 ± 57.22	L
4	2305.9 ± 137.61	L
5	1868.8 ± 107. 48	T
6	1931.3 ± 64.14	T
8	1935.7 ± 69.18	T
10	1880.5 ± 64.34	T
12	1806.9 ± 53.19	T
14	1717.1 ± 55.47	T
16	1651.6 ± 46.78	T
18	1588.4 ± 40.40	T
20	1536.4 ± 33.81	T
22	1485.3 ± 32.74	T
24	1432.4 ± 27.62	T
26	1405.7 ± 24.18	T
28	1361.2 ± 15.40	T
30	1303.1 ± 7.75	T
32	1237.7 ± 4.60	T
Longitudinal wave not observed approximately >4º Transverse wave not observed approximately >38/39º After 28º sample became more difficult to correlate owing to noise levels		

Table 31 – Average ultrasonic velocity with respect to incident angle in the 1-3 plane for average v-CFRP sample

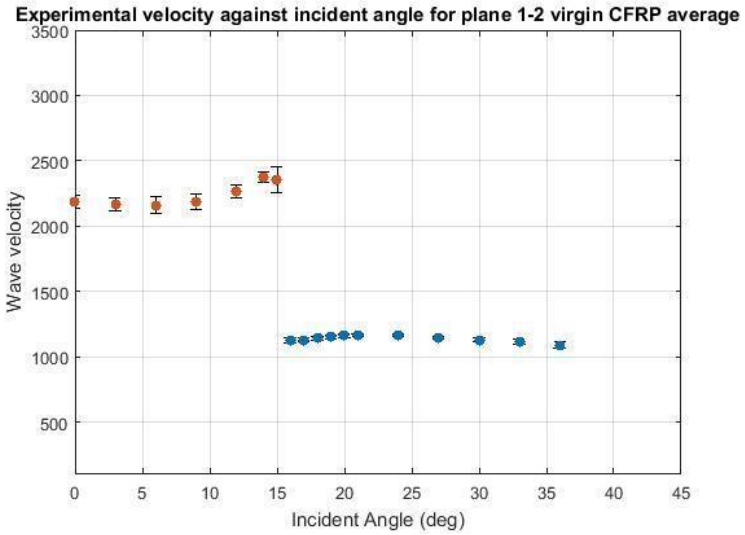

(a)

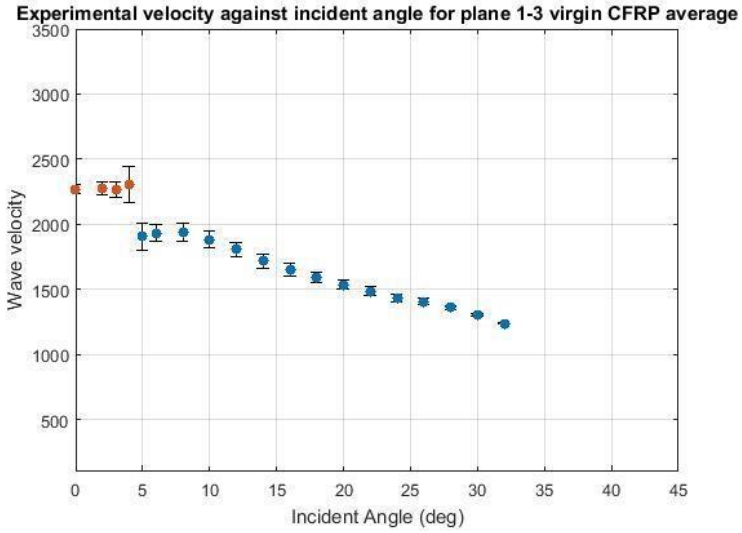

(b)

Figure 42 – Graphical results of the average recorded wave velocities. Figure (a), L and T waves in 1-2 plane. Figure (b,) L and T waves in the 1-3 plane. Red dots are L waves, blue dots are transverse waves.

Examining first Figure 42(a) – wave propagation in the 1-2 plane, it can be stated that for transverse isotropy this plane is under the assumption of isotropy – noting that for an ideal isotropic plane, wave velocity does not change with incident angle. Regarding the longitudinal wave, a

relatively constant average velocity is recorded between 0 and 12 with an increase between 12 and 15. The transverse velocity is more closely related across its whole wave profile, but variation in velocity is recorded. All v-CFRP samples recorded approximately the same velocity profile in the 1-2 plane - low standard deviation values from Table 30 and standard deviation error bars on figure 42 can be observed. Figures 43 (a), (b), (c) and (d), also given to demonstrate the close relationship in sample behaviour.

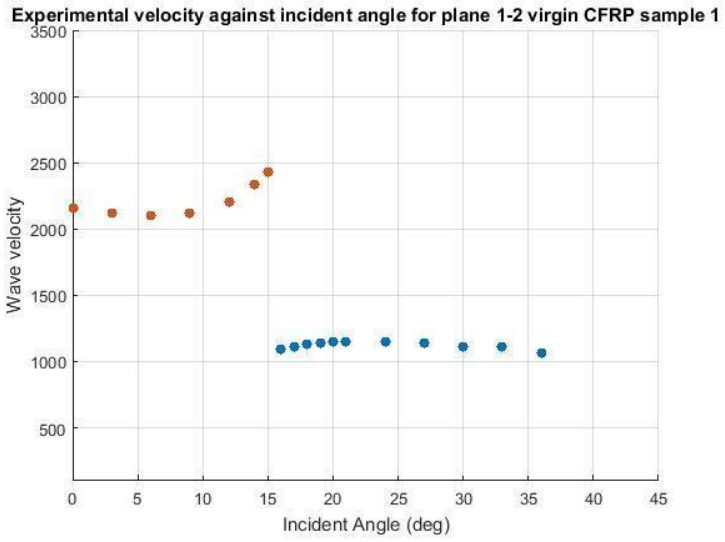
Experimental velocity against incident angle for plane 1-2 virgin CFRP sample 1
Wave velocity
Incident Angle (deg)
3500
3000
2500
2000
1500
1000
500
0
5
10
15
20
25
30
35
40
45

(a)

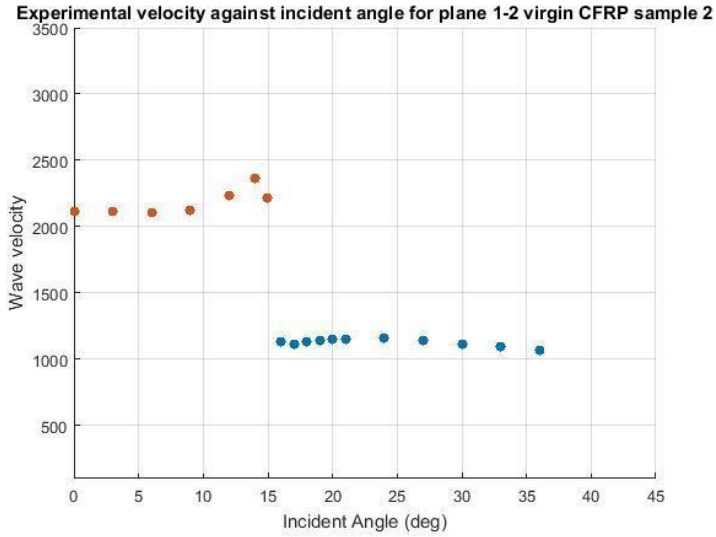
Experimental velocity against incident angle for plane 1-2 virgin CFRP sample 2
Wave velocity
Incident Angle (deg)
3500
3000
2500
2000
1500
1000
500
0
5
10
15
20
25
30
35
40
45

(b)

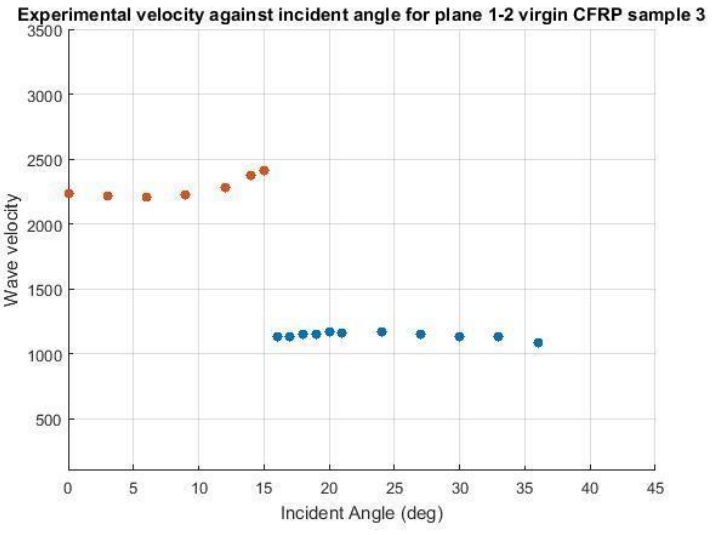
Experimental velocity against incident angle for plane 1-2 virgin CFRP sample 3
Wave velocity
Incident Angle (deg)
3500
3000
2500
2000
1500
1000
500
0
5
10
15
20
25
30
35
40
45

(c)

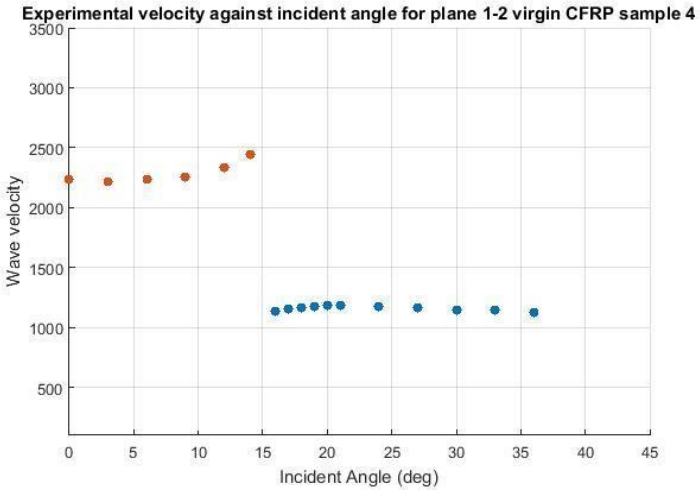

(d)

Figure 43 _ Graphical results of the velocity against incident angle for individual samples in the 1-2 plane. Figures (a), (b), (c) and (d) correspond to samples 1, 2, 3 and 4 respectively. A close relationship in wave velocity profile is observed

The increase in longitudinal velocity as the critical angle was approached is thought to have arisen from two reasons; a) the samples are not perfectly isotropic in this plane and b) experimental error via velocity measurement coupled with the samples having a slightly uneven (bumpy) surface. When compared to findings from literature however, (Castellano et al., 2014; Reddy et al., 2005), the results recorded here do in general mirror what is expected from the isotropic plane of a transversely isotropic composite.

Examining now, Figure 42 (b), in the 1-3 plane the longitudinal velocity is expected to increase with increasing incident angle. The average results record a relatively constant velocity, with a slight increase with incident angle as the angle of around 5, is ^{o} reached. At this point the transverse waves start to emerge independently. Looking closer at the standard deviation values from table 31 and as demonstrated via the standard deviation error bars on figure 42 (b), small values are recorded at angles of 0 , 2 and 3 with a ^{o} ^{o} ^{o} ^{o} larger value recorded at 4, which upon examining the individual curves for the samples is explainable. The wave profile in the 1-3 plane for v-CFRP samples, 1, 2, 3, and 4 are given as Figures 44 (a), (b), (c) and (d) respectively.

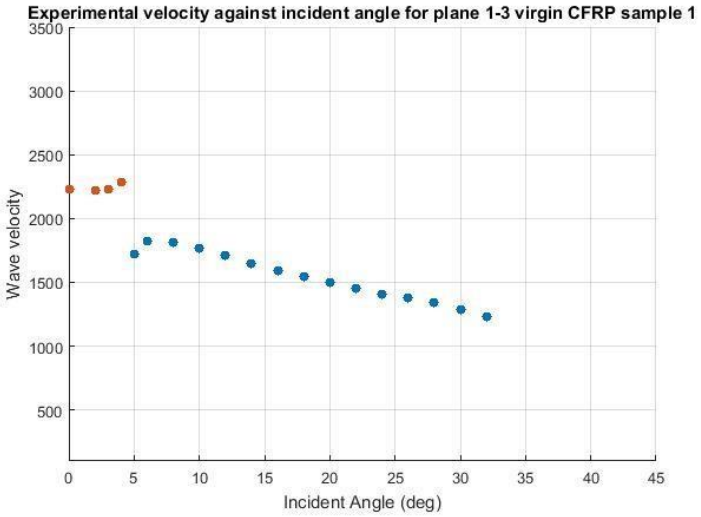
Experimental velocity against incident angle for plane 1-3 virgin CFRP sample 1
Wave velocity
Incident Angle (deg)
3500
3000
2500
2000
1500
1000
500
0
5
10
15
20
25
30
35
40
45

(a)

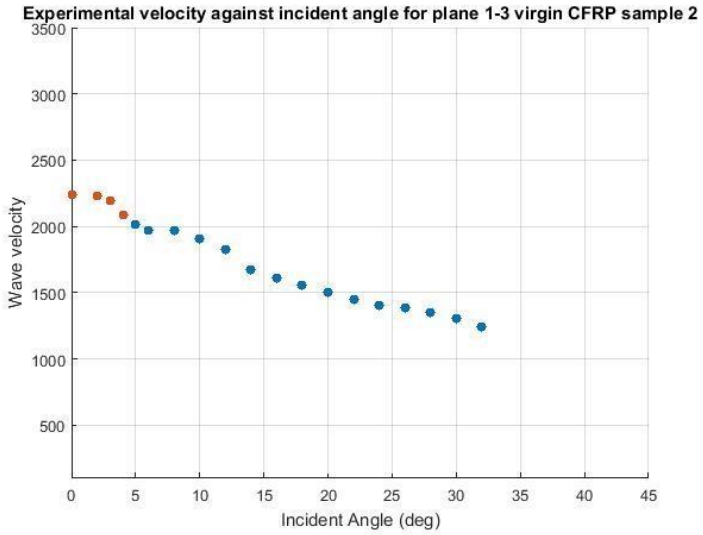
Experimental velocity against incident angle for plane 1-3 virgin CFRP sample 2
Wave velocity
Incident Angle (deg)
3500
3000
2500
2000
1500
1000
500
0
5
10
15
20
25
30
35
40
45

(b)

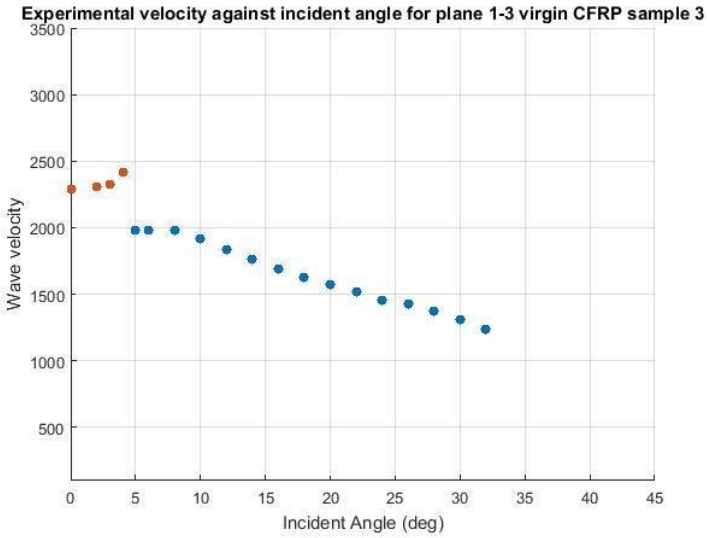
Experimental velocity against incident angle for plane 1-3 virgin CFRP sample 3
Wave velocity
Incident Angle (deg)
3500
3000
2500
2000
1500
1000
500
0
5
10
15
20
25
30
35
40
45

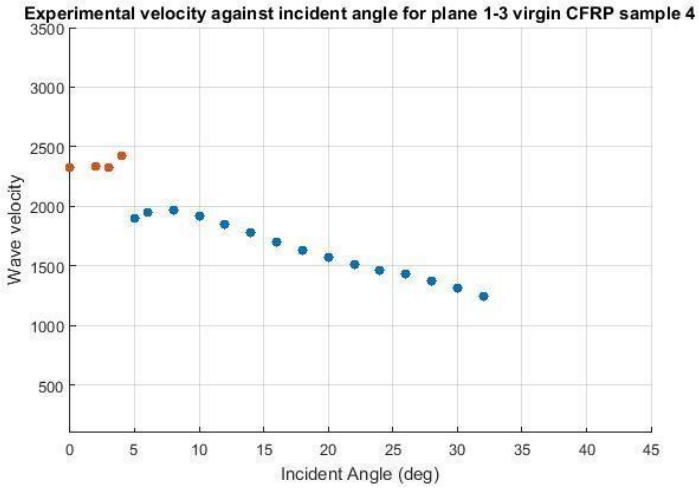

(d)

Figure 44 – Graphical results of the velocity against incident angle for individual samples in the 1-3 plane. Figures (a), (b), (c) and (d) correspond to samples 1, 2, 3 and 4 respectively

It is evident that v-CFRP samples, 1, 3 and 4, Figures (a), (b) and (d) record a similar longitudinal velocity profile with a small increase in velocity with the transverse wave emerging independently around 5^{0}. V -CFRP sample 2 records a decreasing longitudinal velocity with increasing incident angle, which then merges smoothly into the transverse velocity. The reason for the larger standard deviation figure at 4^{0} is due to the different behaviour of v-CFRP sample 2, which also creates the relative constant velocity recorded in the average results, Figure 42 (b). Given the expected behaviour in the 1-2 plane of v-CFRP sample 2, the unexpected velocity profile recorded in the 1-3 plane is thought to have arisen from experimental error coupled with the sample having a slightly uneven surface.

Examining now the average transverse velocity of Figure 42 (b). The wave velocity profile is in agreement with that expected from the 1-3 plane; a small increase in velocity followed by a decreasing velocity with increasing incident angle. On an individual basis, the only real exception was again sample v-CFRP 2, Figure 44 (b). The transverse velocity arises from the decreasing longitudinal velocity making the cross over period difficult to accurately observe. Further, the transverse

(c)

velocity profile differs slightly from that recorded with the v-CFRP samples 1, 3 and 4.

Having now determined the velocity profile for v-CFRP, attention is turn to the determination of v-CFRP elastic constants.

8.3.2 Elastic Constant determination of v-CFRP

The determination of elastic constants, having been discussed in chapter 6, is obtained by measurement of density and the velocity of a wave propagating in a specific direction. Not discussed in chapter 6, but discussed in chapter 7 is the strategy of adopting a non-linear least squares procedure. This method is adopted in this thesis.

A least squares minimization procedure as outlined by (Adamowski et al., 2010, 2009, 2008, 2007; Castellano et al., 2014; Chu et al., 1994; Chu and Rokhlin, 1994c; Lavrentyev and Rokhlin, 1997; Pearson and Murri, 1987; Reddy et al., 2005; Rokhlin and Wang, 1992, 1989a; Wang et al., 2003), may be performed by minimizing the squared sum of the difference between experimental and theoretical velocity. The equation used in this thesis is given as equation (63)

$$\min \sum_{i}^{m} (V^{exp} - V^{calc})^2 \qquad (63)$$

Where m is the number of terms in the summation, V^{exp} is experimental velocity and V^{calc} is the calculated velocity. The principle here is that the calculated velocity is produced by first guessing elastic constants and then subsequently refining this guess in order to minimize the difference between the calculated V and the experimental V. Once the difference has been minimized, the elastic constants used to generate the calculated velocity are reflective of the true constants.

The phase velocity equations for transversely isotropic materials are not derived here but are instead cited directly from literature (Castellano et al., 2014; Reddy et al., 2005). These equations are given in Table 32.

Plane 1-2		
Longitudinal velocity	Fast Transverse velocity	Slow Transverse velocity

$V_l = \sqrt{\frac{C_{11}}{p}}$	$V_{FT} = \sqrt{\frac{C_{44}}{p}}$	$V_{ST} = \sqrt{\frac{C_{66}}{p}}$
Plane 1-3		
Quasi-Longitudinal velocity	Quasi-Transverse velocity	Pure Transverse velocity
$\sqrt{\sqrt{\quad}}$	$\sqrt{\sqrt{\quad}}$	$\sqrt{\quad}$
Where $X = C_{11}cos^2\theta + C_{33}sin^2\theta + C_{44}$ and $Y = C_{11}cos^2\theta + C_{44}sin^2\theta \quad C_{44}cos^2\theta + C_{33}sin^2\theta - (C_{13} + C_{44})^2 sin^2\theta cos^2\theta$		

Table 32 – Equations for determination of elastic constants

Executing the least squares algorithm (iterative repetitions of equation (63)), is done using Matlab. Using the equations listed in Table 32, and adopting an approach from literature, (Adamowski et al., 2010, 2008, 2007), the fminsearch function from Matlab was utilized.

Fminsearch takes an input of some initial user guesses of elastic constants and seeks to find a solution to equation (63). The bespoke Matlab code generated in this work is too cumbersome to be outlined in full in this chapter but is available to review in appendix 4, in this chapter only the main findings are discussed.

Guesses of Elastic constants

Given that C_{11} is obtained by propagating a longitudinal wave at 90 degrees to the fibre direction (Table 32), the average v-CFRP wave velocity in the 1-2 plane and the 1-3 plane at 0ºincidence will provide a reasonable estimate of C_{11}, thus,

$$C_{11} = (1316.2) \cdot (2241.8)^2 = 6.6147\ GPa$$

Where average density of the v-CFRP samples is 1316.2 kg/m^3 ± 17.8218

Similarly from Table 32, for the slower transverse wave in this plane, an estimate of C_{66}, may also be determined. Using a similar procedure as above, and with the velocity defined as the average of the individual velocities, C_{66} was estimated as,

$$C_{66} = (1316.2) \cdot (1138.4)^2 = 1.706\ GPa$$

These values along with additional user estimated constants for C_{33}, C_{44} and C_{13} were inserted into the fminsearch of Matlab.

Elastic Constants from Least Squares Minimization

The values returned from fminsearch are outlined in Table 33.

Elastic constants determined via least squares minimization	
Constant	Value (GPa)
C_{11}	6.59
C_{33}	112.61
C_{13}	9.19
C_{44}	2.02
C_{66}	1.71
C_{12}	3.17

Table 33 – Elastic constants as determined via least squares minimization using fminsearch on Matlab, noting that $C_{12} = (C_{11} - 2\ C_{66})$.

Having determined the elastic constants, it is possible to calculate the average wave velocities predicted by these constants (see Table 32). This process allows for an elegant way to examine the elastic constant values by plotting the superposition of calculated velocities and experimental velocities, both against incident angle. These superimposed results are given as Figure 45 (a) and (b)

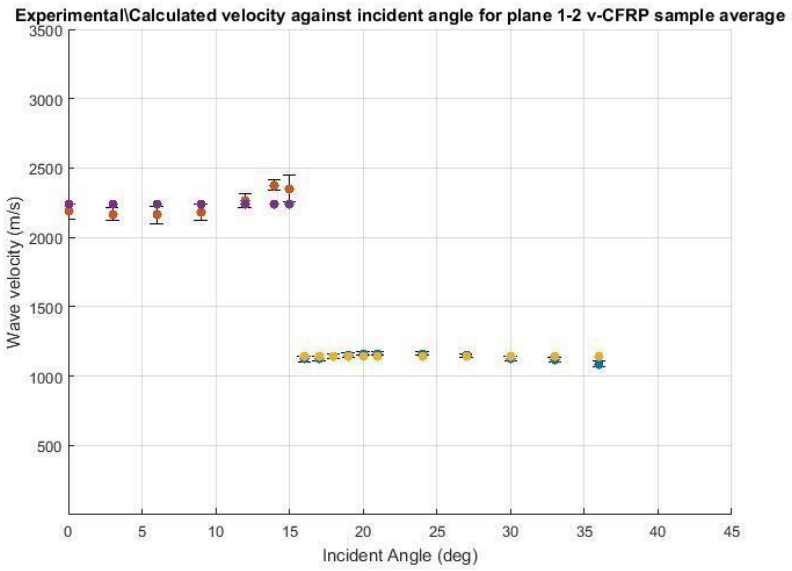

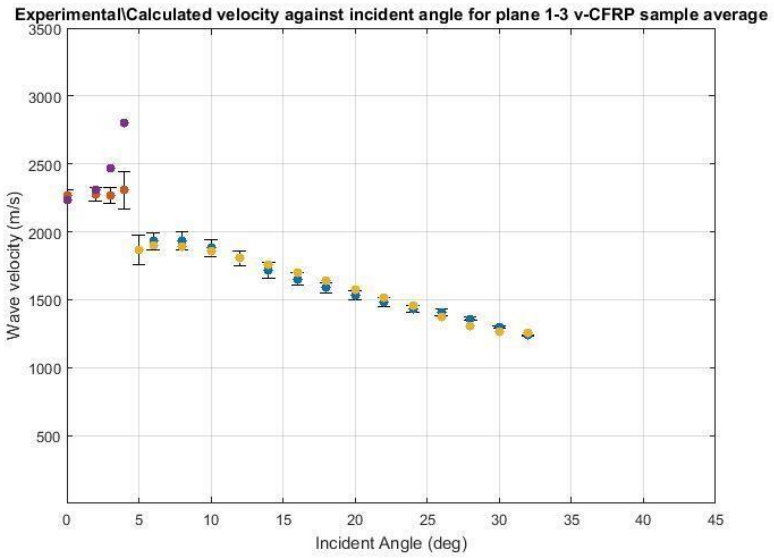

(b)

Figure 45 _ Superimposed calculated and experimental wave velocity against incident angle via ultrasound through transmission. Figure (a), L and T waves in 1-2 plane. Figure (b) L and T waves in the 1-3 plane _ L velocity calculated are colour purple and experimental velocities are colour red. T velocities calculated are colour yellow, experimental velocities are colour blue.

Looking first at Figure 45(a), the calculated longitudinal velocities, which are theoretically independent of incident angle, approach the mean value of the average sample velocity. The calculated velocity at incident angles of 0□, 9□ and 12□ fall within 1 standard deviation of the average sample velocity with the calculated velocity at incident angles of 3□, 6□ and 15□ falling within approximately 1.17-1.33 standard deviations. The largest discrepancy between calculated velocity and longitudinal velocity was at 14□ with the calculated average velocity being approximately 3.5 standard deviations. The calculated transverse velocities also approach the experimental average sample velocities. The calculated velocity at incident angles of 16□, 17□, 18□, 19□, 27□, 30□, and 33□ are within 1 standard deviation of average sample velocity, with calculated average velocity at incident angles of 20□, 22□, and 36□ with a range of 1.6 – 2.2 standard deviations of experimental sample average velocity.

Examining now Figure 45 (b), the calculated velocity at incident angles of 0□ and 2□ approach the experimental velocity, being within 1 standard deviation. As the incident angle is increased, the calculated longitudinal velocity begins to deviate from the

experimental velocity more noticeably at 3° and 4°. These velocities were not used to determine the elastic constants with rationale being a) not all velocities are required for least squares minimization, b) the error at these points is such that it dominates the least squares algorithm thus returning an unrealistic value of C_{33} of approximately 36 GPa and c) possible interplay between a rising longitudinal wave and decreasing transverse wave in this region given the very small first critical angle. The calculated transverse wave profile however did match the expected transverse velocities as can be seen in Figures 45 (b). The calculated velocity at incident angles of 5°, 6°, 8°, 10°, 12°, 14°, 16°, 22° and 24° are within 1 standard deviation of the experimental average sample velocity, with 18°, 20° and 26° within 1,2 - 1.43 standard deviations and as the critical angle is approached the angles of 28, 30 and
32 are within 3.5-4.25 standard deviations.

Table 34 outlines the difference in calculated velocities and experimental velocities at incident angle and may be read in conjunction with Figures 45 (a) and
(b).

% difference of wave velocity based on elastic constants and from experimental values				
Plane	Incident Angle	Velocity (m/s) Experimental	LSM estimated (m/s)	% difference
1 - 2	0		2237.6	2.34
	3		2237.6	3.19
	6		2237.6	3.46
	9		2237.6	2.50
	12		2237.6	1.17
	14		2237.6	6.09
	15		2237.6	5.01
	16		1139.8	1.36

	17	2185.9 ± 51.35 2167.3 ± 48.16 2161.5 ± 59.79 2182.2 ± 59.25 2263.9 ± 49.72 2378.2 ± 39.75 2352.5 ± 164.11 1124.4 ± 19.02 1128.4 ± 16.02 1143.6 ± 15.40 1153.6 ± 15.27 1162.5 ± 13.45 1163.6 ± 11.36 1164.2 ± 9.82 1148.0 ± 12.06 1127.9 ± 14.36 1117.6 ± 19.31	1139.8	1.00
	18		1139.8	0.33
	19		1139.8	1.20
	20		1139.8	1.97
	21		1139.8	2.07
	24		1139.8	2.11
	27		1139.8	0.71
	30		1139.8	1.06
	33		1139.8	1.97
	36	1088.6 ± 23.32	1139.8	4.59
1-3	0	2270.5 ± 36.49	2237.6	1.46
	2		2313.3	1.71
	3		2471.0	8.57
	4		2798.8	19.31
	5		1886.3	0.93
	6		1910.8	1.54
	8		1893.8	2.18
	10		1855.0	1.37

	12	2274.1 ± 49.39 2267.9 ± 57.22 2305.9 ± 137.61 1868.8 ± 107.48 1931.3 ± 64.14 1935.7 ± 69.18 1880.5 ± 64.34 1806.9 ± 53.19 1717.1 ± 55.47 1651.6 ± 46.78 1588.4 ± 40.40 1536.4 ± 33.82 1485.3 ± 32.74 1432.4 ± 27.62 1405.7 ± 24.18 1361.2 ± 15.40	1806.2	0.04
	14		1757.6	2.33
	16		1700.6	2.92
	18		1642.4	3.34
	20		1578.5	2.70
	22		1514.9	1.97
	24		1455.4	1.59
	26		1370.9	2.51
	28		1307.3	4.03
	30	1303.1 ± 7.76	1270.1	2.56
	32	1237.7 ± 4.60	1256.8	1.53

Table 34 – Percentage differences between wave velocity calculated using least squares data and experimental velocity. May be read in conjunction with figures 42 (a) and (b)

Concerning the individual samples, the least squares minimization was also performed. Table 35 provides the elastic constants determined.

Sample	C11 (GPa)	C33 (GPa)	C44 (GPa)	C13 (GPa)	C66 (GPa)	C12 (GPa)
1	6.45	104.31	1.96	10.58	1.68	3.09
2	6.36	141.38	1.94	9.07	1.70	2.96
3	6.67	119.48	2.08	8.54	1.69	3.29

4	6.83	98.62	2.21	8.23	1.75	3.32

Table 35 –Elastic constants of v-CFRP samples 1-4 determined via least squares minimization technique

Similar to Figure 45, the wave profile generated by using the elastic constants obtained via least squares minimization may be superimposed onto the experimental velocities in order to give a visual representation of how closely a fit the constants provide. Of particular interest is sample 2, the sample in which the profile in the 1-3 plane deviated away from the expected behaviour. Figure 46 (a) and (b), documents the superimposed calculated velocity and experimental velocity for this sample.

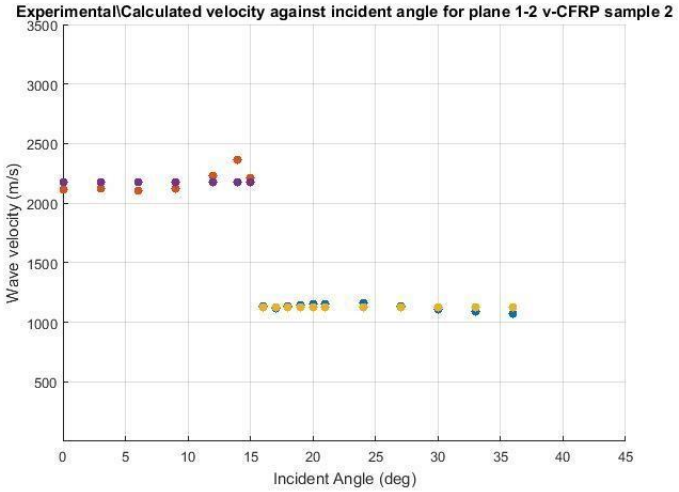

(a)

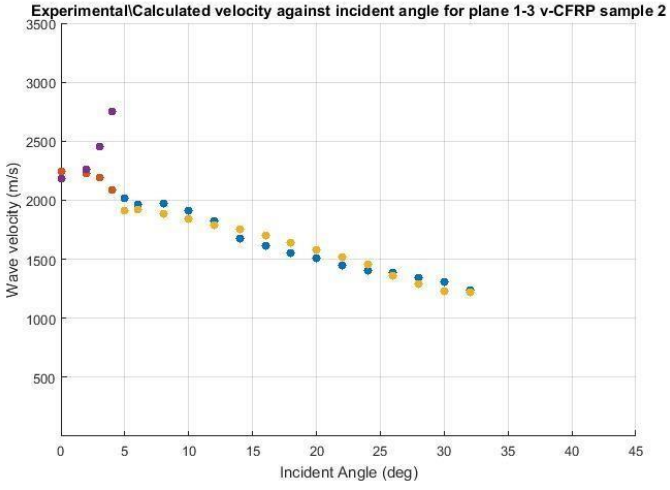

(b)

Figure 46 – Superimposed calculated and experimental wave velocity against incident angle for sample 2. Figure (a), L and T waves in 1-2 plane. Figure (b) L and T waves in the 1-3 plane – L velocity calculated are colour purple and experimental velocities are colour red. T velocities calculated are colour yellow, experimental velocities are colour blue.

Examining Figure 46 (a), it can be seen that the 1-2 plane the calculated longitudinal and transverse average velocities follow the expected experimental velocity profile. The 1-3 plane on the other hand, documents a calculated average velocity which deviates more noticeably from the experimental average velocity when compared to Figure 45. This aspect in covered in more detail in the next section.

Having now determined the elastic constants for the v-CFRP average sample and the individual samples, it is appropriate to examine how the Young‟s modulus derived from these constants compares to a mechanically derived Young‟s modulus and a theoretically derived Young‟s modulus.

8.3.3 Young's Modulus of v-CFRP

Citing from literature various formulas for Young‟s modulus in the fibre direction can be given, (Brinson and Brinson, 2008; Castellano et al., 2014; Reddy et al., 2005; Roylance, 2000). These are presented as equations (64-66).

$$YM_{LSM} = C_{33} - \frac{2{C_{13}}^2}{C_{11} + C_{12}} \qquad (64)$$

$(where\ LSM\ indicates\ least\ squares\ data)$

$$YM_{ROM} = V_f E_f - V_m E_m \qquad (65)$$

$(where\ V_f, V_m, E_f, E_m are\ fibre\ and\ matrix\ volume\ fraction\ and\ Young's\ Modulus)$

$$YM_{Mech} = \frac{\sigma_2 - \sigma_1}{\varepsilon_2 + \varepsilon_1} \qquad (66)$$

$(slope\ of\ stress\ strain\ linear\ section)$

Equations (64), (65) and (66) were executed using bespoke Matlab programmes. In terms of equation (64), the data used were the individually derived elastic constants from Table 35 and the average samples constants from Table 33, for equation (65) data was taken from the data sheet for the uni-directional fibres and epoxy resin accordingly. Equation (66) was obtained using mechanical testing, the details of which are now discussed.

Mechanical testing was conducted at the Advanced Forming Research Centre (AFRC) in Glasgow, United Kingdom. The testing followed ASTM D3039, utilizing a Zwick Z150 tensile testing machine, with a maximum load of 150 kN, operated at room temperature, with a constant strain rate of 2 mm/minute. An extensometer of 50mm-100mm was used to measure strain, with 5 rectangular samples of v-CFRP (samples 6 – 9 from Table 27) tested. The samples were subjected to increased levels of tensile force with the extensometer recording the amount of displacement. The force and displacement data was recorded and used to calculate the samples‟ Young‟s Modulus, i.e. the slope of the stress / strain curve, is given in appendix 5. An example force / displacement relationship, in this case for sample 1 is given as Figure 47.

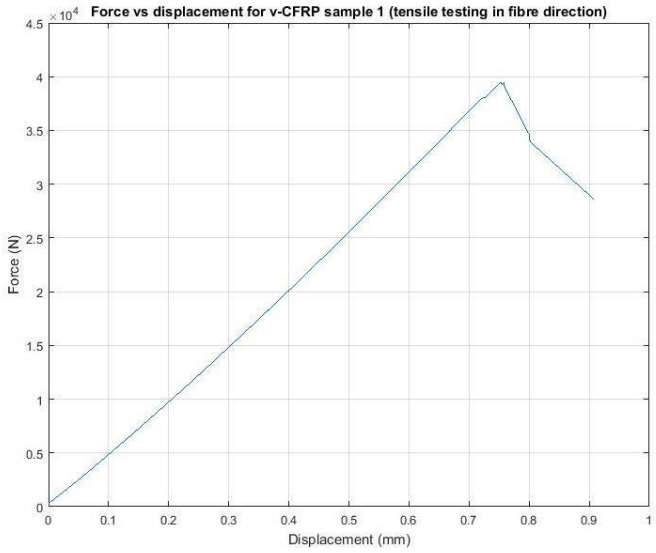

Figure 47 – Force vs displacement curve for v-CFRP sample 1. Young‟s modulus is the slope of this curve.

The Young‟s modulus recorded via the three methods and the % difference between the LSM data, the ROM, and mechanical data is also presented, and is given as Table 36.

Values for Young‟s modulus calculated from elastic constants, the rule of mixtures and mechanical testing alongside % difference						
Sample	YM_{LSM} (GPa)	YM^{ROM} (GPa)	% difference between YM_{LSM} and YM_{ROM}		Average YM_{Mech} (GPa) (from 5 samples)	% difference between YM_{LSM} YM_{Mech} and
v-CFRP 1	80.84	118.14	37.49		96.48 ± 1.63	17.64
v-CFRP 2	123.73	119.62	3.37			24.75
v-CFRP 3	104.84	107.05	2.09			8.31
v-CFRP 4	85.28	107.21	22.79			12.32
Average (1- 4)	98.67 ± 17.1	113.01 ± 5.89	13.55			2.24
Sample average	95.303	112.70	16.73		96.48 ± 1.63	1.23

Table 36 – Values for Young‟s modulus v-CFRP. Data is calculated using equations (64 – 66). The % difference values between the ultrasound derived data and the rule of mixtures and mechanical data is also presented.

It can be seen from Table 36 that the average value of Young‟s modulus calculated using the individual Young‟s Modulus‟s from samples 1 – 4, and the sample average (calculated using the constants from the average velocities – Table 33) agree; which is unsurprising given the small deviation recorded for the average velocities in Table 34. Additionally, the % difference between the ultrasonic derived Young‟s Modulus and the mechanically derived Young‟s Modulus is approximately 1% and 2%. A larger % difference between the Young‟s Modulus‟s and the rule of mixtures (which provides a perfect theoretical result assuming ideal materials) of approximately 13.5% and 17.0% was also recorded.

Examining now the individual samples, sample 3 provides the closest result to both the rule of mixtures and mechanical testing; approximately 2% and 8% differences being recorded in this case. Samples 1 and 4, record a reasonable percentage change of approximately 12% and 18% in the Young‟s Modulus derived ultrasonically and mechanically. Both however record larger % differences in relation to the rule of

mixtures estimate, with figures of 23% and 37% respectively. The closer relationship between the ultrasound data and the mechanical data is not unexpected given that the rule of mixtures is derived using ideal approximations.

Sample 2, is an exceptional case in that the ultrasound derived Young‟s modulus is significantly closer to the theoretical rule of mixtures than to the mechanical derived data, with a % difference of approximately 3% and 25% respectively. As stated previously, the elastic constants derived ultrasonically from this sample provide a less accurate fit to the experimental in the 1-3 plane, (Figure 46(b)), which may explain the high value of ultrasonic derived Young‟s Modulus recorded. Table 37 is given to further highlight this point.

Sample 2				% difference between experimental and individual LSM estimated velocities for samples 1,3,4		
Incident Angle	Experimental (m/s)	LSM estimated (m/s)	% diff	Sample 1	Sample 3	Sample 4
5	2013.3	1912.2	5.15	0.62	1.25	0.15
6	1968.5	1918.2	2.59	2.84	0.37	0.27
8	1974.6	1890.2	4.37	1.64	1.39	1.34
10	1911.8	1842.6	3.69	0.22	0.51	1.08
12	1823.3	1790.9	1.79	0.73	1.07	0.22
14	1676.4	1750.7	4.70	2.35	1.72	0.58
16	1615.7	1699.5	5.05	2.76	2.43	1.42
18	1554.5	1641.8	5.47	3.07	2.45	2.34
20	1507.1	1576.8	4.52	2.36	1.95	1.93
22	1452.5	1517.8	4.39	1.81	0.46	1.18
24	1403.0	1457.8	3.83	1.30	0.86	0.38
26	1388.5	1361.6	1.95	1.12	3.90	3.16
28	1347.7	1293.6	4.10	3.76	4.27	3.93
30	1305.0	1223.5	5.71	2.45	0.97	0.98
32	1239.8	1217.9	1.78	0.92	3.49	3.71

Table 37 –% difference figures between experimental velocity and velocity derived via least mean squares technique for transverse waves in the 1 -3 plane. With sample 2 larger % differences are found indicating that the elastic constants estimated via LMS do not provide as close a relationship to experimental as with the other samples. Note that the experimental velocities for samples 1, 3 and 4 may be found in appendix 3.

Table 37 documents sample 2 having 12 instances of where the % difference is larger than that recorded in samples, 1, 3 and 4. A graph showing some results from Table 37 provides additional clarity on the differences recorded in experimental and theoretical with sample 2. Figures 48 (a) and (b) outline the differences recorded in experimental and theoretical transverse velocity for samples 1 and 2 in the 1-3 plane.

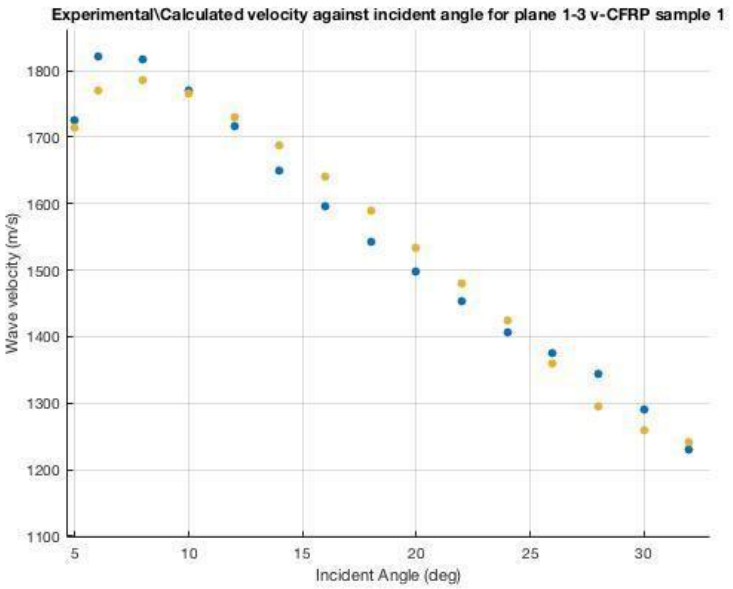

(a)

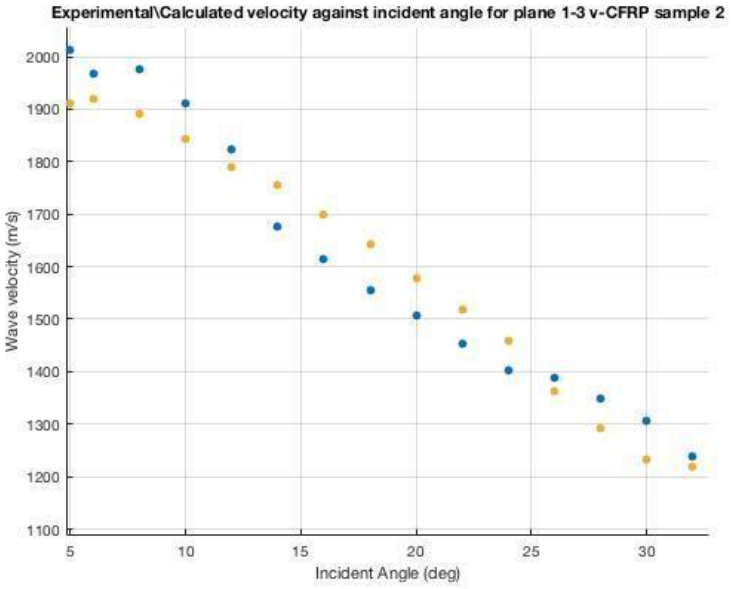

(b)

Figure 48 _ Theoretically derived and experimental transverse 1-3 plane velocities for samples v-CFRP 1 (a) and 2 (b). A closer relationship is observed between the calculated velocity (yellow points) and the experimental velocity (blue points) for sample 1, figure (a), when compared to sample 2, figure (b). This indicates the LSM derived constants do not provide as accurate a velocity prediction when compared to experimental when sample 2 is in comparison with sample 1.

Prior to discussion of rf-CFRP, a final bar graph outlining the Young‟s Modulus recorded via ultrasound through transmission, through the rule of mixtures and through mechanical testing is given as Figure 49.

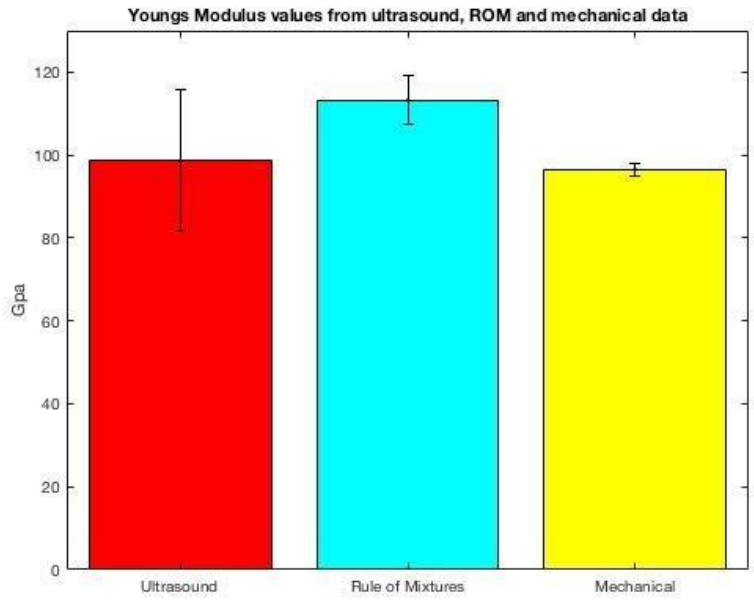

Figure 49 – Average Young‟s modulus and standard deviation figures determined via ultrasound through transmission, rule of mixtures and via mechanical testing.

Having now examined results from ultrasonic through transmission conducted on v-CFRP, it is now appropriate to examine the findings from rf-CFRP.

8.3.4 rf-CFRP ultrasonic analysis

The ultrasonic analysis of rf-CFRP was identical to that conducted on v-CFRP; both longitudinal and transverse waves were propagated through planes 1-2 and 1-3 over a wide range of incident angles. The average results obtained for the rf-CFRP are given in tables 38 and 39.

Sample rf-CFRP Average Plane 1-2

Incident Angle	Velocity m/s	Wave type
0		L
3		L
6		L
9	2287.8 ± 183.65 2182.5 ± 147.98 2235.0 ± 183.75 2164.5 ± 105.61 2295.1 ± 77.88 1746.2 ± 543.50 1226.3 ± 27.86	L
12		L
14		L – T
15		T
16	1237.2 ± 24.18	T
17		T
18		T
19		T
20	1254.3 ± 31.64 1257.5 ± 18.59 1263.3 ± 16.52 1267.4 ± 20.69 1266.3 ± 18.02 1277.0 ± 14.41 1266.3 ± 23.76 1221.0 ± 11.35	T
21		T
24		T
27		T
30		T
33	1173.1 ± 11.85	T
Longitudinal wave not observed approximately >13/14° Transverse wave not observed approximately >38/40°		

Table 38 – Average ultrasonic velocity with respect to incident angle in the 1-2 plane for average rf-CFRP sample

Sample rf-CFRP Average Plane 1-3

Incident Angle	Velocity m/s	Wave type
0	2179.8 ± 147.34	L
2	2169.1 ± 155.00	L
3	2012.9 ± 118.49	L
4	1986.0 ± 144.09	L-T
5	1884.4 ± 80.54	T
6	1906.6 ± 48.61	T
8	1878.1 ± 42.18	T
10	1826.5 ± 36.78	T
12	1781.4 ± 44.65	T
14	1748.0 ± 23.69	T
16	1725.3 ± 44.25	T
18	1701.1 ± 49.54	T
20	1673.0 ± 49.63	T
22	1627.0 ± 38.22	T
24	1546.2 ± 16.54	T
26	1457.5 ± 7.44	T
28	1371.5 ± 7.27	T
30	1276.8 ± 36.39	T
32	1224.0 ± 6.96	T
Longitudinal wave not observed approximately >4° Transverse wave not observed approximately >38/40° After 28 degrees sample became more difficult to correlate owing to noise levels		

Table 39 – Average ultrasonic velocity with respect to incident angle in the 1-3 plane for average rf-CFRP sample

Plots of these average velocities and standard deviations (error bars) against incident angle are given as Figures 50 (a) and (b).

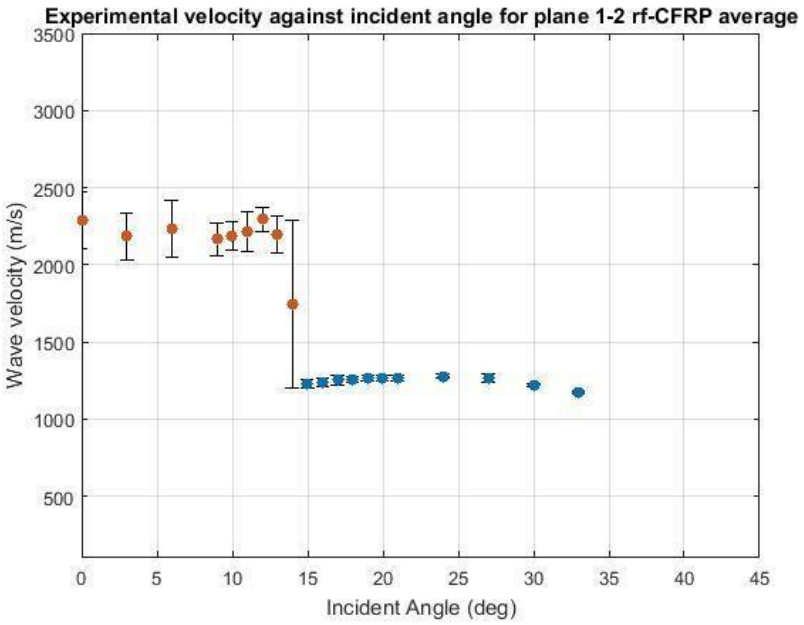

(a)

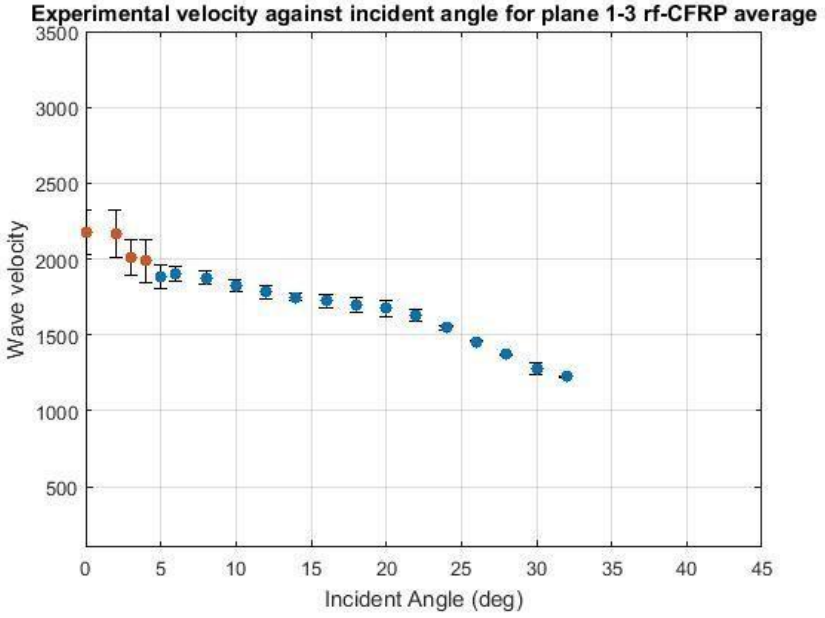

(b)

Figure 50 – Graphical results of the average recorded rf-CFRP wave velocities. Figure (a), L and T waves in the 1-2 plane – notice the point at 14□ corresponding to an average value obtained from two longitudinal and two transverse velocities. Figure (b,) L and T waves in the 1-3 plane.

Examining Figure 50 (a) - the isotropic plane - the average rf-CFRP longitudinal wave velocity records some variation in wave velocity with incidence angle but the general

trend of wave profile when compared to v-CFRP, may be seen. Note, that the value at 14° is at the critical angle transition region; a velocity in keeping with a longitudinal wave was recorded for samples 1 and 2, and a velocity in keeping with a transverse velocity was recoded for samples 3 and 4, hence the very large standard deviation.

On examination of rf-CFRP average longitudinal velocity standard deviation, higher values were found when compared to the standard deviation found with the average v-CFRP longitudinal velocity. This can be observed via comparing Figure 50 to Figure 42 or Table 38 to Table 30 and indicates more variance in longitudinal velocity profile between the rf-CFRP samples when compared to v-CFRP.

Demonstrating this variation, Figures, 50 (a), (b), (c) and (d) which outline the individual wave profiles recorded for rf-CFRP samples 1, 2, 3 and 4 respectively are given.

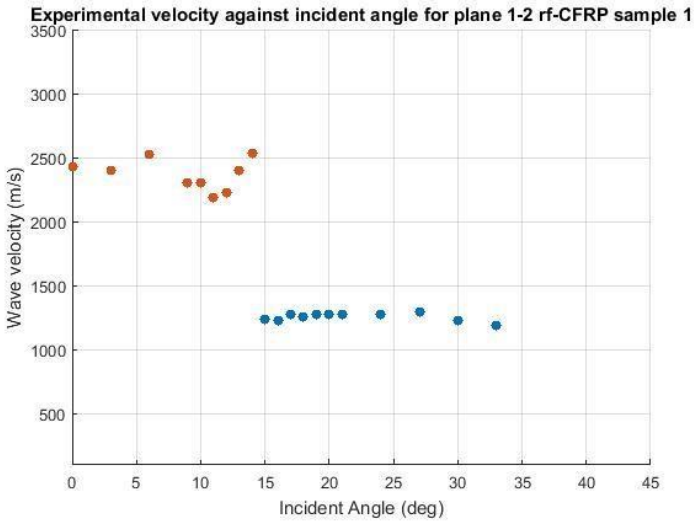
Experimental velocity against incident angle for plane 1-2 rf-CFRP sample 1
Wave velocity (m/s)
Incident Angle (deg)

(a)

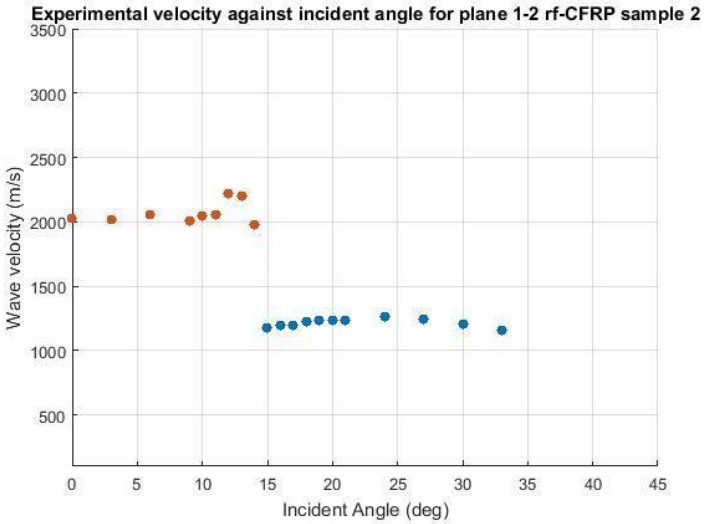
Experimental velocity against incident angle for plane 1-2 rf-CFRP sample 2
Wave velocity (m/s)
Incident Angle (deg)

(b)

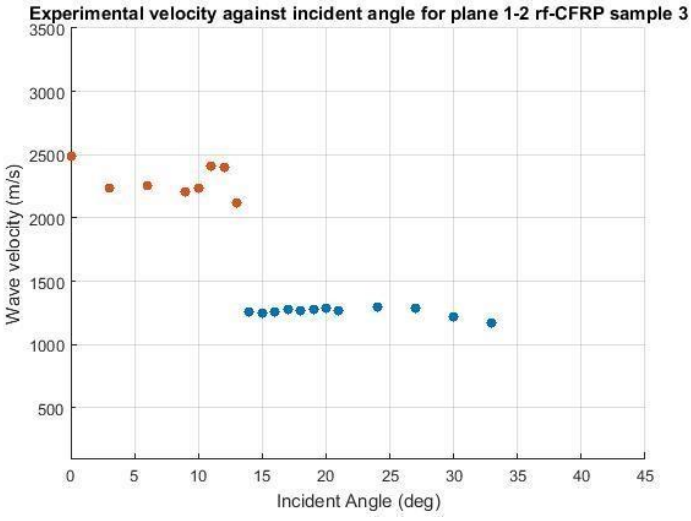
Experimental velocity against incident angle for plane 1-2 rf-CFRP sample 3
Wave velocity (m/s)
Incident Angle (deg)

(c)

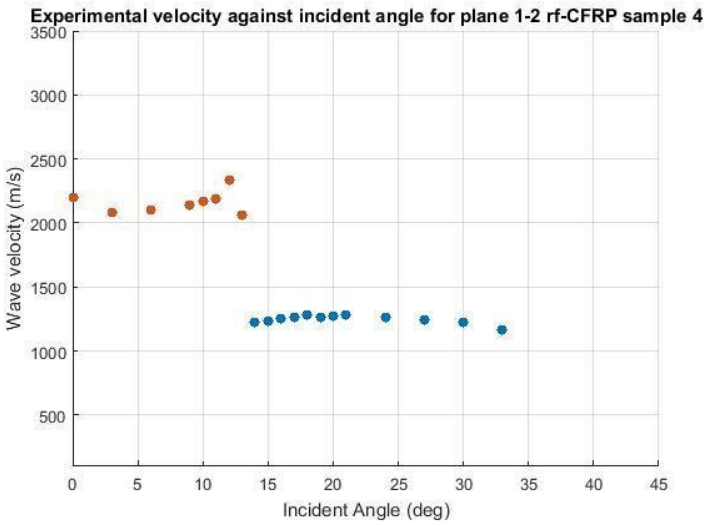

(d)

Figure 51 – Graphical results of the individual rf-CFRP wave velocities in the 1-2 plane. Figure (a), (b), (c) and (d) represent samples 1, 2, 3 and 4 respectively. Samples 2 (b) and 4 (d) recording lower deviation from expected longitudinal wave profile and with sample 1 and sample 3 recording a higher deviation.

It can be seen that sample 2, Figure b, and sample 4, Figure d, bear a relative similarity to that recorded with the v-CFRP, with sample 3, Figure c, and sample 1, Figure a, deviating from the expected curve. In particular, the velocity deviation in sample 1 is such that the wave profile representative of isotropic symmetry is very difficult to identify.

Examining now the rf-CFRP average transverse velocity in the 1-2 plane, Figure 50 (a). When compared to the longitudinal velocity profile, the transverse velocity is in much closer agreement with the expected curve obtained from v-CFRP. This agreement in transverse profile between average v-CFRP and average rf-CFRP may be seen by comparing Figure 42 (a) and Figure 50 (a). Further, the standard deviation figures recorded in Table 38 and via the error bars in Figure 50 for the rf-CFRP average transverse velocities are much smaller than those for the rf-CFRP average longitudinal velocities. The transverse velocities and wave profile was far more stable and repeatable in the 1-2 plane for the rf-CFRP samples 1-4 when compared to longitudinal velocities in the same plane for the rfCFRP samples 1-4 – examination of Figure 50 a, b, c and d demonstrates this close agreement in transverse wave profile between the samples. This result was not found for the v-CFRP samples, in which relatively similar wave profiles were recorded

(Figures 43 (a-d)).

Examining now the rf-CFRP average sample velocity in the 1-3 plane, Figure 50 (b). The longitudinal velocity in this plane is expected to increase with increasing incident angle, this result is not recorded for the average rf-CFRP sample longitudinal velocity however. A steady velocity decrease with increasing incident angle was recorded. This longitudinal velocity profile recorded is similar to that recorded with v-CFRP sample 2, Figure 44 (b); note this sample is one in which the elastic constants derived produced the poorest fit between the calculated velocity and experimental velocity.

Where the rf-CFRP and the v-CFRP do agree however is the early emergence of the transverse wave. Upon rotating the samples around the 2 axis, the transverse wave velocity was observed to emerge independently after only a few degrees. Owing to the close velocity between the longitudinal and transverse waves however, it was difficult to conclusively observe the point at which the transverse wave emerges independently, however a good estimate is approximately 5º.

Further still the standard deviation figures recorded are larger than the figures recorded in the case of v-CFRP as can be saw from Table 39 and Tables 31, indicating again that the longitudinal velocity is more varied across the rf-CFRP Examining the individual velocity profiles, Figures 52 a), b), c) and d) are given.

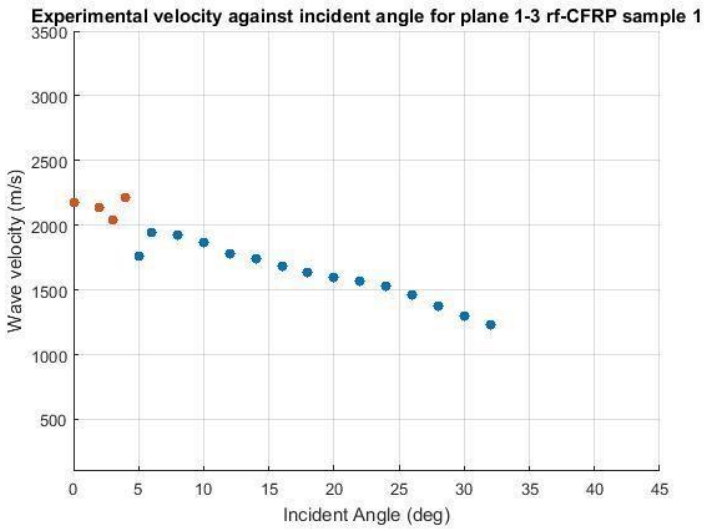

(a)

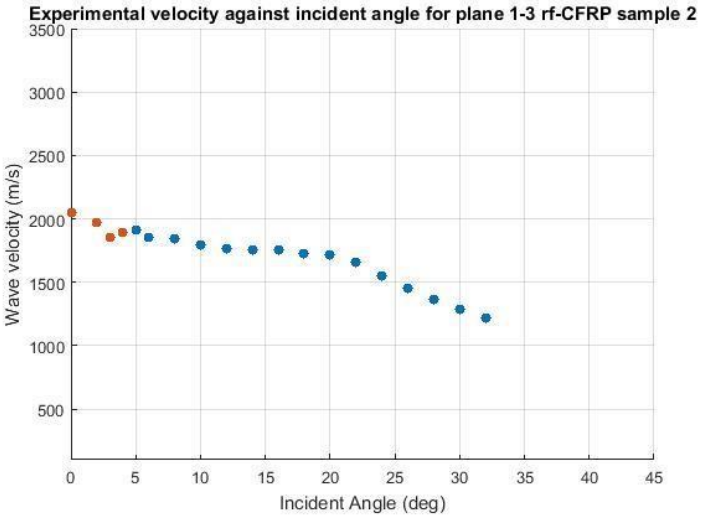
Experimental velocity against incident angle for plane 1-3 rf-CFRP sample 2
Wave velocity (m/s)
Incident Angle (deg)

(b)

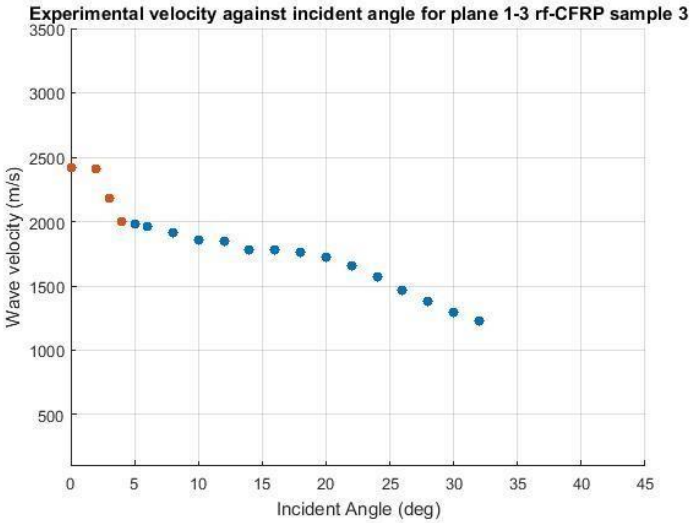
Experimental velocity against incident angle for plane 1-3 rf-CFRP sample 3
Wave velocity (m/s)
Incident Angle (deg)

(c)

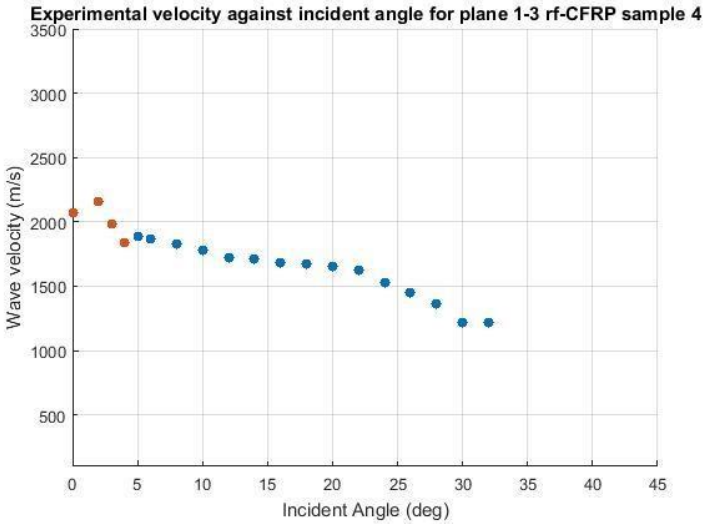
Experimental velocity against incident angle for plane 1-3 rf-CFRP sample 4
Wave velocity (m/s)
Incident Angle (deg)

(d)

Figure 52 – Graphical results of the individual rf-CFRP wave velocities in the 1-3 plane. Figure (a), (b), (c) and (d) represent samples 1, 2, 3 and 4 respectively. Notice the similarity in longitudinal velocity with the v-CFRP sample which provided the least accurate elastic constants, V-CFRP sample 2.

It is evident that rf-CFRP samples, 1, 2, 3 and 4, do not in general record the expected longitudinal wave velocity profile for a wave in the 1-3 plane; an increase in velocity with increasing incident angle is expected.

The closest result to the theoretical and to the individual v-CFRP samples 1, 3 and 4 was rf-CFRP sample 1, which also interestingly recorded a much varied longitudinal velocity profile in the 1-2 plane. Rf-CFRP samples 2, 3 and 4 all recorded a decreasing velocity with increasing incident angle, similar to that of vCFRP sample 2 – the only exception being a velocity increase in sample 4 between
0º and 2º.

It is also the case that the velocity decrease with increasing incident angle should not be assumed to be solely caused by fibre mats suffering possible degradation given that a similar profile was recorded for v-CFRP sample 2. However, such is the variable velocity with the rf-CFRP, an approximate range of 2000 m/s to 2500 m/s at 0º being recorded, it is reasonable to assume some degree of additional sample anisotropy not present in the v-CFRP samples. Examining now the average and individual rf-CFRP transverse velocities. The average transverse velocity, Figure 50 (b), is generally in keeping with that expected from the transverse isotropic plane; a decrease in velocity with increasing incident angle is observed. However, when compared to the average wave profile recorded for v-CFRP, Figure 42 (b), slight differences in profile may be observed.

Examining the samples individually, the velocity variation between the individual samples is smaller than compared to the longitudinal waves, which can be seen by examining the rf-CFRP average sample standard deviation from Table 39 and the Figures 51 (a), (b), (c) and (d). Further, similar to the longitudinal waves, rfCFRP sample 1 bears the closet relationship to both the v-CFRP samples 1, 3 and 4 and to the expected transverse wave behaviour in this plane. The rf-CFRP samples 2, 3 and 4, Figures (b), (c) and (d), also bear similarity but can be observed to differ slightly from that recorded in Figure (a).

Lastly, it is of interest to note that similar to the transverse velocity in the 1-2 plane the transverse velocity in the 1-3 plane follows the expected curve, as produced

by v-CFRP average sample. It can be stated that the transverse velocity in both planes is more in keeping with the theoretical and with that recorded for the v-CFRP samples, when compared to the longitudinal velocity in 1-2 and 1-3 plane of the rf-CFRP samples.

Having now examined the velocity profile for rf-CFRP, the elastic constants are determined.

8.3.5 Elastic Constant determination of rf-CFRP

As with the v-CFRP samples, the average elastic constants were first estimated and then determined using the least mean squares minimization technique - equation (63) and Table 32. This was again performed using bespoke Matlab programming incorporating the fminsearch function.

Guesses of Elastic constants

Similar to the v-CFRP, an estimation of C_{11} is done obtained by realising that the equation for C_{11} may be used for waves propagating at 0º and 90º to the fibre direction. An estimate of C_{11}, is given as

$$C_{11} = (1388.5) \cdot (2233.8)^2 = 6.928\ GPa$$

Where average density of the rf-CFRP samples is 1388.5 kg/m^3 ± 40.0594

Similarly the slower transverse wave in the 1-3 plane is estimated in a similar way to v-CFRP, using the average of individual velocities, C_{66} was estimated as,

$$C_{66} = (1388.5) \cdot (1246.3)^2 = 2.157\ GPa$$

These values along with additional user estimated constants for C_{33}, C_{44} and C_{13} were inserted into the fminsearch of Matlab – note the same measurements as used in the v-CFRP case are used again with the exception of 14º in the 1-2 plane. This velocity sits between the longitudinal and the transverse and was not utilized owing to the impossibility of knowing which type of wave formula to select.

Elastic Constants from Least Squares Minimization

The values returned from fminsearch are outlined in Table 40.

Elastic constants determined via least squares minimization	
Constant	Value (GPa)
C_{11}	6.77
C_{33}	76.60
C_{13}	5.97
C_{44}	2.56
C_{66}	2.16
C_{12}	2.46

Table 40 – Elastic constants for the rf-CFRP average sample as determined via least squares minimization using fminsearch on Matlab, noting that $C_{12} = (C_{11} - 2\,C_{66})$.

Following in a similar vein to the v-CFRP average sample, the calculated or theoretical average velocity, predicted using the elastic constants, is superimposed onto the experimental velocity to get a visual understanding of elastic constants accuracy. The superimposed velocities are given as Figures 53 (a) and (b).

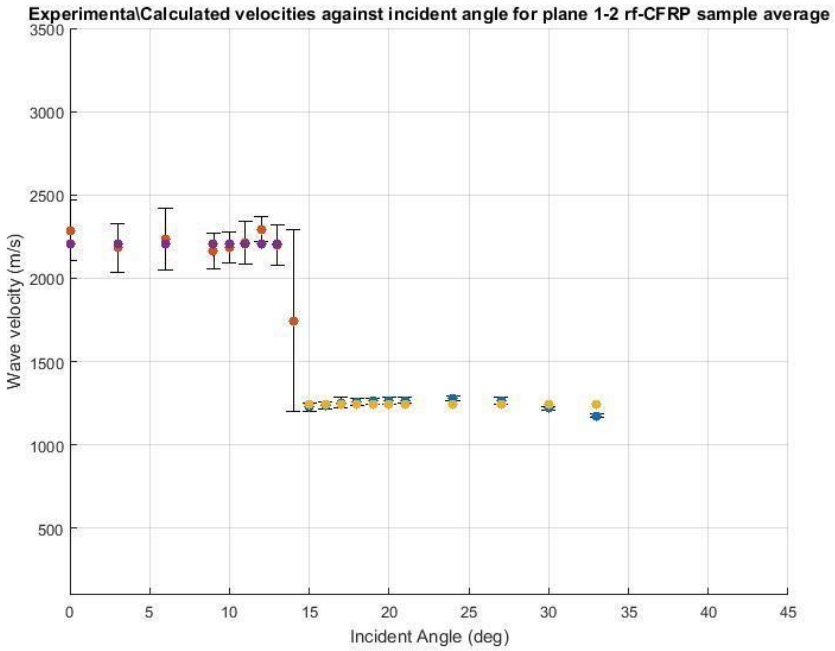

(a)

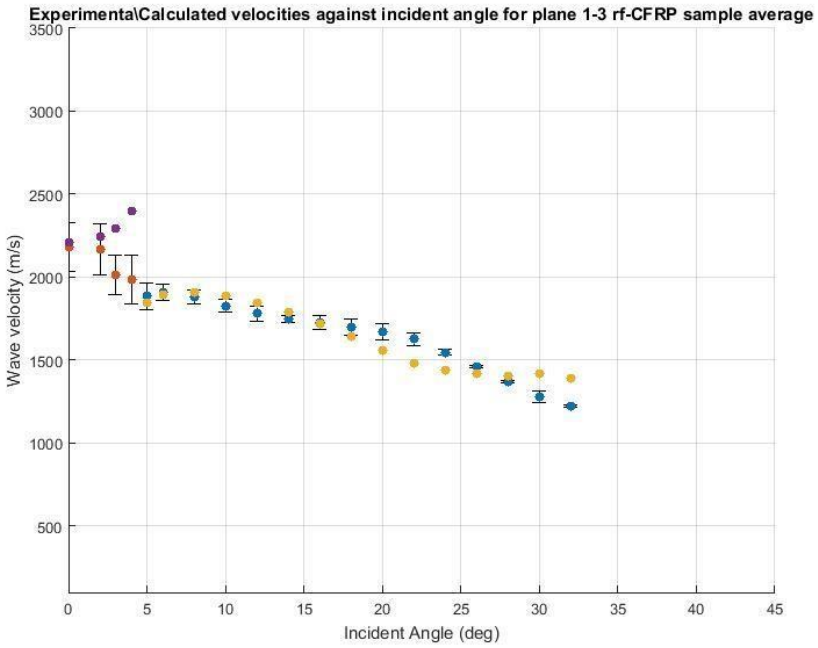

(b)

Figure 53 – Superimposed calculated and experimental wave velocity against incident angle via ultrasound through transmission for sample rf-CFRP average. Figure (a), L and T waves in 1-2 plane. Figure (b) L and T waves in the 1-3 plane – L velocity calculated are colour purple and experimental velocities are colour red. T velocities calculated are colour yellow, experimental velocities are colour blue.

Looking first at Figure 53(a), all calculated average longitudinal velocities are within 1-1.1 standard deviations of the average sample experimental velocity. This result surpasses that of the v-CFRP, however the rf-CFRP recorded significantly larger values of standard deviation for longitudinal velocities in this plane and thus is explainable. The transverse waves, which recorded smaller standard deviations across the rf-CFRP when compared to longitudinal waves, recorded similar results to that of the v-CFRP. At incident angles of 15□, 16□, 17□, 18□, 19□, 20□, 21□, and 27□ are within 1-1.1 standard deviation of experimental mean velocity with 24□, and 30□ within 2.15-2.22 standard deviation of experimental mean velocity with 33□ being 6.14 standard deviations from experimental mean. The large value of 6.14 arises from measurement inaccuracy caused by difficulty in correlating the transverse velocity accurately at this angle and above.

Examining now the relationship between the calculated and experimental velocities in the 1-3 plane. Similar to the v-CFRP the wave profile follows the expected curve with the calculated velocity at incident angles of 0□ and 2□ being within 1

standard deviation of the experimental mean velocity with the angles of 3° and 4° not being considered using similar rationale as with the v-CFRP.

With the calculated transverse velocity, a poorer relationship between experimental and calculated average velocity is observed, particularly for incident angles greater than 20°, when compared to v-CFRP; for instance compare Figure 53 (b) to Figure 45 (b). At incident angles of 5°, 6°, 8°, 16°, 18° are within 1-1.17 standard deviation of the experimental mean velocity, 10°, 12°, 14° are within 1.36 – 1. 67 standard deviation with 20°, 22°, 24°, 26°, 28° and 30° within 2.89-8.10 standard deviations from the experimental mean. The calculated average velocity at incident angle of 32° recorded a large 24 standard deviations from the experimental mean given correlation difficulty increasing as the critical angle region was approached. Further, Table 41 outlines the difference in calculated velocity and experimental velocities at incident angles for both planes of incidence.

% difference of wave velocity based on elastic constants and from experimental values				
Plane	Incident Angle	Velocity (m/s) Experimental	LSM estimated (m/s)	% difference
1 - 2	0		2208.8	3.51
	3		2208.8	1.19
	6		2208.8	1.18
	9	2287.8 ± 183.65 2182.5 ± 147.98 2235.0 ± 183.75 2164.5 ± 105.61 2295.1 ± 77.88 1746.2 ± 543.50 1226.3 ± 27.85	2208.8	2.02
	12		2208.8	3.83
	14		N/A	N/A
	15		1246.4	1.63
	16	1237.2 ± 24.18	1246.4	0.74
	17		1246.4	0.63
	18		1246.4	0.89
	19		1246.4	1.35
	20		1246.4	1.67

	21	1254.3 ± 31.64 1257.5 ± 18.59 1263.3 ± 16.52 1267.4 ± 20.69 1266.3 ± 18.02 1277.0 ± 14.41 1266.3 ± 23.76 1221.0 ± 11.35 1173.1 ± 11.85	1246.4	1.58
	24		1246.4	2.43
	27		1246.4	1.58
	30		1246.4	2.06
	33		1246.4	6.06
1-3	0	2179.8 ± 147.34	2208.8	1.32
	2	2169.1 ± 155.00	2243.6	3.38
	3	2012.9 ± 118.49	2291.9	12.96
	4		2397.6	18.78
	5		1848.4	1.93
	6		1896.0	0.56
	8		1908.9	1.63
	10		1884.0	3.10
	12		1842.3	3.36
	14		1787.5	2.23
	16	1986.0 ± 144.09 1884.4 ± 80.54 1906.6 ± 48.61 1878.1 ± 42.17 1826.5 ± 36.78 1781.4 ± 44.65 1748.0 ± 23.69 1725.3 ± 44.25 1701.1 ± 49.54 1673.0 ± 49.63 1627.0 ± 38.22 1546.2 ± 16.54 1457.5 ± 7.44 1371.5 ± 7.27 1276.8 ± 36.39	1719.6	0.33
	18		1642.7	3.50
	20		1559.3	7.04

	22		1483.1	9.25
	24		1439.6	7.14
	26		1415.9	2.90
	28		1404.0	2.34
	30		1417.2	10.43
	32	1224.0 ± 6.96	1392.4	12.88

Table 41 – Percentage differences between wave velocity calculated using least squares data and experimental velocity for rf-CFRP sample average. May be read in conjunction with figures 52 (a) and (b)

Additionally, the individual elastic constants for rf-CFRP samples 1 – 4 are given in Table 42.

Sample	C11 (GPa)	C33 (GPa)	C44 (GPa)	C13 (GPa)	C66 (GPa)	C12 (GPa)
1	7.07	66.23	2.31	6.87	2.11	2.85
2	6.04	59.81	2.82	1.615	2.13	1.78
3	7.68	84.70	2.77	8.25	2.23	3.18
4	6.33	99.89	2.44	7.44	2.15	2.02

Table 42 –Elastic constants of rf-CFRP samples 1 - 4 determined via least squares minimization technique

Comparing these results to those from the v-CFRP individual constants, Table 35, the constants above vary much more significantly, which is not surprising given the larger standard deviation recorded; v-CFRP samples are more closely related in terms of the recorded velocity. Table 43 is given to outline the observable differences in constants between the rf-CFRP samples and the v-CFRP samples.

Sample	C11 (GPa)	C33 (GPa)	C44 (GPa)	C13 (GPa)	C66 (GPa)	C12 (GPa)
V 1	6.45	104.31	1.96	10.58	1.68	3.09
V 2	6.36	141.38	1.94	9.07	1.70	2.96
V 3	6.67		2.08	8.54	1.69	3.29
V 4	6.83	119.48 98.62 115.95 ±16.55	2.21	8.23	1.75	3.32

Avg and Std dev	6.58 ± 0.18		2.03 ± 0.08	9.10 ± 0.90	1.71 ± 0.029	3.17 ± 0.15
Sample	C11 (GPa)	C33 (GPa)	C44 (GPa)	C13 (GPa)	C66 (GPa)	C12 (GPa)
Rf 1	7.07	66.23	2.31	6.87	2.11	2.85
Rf 2	6.04	59.81	2.82	1.615	2.13	1.78
Rf 3	7.68		2.77	8.25	2.23	3.18
Rf 4	6.33	84.70 99.89 77.66 ± 15.75	2.44	7.44	2.15	2.02
Avg and Std dev	6.78 ± 0.64		2.59 ± 0.21	6.04 ± 2.60	2.16 ± 0.045	2.46 ± 0.57

Table 43 – Individual, average, and standard deviation of elastic constants for v-CFRP (the v samples) and rf-CFRP (the rf samples). The rf-CFRP samples record a larger standard deviation in every case, indicating a more spread data set of elastic constant value (which can be observed from individual constants in the table)

Having now determined the elastic constants for the rf-CFRP average sample and the individual samples, similar to v-CFRP, attention is turned to examination of the Young‟s Modulus.

8.3.6 Young's Modulus of rf-CFRP

To determine the Young‟s modulus of rf-CFRP samples 1-4 similar testing as conducted on v-CFRP was performed, ASTM test standard D3039. Unlike the vCFRP, a theoretical prediction was not recorded with the rf-CFRP; owing to the recycling process, the fibre density figures from the datasheet are no longer considered to be trustworthy. Table 44, outlines the values of Young‟s modulus obtained from the a) individual samples, b) average velocity and c) from mechanical testing - with % difference figures also presented.

Values for Young‟s modulus calculated from elastic constants and mechanical testing alongside % difference

Sample	YM_{LSM} (GPa)	YM_{Mech} Average from 5 samples (GPa)	% difference between YM_{LSM} and YM_{Mech}
1	56.75	98.68 ± 1.69	53.95 %
2	59.14		50.11 %
3	72.211		30.97 %
4	86.65		12.98 %
Average (1- 4)	68.69 ± 11.92		35.83 %
Sample average	64.06	98.68 ± 1.69	42.54 %

Table 44 – Values for Young‟s modulus rf-CFRP. Data is calculated using equations (64 – 66). The % difference values between the ultrasound derived data and mechanical data is also presented.

Examining first the average Young‟s modulus; differences can be observed between the modulus from the individual samples and the modulus derived using the average velocities. The % difference in this instance is approximately 7%, which is larger than the value of approximately 4% for v-CFRP, however the velocity does vary more in the case of the individual rf samples.

The % difference between the average Young‟s Modulus‟s and the mechanical testing was significantly higher than the small figures of 1% and 2% recorded with the v-CFRP. In this instance, values of approximately 36% and 42.5% were recorded. Examining now the individual samples, sample 4 provides the closest result to mechanical testing with a % difference of approximately 13% being recorded, noting this value is line with the performance from the v-CFRP case (see Table 36).

Examining now samples 1 and 2, and 3; these samples recorded the most extreme differences in ultrasound derived Young‟s modulus and mechanically derived Young‟s modulus. In the case of sample 1, a figure of approximately 54% is documented, and in the case of sample 2, a figure of approximately 50% is recorded and in the case of sample 3, approximately 30% being recorded. Compared to vCFRP, sample 1 and 2, have large % differences; the least accurate v-CFRP sample, sample 2, provided a % difference of approximately 25 %. Sample 3 can be roughly equated

to sample 3 from the v-CFRP with figures of approximately 25 and 30% being recorded.

Prior to moving onto a final discussion, Figure 54, presents an additional bar graph documenting the ultrasonic derived individual Young‟s Modulus‟s and the mechanically calculated Young‟s Modulus.

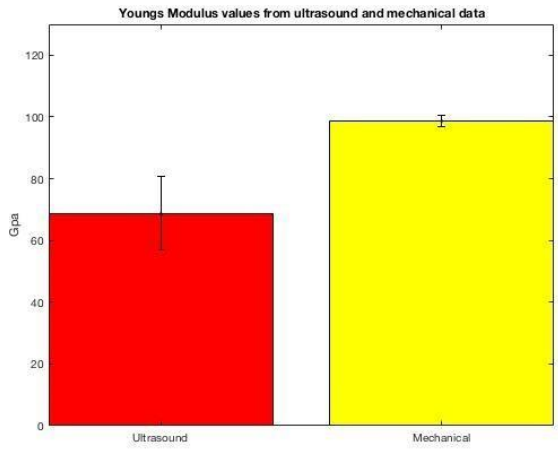

Figure 54 – Young‟s Modulus derived from ultrasound and mechanical data sets.

8.4 Discussion on second research question

Having now outlined the experimental findings, attention is turned back to the second research question (repeated for completeness),

Ultrasonic velocity measurements, specifically, the through transmission technique, have long been used to determine the elastic constants of virgin CFRP. Products denominated as recycled and remanufactured CFRP are not v-CFRP; thus, are the standard ultrasonic through transmission measurements routinely used on v-CFRP applicable to recycled and remanufactured (if these are the correct terms) CFRP?

Exploring this, first consider the application of the technique to both v-CFRP and rfCFRP. In both instances, the same experimental arrangement was used to record the results. That is, no large changes in observed wave profile (i.e. no extreme velocity changes, signification attenuation, or extreme changes in critical angle, all of which could force a change in experimental parameters) for rf-CFRP, when compared to

vCFRP, were recorded. Thus, the experimental technique and arrangement was applicable to both v-CFRP and rf-CFRP.

Examining now a further application of the technique in terms of accuracy. Table 45 provides a summary of findings from the previous sections.

Values for Young‟s modulus calculated from elastic constants and mechanical testing alongside % difference			
Sample	YM_{LSM} (GPa)	Average YM_{Mech} from 5 samples (GPa)	% difference between YM_{LSM} and YM_{Mech}
V-CFRP Average (1- 4)	98.67 ± 17.1	96.48 ± 1.63	2.24 %
V-CFRP average	95.30		1.23 %
rf-CFRP Average (1- 4)	68.69 ± 11.92	98.68 ± 1.69	35.83 %
rf-CFRP Sample average	64.06		42.54 %

Table 45 – Young‟s Modulus for v-CFRP and rf-CFRP derived via ultrasound through transmission and via mechanical testing. % difference values are also given.

From Table 45, it is observed that either the v-CFRP individual average modulus (obtained by the summation of the modulus from individual samples) or the average modulus obtained using average velocity, provides a very good approximation of the mechanically derived Young‟s Modulus. Figures of 2.24% and 1.23% are observed. Using the same derived Modulus‟s in the case of rf-CFRP, it is observed that a poor approximation of mechanically derived Young‟s modulus is obtained. % difference figures of approximately 36% and 42.5% can be observed. Additionally, the rf-CFRP recorded more variation in velocity than the v-CFRP, most noticeably for longitudinal waves, particularly in the 1-2 plane, see standard deviation values listed in Table 39.

Taking these factors into account, it could be concluded, and answering the second research question, that while ultrasound through transmission is applicable for transversely isotropic rf-CFRP, it does not provide as accurate a result when seeking to determine the elastic constants in comparison to v-CFRP.

However, given the additional data presented in section 8.3, this conclusion is premature. Consider first the varying value of Young‟s modulus recorded in the samples for both v-CFRP and rf-CFRP, as evidenced from tables 36 and Table 45. While it is true that rf-CFRP samples 1 and 2 recorded a higher % difference between ultrasound derived Young‟s modulus and the mechanically derived Young‟s modulus, than all four of the v-CFRP samples, sample rf-CFRP 4 recorded a lower value, when compared to v-CFRP sample 1 and 2; this goes against the conclusion that elastic constant determination of v-CFRP via ultrasound through transmission of v-CFRP will always provide a more accurate result when compared to rf-CFRP. RfCFRP sample 3, was not generally better or worse performing than v-CFRP, the rfCFRP sample was roughly on par with the most inaccurate v-CFRP sample, v-CFRP sample 2.

Examining now the argument of using more variation in wave profile as a means of suggesting that elastic constants determination via ultrasound through transmission will always be more accurate for v-CFRP than for rf-CFRP.

The rf-CFRP average longitudinal velocity in the 1-2 plane is more variable when compared to average longitudinal velocity for v-CFRP; Table 38 and Figure 50 (a-d) demonstrate a larger standard deviation, or more varied velocity profile, when compared to a more predictable v-CFRP velocity profile, Table 30 and Figures 42 (ad). Given that an identical composite manufacturing process for both v-CFRP and rfCFRP was employed, this gives credence to the conclusion that ultrasound through transmission of v-CFRP will provide more accurate results, with perhaps some fibre movement or misalignment occurring during the rf-CFRP manufacturing process. However, this reasoning does not factor into account previous research which investigated the robustness of the reconstruction algorithms when faced with velocity scatter of up to 5%, (Rokhlin and Wang, 1992). The authors in this instance inserted a random noise onto their velocity measurements on uni-directional v-CFRP and investigated the robustness of the least means squares algorithm. The authors demonstrated that the elastic constant can be reliably obtained in planes of symmetry with up to 5% velocity scatter. Investigating this, the rand function on MATLAB was used to insert two different variations of 0 - 5% scatter on v-CFRP sample 1 in this plane. The elastic constants were determined using least squares minimization with the Young‟s modulus also calculated. Table 46 provides the before and after elastic constants and Young‟s modulus.

Scatter	C11 (GPa)	C33 (GPa)	C44 (GPa)	C13 (GPa)	C66 (GPa)	C12 (GPa)	YM (GPa)
0-5%	6.69	100.17	1.94	11.03	1.68	3.33	75.89
0-5%	6.44	104.36	1.96	10.58	1.68	3.08	80.84
0 (experimental)	6.45	104.31	1.96	10.58	1.68	3.09	80.84

Table 46 – Young‟s Modulus and elastic constants for v-CFRP sample 1, with two varieties of added scatter and the original experimental values. Version 2 (middle row) of added scatter does not affect the Young‟s modulus result. Version 1 (top row) reduces the result when compared to original experimental findings.

Table 46 documents that additional longitudinal velocity scatter varying from 0-5% in the 1-2 plane can cause almost no change on the elastic constants and Young‟s modulus when compared to experimental. However, it also documents that scatter can cause a change in most notably C_{11} and C_{33}. Therefore, while scatter can influence the value of elastic constants, the assertion that less accurate results will always be obtained with a more varied longitudinal velocity profile in the 1-2 plane, is not justifiable in every situation.

Additionally, the more varied longitudinal profile did not cause any change to elastic constant C_{66}, which is not surprising given the equation for C_{66} in this plane is independent of C_{11} and C_{33}.

A final point which suggests a premature conclusion is that composite recycling processes return more varied fibres as a result of a) how the fibres were obtained and b) composite composition. Taking this into consideration, along with the limited number of samples manufactured and tested, additional experiments are required for a broad conclusion to be sustainable.

Thus, a more realistic conclusion from this research may now be drawn. The manufacturing technique and experimental ultrasonic approach used herein will generally provide smaller percentage differences between mechanical and ultrasound derived Young‟s modulus for v-CFRP than it does for rf-CFRP. This is based on three out of four rf-CFRP samples having larger percentage differences between ultrasonic Young‟s modulus and mechanical Young‟s modulus.

Examining now an unexpected result from this research, rf-CFRP sample 4 recording a result in keeping with the % error of v-CFRP. Given that the recycling process produces fibres more susceptible to misalignment and with reduced matrix adhesion qualities as a result of sizing removal, a more varied velocity profile is expected, and

is generally recorded in the samples. However, after least square minimization, rf-CFRP sample 4 records accuracy figures in keeping with v-CFRP. This is an encouraging result, and given the relative simplicity of the rf-CFRP manufacturing processes used in this work, for more sophisticated rf-CFRP, ultrasound through transmission and least squares minimization could perhaps parallel v-CFRP accuracy in totality.

Additionally, this research has documented a more robust and predictable transverse velocity in rf-CFRP. Smaller standard deviation figures were recorded for the rf-CFRP average sample in both planes when compared to the standard deviation figures of the longitudinal waves in both planes as demonstrated by Figures 51 and 52 and Tables 38 and 39. Further, the velocity in the plane of isotropy was not only consistent but followed the expected velocity profile observed with the v-CFRP case. Expanding on this, Table 47 develops tables 30 and 38 and is given to highlight the close relationship between transverse waves in the plane of isotropy, when compared to longitudinal velocity in this plane. Note these results are also graphed previously Figures 43 and 51 (a-d).

v-CFRP (longitudinal velocity)					
Angle	Sample 1	Sample 2	Sample 3	Sample 4	Average and standard deviation
0	2158	2115.6	2236.5	2233.5	2185.9 ± 51.35
3	2120	2118.4	2212.2	2218.6	2167.3 ± 48.16
6	2103	2102.1	2206.3	2234.6	2161.5 ± 59.79
9	2122.9	2124.6	2227.2	2254.2	2182.2 ± 59.25
12	2207.3	2232	2278.5	2337.8	2263.9 ± 49.72
14	2336.7	2362.3	2370	2443.6	2378.2 ± 39.75
15	2434	2214	2409.9	No correlation	2352.5 ± 98.52
rf-CFRP (longitudinal velocity)					
Angle	Sample 1	Sample 2	Sample 3	Sample 4	Average and standard deviation
0	2430.2	2029	2489.5	2201.6	2287.8 ± 183.65 2182.5 ± 147.98
3	2398.2	2012.5	2234.3	2085.1	
6	2527.1	2054.5	2253	2105.3	2235.0 ± 183.75 2164.5 ± 105.61
9	2299.8	2000.8	2205.2	2144.3	
12	2226.2	2216	2403.4	2334.5	2295.1 ± 77.88
14	2530.6	1975.1	T wave	T wave	2252.8 ± 277.45
v-CFRP (Transverse velocity)					

Angle	Sample 1	Sample 2	Sample 3	Sample 4	Average and standard deviation
16	1091.5	1134.7	1136.8	1134.6	1124.4 ± 19.02
17	1112.4	1117.2	1130.5	1153.7	1128.5 ± 16.02
18	1127.1	1132.3	1148.5	1166.5	1143.6 ± 15.40
19	1140.8	1140.7	1154.9	1178.1	1153.6 ± 15.27
20	1147.9	1153.7	1165.4	1183.1	1162.5 ± 13.45
21	1153.8	1154.4	1164.6	1181.9	1163.6 ± 11.36
24	1149.3	1165.7	1165.4	1176	1164.2 ± 9.82
27	1136.1	1137.9	1151.8	1166	1148.0 ± 12.06
30	1114.8	1113.5	1135.5	1147.6	1127.9 ± 14.36
33	1108.2	1091.5	1128.4	1142.2	1117.6 ± 19.31
rf-CFRP (Transverse velocity)					
Angle	Sample 1	Sample 2	Sample 3	Sample 4	Average and standard deviation
14	L wave	L wave	1255.6	1223.5	1239.6 ± 16.05
15	1241.4	1178.2	1245.9	1239.6	1226.3 ± 27.85
16	1233.3	1199.4	1261.6	1254.5	1237.2 ± 24.18
17	1273.5	1199.7	1275.9	1268	1254.3 ± 31.64
18	1258.8	1228.3	1263.1	1279.8	1257.5 ± 18.59
19	1277.4	1235.6	1274.2	1265.9	1263.3 ± 16.52
20	1279.8	1232	1283.4	1274.4	1267.4 ± 20.69
21	1280.2	1236.5	1267.3	1281	1266.3 ± 18.02
24	1278.5	1261.7	1299.7	1268.1	1277.0 ± 14.41
27	1295.7	1244.3	1283.6	1241.6	1266.3 ± 23.76
30	1233	1202.4	1223.0	1225.6	1221.0 ± 11.35
33	1191.8	1158.9	1170.5	1171.1	1173.1 ± 11.85

Table 47 – Velocities recorded in the 1-2 plane for both v-CFRP and rf-CFRP. Larger differences in longitudinal velocity between rf- CFRP samples when compared to differences between v-CFRP may be observed. Transverse velocities for both rf-CFRP and v-CFRP behaviour more similarly.

Additionally, similar research conducted on quasi-isotropic CFRP, (Paterson et al., 2018), found that % differences between rf-CFRP samples for transverse velocity were smaller than % percentage differences found with longitudinal velocities when propagating in an isotropic plane (i.e. the transverse velocities across the rf-CFRP samples behaved more uniformly in terms of velocity and profile). While in the case of Paterson et al there is a different less accurate manufacturing process, these early results suggest that transverse wave velocity profile could be relatively more stable in the plane of isotropy than longitudinal waves for rf-CFRP for both transversely isotropic and quasi-isotropic rf-CFRP. However, further analysis on additional samples is required to confirm these early indications.

Staying with the research on quasi-isotropic CFRP (see appendix 6), a hypothesis arising from this work, was that for a similar manufacturing process, the same wave profile for v-CFRP will be returned for rf-CFRP. Figures 43, 44, 51 and 52 (a-d) appear to suggest the hypothesis of similar wave profile has some degree of legitimacy, particularly when the transverse waves are examined, but there is however noticeable variation between v-CFRP and rf-CFRP samples in this work; the longitudinal velocity varied more in the 1-2 plane and the rf-CFRP samples matched only v-CFRP samples 2 in the 1-3 plane.

Additionally, the point at which the longitudinal wave was no longer recorded in the 1-2 plane was more varied for the rf-CFRP than with the v-CFRP; samples 1 and 2 recorded a longitudinal wave for incident angle of 14, with samples 2 and 4 recording a transverse wave for samples 3 and 4. Thus, further research is again required to gauge the accuracy of this hypothesis.

8.4.1 Measurement Enhancement

As stated the findings in this chapter are limited by the experimental technique and manufacturing process adopted. Given practical constrains of this thesis in addition to this being the first time in open literature that the elastic constants of rf-CFRP are sought via ultrasound through transmission this chapter reports on initial results which can be built and expanded upon. The literature review presented in chapter 7 identifies methods in which to refine and further develop the findings in this chapter.

These methods are again discussed with relevance to building on this work.

Group Velocity Effect

As stated, the group velocity effect can cause the path of the ultrasonic beam to skew from the path taken by a plane wave travelling under Snell‟s laws when propagating in an anisotropic medium. Further, solutions to the combat the group velocity effect, namely the double through transmission system, are reported in literature, (Pearson and Murri, 1987; Rokhlin and Wang, 1992, 1989a).

Moving forward and building on this work it is of merit to investigate the role of group velocity in rf-CFRP. Similar to existing literature, the elastic constants should be

determined via the double through transmission method and the Markham method (this work) with a reporting of disparities. The effect of beam deviation will be determined in addition to any measurement inaccuracy associated with the Markham technique (resulting from group velocity effect) being determined.

Self-Reference Model (SRM)

Similar to group velocity analysis, investigating SRM should be performed as with existing literature (Chu and Rokhlin, 1994a, 1994b, 1992). Given that the SRM is focused on increasing the accuracy of the phase reference velocity measurement, future analysis can be performed on rf-CFRP using either the Markham method (this work) or the double through transmission arrangement. This type of analysis would provide more insight into how effective the SRM is in reducing measurement error for rf-CFRP.

Automation

In this work, 4 samples of rf-CFRP and 4 samples of v-CFRP were subject to ultrasound through transmission. Ultrasonic transducers were excited using a manually operated function generator with velocity measurement conducted via a MATLAB correlation technique found with literature, (Trogé et al., 2016). The
CFRP samples were manually rotated using a rotary device with angular rotation
0.01° resolution over 360°.
Moving forward it is appropriate to increase the number of samples and number of measurements taken on each sample. A process similar to (Castellano et al., 2014) in where LabVIEW is incorporated into the experimental apparatus is suggested. In this work, the authors determined the elastic constants of unidirectional v-CFRP via the double through transmission system but critically the signal acquisition, oscilloscope, rotation via stepper motor and processing of experimental data are controlled automatically via LabVIEW. Automating the manual methods outlined in this chapter will allow for a) samples to be tested quicker (quicker testing allows for more samples to be tested and thus the development of a broader conclusion) and b) more tests can be conducted on samples (100+ measurements can be taken and averaged to reduce the effects of noise in the data).

Further work

As part of the literature review outlined in chapter 7 two novel information tables are presented. These tables highlight some 40 contributions to knowledge. It is also the case that this work is the first in open literature to determine the elastic constants of rf-CFRP via ultrasound through transmission. Thus in addition to investigating group velocity effects, the SRM, and automation as mechanisms to reduce measurement inaccuracy the novel information tables in conjunction with varying composite recycling and manufacturing processes may be consulted moving forward.

8.5 Conclusion

This chapter has investigated the application of ultrasound through transmission as a means to determine the elastic constants of transversely isotropic rf-CFRP. To provide a frame of reference the elastic constants of v-CFRP were first evaluated.

These constants were used to determine the Young‟s modulus which was compared with a mechanically determined result. The v-CFRP returned reasonable results with the closest % difference between ultrasound and mechanical being 8%. Examination of the rf-CFRP samples demonstrated that the ultrasound through transmission technique is applicable to transversely isotropic rf-CFRP. No large changes in velocity, critical angles, or attenuation, which all have the potential to cause the experimental set up to be altered, were recorded. For the experimental configuration and manufacturing process used in this work a larger % difference between ultrasonically derived Young‟s modulus and mechanically derived Young‟s modulus when compared to v-CFRP was recorded for 3 out 4 samples of rf-CFRP when compared to v-CFRP. With the rf-CFRP samples, the elastic constants C_{11}, C_{33} and C_{13}, recorded the most variation in value with little variation recorded in C_{44} and C_{66} (the constants determined using transverse velocity in plane of isotropy). A broad conclusion that rf-CFRP will always record a less accurate result was not able to be drawn given the instance of sample rf-CFRP 2 recording a % error figure in keeping with the results from v-CFRP. Further, it was shown that a random longitudinal velocity scatter of 0-5% in the 1-2 plane did not always influence the elastic constants when compared to experimental velocities with no scatter, but has the capacity to do so. Additionally, it

was also recorded that the transverse waves in the plane of isotropy for a transversely isotropic rf-CFRP were relatively constant and predictable across the samples. Further, the transverse wave profiles were also in keeping with the experimental results from v-CFRP. Further still, similar experiments on quasi-isotropic rf-CFRP also found that transverse waves were more closely related in a plane of isotropy than their longitudinal counter parts for rf-CFRP. Given the limited data set however, the assertion that transverse waves are more stable than longitudinal waves for rfCFRP was not able to be confirmed at this point, but is an area worthy of further investigation.

Lastly, this research also gave an indication that a similar wave profile for rfCFRP and v-CFRP will be returned, a hypothesis arising from earlier research on quasi-isotropic CFRP (see appendix 6), but did not confirm it.

With the conclusion of this chapter limited by the experimental arrangement and manufacturing process outlined, building on the findings from the literature (chapter 7), this chapter has also document future work to allow for increased measurement accuracy. Areas such as group velocity effects, automation, reference velocity measurement were put forward as the next stage of research to be conducted.

Moving forward in this thesis, chapter 9 documents an overall conclusion to this thesis. Additional work arising from this chapter is held off and is presented at the end of chapter 9, along with additional work arising from the previous chapters.

Chapter 9: Thesis Conclusion

The expected proliferation of both carbon fibre and CFRP (Kraus and Kühnel, 2015), coupled with the expense of manufacturing such materials, (Carberry, 2008), and increasing legislation designed to tackle waste and force landfilling as a last resort, (European Parliament and Council, 2012, 2008, 2000a), has led to on-going research as to what to do with such EOL materials.

An EOL option which has received significant attention is recycling, a strategy aimed at extracting the fibres from CFRP by means of mechanical, thermal or chemical processes, (Oliveux et al., 2017, 2015; Pickering, 2006; Pimenta et al., 2010; Pimenta and Pinho, 2012, 2011). Researchers have also considered the process of remanufacturing new composite using these extracted fibres, (Morin et al., 2012; Oliveux et al., 2017, 2015; Perry et al., 2012; Pimenta and Pinho, 2012, 2011, Shi et al., 2014, 2012a; Tian et al., 2017).

While recycling and remanufacturing are widely discussed in literature, these processes are defined externally from the CFRP re-use industry. No study to date has investigated if recycling and remanufacturing are the appropriate terms to describe the processes conducted by EOL CFRP researchers.

Additionally, CFRP parameters such as Young‟s modulus and the determination of elastic constants are achievable via a non-destructive ultrasonic based velocity system, also known as „the through transmission technique“,

(Markham, 1970; Pearson and Murri, 1987; Rokhlin et al., 2011; Rokhlin and Wang, 1992; Zimmer and Cost, 1970). However, this type of testing has generally not been performed by practitioners involved in re-use of EOL CFRP, who instead favour a mechanical based testing approach.

Thus, this research has sought to investigate a) the terminology surrounding the CFRP re-use industry, including a justification as to the importance of this issue, and b) the application of the through transmission technique to CFRP manufactured using the fibres obtained via composite recycling.

9.1 Findings

The findings from this research are expressed below in relation to the research questions driving this research.

9.1.1 Terminology surrounding the CFRP re-use industry

Research question 1 is repeated for clarity

"Are the products denominated as recycled CFRP and remanufactured (remanufactured) CFRP actually by definition, recycled and remanufactured CFRP? If not, why not? And is there a more accurate way of describing these products?"

Through investigation of this question, this research has identified problems associated with using both recycling and remanufactured terminology to describe the processes and products conducted by CFRP EOL researchers. Additionally, new terminology which more accurately describes the products created by industry and academia was also presented.

Considering first recycling terminology. By comparing a standard definition of recycling (BS 8887-2, 2009; European Parliament and Council, 2012, 2008), against the practices of mechanical, thermal and chemical CFRP recycling, it was shown that the processes conducted by CFRP researchers are indeed recycling operations.

However, it was also shown using a similar methodology that recycled CFRP and recycled fibres are not always the most accurate terminology to describe products. Recycled CFRP, or CFRP recyclate, is the product created by recycling the original composite (i.e. the reclaimed fibres). Thus, defining recycled CFRP as the product

arising from using reclaimed fibres to manufacture new CFRP, incorporating virgin resin, was found to be an inaccurate way of describing these products. Further, given that composite recycling returned the fibres in a state largely resembling the pre-impregnated state (when compared to the original raw materials), and the desire to obtain the fibres in an exact pre-impregnated like state moving forward, the term recycled fibres was shown in general as not being an applicable way to describe fibres obtained via CFRP recycling.

Taking both of these findings into consideration, new terminology in keeping with existing European Union terminology was given to describe such products i.e. reused fibre CFRP (rf-CFRP or CFRP-rf).

Examining now remanufacturing terminology. A similar methodology was used to compare the processes conducted by EOL CFRP researchers against established remanufacturing terminology. Here it was found that CFRP remanufacturing is not occurring. It was also found that CFRP cannot be remanufactured.

9.1.2 Creation of novel tool

Given that incorrect usage of terminology was found in this sector, this research also sought to develop a novel way of differentiating between recycled, repaired, re-used, reconditioned, and remanufactured products in general.

This research has shown that to correctly designate a product as recycled, reused, repaired, reconditioned, or remanufactured, then existing definitions or existing tools had to be examined, interpreted by the reader, and then applied by the reader. Thus, a gap in literature was identified in that a tool which could remove the decision from the reader, and therefore inform the reader itself, was not available.

To fill this gap in knowledge a novel tool was developed. The tool was built on the premise that by defining the stages of remanufacturing, and therefore a remanufactured product, then all other processes must also be tacitly defined (given that remanufacturing involves the most labour content). An initial tool was presented and reviewed at ICoR 2015. An updated tool then received further independent review by industrial and academic bodies. Lastly the updated tool was subject to additional review via journal publication, resulting in a final version which appears in this thesis.

In addition to providing a novel tool for researchers to develop future manufacturing sustainability research upon, this tool also served as a means to express only the essential list of remanufacturing characteristics, and therefore develop a distinction between the essential characteristics of a remanufactured product and the general expected characteristics of a remanufactured product within literature. Lastly, this novel tool may also be used by academia to quickly assess if a given industry is actually producing remanufactured products, given its ease of use, quickness of use, and the fact that no knowledge of re-based processes is required to use it.

9.1.3 Ultrasonic determination of rf-CFRP elastic constants

Research question 2 is repeated for clarity

"Ultrasonic velocity measurements, specifically, the through transmission technique, have long been used to determine the elastic constants of virgin CFRP. Products denominated as recycled and remanufactured CFRP are not v-CFRP; thus, are the standard ultrasonic through transmission measurements routinely used on v-CFRP applicable to recycled and remanufactured (if these are the correct terms) CFRP?"

Investigation of this question firstly examined the relationship between acoustic wave velocity and the elastic constants of a solid, along with examining the experimental technique required to measure the elastic constants. Looking first at the theoretical principles, a thorough derivation of the Christoffel equation was presented in this thesis. This derivation incorporated existing knowledge from various researchers and presented this information as a single document. Thus, new or existing practitioners involved in this area have now an additional relatively thorough text, which draws information from various sources, on which to build future research. This research also created a literature review of the determination of elastic constants on uni-directional v-CFRP via ultrasound through transmission. A thorough review dating from circa 1970-2014 was undertaken, with the chronological progression of how the through transmission technique grew over time, clearly mapped out. Thus, again new or existing practitioners now have an additional document, citing many seminal works, on which future research may be built.

This research also documented the manufacture of uni-directional v-CFRP via vacuum assisted resin transfusion. Further, the elastic constants were also derived ultrasonically, with a comparison of mechanically derived Young‟s modulus, a theoretical Young‟s modulus and the ultrasonically derived Young‟s modulus also conducted.

Four samples were ultrasonically tested with the Young‟s modulus from these samples used to calculate an average figure. This average figure recorded approximately 2% difference from the mechanically derived Young‟s modulus and approximately 14% difference from the theoretical value. Of the individual samples, maxima and minima % difference figures between ultrasonic modulus and mechanical modulus was also found, figures of 25% and 8% respectively were reported.

Building on this, this research also presented for the first time in literature, the determination of elastic constants of rf-CFRP via ultrasound through transmission. Manufacture of the rf-CFRP was via pyrolysis of v-CFRP followed by a vacuum assisted resin transfusion. Similar to v-CFRP, the elastic constants were used to calculate individual and subsequently an average Young‟s modulus which was compared to a mechanically derived Young‟s modulus. Unlike the v-CFRP, the rf-CFRP recorded % difference values of approximately 36%. A more varied longitudinal wave profile in the 1-2 plane was also found when compared to the vCFRP, however a more stable transverse profile was also found in the same plane. On an individual sample basis the maxima and minima % difference figures between ultrasonic modulus and mechanical modulus were found to be approximately 54% and 13%. This research demonstrated that given a similar ultrasound through transmission experimental arrangement, for the manufacturing procedure outlined in this thesis, v-CFRP will generally return a smaller % difference figure (between ultrasonic Young‟s modulus and mechanical Young‟s modulus) when compared to v-CFRP.

9.1.4 Recap of thesis findings

<u>In relation to terminology surrounding the CFRP re-use industry</u>

- Literature survey outlining the practices and instances within industry where the terms recycling and remanufacturing are occurring in relation to carbon fibre reinforced plastic.

- Presentation of accepted definitions of recycled and remanufactured products from industry and academia
- Identification that existing incorrect application of remanufacturing terminology along with both correct and liberal use of recycling terminology is used in this sector.
- Identification that CFRP is not capable of being remanufactured
- Proposal of new terminology better positioned to denominate these products

In relation to creation of novel tool

- Literature review to establish existing means to differentiate between recycled, re-used, repaired, reconditioned and remanufactured products. It was found that the reader must form their form their own decision as to the status of a product which has received re-based process
- Creation of novel tool designed to remove the decision as to which process a product has received from the user i.e. the tools informs the user directly via novel interaction element, requiring no previous knowledge of processes.
- Industrial and academic review of novel tool
- A list of only essential characteristics of remanufactured products, which is distinct from general characteristics of remanufactured products

In relation to Ultrasonic determination of rf-CFRP elastic constants

- Derivation of the Christoffel equation, an equation governing the relationship between wave velocity and elastic constants of a solid, from first principles
- Literature review on determination of elastic constants of v-CFRP highlighting the long established experimental arrangements and existing knowledge on the subject
- Determination of elastic constants of v-CFRP via an ultrasonic immersion based velocity measurement and via mechanical testing with comparison of result
- Recycling of v-CFRP and subsequent manufacture of rf-CFRP.
- Determination of elastic constants of rf-CFRP via similar ultrasonic immersion based velocity measurement and via mechanical testing with comparison of result
- For the given ultrasonic immersion technique and manufacturing processes used in this work, generally a smaller percentage error between the ultrasonic derived Young‟s modulus and the mechanically derived Young‟s modulus will be obtained for v-CFRP when compared to rf-CFRP
- Observation of more stable transverse velocities, particularly in the plane of isotropy when compared to longitudinal velocity for rf-CFRP, building on similar observed transverse velocities for quasi-isotropic rf-CFRP.
- Bespoke Matlab programmes to serve both as a teaching aid in this research area and also to identify and present the findings recorded from experiment

9.3 Recap of contributions to knowledge

- Cross examination of practices, in relation to CFRP, conducted within industry and academia currently labelled as recycling and remanufacturing with accepted definitions of recycling and remanufacturing.

- Identification that CFRP remanufacturing terminology is used incorrectly, recycling terminology is used both correctly and in a somewhat liberal manner to describe products and processes created by academia and industry and that CFRP is not capable of being remanufactured.

- Identification of new terminology which more accurately describes the products created by academia and industry, terminology which is in keeping with accepted definitions and also in accordance with existing EU directives.

- Development and presentation of a novel EOL decision making tool which may be used to form a decision as to whether a product has been recycled, repaired, re-used, reconditioned or remanufactured and as means to quickly and efficiently determine remanufacturing synonyms.

- Review documenting a chronological progression of findings and contributions to knowledge within literature concerning the immersion based ultrasonic through transmission determination of elastic constants of unidirectional v-CFRP, circa 1970-2014.

- Determination that while applicable as a means to investigate elastic constants and Young‟s modulus of rf-CFRP, for the manufacturing procedure and experimental arrangement outlined in this research, generally a lower % difference between ultrasound derived Young‟s modulus and Mechanical derived Young‟s modulus is found for v-CFRP when compared to rf-CFRP.

- Development and presentation of bespoke Matlab programmes that construct and execute the Christoffel equation, provide information on wave polarization, serve as means to determine elastic constants, and provide graphical outputs to the user.

9.4 Recap of research beneficiaries

Both industry and academia benefit from this research. Listed below is the rationale as to why both sectors will benefit.

- Using the correct terminology to describe recovery strategies allows for
    1. Greater potential for effective research
    2. Improved dialogue between industry and academia
    3. Increased likelihood of gauging market more accurately
    4. Better compliance with new or existing legislation
    5. Increased awareness of remanufacturing within the field
    6. More accurate description of products created

- Novel tool, identifying and informing the user of which EOL operation conducted allows for
    1. More accurate description of products
    2. Quick test to identify remanufacturing and to identify remanufacturing synonyms such as „overhaul“ or „rebuild“
    3. Reduction of user error (removes final decision from user)
    4. Increased awareness of a remanufactured product (when used in conjunction with existing tools)

- Development of bespoke Matlab programmes and conducting experimental results on rf-CFRP allows for,
    1. Analysis of ultrasound through transmission on rf-CFRP, when compared to v-CFRP
    2. The accuracy of „remanufactured“ CFRP Young“s modulus determination via ultrasound through transmission for the manufacturing and experimental procedure outlined, when compared to v-CFRP.
    3. Increased awareness in the ultrasonic research community of relatively new and novel products, rf-CFRP
    4. Teaching aid for students via
        - Thorough derivation of Christoffel equation from first principles
        - Matlab programme outlining the relationship in solids between the elastic wave velocity and the elastic properties of the material.
    5. Fully customizable Matlab programmes able to determine elastic solids of materials and document findings using these data sets

9.4 Future work

Building on this research, various themes for future work have been identified across the research undertaken, as described below.

Definitions of rf-CFRP

This research has presented a new definition for materials also known as remanufactured CFRP or recycled CFRP. This definition is in keeping with existing terminology and more accurately describes these products. Moving forward, research should be geared towards seeking to get this terminology established within industry and academia. This process would involve diverse activities such as networking and presenting, and promotion of the research at conferences, workshops and focus groups, along with further research, for instance NDT/E based research on rf-CFRP materials.

Ultrasonic NDT/E of rf-CFRP

This work has conducted an investigation into ultrasound through transmission and found a conclusion limited to the manufacturing process and testing mechanism used here in. Moving forward, the literature review has identified many areas of future research. These areas include but are not limited to,

- Different sample architectures
- Sample width variation
- Different recycling systems
- Different types of fibre composites
- Sample manufacturing improvements
- Frequency variation
- Adoption of double through transmission
- Reference wave determination
- Robustness of reconstruction algorithms for rf-CFRP
- Dispersion effects
- Group velocity effects
- Phase shift effects
- Critical angle measurements

Novel EOL tool

An output of this research was the development of a novel tool to help both researchers and industrialists‟ better articulate products which have received a rebased process. This tool has received endorsement and was refined and by two independent rounds of academic and industrial feedback, along with review and publication by the Journal of Cleaner Production. Moving forward further endorsement could be sought by sending out the tool to companies known to offer a variety of re-based services in addition to working in collaboration with government agencies such as British Standards. Further, given that the lay person may be unfamiliar with some terminology, for example emergy, additional focus may be placed upon clarification of language in within the tool.

Additionally, future research may also be geared towards investigating differences and understanding between this tool and similar tools within literature. This type of knowledge would provide insight for researchers to develop future tools to help the industry meets specific needs, such as understanding the differences in rebased processes, identifying a re-based product, educating the wider public on the rebased processes and so forth.

References

Abbey, J.D., Meloy, M.G., Blackburn, J., Guide Jr., V.D.R., 2015. Consumer Markets for Remanufactured and Refurbished Products. California Management Review 57, 26–43. doi:10.1017/CBO9781107415324.004

Abbey, J.D., Meloy, M.G., Guide, V.D.R., Atalay, S., 2014. Remanufactured products in closed-loop supply chains for consumer goods. Production and Operations Management 24, 488–503. doi:10.1111/poms.12238

Adamowski, J.C., Andrade, M.A.B., Buiochi, F., Alvarez, N.., 2009. The ultrasonic determination of elastic constants of composite materials using a diffraction free receiver, in: 20th International Congress of Mechanical Engineering.

Adamowski, J.C., Andrade, M.A.B., Buiochi, F., Franco, E.E., 2007. Ultrasonic through transmission measurement of elastic constants of fiber reinforced

composites using a large aperture receiver, in: 19th International Congress of Mechanical Engineering.

Adamowski, J.C., Andrade, M. a B., Perez, N., Buiochi, F., 2008. A Large Aperture Ultrasonic Receiver for Through- Transmission Determination of Elastic Constants of Composite Materials, in: Proceedings - IEEE Ultrasonics Symposium. pp. 1524–1527. doi:10.1109/ULTSYM.2008.0371

Adamowski, J.C., Buiochi, F., Higuti, R.T., 2010. Ultrasonic material characterization using large-aperture PVDF receivers. Ultrasonics 50, 110–115. doi:10.1016/j.ultras.2009.09.018

Adams, R.D., Collins, A., Cooper, D., Wingfield-Digby, M., Watts-Farmer, A., Laurence, A., Patel, K., Stevens, M., Watkins, R., 2014. Recycling of reinforced plastics. Applied Composite Materials 21, 263–284. doi:10.1007/s10443-0139380-1

Anderson, P.F., 1983. Marketing , Progress , and Scientific Scientific Method. Journal of Marketing 47, 18–31. doi:10.2307/1251395

Andreu, J., 1995. The remanufacturing Process, Internal Paper from Manchester Metropolitian University. Manchester.

Arist gui, C., Baste, S., 1997. Optimal recovery of the elasticity tensor of general anisotropic materials from ultrasonic velocity data. The Journal of the Acoustical Society of America 101, 813–833. doi:10.1121/1.418040

Asmatulu, E., Twomey, J., Overcash, M., 2013. Recycling of fiber-reinforced composites and direct structural composite recycling concept. Journal of Composite Materials 48, 593–608. doi:10.1177/0021998313476325

ASTM D 3039/D 3039M–14, 2014. ASTM International. Standard test method for tensile properties of polymer matrix composite materials. ASTM D 3039/D 3039M-14., in: Anual Book of ASTM Standards, Vol. 08,.

ASTM D 3518/D 3518M–94, 2008. ASTM International. Standard test method for in-plane shear response of polymer matrix composite materials by tensile test of a ±45? laminate, ASTM D 3518/D 3518M–94, in: Anual Book of ASTM Standards, Vol. 08.

ASTM D 5379/D 5379M–05, 2008. ASTM International, Standard Test Method for Shear Properties of Polymer Matrix Composite Materials by the V-Notched Beam Method, ASTM D 5379/D 5379M–05, in: Anual Book of ASTM Standards,Vol. 08,.

Auld, B.A., 1990. Acoustic fields and waves in solids, Volume 1, 2nd ed. Krieger publishing company.

Balasubramaniam, K., Rao, N.S., 1998. Inversion of composite material elastic constants from ultrasonic bulk wave phase velocity data using genetic algorithms. Composites Part B: Engineering 29, 171–180. doi:10.1016/S13598368(97)00007-3

Barquet, A.P., Rozenfeld, H., Forcellini, F.A., 2013. An integrated approach to remanufacturing: model of a remanufacturing system. Journal of Remanufacturing 3, 1–11. doi:10.1186/2210-4690-3-1

Baudouin, S., Hosten, B., 1997. Comparison between prediction and measurement of viscoelastic moduli in composite materials versus temperature using ultrasonic immersion technique with oil. The Journal of the Acoustical Society of America 102, 3450–3457. doi:10.1121/1.419587

Baudouin, S., Hosten, B., 1996. Immersion ultrasonic method to measure elastic constants and anisotropic attenuation in polymer-matrix and fiber-reinforced composite materials. Ultrasonics 34, 379–382. doi:10.1016/0041624X(96)00021-2

Boucher, S., 1976. Effective moduli of quasi-homogeneous quasi-isotropic composite materials composed of elastic inclusions in an elastic matrix.(ii) Finite concentration of inclusions. Revue M 22.

Boucher, S., 1975. Effective moduli of quasi-homogeneous quasi-isotropic composite materials. (I) Infinitesimal concentrations of inclusions. Revue M 21.

Brinson, H.., Brinson, L.., 2008. Polymer engineering science and viscoelasticity. Springer. doi:10.1007/978-1-4899-7485-3

BS 8887-2, 2009. BSI Standards Publication Design for manufacture , assembly , disassembly and end - of - life processing (MADE) Part 2 : Terms and definitions.

Bunsell, A.R., Renard, J., 2005. Fundamentals of fibre reinforced composite materials, 1st ed. Institute of Physics, Bristol.

Carberry, W., 2008. Aero. Boeing Commercial Magazine Qtr 4, 8.

Carey, S.S., 2011. A Beginner"s Guide to Scientific Method, 4th ed. CENGAGE Learning Custom Publishing.

Castagnede, B., Jenkins, J.T., Sachse, W., 1990. Optimai determination of the elastic constants of composite materials from ultrasonic wave - speed measurements. American Institute of Physics 67, 2753–2761.

Castagnede, B., Roux, J., Hosten, B., 1989. Correlation method for normal mode tracking in anisotropic media using an ultrasonic immersion system. Ultrasonics 27, 280–287.

Castellano, A., Foti, P., Fraddosio, A., Marzano, S., Piccioni, M.D., 2014. Mechanical characterization of CFRP composites by ultrasonic immersion tests: Experimental and numerical approaches. Composites Part B: Engineering 66, 299–310. doi:10.1016/j.compositesb.2014.04.024

Cawley, P., Hosten, B., 1997. The use of large ultrasonic transducers to improve transmission coefficient measurements on viscoelastic anisotropic plates. The Journal of the Acoustical Society of America 101, 1373–1379. doi:10.1121/1.418103

Chaves, E., 2013. Notes on Continuum Mechanics, First. ed. Springer Netherlands. doi:10.1007/978-94-007-5986-2

Chimenti, D.E., 2014. Review of air-coupled ultrasonic materials characterization. Ultrasonics 54, 1804–1816. doi:10.1016/j.ultras.2014.02.006

Chu, Y.C., Degtyar, A.D., Rokhlin, S.I., 1994. On determination of orthotropic material moduli from ultrasonic velocity data in nonsymmetry planes. The Journal of the Acoustical Society of America 95, 3191–3203. doi:10.1121/1.409983

Chu, Y.C., Rokhlin, S.I., 1994a. comparative analysis of through transmission ultrasonic bulk wave methods for phase velocity measurements in anisotropic materials. Acoustical Society of America 95, 3204–3212.

Chu, Y.C., Rokhlin, S.I., 1994b. A method for determination of elastic constants of a unidirectional lamina from ultrasonic bulk velocity measurements on [0/90] cross-ply composites. Acoustical Society of America 96, 342–352.

Chu, Y.C., Rokhlin, S.I., 1994c. Stability of determination of composite moduli from velocity data in planes of symmetry for weak and strong anistropies. Acoustical Society of America 95, 213–225.

Chu, Y.C., Rokhlin, S.I., 1992. Determination of macro- and micromechanical and interfacial elastic properties of composites from ultrasonic data. Acoustical Society of America 92, 920–931.

Cleland, A., 2003. Foundations of Nanomechanics: From Solid-State Theory to Device Applications, 1st ed. Springer-Verlag Berlin Heidelberg.

Council of The European Communities, 1975. 75/442/EEC - Council Directive on Waste. Official Journal of the European Communities L 0442, 1–10.

Dean, G.D., 1971. A Comparison of the Use of Elastic Moduli and X-ray Measurements for the Assessment of Fibre Orientation in Chopped Carbon Fibre Composites. National Physics Laboratory, Teddington, Middlesex.

Dean, G.D., Lockett, F.J., 1973. Determination of the Mechanical Properties of Fiber Composites by Ultrasonic Techniques. Analysis of the Test Methods for High Modulus FIbers and Compoistes. ASTM STP 521, American Society for Testing and Materials 326–346.

Dean, G.D., Turner, P., 1973. The elastic properties of carbon fibres and thier composites. Composites 4, 174–180. doi:10.1016/0010-4361(73)90109-2

Degtyar, a. D., Rokhlin, S.I., 1997. Comparison of elastic constant determination in anisotropic materials from ultrasonic group and phase velocity data. The Journal of the Acoustical Society of America 102, 3458–3466. doi:10.1121/1.419588

Deschamps, M., Bescond, C., 1995. Numerical method to recover the elastic constants from ultrasound group velocities. Ultrasonics 33, 205–211. doi:10.1016/0041-624X(95)00024-W

Deschamps, M., Hosten, B., 1992. Viscoelasticity influence on frequency dependence of the ultrasonic transmission through plates of composite materials. Rev. Prog. Quantitative NDE 11, 201–208.

Deschamps, M., Hosten, B., 1992. The effects of viscoelasticity on the reflection and transmission of ultrasonic waves by an orhtotropic plate. Acoustical Society of America 91, 2007–2015.

Easterby-Smith, M., Thorpe, R., Jackson, P., 2012. Management Research, 4th ed. Sage Publishing.

Elliot, G.J., 1973. An investigation of ultrasonic goniometry methods applied to carbon fibre composite materials. Nondestructive testing centre, Atomic Energy Research Establishment.

EU, 2017. End of Life vehicles [WWW Document]. URL http://ec.europa.eu/environment/waste/elv/ (accessed 9.22.17).

European Action Plan, 2015. European Union Action Plan for the Circular Economy [WWW Document]. URL http://eur-lex.europa.eu/legalcontent/EN/TXT/?uri=CELEX:52015DC0614 (accessed 8.17.16).

European Commission, 2012. Guidance on the interpretation of key provisions of Directive 2008/98/EC on waste.

European Parliament and Council, 2012. Directive 2012/19/EU of the European Parliament and of the Council of 4 July 2012 on waste electrical and electronic equipment (WEEE). Official Journal of European Union L 197, 38–71. doi:10.3000/19770677.L_2012.197.eng

European Parliament and Council, 2008. Directive 2008/98/EC of the European Parliament and of the Council of 19 November 2008 on waste and repealing certain directives (Waste framework. Official Journal of European Union L 312, 3–30. doi:2008/98/EC.; 32008L0098

European Parliament and Council, 2006. Regulation No 1013/2006 of the European Parliament and the Council of 14 June 2006 on shipments of waste. Official Journal of the European Union L 190, 1–98.

European Parliament and Council, 2003. Directive 2002/96/EC of the European Parliament and of the Council on waste electrical and electronic equipment (WEEE). Official Journal of the European Union L 37, 24–38. doi:10.3000/19770677.L_2012.197.eng

European Parliament and Council, 2000a. Directive 2000/53/EC - End-of-Life Vehicles. Official Journal of the European Communities L 269, 34–42.

European Parliament and Council, 2000b. Directive 2000/76/EC of the European Paliament and of the Council of 4 December 2000 on the incineration of waste. Official Journal of the European Communities L 332, 91–111.

European Parliament and Council, 1999. Council Directive 1999/31/EC. Official Journal of the European Communities L 182, 1–19. doi:10.1039/ap9842100196

European Parliament And The Council, 2008. Directive 2008/1/EC concerning integrated pollution prevention and control (Codified version). Official Journal of the European Union L 24/8, 8–29.

Every, A.G., Sachse, W., 1992. Sensitivity of inversion algorithms for recovering elastic constants of anisotropic solids from longitudinal wavespead data. Ultrasonics 30, 43–48. doi:10.1016/0041-624X(92)90031-G

Every, a. G., Sachse, W., 1990. Determination of the elastic constants of anisotropic solids from acoustic-wave group-velocity measurements. Physical Review B 42, 8196–8205. doi:10.1103/PhysRevB.42.8196

Federal Act, 2015. United States Government – Federal repair cost savings act of 2015 [WWW Document]. URL https://www.congress.gov/bill/114thcongress/%0Asenate-bill/565/text/pl (accessed 8.17.16).

Feraboli, P., Kawakami, H., Wade, B., Gasco, F., Deoto, L., Masini, A., 2012. Recyclability and reutilization of carbon fiber fabric / epoxy composites.

Journal of Composite Materials 46, 1459–1473. doi:10.1177/0021998311420604

Gao, J., Chen, X., Zheng, D., 2010. Remanufacturing oriented adaptive repair system for worn components. 5th International Conference on Responsive Manufacturing - Green Manufacturing (ICRM 2010) 13–18. doi:10.1049/cp.2010.0406

Gholizadeh, S., 2016. A review of non-destructive testing methods of composite materials. Procedia Structural Integrity 1, 50–57. doi:10.1016/j.prostr.2016.02.008

Gieske, J.H., Allred, R.E., 1974. Elastic constants of B-A1 comopsites by ultrasonic velocity measurements. Experimental Mechanics 14, 158–165.

Giuntini, R., Gaudette, K., 2003. Remanufacturing: The next great opportunity for boosting US productivity. Business Horizons 46, 41–48. doi:10.1016/S00076813(03)00087-9

Glavič, P., Lukman, R., 2007. Review of sustainability terms and their definitions. Journal of Cleaner Production 15, 1875–1885. doi:10.1016/j.jclepro.2006.12.006

Go, T., Wahab, D., Rahman, M., Ramli, R., Azhari, C., 2011. Disassemblability of end-of-life vehicle: a critical review of evaluation methods. Journal of Cleaner Production 19, 1536–1546. doi:10.1016/j.jclepro.2011.05.003

Go, T.F., Wahab, D. a., Hishamuddin, H., 2015. Multiple Generation Life-Cycles for Product Sustainability: The Way Forward. Journal of Cleaner Production 95, 16–29. doi:10.1016/j.jclepro.2015.02.065

Gold, L., 1950. Compilation of Body Wave Velocity Data for Cubic and Hexagonal Metals. Journal of Applied Physics 21, 541–546. doi:10.1063/1.1699703

Goodall, P., Rosamond, E., Harding, J., 2014. A review of the state of the art in tools and techniques used to evaluate remanufacturing feasibility. Journal of Cleaner Production 81, 1–15. doi:10.1016/j.jclepro.2014.06.014

Goodship, V. (Ed.), 2010. Management, Recycling and Reuse of Waste Composites. Woodhead Publishing Limited.

Gopalakrishnan, S., Ruzzene, M., Hanagud, S., 2011. Computational Techniques for Structural Health Monitoring, 1st ed. Springer-Verlag London. doi:10.1007/978-0-85729-284-1

Graciet, C., Hosten, B., 1994. Simultaneous measurement of speed, attenuation, thickness and density with reflected ultrasonic waves in plates, in: Ultrasonics Symposium Proceedings. pp. 1219–1222.

Gray, C., Charter, M., 2007. Remanufacturing and product design [WWW Document]. URL http://cfsd.org.uk/Remanufacturing and Product Design.pdf

Gurler, I., 2011. The Analysis and Impact of Remanufacturing Industry Practices. International Journal of Contemporary Economics and Administrative Sciences 1, 25–39.

Hamzaoui-Essoussi, L., Linton, J.D., 2014. Offering branded remanufactured/recycled products: at what price? Journal of Remanufacturing 4, 1–15. doi:10.1186/s13243-014-0009-9

Hashin, Z., 1972. Theory of fiber reinforced materials. (NASA-CR-1974) National Aeronautics and Space Administration, Langley Research Center.

Hazen, B.T., Overstreet, R.E., Jones-Farmer, L.A., Field, H.S., 2012. The role of ambiguity tolerance in consumer perception of remanufactured products. International Journal of Production Economics 135, 781–790. doi:10.1016/j.ijpe.2011.10.011

Heil, J.P., 2011. Study and Analysis of Carbon Fiber Recycling. Raleigh, North Carolina.

Hollman, K.W., Fortunko, C.M., 1998. An accurate method for measurement of transverse elastic-wave velocities. Measurement Science and Technology 9, 1721–1727. doi:10.1088/0957-0233/9/10/012

Hosten, B., 2001. Ultrasonic through-transmission method for measuring the complex stiffness moduli of composite materials, in: Every, A.G., Sachse, W. (Eds.),

Handbook of Elastic Properties of Solids, Liquids and Gases. Academic press, San Diego, pp. 67–86.

Hosten, B., 1991. Reflection and transmission of acoustic plane waves on an immersed orthotropic and viscoelastic solid layer. The Journal of the Acoustical Society of America 89, 2745–2752. doi:10.1121/1.400685

Hosten, B., Baudouin, S., 1995. Ultrasonic Measurements of elastic constants in polymeric matrix/glass fibres composite materials versus temperature. Rev. Prog. Quantitative NDE 14, 1209–1216.

Hosten, B., Castaings, M., 1993a. Validation at lower frequencies of the effective elastic constants measurements for orthotropic composite materials. Rev. Prog. Quantitative NDE 12, 1193–1199.

Hosten, B., Castaings, M., 1993b. Transfer matrix of multilayered absorbing and anisotropic media. Measurements and simulations of ultrasonic wave propagation through composite materials. Acoustical Society of America 94, 1488–1495.

Hosten, B., Deschamps, M., Tittmann, B.R., 1987. Inhomogeneous wave generation and propagation in lossy anisotropic solids application to the characterisation of viscoelastic composite materials. Acoustical Society of America 82, 1763–1770.

Hosten, B., Hutchins, D.A., Schindel, D.W., 1996. Measurement of elastic constants in composite materials using air-coupled ultrasonic bulk waves. Acoustical Society of America 99, 2116–2123. doi:10.1121/1.415398

Howarth, J., Mareddy, S.S.R., Mativenga, P.T., 2014. Energy intensity and environmental analysis of mechanical recycling of carbon fibre composite. Journal of Cleaner Production 81, 46–50. doi:10.1016/j.jclepro.2014.06.023

Ibrahim, M.E., 2014. Nondestructive evaluation of thick-section composites and sandwich structures: A review. Composites Part A: Applied Science and Manufacturing 64, 36–48. doi:10.1016/j.compositesa.2014.04.010

Ijomah, W., 2009. Addressing decision making for remanufacturing operations and design-for-remanufacture. International Journal of Sustainable Engineering 2, 91–202. doi:10.1080/19397030902953080

Ijomah, W., 2002. A model-based definition of the generic remanufacturing business process. Plymouth University. doi:10026.1/601

Ijomah, W., McMahon, C., Hammond, G., Newman, S., 2007. Development of design for remanufacturing guidelines to support sustainable manufacturing. Robotics and Computer-Integrated Manufacturing 23, 712–719. doi:10.1016/j.rcim.2007.02.017

Ijomah, W.L., Childe, S., McMahon, C., 2004. Remanufacturing: a key strategy for sustainable development, in: Proceedings of the 3rd International Conference on Design and Manufacture for Sustainable Development. Cambridge university press. doi:10.1016/j.buildenv.2006.10.027

Ijomah, W.L., Childe, S.J., Hammond, G.P., Mcmahon, C.A., 2005. A robust description and tool for remanufacturing: A resource and energy recovery strategy, in: Proceedings - Fourth International Symposium on Environmentally Conscious Design and Inverse Manufacturing, Eco Design. IEEE, Tokyo, pp. 472–479. doi:10.1109/ECODIM.2005.1619269

Irgens, F., 2008. Continuum Mechanics, 1st ed. Springer-Verlag Berlin Heidelberg.

Jolly, M., Prabhakar, A., Sturzu, B., Hollstein, K., Singh, R., Thomas, S., Foote, P., Shaw, A., 2015. Review of Non-destructive Testing (NDT) Techniques and their Applicability to Thick Walled Composites. Procedia CIRP 38, 129–136. doi:10.1016/j.procir.2015.07.043

Jones, B.R., Stone, D.E.W., 1976. Towards an ultrasonic-attenuation technique to measure void content in carbon-fibre composites. Non-Destructive Testing 9, 71–79. doi:10.1016/0029-1021(76)90004-9

Ke, Q., Zhang, H.-C., Liu, G., Li, B., 2011. Glocalized Solutions for Sustainability in Manufacturing: Proceedings of the 18th CIRP International 437 Conference on Life Cycle Engineering. Springer, Braunschweig, Germany. doi:10.1007/978-3642-19692-8_75

Khor, K., Udin, Z., 2012. Impact of Reverse Logistics Product Disposition towards Business Performance in Malaysian E&E Companies. Journal of Supply Chain and Customer Relationship Management 1–19. doi:10.5171/2012.699469

Kim, K.Y., 1994. Analytic relations between the elastic constants and the group velocity in an arbitrary direction of symmetry planes of media with orthorhombic or higher symmetry. Physical Review B 49, 3713–3724. doi:10.1103/PhysRevB.49.3713

Kim, K.Y., Ohtani, T., Baker, a. R., Sachse, W., 1995. Determination of All Elastic Constants of Orthotropic Plate Specimens from Group Velocity Data. Research in Nondestructive Evaluation 7, 13–29. doi:10.1080/09349849509409563

Kim, K.Y., Sribar, R., Sachse, W., 1995. Analytical and optimization procedures for determination of all elastic constants of anisotropic solids from group velocity data measured in symmetry planes. Journal of Applied Physics 77, 5589–5600. doi:10.1063/1.359201

King, A., Barker, S., 2007. Using The Delphi Technique To Establish A Robust Research Agenda For Remanufacturing, in: 14th CIRP Conference on Life Cycle Engineering. Japan, pp. 219–224.

King, A., Burgess, S., Ijomah, W., Mcmahon, C., 2006. Reducing Waste: Repair, Recondition, Remanufacture or Recycle? Sustainable Development 267, 257–267. doi:10.1002/sd

King, A., Gu, J., 2010. Calculating the environmental benefits of remanufacturing. Proceedings of the ICE - Waste and Resource Management 163, 149–155. doi:10.1680/warm.2010.163.4.149

Kinsler, L., Frey, A., Coppens, A., Sanders, J., 1982. Fundamentals of Acoustics. John Wiley and Sons.

Kothari, C.R., 2004. Research Metholodogy Methods and Tecnhiques, 2nd (revis. ed. New Age International.

Kraus, T., Kühnel, M., 2015. Composites Market Report 2015, Federation of Reinforced Plastics (AVK) and Carbon Composite e.v. (CCeV).

Kriz, R.D., Stinchcomb, W.W., 1979. Elastic moduli of transversely isotropic graphite fibers and their composites. Experimental Mechanics 19, 41–49.

Lavrentyev, A.., Rokhlin, S.I., 1997. Phase correction fo ultrasonic bulk wave measurements of elastic constants in anisotropic materials. Review of Progress in Quantitative Nondestructive Evaluation 16B, 1367–1374.

Ledbetter, H.M., Kriz, R.D., 1982. Elastic Wave Surfaces in Solids. physica status solidi 114, 475–480.

Lewis, A., 2014. Making composite repairs to the 787. Boeing Commercial Magazine Qtr 4, 5–13.

Linder, M., Williander, M., 2015. Circular Business Model Innovation: Inherent Uncertainties. Business Strategy and the Environment, Online prepublished version. doi:10.1002/bse.1906

Lund, R., 1996. The Remanufacturing Industry: Hidden Giant, Boston University press. Boston.

Lund, R., Hauser, W., 2010. An American Perspective, in: 5th International Conference on Responsive Manufacturing - Green Manufacturing. doi:10.1049/cp.2010.0404

Lund, R.T., 1985. Remanufacturing : the experience of the United States and implications for developing countries. World bank technical paper No.31 1– 126.

Marder, M.M., 2011. No TitleResearch Methods for Science, 1st ed. Cambridge University Press.

Markham, M.F., 1970. Measurement of the elastic constants of fibre composites by ultrasonics. Composites 1, 145–149.

Marsh, G., 2009. Carbon recycling: a soluble problem. Reinforced Plastics 53, 2223-27. doi:10.1016/S0034-3617(09)70149-3

Matsumoto, M., Ijomah, W., 2013. Remanufacturing, in: Kauffman, J., Lee, K. (Eds.), Handbook of Sustainable Engineering. pp. 389–408. doi:10.1007/978-1-4020-8939-8

McConnell, V.P., 2010. Launching the carbon fibre recycling industry. Reinforced Plastics 54, 33–37. doi:10.1016/S0034-3617(10)70063-1

Meftah, H., Tamboura, S., Fitoussi, J., BenDaly, H., Tcharkhtchi, A., Compos Mater, A., Tcharkhtchi abbastcharkhtchi, A., 2017. Characterization of a New Fully Recycled Carbon Fiber Reinforced Composite Subjected to High Strain Rate Tension. Applied Composite M. doi:10.1007/s10443-017-9632-6

Meredith, J., Cozien-cazuc, S., Collings, E., Carter, S., Alsop, S., Lever, J., Coles, S.R., Wood, B.M., Kirwan, K., 2012. Recycled carbon fibre for high performance energy absorption. Composites Science and Technology 72, 688–695. doi:10.1016/j.compscitech.2012.01.017

Meyer, L.O., Schulte, K., Grove-Nielsen, E., 2009. CFRP-Recycling Following a Pyrolysis Route: Process Optimization and Potentials. Journal of Composite Materials 43, 1121–1132. doi:10.1177/0021998308097737

Miller, G.F., Musgrave, M.J.P., 1956. On the propagation of elastic waves in aeolotropic media. III. Media of cubic symmetry. Proceddings of the Royal Society 236, 352–383. doi:10.1098/rspa.1956.0142

Morgan, P., 2005. Carbon fibres and thier composites, 1st ed. CRC Press.

Morin, C., Loppinet-Serani, A., Cansell, F., Aymonier, C., 2012. Near- and supercritical solvolysis of carbon fibre reinforced polymers (CFRPs) for recycling carbon fibers as a valuable resource: State of the art. Journal of Supercritical Fluids 66, 232–240. doi:10.1016/j.supflu.2012.02.001

Musgrave, M.J.P., 1954a. On the propagation of elastic waves in aeleotropic media:I General Principals. Proceddings of the Royal Society 226, 339–356. doi:10.1098/rspa.1954.0258

Musgrave, M.J.P., 1954b. On the propagation of elastic waves in aeleotropic media:II media of hexagonal symmetry. Proceddings of the Royal Society 226, 356–366. doi:10.1098/rspa.1954.0259

Nasr, N., Thurston, M., 2006. Remanufacturing : A Key Enabler to Sustainable Product Systems, in: Proceedings of the 13th CIRP International Conference on Life Cycle Engineering. pp. 15–18.

OECD, 2015. Municipal Waste Generation and Treatment [WWW Document]. URL https://stats.oecd.org/Index.aspx?DataSetCode=MUNW# (accessed 5.11.17).

Ogi, K., Nishikawa, T., Okano, Y., Taketa, I., 2007. Mechanical properties of ABS resin reinforced with recycled CFRP. Advanced Composite Materials 16, 181–194. doi:10.1163/156855107780918982

Okayasu, M., Yamazaki, T., Ota, K., Ogi, K., Shiraishi, T., 2013. Mechanical properties and failure characteristics of a recycled CFRP under tensile and cyclic loading. International Journal of Fatigue 55, 257–267. doi:10.1016/j.ijfatigue.2013.07.005

Oliveux, G., Bailleul, J., Gillet, A., Mantaux, O., Leeke, G. a., 2017. Recovery and reuse of discontinuous carbon fi bres by solvolysis : Realignment and properties of remanufactured materials. Composites Science and Technology 139, 99–108. doi:10.1016/j.compscitech.2016.11.001

Oliveux, G., Dandy, L.O., Leeke, G. a., 2015. Current Status of Recycling of Fibre Reinforced Polymers: review of technologies, reuse and resulting properties. Progress in Materials Science 72, 61–99. doi:10.1016/j.pmatsci.2015.01.004

Pain, H., 2005. The physics of vibrations and waves, 6th Editio. ed. John Wiley and Sons.

Parker, D., 2010. Briefing: remanufacturing and reuse – trends and prospects. Proceedings of the ICE - Waste and Resource Management 163, 141–147. doi:10.1680/warm.2010.163.4.141

Paterson, D.A.P., Ijomah, W., Windmill, J., 2016. An analysis of end-of-life terminology in the carbon fiber reinforced plastic industry. International Journal of Sustainable Engineering 9, 130–140. doi:10.1080/19397038.2015.1136361

Paterson, D.A.P., Ijomah, W., Windmill, J., 2015. Carbon fibre reinforced plastic EOL : protecting remanufacturing status and life cycle route analysis, in: International Conference on Remanufacturing. pp. 1753–1759. doi:http://strathprints.strath.ac.uk/53781/

Paterson, D.A.P., Ijomah, W.L., Windmill, J.F.C., 2017. End-of-Life decision tool with emphasis on Remanufacturing. Journal of Cleaner Production 148, 653–664. doi:10.1016/j.jclepro.2017.02.011

Paterson, D.A.P., Ijomah, W.L., Windmill, J.F.C., Kao, C.C., Smilie, G., 2018. Ultrasonic Bulk Wave Measurements on Composites using Fibres from Recycled CFRP. Review of Progress in Quantitative Nondestructive Evaluation AIP Conference Proceedings, vol 1949, 130010. DOI: 10.1063/1.5031605

Paterson, D.A.P., Ijomah, W., Windmill, J., 2018a Elastic constant determination of unidirectional composite via ultrasonic bulk wave through transmission measurements A review. Progress in materials Science. In Press:AAM https://doi.org/10.1016/j.pmatsci.2018.04.001

Pearson, L.H., Murri, W.J., 1987. Measurement of ultrasonic wavespeeds in off-axis directions of composite materials, in: Thompson, D.O., Chimenti, D.E. (Eds.), Review of Progress in Quantitative Nondestructive Evaluation. Springer US, pp. 1093–1101. doi:10.1007/978-1-4613-1893-4_125

Perry, N., Bernard, a., Laroche, F., Pompidou, S., 2012. Improving design for recycling - Application to composites. CIRP Annals - Manufacturing Technology 61, 151–154. doi:10.1016/j.cirp.2012.03.081

Pickering, S.J., 2006. Recycling technologies for thermoset composite materialscurrent status. Composites Part A: Applied Science and Manufacturing 37, 1206–1215. doi:10.1016/j.compositesa.2005.05.030

Pigosso, D., Zanette, E., Filho, A., Ometto, A., Rozenfeld, H., 2010. Ecodesign methods focused on remanufacturing. Journal of Cleaner Production 18, 21–31. doi:10.1016/j.jclepro.2009.09.005

Pimenta, S., Pinho, S., 2012. The effect of recycling on the mechanical response of carbon fibres and their composites. Composite Structures 94, 3669–3684. doi:10.1016/j.compstruct.2012.05.024

Pimenta, S., Pinho, S., 2011. Recycling carbon fibre reinforced polymers for structural applications: Technology review and market outlook. Waste Management 31, 378–392. doi:10.1016/j.wasman.2010.09.019

Pimenta, S., Pinho, S.T., Robinson, P., Wong, K.H., Stephen, J., 2010. Mechanical analysis and toughening mechanisms of a multiphase recycled CFRP. Composites Science and Technology 70, 1713–1725. doi:10.1016/j.compscitech.2010.06.017

Prosser, W.H., 1987. Ultrasonic characterization of the nonlinear elastic properties of unidirectional graphite/epoxy composites, NASA Contractor Report 4100, Nasa Virginia Research Centre.

Rajendra Kumar, C., 2008. Research Methodology, 1st ed. APH Publishing Coporation.

Reddy, S.S.S., Balasubramaniam, K., Krishnamurthy, C. V., Shankar, M., 2005. Ultrasonic goniometry immersion techniques for the measurement of elastic moduli. Composite Structures 67, 3–17. doi:10.1016/j.compstruct.2004.01.008

Reynolds, W.N., 1971. Problems of nondestructive testing in carbon fibres and their composites, in: In International Conference on Carbon Fibres. London, The Plastics institute.

Reynolds, W.N., Wilkinson, S.J., 1978. The analysis of fibre-reinforced porous composite materials by the measurement of ultrasonic wave velocities. Ultrasonics 16, 159–163. doi:10.1016/0041-624X(78)90071-9

Reynolds, W.N., Wilkinson, S.J., 1974. The propagation of ultrasonic waves in CFRP laminates. Ultrasonics 12, 109–114. doi:10.1016/0041-624X(74)90067-5

Ribeiro, J.S., Gomes, J.D.O., 2014. A framework to integrate the end-of-life aircraft in preliminary design, in: 21st CIRP Conference on Life Cycle Engineering. Elsevier B.V., pp. 508–513. doi:10.1016/j.procir.2014.06.077

Rokhlin, S.I., Chimenti, D.E., Nagy, P.B., 2011. Physical Ultrasonics of Composites. Oxford university press.

Rokhlin, S.I., Wang, W., 1992. Double through transmission bulk wave method for ultrasonic phase velocity measurement and determination of elastic constants of composite materials. Acoustical Society of America 91, 3303–3312.

Rokhlin, S.I., Wang, W., 1989a. Ultrasonic evaluation of in-plane and out-of-plane elastic properties of composite materials, in: Thompson, D.O., Chimenti, D.E. (Eds.), Review of Progress in Quantitative Nondestructive Evaluation. Springer US, pp. 1489–1497. doi:10.1007/978-1-4613-0817-1_187

Rokhlin, S.I., Wang, W., 1989b. Critical angle measurement of elastic constants in composite material. The Journal of the Acoustical Society of America 86, 1876–1882. doi:10.1121/1.398566

Rose, J.L., 2014. Ultrasonic guided waves in solid media. Cambridge university press.

Roux, J., 1990. Elastic wave propagation in anisotropic materials. ultrasonics Symposium Proceedings 1065–1073. doi:10.1017/CBO9781107415324.004

Royer, D., Dieulesaint, E., 2000. Elastic Waves in Solids I, 1st ed. Springer-Verlag Berlin Heidelberg.

Roylance, D., 2000. Introduction to composites materials [WWW Document]. URL http://web.mit.edu/course/3/3.11/www/modules/composites.pdf (accessed 8.9.17).

Rybicka, J., Tiwari, A., Leeke, G.A., 2014. Technology readiness level assessment of composites recycling technologies. Journal of Cleaner Production 112, 1001–1012. doi:10.1016/j.jclepro.2015.08.104

Scott, I.G., Scala, C.M., 1982. A review of non-destructive testing of composite materials. NDT International 15, 75–86. doi:10.1016/0308-9126(82)90001-3

Seiner, H., Landa, M., 2004. Sensitivity analysis of an inverse procedure for determination of elastic coefficients for strong anisotropy. Ultrasonics 43, 253– 263. doi:10.1016/j.ultras.2004.07.004

Shi, J., Bao, L., Kemmochi, K., 2014. Low-Velocity Impact Response and Compression After Impact Assessment of Recycled Carbon Fiber-Reinforced Polymer Composites for Future Applications. Polymer Composites 35. doi:10.1002/pc

Shi, J., Bao, L., Kobayashi, R., Kato, J., Kemmochi, K., 2012a. Reusing recycled fibers in high-value fiber-reinforced polymer composites: Improving bending strength by surface cleaning. Composites Science and Technology 72, 1298–1303. doi:10.1016/j.compscitech.2012.05.003

Shi, J., Kemmochi, K., Bao, L.M., 2012b. Research in Recycling Technology of Fiber Reinforced Polymers for Reduction of Environmental Load: Optimum Decomposition Conditions of Carbon Fiber Reinforced Polymers in the Purpose of Fiber Reuse. Advanced Materials Research 343–344, 142–149. doi:10.4028/www.scientific.net/AMR.343-344.142

Shu, L.H., Flowers, W.C., 1999. Application of a design-for-remanufacture framework to the selection of product life-cycle fastening and joining methods.

Robotics and Computer-Integrated Manufacturing 15, 179–190. doi:10.1016/S0736-5845(98)00032-5

Shu, L.H., Flowers, W.C., 1995. Considering Remanufacture and other End-of-Life Options in Selection of Fastening and Joining Methods, in: Electronics and the Environment, 1995. ISEE., Proceedings of the 1995 IEEE International Symposium on. IEEE, pp. 75–80. doi:10.1109/ISEE.1995.514953

Smith-Gillespie, A., Peace, B., Walsh, B., Stewart, D., 2015. Supporting excellence in UK remanufacturing.

Smith, R.E., 1972. Ultrasonic elastic constants of carbon fibers and their composites. Journal of Applied Physics 43, 2555–2561. doi:10.1063/1.1661559

Snudden, J.P., Ward, C., Potter, K., 2014. Reusing automotive composites production waste. Reinforced Plastics 58, 20–27. doi:10.1016/S0034-3617(14)70246-2

Song, Y.S., Youn, J.R., Gutowski, T.G., 2009. Life cycle energy analysis of fiberreinforced composites. Composites Part A: Applied Science and Manufacturing 40, 1257–1265. doi:10.1016/j.compositesa.2009.05.020

Spelman, C., Sheerman, B., 2014. Triple Win: The Social, economic and environmental case for remanufacture, A report by the All-party Parliamentary Sustainable Resource Group and the All-Party Parliamentary Manufacturing Group. United Kingdom.

Stijnman, P.W.A., 1995. Determination of the elastic constants of some composites by using ultrasonic velocity measurements. Composites 26, 597–604. doi:10.1016/0010-4361(95)92624-L

Stone, D.E.W., Clarke, B., 1975. Ultrasonic attenuation as a measure of void content in carbon-fibre reinforced plastics. Non-Destructive Testing 8, 137–145. doi:10.1016/0029-1021(75)90023-7

Summerscales, J. (Ed.), 1990. Non-destructive testing of fibre-reinforced plastics composites, Vol. 2. ed. Elsvier applied science.

Summerscales, J. (Ed.), 1987. Non-destructive testing of fibre-reinforced plastics composites, Vol. 1. ed. Elsvier applied science.

Sundin, E., 2004. Product and process design for successful remanufacturing. Linkoping Univeristy.

Sundin, E., Lindahl, M., Ijomah, W., 2009. Product design for product/service systems. Journal of Manufacturing Technology Management 20, 723–753. doi:http://dx.doi.org/10.1108/17410380910961073

Suzuki, T., Takahashi, J., 2005. Prediction of Energy Intensity of Carbon Fiber Reinforced Plastics for Mass-Produced Passenger Cars. Materials Research Bulletin 14–19.

Tian, X., Liu, T., Wang, Q., Dilmurat, A., Li, D., Ziegmann, G., 2017. Recycling and remanufacturing of 3D printed continuous carbon fi ber reinforced PLA composites. Journal of Cleaner Production 142, 1609–1618. doi:10.1016/j.jclepro.2016.11.139

Trog , A., O"Leary, R.L., Hayward, G., Pethrick, R.A., Mullholland, A.J., 2016. Properties of photocured epoxy resin materials for application in piezoelectric ultrasonic transducer matching layers. Acoustical Society of America 128, 2704–2714. doi:10.1121/1.3483734

Tuttle, M., 2015. Resistive Strain Measurement Devices, in: Kutz, M. (Ed.), Mechanical Engineers" Handbook, Volume 1, Materials and Engineering Mechanics, 4th Edition. John Wiley and Sons, Hobeken, New Jersey, pp. 659–681.

Vergani, L., Colombo, C., Libonati, F., 2014. A review of thermographic techniques for damage investigation in composites. Frattura ed Integrita Strutturale 8, 1–12. doi:10.3221/IGF-ESIS.27.01

Wang, L., Lavrentyev, A.I., Rokhlin, S.I., 2003. Beam and phase effects in anglebeam-through-transmission method of ultrasonic velocity measurement. The Journal of the Acoustical Society of America 113, 1551–1559. doi:10.1121/1.1548151

Watson, M., 2009. A review of literature and research on public attitudes, perceptions and behaviour relating to remanufactured, repaired and reused products.

Wei, S., 2014. Core Acquisition Management in Remanufacturing. Linkoping Univeristy.

Wilkinson, S.J., Reynolds, W.N., 1974. The propagation of ultrasonic waves in carbon-fibre-reinforced plastics. Journal of Physics D: Applied Physics 7, 50–57. doi:10.1088/0022-3727/7/1/313

Winkler, H., 2010. Sustainability through the implementation of sustainable supply chain networks. Int. J. Sustainable Economy 2, 293–309. doi:10.1504/IJSE.2010.033396

Witik, R. a., Teuscher, R., Michaud, V., Ludwig, C., Månson, J.A.E., 2013. Carbon fibre reinforced composite waste: An environmental assessment of recycling, energy recovery and landfilling. Composites Part A: Applied Science and Manufacturing 49, 89–99. doi:10.1016/j.compositesa.2013.02.009

Yang, Y., Boom, R., Irion, B., van Heerden, D.J., Kuiper, P., de Wit, H., 2012. Recycling of composite materials. Chemical Engineering and Processing: Process Intensification 51, 53–68. doi:10.1016/j.cep.2011.09.007

Zimmer, J.E., Cost, J.R., 1970. Determination of the elastic constants of a unidirectional fiber composite using ultrasonic velocity measurements. Acoustical Society of America 47, 795–803.

Zuidwijk, R., Krikke, H., 2008. Strategic response to EEE returns: European Journal of Operational Research 191, 1206–1222. doi:10.1016/j.ejor.2007.08.004

Appendix 1: Supplementary mathematical verification

Note that in this appendix equation numbering and figure numbering is listed independently of the thesis chapters - this to eliminate any confusion between this appendix and the chapters. If an equation or figure from the chapters is cited, it is clearly done so with italics.

1.1 Simplifying equation (9)

Equation (9) rewritten now as equation (67)

$$\Delta'(\vec{P},t) = dQ^2(\vec{P},t) - dP^2 \qquad (67)$$

Turning equation (67) into a far more user friendly equation is done through by expressing dQ(**P**,t) - the infinitesimal change in Q arising from the infinitesimal change in P - in terms of the particle displacement scalar u**.** This is done so by first rewriting equation (1) in differential form and solving for dQ(**P**,t), given as equation (68).

$$dQ(\vec{P},t) = du(\vec{P},t) + dP \qquad (68)$$

In equation (6) the vector form of the differential displacement d**u** is outlined, and so the scalar form for the x, y and z components of equation (6), *(from chapter 6)*, may be given by equation (69),

$$du_x(\vec{P},t) = \frac{\partial u_x(\vec{P},t)}{\partial P_x}dP_x + \frac{\partial u_x(\vec{P},t)}{\partial P_y}dP_y + \frac{\partial u_x(\vec{P},t)}{\partial P_z}dP_z$$

$$du_y(\vec{P},t) = \frac{\partial u_y(\vec{P},t)}{\partial P_x}dP_x + \frac{\partial u_y(\vec{P},t)}{\partial P_y}dP_y + \frac{\partial u_y(\vec{P},t)}{\partial P_z}dP_z$$

$$du_z(\vec{P},t) = \frac{\partial u_z(\vec{P},t)}{\partial P_x}dP_x + \frac{\partial u_z(\vec{P},t)}{\partial P_y}dP_y + \frac{\partial u_z(\vec{P},t)}{\partial P_z}dP_z \qquad (69)$$

To solve for Δ‟, it is first required to Solve for $dQ^2(\mathbf{P},t)$ which may be done so by considering three manageable sections of dQ, i.e., dQ_x, dQ_y and dQ_z. Once solved, the terms may be grouped together and equation (67), the deformation, may be realised.

$$dQ_x^2(\vec{P},t) = {dP_x}^2 + 2\left(dP_x\left(\frac{\partial u_x(\vec{P},t)}{\partial P_x}dP_x + \frac{\partial u_x(\vec{P},t)}{\partial P_y}dP_y + \frac{\partial u_x(\vec{P},t)}{\partial P_z}dP_z\right)\right) + Q'x \qquad (70)$$

$$dQ_y^2(\vec{P},t) = {dP_y}^2 + 2\left(dP_y\left(\frac{\partial u_y(\vec{P},t)}{\partial P_x}dP_x + \frac{\partial u_y(\vec{P},t)}{\partial P_y}dP_y + \frac{\partial u_y(\vec{P},t)}{\partial P_z}dP_z\right)\right) + Q'y \qquad (71)$$

$$dQ_z^2(\vec{P},t) = {dP_z}^2 + 2\left(dP_z\left(\frac{\partial u_z(\vec{P},t)}{\partial P_x}dP_x + \frac{\partial u_z(\vec{P},t)}{\partial P_y}dP_y + \frac{\partial u_z(\vec{P},t)}{\partial P_z}dP_z\right)\right) + Q'y \qquad (72)$$

With $Q'x$ equal to,

$$\begin{aligned} Q'x = \Bigg(& \left(\frac{\partial u_x(\vec{P},t)}{\partial P_x}dP_x\right)^2 + \frac{\partial u_x(\vec{P},t)}{\partial P_x}\frac{\partial u_x(\vec{P},t)}{\partial P_y}dP_xdP_y + \frac{\partial u_x(\vec{P},t)}{\partial P_x}\frac{\partial u_x(\vec{P},t)}{\partial P_z}dP_xdP_z \\ & + \frac{\partial u_x(\vec{P},t)}{\partial P_y}\frac{\partial u_x(\vec{P},t)}{\partial P_x}dP_ydP_x + \left(\frac{\partial u_x(\vec{P},t)}{\partial P_y}dP_y\right)^2 + \frac{\partial u_x(\vec{P},t)}{\partial P_y}\frac{\partial u_x(\vec{P},t)}{\partial P_z}dP_ydP_z \\ & \frac{\partial u_x(\vec{P},t)}{\partial P_z}\frac{\partial u_x(\vec{P},t)}{\partial P_x}dP_zdP_x + \frac{\partial u_x(\vec{P},t)}{\partial P_z}\frac{\partial u_x(\vec{P},t)}{\partial P_y}dP_zdP_y + \left(\frac{\partial u_x(\vec{P},t)}{\partial P_z}dP_z\right)^2\Bigg) \end{aligned}$$

and $Q'y$ and $Q'z$ equal to $Q'x$ with all $\partial u_x(\vec{P},t)$ changed to $\partial u_y(\vec{P},t)$ and $\partial u_z(\vec{P},t)$ respectively.

Grouping, respective terms together and solving equation (1) for Δ‟ gives,

$$\Delta'(\vec{P},t) = dQ^2(\vec{P},t) - dP^2 =$$

$$\left(2\frac{\partial u_x(\vec{P},t)}{\partial P_x} + \left(\frac{\partial u_x(\vec{P},t)}{\partial P_x}\right)^2 + \left(\frac{\partial u_y(\vec{P},t)}{\partial P_x}\right)^2 + \left(\frac{\partial u_z(\vec{P},t)}{\partial P_x}\right)^2\right){dP_x}^2 \qquad (a)$$

$$+$$

$$\left(2\frac{\partial u_y(\vec{P},t)}{\partial P_y} + \left(\frac{\partial u_x(\vec{P},t)}{\partial P_y}\right)^2 + \left(\frac{\partial u_y(\vec{P},t)}{\partial P_y}\right)^2 + \left(\frac{\partial u_z(\vec{P},t)}{\partial P_y}\right)^2\right){dP_y}^2 \qquad (b)$$

$$\left(2\frac{\partial u_z(\vec{P},t)}{\partial P_z} + \left(\frac{\partial u_x(\vec{P},t)}{\partial P_z}\right)^2 + \left(\frac{\partial u_y(\vec{P},t)}{\partial P_z}\right)^2 + \left(\frac{\partial u_z(\vec{P},t)}{\partial P_z}\right)^2\right){dP_z}^2 \qquad (c)$$

$$+$$

$$2\left(\frac{\partial u_x(\vec{P},t)}{\partial P_x}\frac{\partial u_x(\vec{P},t)}{\partial P_y}+\frac{\partial u_y(\vec{P},t)}{\partial P_x}\frac{\partial u_y(\vec{P},t)}{\partial P_y}+\frac{\partial u_z(\vec{P},t)}{\partial P_x}\frac{\partial u_z(\vec{P},t)}{\partial P_y}+\frac{\partial u_x(\vec{P},t)}{\partial P_y}+\frac{\partial u_y(\vec{P},t)}{\partial P_x}\right)dP_x dP_y \quad (d)$$

$$+$$

$$2\left(\frac{\partial u_x(\vec{P},t)}{\partial P_x}\frac{\partial u_x(\vec{P},t)}{\partial P_z}+\frac{\partial u_y(\vec{P},t)}{\partial P_x}\frac{\partial u_y(\vec{P},t)}{\partial P_z}+\frac{\partial u_z(\vec{P},t)}{\partial P_x}\frac{\partial u_z(\vec{P},t)}{\partial P_z}+\frac{\partial u_x(\vec{P},t)}{\partial P_z}+\frac{\partial u_z(\vec{P},t)}{\partial P_x}\right)dP_x dP_z \quad (e)$$

$$+$$

$$2\left(\frac{\partial u_x(\vec{P},t)}{\partial P_y}\frac{\partial u_x(\vec{P},t)}{\partial P_z}+\frac{\partial u_y(\vec{P},t)}{\partial P_y}\frac{\partial u_y(\vec{P},t)}{\partial P_z}+\frac{\partial u_z(\vec{P},t)}{\partial P_y}\frac{\partial u_z(\vec{P},t)}{\partial P_z}+\frac{\partial u_y(\vec{P},t)}{\partial P_z}+\frac{\partial u_z(\vec{P},t)}{\partial P_y}\right)dP_y dP_z \quad (f)$$

All of which is able to be expressed in more manageable matrix notation,

$$2\left((dP_x \quad dP_y \quad dP_z)\begin{pmatrix}\varepsilon_{xx} & \varepsilon_{xy} & \varepsilon_{xz}\\ \varepsilon_{yx} & \varepsilon_{yy} & \varepsilon_{yz}\\ \varepsilon_{zx} & \varepsilon_{zy} & \varepsilon_{zz}\end{pmatrix}\begin{pmatrix}dP_x\\ dP_y\\ dP_z\end{pmatrix}\right) \qquad (73)$$

Noting a symmetric ε matrix, ε_{ij} may be equated to the bracketed terms in $(a)-(f)$ and given by,

$$\varepsilon_{ij}(\vec{P},t)=\frac{1}{2}\left(\frac{\partial u_i(\vec{P},t)}{\partial P_j}+\frac{\partial u_j(\vec{P},t)}{\partial P_i}+\frac{\partial u_k(\vec{P},t)}{\partial P_i}\frac{\partial u_k(\vec{P},t)}{\partial P_j}\right) \qquad (74)$$

$$for\ i,j,k=x,y,z$$

Noting here that the convention within academia is to perform a summation over any repeated subscripts which appear solely on the right hand side of the equation, in this instance, k. Attention may be drawn to appendix 1.1.1 for additional clarity of matrix notation and abbreviated subscripts notation.

Using the contracted notation in equation (9), the global measure of deformation, equation (67), is now able to be expressed in terms of particle displacement, in a concise mathematical way.

$$\Delta'(\vec{P},t)=\ dQ^2(\vec{P},t)-\ dP^2=\ 2\varepsilon_{ij}(\vec{P},t)dP_i dP_j \qquad (75)$$

1.1.1 Matrix notation and abbreviated subscript notation

Matrix notation is convenient to allow for long and complex mathematical equations to be expressed in a more desirable format. Once the matrices‟ are multiplied out, the

equation will return to its pre matrix state. The process of matrix multiplication for equation (7) is given below,

$$2\left((dP_x \quad dP_y \quad dP_z)\begin{pmatrix}\varepsilon_{xx} & \varepsilon_{xy} & \varepsilon_{xz}\\ \varepsilon_{yx} & \varepsilon_{yy} & \varepsilon_{yz}\\ \varepsilon_{zx} & \varepsilon_{zy} & \varepsilon_{zz}\end{pmatrix}\begin{pmatrix}dP_x\\ dP_y\\ dP_z\end{pmatrix}\right) \qquad (7)$$

Noting that

$$\begin{pmatrix}\varepsilon_{xx} & \varepsilon_{xy} & \varepsilon_{xz}\\ \varepsilon_{yx} & \varepsilon_{yy} & \varepsilon_{yz}\\ \varepsilon_{zx} & \varepsilon_{zy} & \varepsilon_{zz}\end{pmatrix}\begin{pmatrix}dP_x\\ dP_y\\ dP_z\end{pmatrix}$$

Is equal to

$$\begin{pmatrix}\varepsilon_{xx}dP_x+\varepsilon_{xy}dP_y+\varepsilon_{xz}dP_z\\ \varepsilon_{yx}dP_x+\varepsilon_{yy}dP_y+\varepsilon_{yz}dP_z\\ \varepsilon_{xz}dP_x+\varepsilon_{yz}dP_y+\varepsilon_{zz}dP_z\end{pmatrix}$$

Equation (7) becomes,

$$2(dP_x \quad dP_y \quad dP_z)\begin{pmatrix}\varepsilon_{xx}dP_x+\varepsilon_{xy}dP_y+\varepsilon_{xz}dP_z\\ \varepsilon_{yx}dP_x+\varepsilon_{yy}dP_y+\varepsilon_{yz}dP_z\\ \varepsilon_{xz}dP_x+\varepsilon_{yz}dP_y+\varepsilon_{zz}dP_z\end{pmatrix}$$

Further,

$$(A \quad B \quad C)\begin{pmatrix}X\\ Y\\ Z\end{pmatrix}$$

Is given by,

$$A\cdot X + B\cdot Y + C\cdot Z$$

And so,

$$2(dP_x \quad dP_y \quad dP_z)\begin{pmatrix}\varepsilon_{xx}dP_x+\varepsilon_{xy}dP_y+\varepsilon_{xz}dP_z\\ \varepsilon_{yx}dP_x+\varepsilon_{yy}dP_y+\varepsilon_{yz}dP_z\\ \varepsilon_{xz}dP_x+\varepsilon_{yz}dP_y+\varepsilon_{zz}dP_z\end{pmatrix}$$

May be expressed as,

$$2\varepsilon_{xx}{dP_x}^2 + 2\varepsilon_{yy}{dP_y}^2 + 2\varepsilon_{zz}{dP_z}^2 + 2\left(\varepsilon_{xy}+\varepsilon_{yx}\right)dP_x dP_y$$

$$+$$

$$2(\varepsilon_{xz}+\varepsilon_{zx})dP_x dP_z + 2\left(\varepsilon_{yz}+\varepsilon_{zy}\right)dP_y dP_z$$

With ε_{ij} having already been documented previously in equation 8, abbreviated subscripts are now given more clarity. An example variable is calculated using equation (8),

$$\varepsilon_{ij}(\vec{P},t) = \frac{1}{2}\left(\frac{\partial u_i(\vec{P},t)}{\partial P_j} + \frac{\partial u_j(\vec{P},t)}{\partial P_i} + \frac{\partial u_k(\vec{P},t)}{\partial P_i}\frac{\partial u_k(\vec{P},t)}{\partial P_j}\right) \qquad (8)$$

ε_{yz} is given as,

$$\left(\frac{\partial u_y(\vec{P},t)}{\partial P_z} + \frac{\partial u_z(\vec{P},t)}{\partial P_y} + \frac{\partial u_x(\vec{P},t)}{\partial P_y}\frac{\partial u_x(\vec{P},t)}{\partial P_z} + \frac{\partial u_y(\vec{P},t)}{\partial P_y}\frac{\partial u_y(\vec{P},t)}{\partial P_z} + \frac{\partial u_z(\vec{P},t)}{\partial P_y}\frac{\partial u_z(\vec{P},t)}{\partial P_z}\right)$$

Noting that ε_{zy} is identical then $\varepsilon_{yz} + \varepsilon_{zy}$ is given as,

$$\left(\frac{\partial u_x(\vec{P},t)}{\partial P_y}\frac{\partial u_x(\vec{P},t)}{\partial P_z} + \frac{\partial u_y(\vec{P},t)}{\partial P_y}\frac{\partial u_y(\vec{P},t)}{\partial P_z} + \frac{\partial u_z(\vec{P},t)}{\partial P_y}\frac{\partial u_z(\vec{P},t)}{\partial P_z} + \frac{\partial u_y(\vec{P},t)}{\partial P_z} + \frac{\partial u_z(\vec{P},t)}{\partial P_y}\right)$$

Which is equal to the bracketed term corresponding to selection (f) in 4.1.

1.2 Derivation of strain equations

In the case of normal strain, this is evidenced as follows. Considering *Figure 18 (from chapter 6)*, particle a and particle b, and the distance between them, ΔP, may be redrawn as Figure 55,

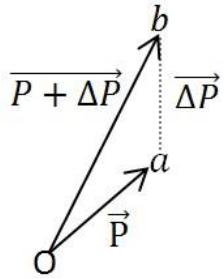

Figure 55 – Position vector from origin to particle a and particle b, with the distance between equal to

Now for a lateral displacement in the x direction only, as evidence by particle displacement vector, **u**, particle a moves to a‟ and particle b moves to b‟, this action is shown in Figure 56,

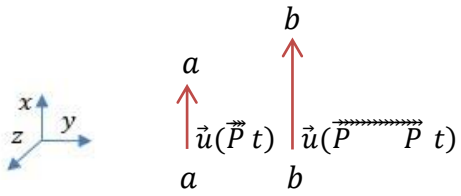

Figure 56 _ Displacement of particles a and b from equilibrium, documenting relative particle displacement in x direction only

For a rigid translation, the distance between a‟ and b‟ will be the same as the distance between a and b and therefore d**u** will equal zero, as per the principle outlined using *Figure 19.* However, in this case deformation in the x direction has occurred and so the difference between a‟ and b‟ will not equal the distance between a and b, ΔP. Thus, knowing that normal strain is equal to change in length over reference length, normal strain may be considered as

$$\frac{Change\ in\ length}{Reference\ length} = \frac{\vec{u}(\overrightarrow{P+\Delta P}, t) - \vec{u}(\vec{P}, t)}{\overrightarrow{\Delta P}} \qquad (76)$$

Noting that **u** is of course a function of x, y and z, as given by equation (77),

$$\vec{u}(\vec{P}, t) = \hat{x}u_x(\vec{P}, t) + \hat{y}u_y(\vec{P}, t) + \hat{z}u_z(\vec{P}, t) \qquad (77)$$

And that **P** is of course a function of x, y and z, then for a normal strain in the x direction only, i.e. **P** + Δ**P** only differs from **P** in that only a change in $\mathbf{P}_x$ is recorded, the right hand side of equation (77) may be rewritten as,

$$\left(\frac{u_x(P_x + \Delta P_x, P_y, P_z, t) - u_x(P_x, P_y, P_z, t)}{\Delta P_x}\right)\hat{x}$$

$$+$$

$$\left(\frac{u_y(P_x + \Delta P_x, P_y, P_z, t) - u_y(P_x, P_y, P_z, t)}{\Delta P_x}\right)\hat{y}$$

$$+$$

$$\left(\frac{u_z(P_x + \Delta P_x, P_y, P_z, t) - u_z(P_x, P_y, P_z, t)}{\Delta P_x}\right)\hat{z}$$

However, for a normal strain in the x direction only, both u_y and u_z will equal zero. thus equation (77) may then be written as equation (78).

$$\varepsilon_{xx} = \frac{Change\ in\ length}{Reference\ length} = \left(\frac{u_x(P_x + \Delta P_x, P_y, P_z, t) - u_x(\vec{P}, t)}{\Delta P_x}\right) \qquad (78)$$

Noting that in equation (78), the unit vector notation is dropped with the variable ε_{xx}, which means an x extension along x, being used to identify the x normal strain. It is also the case that equation (78) defines the average strain; however, the point strain defines strain in terms of particle displacement vector, **u**, at a given point.

This is found by taking the limit with, the distance, between two particles, going towards zero. That is,

$$\varepsilon_{xx} = \lim_{\Delta P_x \to 0}\left(\frac{u_x(P_x + \Delta P_x, P_y, P_z, t) - u_x(\vec{P}, t)}{\Delta P_x}\right) \qquad (79)$$

With this limit of P going towards zero, looking closer at equation (79), it can be seen that this equation is actually the fundamental equation of a partial derivative; in this case, **u** being a function of **P** (ignoring a dependency on time, t i.e. taking derivative at constant time), equation (79) may be rewritten as equation (80),

$$\varepsilon_{xx} = \frac{\partial u_x}{\partial P_x} \qquad (80)$$

Note additionally, that the same argument holds for normal strain in the y direction and normal strain in the z direction. That is,

$$\varepsilon_{yy} = \frac{\partial u_y}{\partial P_y} \qquad \varepsilon_{zz} = \frac{\partial u_z}{\partial P_z} \qquad (81)$$

Considering now, shear strain, initially consider Figure 57, which documents an arrangement of four particles at equilibrium position.

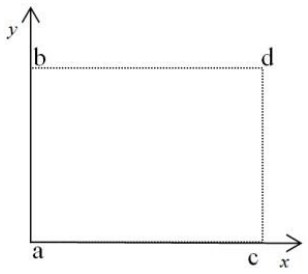

Figure 57 – Outlining 4 particles a, b, c and d which are all at equilibrium position

Examine now, an x, y shear strain as shown Figure 58, noting that $\mathbf{u}_y$ and $\mathbf{u}_x$ are not equal.

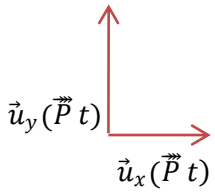

Figure 58 - Documenting position vectors arising from particle displacement, noting that length of vector is not equated to magnitude in this instance.

If the particles in Figure 57 are subjected to the type of shear strain shown in Figure 58, then deformation will arise. Figure 59 documents a case of resulting deformation with the deformed arrangement superimposed onto the equilibrium case.

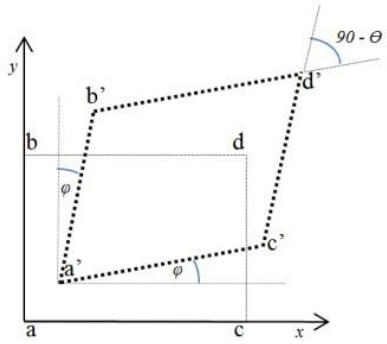

Figure 59 – Deformed particle arrangement, a‟, b‟, c‟ and d‟, is superimposed onto the equilibrium case. The reduction in angle between x and y axis, θ, is the defined as the shear strain, noting that φ is defined as $\theta/2$.

Noting that shear strain, is the reduction in angle between orthogonal axes, in this case, θ, with φ equal to$\theta/2$ then, θ is equal to,

$$\theta = \varphi_1 + \varphi_2 \qquad (82)$$

Isolating particle a, a‟, c and c‟ from Figure 59, and denoting the distance between particle a and particle c as $\Delta\mathbf{P}$, with the distance between a and (not shown) origin being **P** as in Figure 17 *(chapter 6)*, and noting that the displacement between particle a‟ and c‟, has both a vertical and horizontal component, then the tangent of φ_1 may be realised, this is given as follows;

Examining first the vertical displacement, consider Figure 60, which ignores the horizontal part of displacement vector, therefore a‟ and c‟ projection onto the x axis may be thought of as the original positions of these particles.

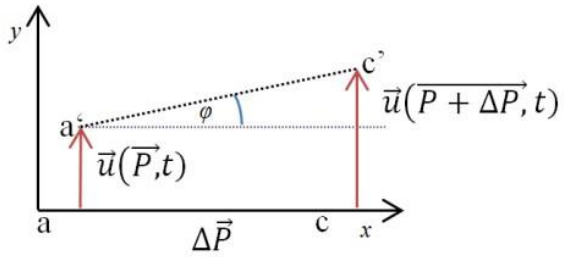

Figure 60 – Documenting the vertical displacement vector between particle a and particle c. The horizontal part of displacement vector has in this example been ignored.

From Figure 60, the length of the side opposite the angle, φ, is therefore equal to Δ**u**(**P**,t), noting that there is only displacement in the y direction and only change, ΔP_x, is recorded then using the same argument that led to equation (76) then the length may be expressed as,

$$u_y(P_x + \Delta P_x, P_y, P_z, t) - u_y(P_x, P_y, P_z, t)$$

Noting again that as the requirement is length (scalar value) and not position then the unit vector notation may be dropped.

Considering now the horizontal part of the displacement vector, the original distance between both vectors is Δ**P**, however, when the vertical displacement is ignored only displacement in the x direction is recorded, that is, Δ**P**, will become solely, $\Delta P_x\hat{x}$, and so, the length of the side adjacent to angle φ is equal to ΔP_x + any changes along x. Noting again the unit vector notation has been dropped. Thus, the tangent of angle φ is equal to

$$\text{Tangent } \varphi = \frac{oppostite}{adjacent} = \frac{u_y(P_x + \Delta P_x, P_y, P_z, t) - u_y(P_x, P_y, P_z, t)}{\Delta P_x + (\Delta P_{x(a' \text{and } c')})} \qquad (83)$$

Noting however, for small displacement, ΔP_x will be significantly larger than any change in x arising from displacement between a‟ and c‟ and so the denominator may be regarded as ΔP_x, further, under small deviation conditions the tangent of φ will be approximately equal to just φ, thus, equation (83) may be written as equation (84)

$$\varphi = \frac{u_y(P_x + \Delta P_x, P_y, P_z, t) - u_y(P_x, P_y, P_z, t)}{\Delta P_x} \qquad (84)$$

Following a similar argument allows for the other angle to be evaluated, which is given as equation (85),

$$\varphi = \frac{u_x(P_x, P_y + \Delta P_y, P_z, t) - u_x(P_x, P_y, P_z, t)}{\Delta P_y} \qquad (85)$$

Thus the total angle, θ, and therefore total average shear may be found through equation (86),

$$\theta = \frac{u_y(P_x + \Delta P_x, P_y, P_z, t) - u_y(P_x, P_y, P_z, t)}{\Delta P_x} + \frac{u_x(P_x, P_y + \Delta P_y, P_z, t) - u_x(P_x, P_y, P_z, t)}{\Delta P_y} \qquad (86)$$

Similar to equation (79), the point strain, is therefore found by reducing distance between particles to zero, upon rewriting the numerator of equation (86) in more compact form, the point strain may be given as equation (87),

$$\gamma_{xy} = \lim_{\Delta P_x \to 0, \Delta P_y \to 0} \left(\frac{\Delta u_y(\vec{P}, t)}{\Delta P_x} + \frac{\Delta u_x(\vec{P}, t)}{\Delta P_y} \right) \qquad (87)$$

Which gives

$$\gamma_{xy} = \frac{\partial u_x}{\partial P_y} + \frac{\partial u_y}{\partial P_x} \qquad (88)$$

Noting that switching the x and y‟s from equation (88) does not alter it and so,

$$\gamma_{xy} = \gamma_{yx}$$

Similar arguments hold for the remaining shear strains,

$$\gamma_{xz} = \gamma_{zx} = \frac{\partial u_x}{\partial P_z} + \frac{\partial u_z}{\partial P_x} \ , \quad \gamma_{yz} = \gamma_{zy} = \frac{\partial u_y}{\partial P_z} + \frac{\partial u_z}{\partial P_y} \qquad (89)$$

All strain elements having now been documented, relating these elements to equation (11) *form chapter 6*, given here as equation (90), i.e.

$$\varepsilon_{ij}(\vec{P}, t) = \frac{1}{2} \left(\frac{\partial u_i(\vec{P}, t)}{\partial P_j} + \frac{\partial u_j(\vec{P}, t)}{\partial P_i} + \frac{\partial u_k(\vec{P}, t)}{\partial P_i} \frac{\partial u_k(\vec{P}, t)}{\partial P_j} \right) \qquad (90)$$

requires two remaining aspects to be discussed; the difference between engineering strain and shearing strain (also called tensor strain) and also linearized assumptions. Looking first at engineering strain and shearing strain; it can be said that equations (88) and (89) describe engineering strain, thus engineering strain describes the total reduction in angle between two sets of orthogonal axes. Shearing strain or tensor strain, is considered to be the average of the angles φ_1 and φ_2, that is,

$$\frac{\varphi_1 + \varphi_2}{2}$$

Thus, shearing strain may be thought of half the engineering strain. In the elastic theory of solids discipline, shearing strains are often preferred over engineering strains. Looking now at linearized assumptions, for small particle deviation the quadratic terms in equation (90) are significantly smaller than the non-quadratic terms and so equation (90) may be written as equation (91)

$$\varepsilon_{ij}(\vec{P},t)=\frac{1}{2}\left(\frac{\partial u_i(\vec{P},t)}{\partial P_j}+\frac{\partial u_j(\vec{P},t)}{\partial P_i}\right) \qquad (91)$$

Further, with i and j being equal to x, y and z, all strain elements are able to be expressed compactly as equation (92), which is regarded as a tensor, noting that for the remainder of this thesis a tensor quantity is always given in bold.

$$[\boldsymbol{\varepsilon}]=\begin{bmatrix} \frac{\partial u_x}{\partial P_x} & \frac{1}{2}\left(\frac{\partial u_x}{\partial P_y}+\frac{\partial u_y}{\partial P_x}\right) & \frac{1}{2}\left(\frac{\partial u_x}{\partial P_z}+\frac{\partial u_z}{\partial P_x}\right) \\ \frac{1}{2}\left(\frac{\partial u_x}{\partial P_y}+\frac{\partial u_y}{\partial P_x}\right) & \frac{\partial u_y}{\partial P_y} & \frac{1}{2}\left(\frac{\partial u_y}{\partial P_z}+\frac{\partial u_z}{\partial P_y}\right) \\ \frac{1}{2}\left(\frac{\partial u_x}{\partial P_z}+\frac{\partial u_z}{\partial P_x}\right) & \frac{1}{2}\left(\frac{\partial u_y}{\partial P_z}+\frac{\partial u_z}{\partial P_y}\right) & \frac{\partial u_z}{\partial P_z} \end{bmatrix} \qquad (92)$$

Further, the relationship given below as equation (93) also holds true.

$$[\boldsymbol{\varepsilon}]=\begin{bmatrix} \frac{\partial u_x}{\partial P_x} & \frac{1}{2}\left(\frac{\partial u_x}{\partial P_y}+\frac{\partial u_y}{\partial P_x}\right) & \frac{1}{2}\left(\frac{\partial u_x}{\partial P_z}+\frac{\partial u_z}{\partial P_x}\right) \\ \frac{1}{2}\left(\frac{\partial u_x}{\partial P_y}+\frac{\partial u_y}{\partial P_x}\right) & \frac{\partial u_y}{\partial P_y} & \frac{1}{2}\left(\frac{\partial u_y}{\partial P_z}+\frac{\partial u_z}{\partial P_y}\right) \\ \frac{1}{2}\left(\frac{\partial u_x}{\partial P_z}+\frac{\partial u_z}{\partial P_x}\right) & \frac{1}{2}\left(\frac{\partial u_y}{\partial P_z}+\frac{\partial u_z}{\partial P_y}\right) & \frac{\partial u_z}{\partial P_z} \end{bmatrix}=\begin{bmatrix} \varepsilon_{xx} & \varepsilon_{xy} & \varepsilon_{xz} \\ \varepsilon_{xy} & \varepsilon_{yy} & \varepsilon_{yz} \\ \varepsilon_{xz} & \varepsilon_{yz} & \varepsilon_{zz} \end{bmatrix} \qquad (93)$$

1.3 Derivation of general stress equations

The general form of the traction force stress relationship stems from considering the traction forces applied to a face not necessarily solely facing the x, y, or z axis, i.e. a

face with a normal vector encompassing more than one directional (x, y or z) component. A standard tetrahedron based argument is now given, consider Figure 61.

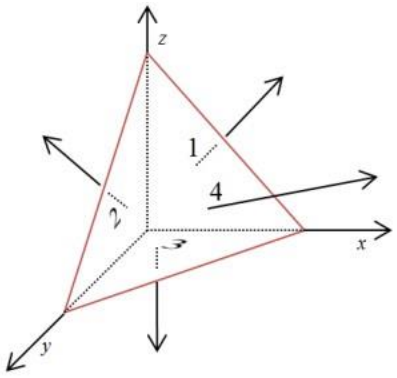

Figure 61 - Tetrahedron, with sides 1, 2, 3 and 4 having on outward traction force impacting on a neighbouring volume element (not shown in dependence. figure). The outward normal of side 4 has x, y and z

Figure 61 documents a tetrahedron with sides 1, 2 and 3 facing the x, y and z direction as in *Figure 21* (*from chapter 6*). The tetrahedron has another side, side 4, which faces an outward direction noting that this side has a normal vector with x, y and z components. The vector direction for this outward face be given as $\vec{n}$and the unit vector may be considered as, $\hat{n}$**,** further, anticipating the forthcoming derivation, the areas of sides 1, 2, 3 and 4 may be given by a1, a2, a3 and a4.

If Figure 61 is considered to be in static equilibrium then the forces on the outer face of the tetrahedron must be in equilibrium, and so for the traction forces given by equations

$$\overrightarrow{T_x} = \sigma_{xx}\hat{x} + \sigma_{yx}\hat{y} + \sigma_{zx}\hat{z} \quad (94)$$

$$\overrightarrow{T_y} = \sigma_{xy}\hat{x} + \sigma_{yy}\hat{y} + \sigma_{zy}\hat{z} \quad (95)$$

$$\overrightarrow{T_z} = \sigma_{xz}\hat{x} + \sigma_{yz}\hat{y} + \sigma_{zz}\hat{z} \quad (96)$$

and the traction force on surface 4 (the outward surface) being given as $\overrightarrow{T_n}$ then equation (97) is presented.

$$\vec{F} = \overrightarrow{T_n}a4 - \overrightarrow{T_x}a1 - \overrightarrow{T_y}a2 - \overrightarrow{T_z}a3 = 0 \qquad (97)$$

Noting that faces 1, 2, 3 face the negative x, y and z direction and so for static equilibrium the traction force must oppose traction force for the inward 1, 2 and 3 faces which face the positive x, y and z direction. Noting additionally, that the traction force is force per unit area and so for total force, the areas, a1, a2, a3 and a4 are required.

Inserting equation (97) into Newton‟s second law, gives equation (98)

$$\vec{F} = \overrightarrow{T_n}a4 - \overrightarrow{T_x}a1 - \overrightarrow{T_y}a2 - \overrightarrow{T_z}a3 = m\vec{a} \qquad (98)$$

It is also the case that areas, 1, 2, and 3 may be expressed as the respective component of unit normal vector, $\hat{n}$, multiplied by a4, or, put another way; areas 1, 2, and 3 are equal to the area a4 projected onto it. Thus, equation (98) may be written as equation (99),

$$\overrightarrow{T_n}a4 - \overrightarrow{T_x}n_x a4 - \overrightarrow{T_y}n_y a4 - \overrightarrow{T_z}n_z a4 = m\vec{a} \qquad (99)$$

Noting that the mass is volume multiplied by density then forcing the tetrahedron to become infinitesimal, so as to allow for traction force stress relationship at a point to be evaluated, is performed by inserting a limit where the volume tends to zero, i.e.,

$$\lim_{V\to 0}\left(\overrightarrow{T_n}a4 - \overrightarrow{T_x}n_x a4 - \overrightarrow{T_y}n_y a4 - \overrightarrow{T_z}n_z a4 = \rho V\vec{a}\ \right) \quad (100)$$

Thus, upon evaluation and rearranging equation (100) may be given as

$$\overrightarrow{T_n}a4 = \overrightarrow{T_x}n_x a4 + \overrightarrow{T_y}n_y a4 + \overrightarrow{T_z}n_z a4$$

Further, upon noticing that the area, a4, is now effectively a constant scalar multiplier across the whole equation it may be omitted and so equation (101) is given to express the point traction force stress relationship,

$$\overrightarrow{T_n} = \overrightarrow{T_x}n_x + \overrightarrow{T_y}n_y + \overrightarrow{T_z}n_z \qquad (101)$$

Note that $\overrightarrow{T_x}, \overrightarrow{T_y}, \overrightarrow{T_z}$ were defined earlier by equations (94-96), thus equation (101) may be expanded that is,

$$\overrightarrow{T_n} = \left(\sigma_{xx}\hat{x} + \sigma_{yx}\hat{y} + \sigma_{zx}\hat{z}\right)n_x + \left(\sigma_{xy}\hat{x} + \sigma_{yy}\hat{y} + \sigma_{zy}\hat{z}\right)n_y + \left(\sigma_{xz}\hat{x} + \sigma_{yz}\hat{y} + \sigma_{zz}\hat{z}\right)n_z \qquad (102)$$

Now grouping together the x, y and z directed forces and allowing these to equal $\overrightarrow{T_{in}}$ (where i may be x, y or z) gives

$$\overrightarrow{T_{xn}} = (\sigma_{xx}n_x + \sigma_{xy}n_y + \sigma_{xz}n_z)\hat{x} \qquad (103)$$

$$\overrightarrow{T_{yn}} = (\sigma_{yx}n_x + \sigma_{yy}n_y + \sigma_{yz}n_z)\hat{y} \qquad (104)$$

$$\overrightarrow{T_{zn}} = (\sigma_{zx}n_x + \sigma_{zy}n_y + \sigma_{zz}n_z)\hat{z} \qquad (105)$$

Noting that now, $\overrightarrow{T_{xn}}, \overrightarrow{T_{yn}},$ and $\overrightarrow{T_{zn}}$ give the x, y or z directed force on a surface which faces the unit vector, $\hat{n},$ direction, with $\hat{n},$ having a unit vector encompassing x, y and z elements (that is, n_x, n_y, n_z). Additionally within literature the unit vector notation $,\hat{x}, \hat{y}, \hat{z},$ tends to be omitted, noting that the first component of the traction force identifies force direction and that the second component is the surface which the stress acts upon, and so is omitted in this thesis also. The compact form, incorporating the Cauchy stress tensor, outlining the traction force stress relationship at a given point is now given as,

$$\begin{bmatrix} T_{xn} \\ T_{yn} \\ T_{zn} \end{bmatrix} = \begin{bmatrix} \sigma_{xx} & \sigma_{xy} & \sigma_{xz} \\ \sigma_{yx} & \sigma_{yy} & \sigma_{yz} \\ \sigma_{zx} & \sigma_{zy} & \sigma_{zz} \end{bmatrix} \begin{bmatrix} n_x \\ n_y \\ n_z \end{bmatrix} \quad (106)$$

And so,

$$\left[\overrightarrow{T_n}\right] = [\boldsymbol{\sigma}][\hat{n}] \; or \; \overrightarrow{T_n} = \boldsymbol{\sigma} \cdot \hat{n} \quad (107)$$

Where,

$$\overrightarrow{T_n} = \overrightarrow{T_{xn}} + \overrightarrow{T_{yn}} + \overrightarrow{T_{zn}} \qquad (108)$$

Noting that x, y and z unit vectors are omitted and that under the assumption of linearized theory (very small particle deviations) the Cauchy stress tensor is also symmetric in that $\sigma_{ij} = \sigma_{ji}$.

1.4 Relating stress to strain the constitutive equations

Section 6.2.5 outlines the relationship between stress and strain and expresses the simplified version of the constitutive relation. A more detailed examination of deriving the simplified version is now given.

As outlined by (Auld, 1990; Bunsell and Renard, 2005; Chaves, 2013; Rokhlin et al., 2011; Rose, 2014; Royer and Dieulesaint, 2000), the strain associated with a given stress component may be found from equation, (109)

$$\begin{bmatrix}\sigma_{xx}\\ \sigma_{xy}\\ \sigma_{xz}\\ \sigma_{yx}\\ \sigma_{yy}\\ \sigma_{yz}\\ \sigma_{zx}\\ \sigma_{zy}\\ \sigma_{zz}\end{bmatrix} = \begin{bmatrix} C_{xxxx} & C_{xxxy} & C_{xxxz} & C_{xxyx} & C_{xxyy} & C_{xxyz} & C_{xxzx} & C_{xxzy} & C_{xxzz}\\ C_{xyxx} & C_{xyxy} & C_{xyxz} & C_{xyyx} & C_{xyyy} & C_{xyyz} & C_{xyzx} & C_{xyzy} & C_{xyzz}\\ C_{xzxx} & C_{xzxy} & C_{xzxz} & C_{xzyx} & C_{xzyy} & C_{xzyz} & C_{xzzx} & C_{xzzy} & C_{xzzz}\\ C_{yxxx} & C_{yxxy} & C_{yxxz} & C_{yxyx} & C_{yxyy} & C_{yxyz} & C_{yxzx} & C_{yxzy} & C_{yxzz}\\ C_{yyxx} & C_{yyxy} & C_{yyxz} & C_{yyyx} & C_{yyyy} & C_{yyyz} & C_{yyzx} & C_{yyzy} & C_{yyzz}\\ C_{yzxx} & C_{yzxy} & C_{yzxz} & C_{yzyx} & C_{yzyy} & C_{yzyz} & C_{yzzx} & C_{yzzy} & C_{yzzz}\\ C_{zxxx} & C_{zxxy} & C_{zxxz} & C_{zxyx} & C_{zxyy} & C_{zxyz} & C_{zxzx} & C_{zxzy} & C_{zxzz}\\ C_{zyxx} & C_{zyxy} & C_{zyxz} & C_{zyyx} & C_{zyyy} & C_{zyyz} & C_{zyzx} & C_{zyzy} & C_{zyzz}\\ C_{zzxx} & C_{zzxy} & C_{zzxz} & C_{zzyx} & C_{zzyy} & C_{zzyz} & C_{zzzx} & C_{zzzy} & C_{zzzz}\end{bmatrix}\begin{bmatrix}\varepsilon_{xx}\\ \varepsilon_{xy}\\ \varepsilon_{xz}\\ \varepsilon_{yx}\\ \varepsilon_{yy}\\ \varepsilon_{yz}\\ \varepsilon_{zx}\\ \varepsilon_{zy}\\ \varepsilon_{zz}\end{bmatrix} \quad (109)$$

In addition to the Cauchy stress tensor and the strain tensor being symmetrical, a degree of symmetry is also found within the tensor of elasticity. That is,

$$C_{ijkl} = C_{jikl} = C_{ijlk} = C_{jilk}$$

Thus, upon highlighting the excess variables from equation (109), that is,

$$\begin{bmatrix}\sigma_{xx}\\ \sigma_{xy}\\ \sigma_{xz}\\ \sigma_{yx}\\ \sigma_{yy}\\ \sigma_{yz}\\ \sigma_{zx}\\ \sigma_{zy}\\ \sigma_{zz}\end{bmatrix} = \begin{bmatrix} C_{xxxx} & C_{xxxy} & C_{xxxz} & C_{xxyx} & C_{xxyy} & C_{xxyz} & C_{xxzx} & C_{xxzy} & C_{xxzz}\\ C_{xyxx} & C_{xyxy} & C_{xyxz} & C_{xyyx} & C_{xyyy} & C_{xyyz} & C_{xyzx} & C_{xyzy} & C_{xyzz}\\ C_{xzxx} & C_{xzxy} & C_{xzxz} & C_{xzyx} & C_{xzyy} & C_{xzyz} & C_{xzzx} & C_{xzzy} & C_{xzzz}\\ C_{yxxx} & C_{yxxy} & C_{yxxz} & C_{yxyx} & C_{yxyy} & C_{yxyz} & C_{yxzx} & C_{yxzy} & C_{yxzz}\\ C_{yyxx} & C_{yyxy} & C_{yyxz} & C_{yyyx} & C_{yyyy} & C_{yyyz} & C_{yyzx} & C_{yyzy} & C_{yyzz}\\ C_{yzxx} & C_{yzxy} & C_{yzxz} & C_{yzyx} & C_{yzyy} & C_{yzyz} & C_{yzzx} & C_{yzzy} & C_{yzzz}\\ C_{zxxx} & C_{zxxy} & C_{zxxz} & C_{zxyx} & C_{zxyy} & C_{zxyz} & C_{zxzx} & C_{zxzy} & C_{zxzz}\\ C_{zyxx} & C_{zyxy} & C_{zyxz} & C_{zyyx} & C_{zyyy} & C_{zyyz} & C_{zyzx} & C_{zyzy} & C_{zyzz}\\ C_{zzxx} & C_{zzxy} & C_{zzxz} & C_{zzyx} & C_{zzyy} & C_{zzyz} & C_{zzzx} & C_{zzzy} & C_{zzzz}\end{bmatrix}\begin{bmatrix}\varepsilon_{xx}\\ \varepsilon_{xy}\\ \varepsilon_{xz}\\ \varepsilon_{yx}\\ \varepsilon_{yy}\\ \varepsilon_{yz}\\ \varepsilon_{zx}\\ \varepsilon_{zy}\\ \varepsilon_{zz}\end{bmatrix}$$

Equation (109) may be rewritten as,

$$\begin{bmatrix}\sigma_{xx}\\ \sigma_{yy}\\ \sigma_{zz}\\ \sigma_{yz} = \sigma_{zy}\\ \sigma_{xz} = \sigma_{zx}\\ \sigma_{xy} = \sigma_{yx}\end{bmatrix} = \begin{bmatrix} C_{xxxx} & C_{xxyy} & C_{xxzz} & C_{xxyz} & C_{xxxz} & C_{xxxy}\\ C_{yyxx} & C_{yyyy} & C_{yyzz} & C_{yyyz} & C_{yyxz} & C_{yyxy}\\ C_{zzxx} & C_{zzyy} & C_{zzzz} & C_{zzyz} & C_{zzxz} & C_{zzxy}\\ C_{yzxx} & C_{yzyy} & C_{yzzz} & C_{yzyz} & C_{yzxz} & C_{yzxy}\\ C_{xzxx} & C_{xzyy} & C_{xzzz} & C_{xzyz} & C_{xzxz} & C_{xzxy}\\ C_{xyxx} & C_{xyyy} & C_{xyzz} & C_{xyyz} & C_{xyxz} & C_{xyxy}\end{bmatrix}\begin{bmatrix}\varepsilon_{xx}\\ \varepsilon_{yy}\\ \varepsilon_{zz}\\ \varepsilon_{yz} = \varepsilon_{zy}\\ \varepsilon_{xz} = \varepsilon_{zx}\\ \varepsilon_{xy} = \varepsilon_{yx}\end{bmatrix} \quad (110)$$

Additionally, it is also true that $C_{ijkl} = C_{klij}$ and so equation (110) may be reduced again, with the reduction equating to the tensor becoming symmetrical, that is.

$$\begin{bmatrix}\sigma_{xx}\\ \sigma_{yy}\\ \sigma_{zz}\\ \sigma_{yz} = \sigma_{zy}\\ \sigma_{xz} = \sigma_{zx}\\ \sigma_{xy} = \sigma_{yx}\end{bmatrix} = \begin{bmatrix} C_{xxxx} & C_{xxyy} & C_{xxzz} & C_{xxyz} & C_{xxxz} & C_{xxxy}\\ C_{xxyy} & C_{yyyy} & C_{yyzz} & C_{yyyz} & C_{yyxz} & C_{yyxy}\\ C_{xxzz} & C_{yyzz} & C_{zzzz} & C_{zzyz} & C_{zzxz} & C_{zzxy}\\ C_{xxyz} & C_{yyyz} & C_{zzyz} & C_{yzyz} & C_{yzxz} & C_{yzxy}\\ C_{xxxz} & C_{yyxz} & C_{zzxz} & C_{yzxz} & C_{xzxz} & C_{xzxy}\\ C_{xxxy} & C_{yyxy} & C_{zzxy} & C_{yzxy} & C_{xzxy} & C_{xyxy}\end{bmatrix}\begin{bmatrix}\varepsilon_{xx}\\ \varepsilon_{yy}\\ \varepsilon_{zz}\\ \varepsilon_{yz} = \varepsilon_{zy}\\ \varepsilon_{xz} = \varepsilon_{zx}\\ \varepsilon_{xy} = \varepsilon_{yx}\end{bmatrix} \quad (111)$$

Equation (111) being the equation (31) from section 6.2.5.

1.5 Plane wave propagation

Mechanical waves (noting that ultrasonic waves are a variety of mechanical waves) may in the general sense be thought of as a disturbance or vibration propagating through a medium. For the large part, in the context of this thesis, wave motion may be considered as the resultant propagating disturbance caused by traction forces impacting on the surface of a solid; with these traction forces causing particles (and subsequently, neighbouring particles) to deviate from equilibrium and oscillate around their equilibrium position. Additionally, a disturbance will propagate through the solid, by virtue of a combination of elastic restoring forces, traction force and inertia of the particles.

Mathematically, for a particular function argument, a disturbance may be modelled as a variable which is any function of this particular argument on the proviso that the disturbance or variable is able to act as a solution to an equation known as the wave equation. For instance, when y may be expressed as a function of x and t, for a one dimensional disturbance the wave equation is given by equation (112),

$$\frac{\partial^2 y}{\partial x^2} = \frac{1}{c^2}\frac{\partial^2 y}{\partial t^2} \quad (112)$$

The solution to this equation, is given by any single valued function, assuming it may be differentiated twice, whose argument is given by

$$(x \pm ct)$$

Where c and t are the speed and point in time. The stated argument may further be manipulated, by multiplying by wave number k, (not yet defined) to allow it to be expressed in terms of radians, without loss of generality, and so a solution of the wave equation (112) may be given as,

$$f(kx \pm wt) \quad (113)$$

Where f may be thought of as either a cosine function or a sinusoidal function. Noting that y, which is a function of x and t, is equal to the amplitude of the wave at a given point in this instance. This reasoning also holds for 3 dimensional

disturbance, that is, for,

$$\frac{\partial^2 F}{\partial x^2} + \frac{\partial^2 F}{\partial y^2} + \frac{\partial^2 F}{\partial z} = \frac{1}{c^2}\frac{\partial^2 F}{\partial t^2} \quad (114)$$

Where F is a function of x, y, z and t, a particular plane wave solution may be given as,

$$sin\left(k_x x + k_y y + k_z z \pm wt\right) \quad (115)$$

Explaining now the terms w and $\boldsymbol{k}$. For a plane wave travelling in a given direction, in this case equation (115), the equation describing the disturbance must by definition describe the direction the wave is travelling and also identify the point at which the wave is to be evaluated.

Considering the direction of propagation, the vector variable $\boldsymbol{k}$ may be introduced. The direction of $\boldsymbol{k}$ is at a right angle to the plane wave surfaces, Figure 62 is given to exemplify this.

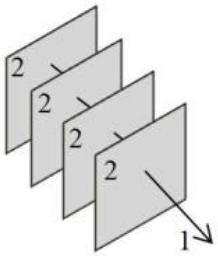

1 = $\vec{k}$

2 = Plane wave surfaces

Figure 62 – Plane wave surfaces with the $\vec{k}$ vector pointing in the direction of wave propagation, that is, 90° to plane wave surface.

Relating $\boldsymbol{k}$ to the variables which appear in equation (115), that is, k_x, k_y, k_z, equation (116) is given,

$$\vec{k} = k_x\hat{x} + k_y\hat{y} + k_z\hat{z} \quad (116)$$

Additionally, a wave will undergo one compete revolution every 2π radians (360°), regarded as the wave cycle of the wave and the wavelength of the wave may be understood as the distance, in meters, between points of respective position on neighbouring wave cycles of a given plane wave. This concept is shown in Figure 63.

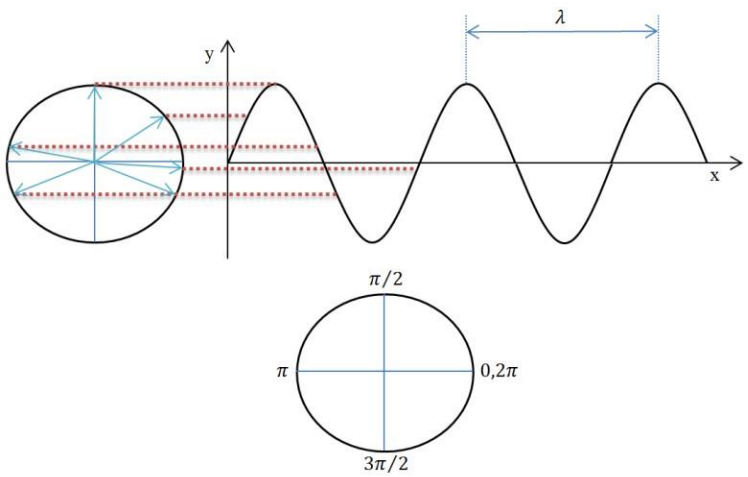

Figure 63 – Sine wave traversing from left to right. The red dots indicate the amount of degrees the wave has gone through as it oscillates; the concept of wave length is also shown. For clarity, the bottom second circle is included to demonstrate the angles the red dashed lines approximately equate to.

Returning to **k**, the wave number may be introduced. The wave number of a wave is given by,

$$|\vec{k}| = k = \frac{2\pi\ (radians)}{\lambda\ (meters)} = \sqrt{{k_x}^2 + {k_y}^2 + {k_z}^2} = \ wavenumber$$

That is, the wave number is a measure of the amount of radians a wave travels through in 1 metre space, noting that each complete wave cycle is equal to 2π radians or 360o.

Noting additionally, the components of **k** are found using the following formula, where **d** is a unit vector in the direction of wave propagation.

$$\vec{k} = k\hat{d}$$

Looking now at what is known as angular frequency. Angular frequency, *w*, may be thought of as the amount of radians a wave travels through in 1 second (measured in radians/s). Mathematically, this is expressed as

$$w = 2\pi f = angular\ frequency$$

Noting that f is given as the frequency, which is measured in hertz, and is a non angular based measurement of how many wave cycles occur in 1 second. Additionally, the inverse of the frequency is given as the period, this being a time value associated to the amount of time taken for one full wave cycle. Figure 64 is given to reinforce this concept.

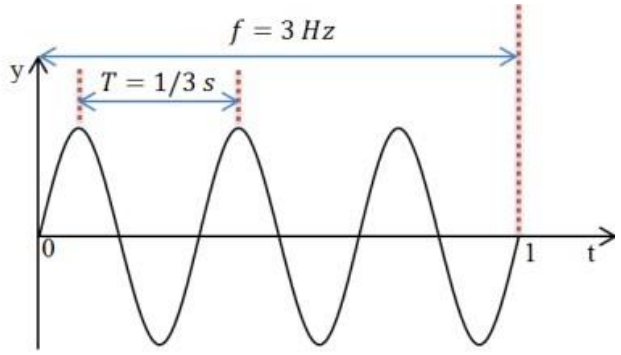

Figure 64 - Plane sinusoidal wave propagating from left to right with the frequency and period both shown

Having now outlined all necessary criteria to describe plane travelling waves, the academic notation convention is now able to be realised. This is made possible using Euler‟s formula.

$$e^{i\theta} = \cos(\theta) + isin(\theta) \qquad (117)$$

Where e is the exponential function and i the imaginary number,$\sqrt{-1}$. Noting that when using equation (117) to document a sine or cosine, only the imaginary part in the case of sine is used or only the real part in the case of a cosine is used. Thus, equation (117) may be expressed as equation (118),

$$e^{i(k_x x + k_y y + k_z z \pm wt)} \qquad (118)$$

As with academic convention, this thesis further manipulates equation (118) to allow for a more compact equation to be expressed. This is outlined by first considering how a one dimensional wave (a wave only having an x displacement component) is evaluated.

If the altered argument of equation (118) is considered along with a known frequency, velocity and wavelength, then the wave will have a set distance. Thus, for a wave given by equation (115) or (118), the wave amplitude between the origin and a fixed distance from the origin is able to be evaluated by selecting an appropriate time period, t, and displacement, x, (assuming the x, is below or equal to the maximum distance (in meters) travelled by the wave in this time period). That is, for a given distance from the origin, say for instance 5 meters, and for a given point in time, say 5 seconds, the above equation returns the wave amplitude value associated at this point. Noting, that if the distance from the origin is kept at 5 meters and different time point is selected, a different and new amplitude value would be returned. Note additionally that the argument of both equation (115) and equation (118) is measured in radians and the choice as where the wave should be evaluated in terms of amplitude is through the choice of x and so x may be thought of as a position vector pointing in the direction of wave travel. For a wave of 3 Hz, and wavelength of 1 m, Figure 65 exemplifies this concept,

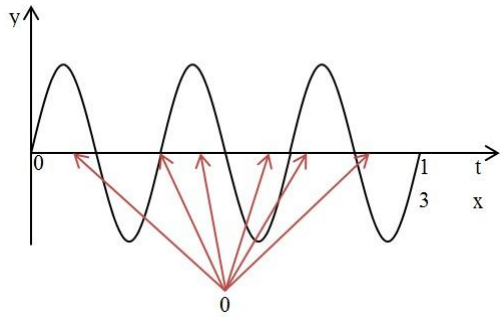

Figure 65 – Wave travelling in x direction with position vectors pointing to various directions on the x axis. Note that the way the position vectors and origin point is shown in this figure is only for clarity

Noting that in Figure 65, the position vectors would not originate from the origin shown and would originate from the origin at the intersection of the axes where the true origin is documented; the vectors would lie solely on the x axis also.

Scaling up to 3 dimensions, this same argument holds true and so by introducing a position vector from the origin with an x, y and z component as, $\vec{D}$, given as

$$\vec{D} = x\hat{x} + y\hat{y} + z\hat{z} \qquad (119)$$

And noting equation (116),

$$\vec{k} = k_x\hat{x} + k_y\hat{y} + k_z\hat{z} \qquad (116)$$

Then equation (118) may be more compactly written using the dot product of equation (116) and equation (119), that is equation (120) defines a positive travelling wave (from left to right) as in keeping with academic convention.

$$e^{i(k_x x + k_y y + k_z z - wt)} = e^{i(\vec{k}\cdot\vec{D} - wt)} = e^{i\left(\left(k(\hat{k})\right)\cdot\vec{D} - wt\right)} \qquad (120)$$

1.6 Christoffel Matrices

1.6.1 Isotropic material

For an isotropic medium, the stiffness tensor is given by equation (121). This is not proven but is able to be found from references cited in the chapter.

$$[\boldsymbol{C}] = \begin{bmatrix} C_{11} & C_{12} & C_{12} & 0 & 0 & 0 \\ C_{12} & C_{11} & C_{12} & 0 & 0 & 0 \\ C_{12} & C_{12} & C_{11} & 0 & 0 & 0 \\ 0 & 0 & 0 & C_{44} & 0 & 0 \\ 0 & 0 & 0 & 0 & C_{44} & 0 \\ 0 & 0 & 0 & 0 & 0 & C_{44} \end{bmatrix} \qquad (121)$$

Noting $C_{12} = C_{11} - 2C_{44}$ and so only 2 elastic constants are independent. Calculating now the Christoffel matrix, equation (58) from chapter 6, and starting with the first element, i.e.

$$\Gamma_{ij} = \Gamma_{xx}$$

Then

$$\Gamma_{ij} = \begin{bmatrix} k_x & 0 & 0 & 0 & k_z & k_y \\ 0 & k_y & 0 & k_z & 0 & k_x \\ 0 & 0 & k_z & k_y & k_x & 0 \end{bmatrix} [\boldsymbol{C}] \begin{bmatrix} k_x & 0 & 0 \\ 0 & k_y & 0 \\ 0 & 0 & k_x \\ 0 & k_z & k_y \\ k_z & 0 & k_x \\ k_y & k_x & 0 \end{bmatrix} = k_{iK} C_{KL} k_{Lj} \qquad (122)$$

may be rewritten as,

$$\Gamma_{xx} = k_{xK} C_{KL} k_{Lx} \qquad (122)$$

Equation (122) requires a summation over repeated subscripts, as per academic convention, and also C_{KL}. The following two expressions are used to simply this analysis.

Elements	
k_{xK}	k_{Lx}
$k_{x1} = k_x$	$k_{1x} = k_x$
$k_{x2} = 0$	$k_{2x} = 0$
$k_{x3} = 0$	$k_{3x} = 0$
$k_{x4} = 0$	$k_{4x} = 0$
$k_{x5} = k_z$	$k_{5x} = k_z$
$k_{x6} = k_y$	$k_{6x} = k_y$

$$[\boldsymbol{C}] = \begin{bmatrix} C_{11} & C_{12} & C_{13} & C_{14} & C_{15} & C_{16} \\ C_{21} & C_{22} & C_{23} & C_{24} & C_{25} & C_{26} \\ C_{31} & C_{32} & C_{33} & C_{34} & C_{35} & C_{36} \\ C_{41} & C_{42} & C_{43} & C_{44} & C_{45} & C_{46} \\ C_{51} & C_{52} & C_{53} & C_{54} & C_{55} & C_{56} \\ C_{61} & C_{62} & C_{63} & C_{64} & C_{65} & C_{66} \end{bmatrix}$$

The table represents the values taken from the first row and first column of unit vector propagation direction matrices in equation (122) i.e. for (i.e. K = 1 and L = 1). The elastic constant matrix is not the matrix given as equation (51) but instead the full matrix. This allows for a simpler analysis moving forward. Calculation of equation (122) now follows the pattern outlined below. Hold K = 1 and go through L and perform a summation.

K =1, L (1-6)

Subscript	Value
$k_{x1}C_{11}k_{1x}$	$k_xC_{11}k_x$
$k_{x1}C_{12}k_{2x}$	$k_xC_{12}0$
$k_{x1}C_{13}k_{3x}$	$k_xC_{13}0$
$k_{x1}C_{14}k_{4x}$	$k_xC_{14}0$
$k_{x1}C_{15}k_{5x}$	$k_xC_{15}k_z$
$k_{x1}C_{16}k_{6x}$	$k_xC_{16}k_y$
Summation	${k_x}^2C_{11}$

Having used the full matrix of elastic constants, the values from equation (121) are now substituted and it can be shown that $C_{14,}$ C_{15}, C_{16}, are 0. Performing now a similar analysis for K = 2, K = 3, K = 4, K = 5 and K = 6 yields,

K =2,3,4,5,6, L (1-6)	
Summation	Value
K = 2	0
K = 3	0
K = 4	0
K = 5	${k_z}^2C_{44}$
K = 6	${k_y}^2C_{44}$

Performing the final summation that is, adding up the individual summations of K =1, 2, 3…6 while allowing L to increase from 1-6 for each individual K, gives,Γ_{xx}

$$\Gamma_{xx} = {k_x}^2C_{11} + {k_y}^2C_{44} + {k_z}^2C_{44}$$

Which upon realising,

$$\hat{k} = k_x\hat{x} + k_y\hat{y} + k_z\hat{z}$$

Thus,

$$|\hat{k}| = \sqrt{{k_x}^2 + {k_y}^2 + {k_z}^2} = 1$$

Thus,

$${k_x}^2 + {k_y}^2 + {k_z}^2 = 1^2$$

$$\downarrow$$

$$1 - {k_x}^2 = {k_y}^2 + {k_z}^2$$

And so Γ_{xx} may be expressed as,

$$\Gamma_{xx} = {k_x}^2 C_{11} + C_{44}\left(1 - {k_x}^2\right) \quad (123)$$

Performing a similar process for the remaining elements of the Christoffel matrix leads to the development of the complete Christoffel matrix for isotropic solids, i.e. equation (58) from chapter 6, given here as equation (124).

$$[\Gamma] = \begin{bmatrix} C_{11}{k_x}^2 + C_{44}\left(1 - {k_x}^2\right) & (C_{12} + C_{44})k_x k_y & (C_{12} + C_{44})k_x k_z \\ (C_{12} + C_{44})k_y k_x & C_{11}{k_y}^2 + C_{44}\left(1 - {k_y}^2\right) & (C_{12} + C_{44})k_y k_z \\ (C_{12} + C_{44})k_z k_x & (C_{12} + C_{44})k_z k_y & C_{11}{k_z}^2 + C_{44}\left(1 - {k_z}^2\right) \end{bmatrix} \quad (124)$$

1.6.2 Anisotropic material

The process of deriving the Christoffel matrix for the case of anisotropic symmetry is the same as for the isotropic, and so therefore not repeated. The anisotropic Christoffel matrix is given as equation (125).

$$[\Gamma] = \begin{bmatrix} \Gamma_{xx}' & \Gamma_{xy}' & \Gamma_{xz}' \\ \Gamma_{xy}' & \Gamma_{yy}' & \Gamma_{yz}' \\ \Gamma_{xz}' & \Gamma_{yz}' & \Gamma_{zz}' \end{bmatrix} \quad (125)$$

$$\Gamma_{xx}' = C_{11}{k_x}^2 + C_{66}{k_y}^2 + C_{55}{k_z}^2 + 2C_{56}k_y k_z + 2C_{15}k_z k_x + 2C_{16}k_x k_y$$

$$\Gamma_{yy}' = C_{66}{k_x}^2 + C_{22}{k_y}^2 + C_{44}{k_z}^2 + 2C_{24}k_y k_z + 2C_{46}k_z k_x + 2C_{26}k_x k_y$$

$$\Gamma_{zz}' = C_{55}{k_x}^2 + C_{44}{k_y}^2 + C_{33}{k_z}^2 + 2C_{34}k_y k_z + 2C_{35}k_z k_x + 2C_{45}k_x k_y$$

$$\Gamma_{xy}' = C_{16}{k_x}^2 + C_{26}{k_y}^2 + C_{45}{k_z}^2 + (C_{46} + C_{25})k_y k_z + (C_{14} + C_{56})k_z k_x + (C_{12} + C_{66})k_x k_y$$

$$\Gamma_{xz}' = C_{16}{k_x}^2 + C_{26}{k_y}^2 + C_{45}{k_z}^2 + (C_{45} + C_{36})k_y k_z + (C_{13} + C_{55})k_z k_x + (C_{14} + C_{56})k_x k_y$$

$$\Gamma_{yz}' = C_{16}{k_x}^2 + C_{26}{k_y}^2 + C_{45}{k_z}^2 + (C_{44} + C_{23})k_y k_z + (C_{36} + C_{45})k_z k_x + (C_{25} + C_{46})k_x k_y$$

1.7 Executing the Christoffel equation

1.7.1 Isotropic medium

Executing the Christoffel equation in isotropic medium is most easily is done so by picking a direction that simplifies the Christoffel equation the most (which is akin to saying, which direction simplifies equation (124) to its simplest form). This may be either, the x, the y, or the z direction only. The x direction is considered here, that is,

$$\hat{k} = \hat{x} = k_x$$

Remembering that k_x refers to the x component of the wave propagation unit vector and not the x component of the wave propagation vector. Equation (124) thus becomes,

$$[\Gamma] = \begin{bmatrix} C_{11} & 0 & 0 \\ 0 & C_{44} & 0 \\ 0 & 0 & C_{44} \end{bmatrix}$$

And so the Christoffel equation (eqn 56) thus becomes,

$$k^2 \begin{bmatrix} C_{11} & 0 & 0 \\ 0 & C_{44} & 0 \\ 0 & 0 & C_{44} \end{bmatrix} \begin{bmatrix} v_x \\ v_y \\ v_z \end{bmatrix} = \rho w^2 \begin{bmatrix} v_x \\ v_y \\ v_z \end{bmatrix}$$

And so three phase velocity equations are now realisable, that is,

$$k^2 C_{11} v_x = \rho w^2 v_x \quad (126)$$

$$k^2 C_{44} v_y = \rho w^2 v_y \quad (127)$$

$$k^2 C_{44} v_z = \rho w^2 v_z \quad (128)$$

Noting that equation (126) concerns the velocity of a longitudinal wave propagating in the x direction, equation (127) concerns a shear wave propagating in the x direction and polarized in the y direction and equation (128) describes another shear wave propagating in the x direction this time polarized in the z direction. It is apparent from the above equations that,

$$k^2 C_{11} v_x = \rho w^2 v_x \rightarrow k^2 C_{11} = \rho w^2 \rightarrow \sqrt{\frac{C_{11}}{\rho}} = \frac{w}{k} \rightarrow v_x = \sqrt{\frac{C_{11}}{\rho}}$$

$$k^2 C_{44} v_y = \rho w^2 v_y \rightarrow k^2 C_{44} = \rho w^2 \rightarrow \sqrt{\frac{C_{44}}{\rho}} = \frac{w}{k} \rightarrow v_y = \sqrt{\frac{C_{44}}{\rho}}$$

$$k^2 C_{44} v_y = \rho w^2 v_y \rightarrow k^2 C_{44} = \rho w^2 \rightarrow \sqrt{\frac{C_{44}}{\rho}} = \frac{w}{k} \rightarrow v_z = \sqrt{\frac{C_{44}}{\rho}}$$

Where the subscript attached to the velocity component indicates the polarization direction. For an isotropic medium, it is now shown that the two independent elastic constants C_{11} and C_{44} may be determined from velocity measurements of shear waves in the x direction and a longitudinal wave in the x direction. That is,

$$velocity\ of\ longitudinal\ wave\ in\ x\ direction = v_x = \sqrt{\frac{C_{11}}{\rho}} \qquad (129)$$

$$velocity\ of\ shear\ wave\ polarized\ in\ y\ direction = v_y = \sqrt{\frac{C_{44}}{\rho}} \qquad (130)$$

$$velocity\ of\ shear\ wave\ polarized\ in\ z\ direction = v_z = \sqrt{\frac{C_{44}}{\rho}} \qquad (131)$$

Thus for a known velocity and density the elastic constants may be determined that is,

$$C_{11} = \rho {v_x}^2 \qquad (132)$$

$$C_{44} = \rho {v_y}^2 = \rho {v_z}^2 \qquad (133)$$

1.7.2 Anisotropic medium

Looking now at the anisotropic case, the anisotropic case is more complicated, in that the polarization direction is such that there is no guarantee of a pure wave (longitudinal or transverse) in a given direction. Additionally, the Christoffel matrix is also more complicated, and so prior to executing the equation to solve for elastic constants, some light groundwork is required. This ground work is given as follows; initially the general form of the Christoffel equation, equation (56) from chapter 6, may be rewritten in the form,

$$\left[k^2 \Gamma_{ij} - \rho w^2 \delta_{ij}\right]\left[v_j\right] = 0$$

Noting that δ_{ij} is a function called the Kronecker Delta, such that,

$$\delta_{ij} = 1\ when\ i = j$$
$$\delta_{ij} = 0\ when\ i \neq j$$

Further dividing by k^2 gives,

$$[\Gamma_{ij} - \rho v^2 \delta_{ij}][v_j] = 0 \quad (134)$$

Additionally, going through the Γ_{ij} elements from Γ_{xx}toΓ_{zz}, and noting that Γ_{ij} are elements of the anisotropic Christoffel matrix, then the Christoffel matrix, with the appropriate subtractions, may be expressed as,

$$\begin{bmatrix} \Gamma_{xx}' - pv^2 & \Gamma_{xy}' & \Gamma_{xz}' \\ \Gamma_{xy}' & \Gamma_{yy}' - pv^2 & \Gamma_{yz}' \\ \Gamma_{xz}' & \Gamma_{yz}' & \Gamma_{zz}' - pv^2 \end{bmatrix} \quad (135)$$

Further, dropping the subscript notation then $[\Gamma_{ij} - \rho v^2 \delta_{ij}]$ is akin to what would be expressed from,

$$[\Gamma - \mathrm{I}\rho v^2] \; with \; \mathrm{I} = \begin{bmatrix} 1 & 0 & 0 \\ 0 & 1 & 0 \\ 0 & 0 & 1 \end{bmatrix}$$

Inserting $[\Gamma - \mathrm{I}\rho v^2]$ into equation (134) and again dropping the subscript notation gives,

$$[\Gamma - \mathrm{I}\rho v^2][\vec{v}] \quad or \quad [\Gamma][\vec{v}] = \rho v^2 [\vec{v}] \quad (136)$$

Thus equation (136) may be thought of as a classic eigenvector eigenvalue problem; i.e. for a given matrix,$[\Gamma]$, and a scalar quantity, ρv^2, there exists another vector quantity which if multiplied by both$[\Gamma]$ and ρv^2 returns the same value. Noting that the vector quantity$\vec{v}$ is in this instance the vector of particle polarization (the x, y and z components of $\vec{v}$ are the directions to which a given particle deviates from its equilibrium position). Thus, it can be said that ρv^2 may be regarded as the eigenvalue of $[\Gamma]$ and $\vec{v}$ may be regarded as the eigenvector of$[\Gamma]$.

Note that when equation (136) was rearranged, the identity matrix may be dropped as it has does not change the polarization vector. However, for the original form of the equation the identity matrix is required as without it a 3x3 matrix, (Γ), minus a 3x1 matrix is not permitted.

Relating this fact to equation (134) is done so by first expressing all vector elements of equation (134), given here as equation (137),

$$\begin{bmatrix} \Gamma_{xx}' - pv^2 & \Gamma_{xy}' & \Gamma_{xz}' \\ \Gamma_{xy}' & \Gamma_{yy}' - pv^2 & \Gamma_{yz}' \\ \Gamma_{xz}' & \Gamma_{yz}' & \Gamma_{zz}' - pv^2 \end{bmatrix} \begin{bmatrix} v_x \\ v_y \\ v_z \end{bmatrix} = 0 \quad (137)$$

Now for a non-trivial solution, which in this case means avoiding the possibility that the vector $\vec{v}$ is equal to zero, the determinant of $[\Gamma - \mathrm{I}\rho v^2]$ must be equal zero. That is,

$$DET\begin{vmatrix} \Gamma_{xx}' - pv^2 & \Gamma_{xy}' & \Gamma_{xz}' \\ \Gamma_{xy}' & \Gamma_{yy}' - pv^2 & \Gamma_{yz}' \\ \Gamma_{xz}' & \Gamma_{yz}' & \Gamma_{zz}' - pv^2 \end{vmatrix} = 0 \qquad (138)$$

Obtaining the velocity of wave propagation in terms of the elastic constants is done so by solving equation (138) for $v$noting that three roots exist i.e. three different v may be selected and equation (137) may still be solved.

A reference execution of the Christoffel equation is now performed for a symmetry class of transverse isotropy, or hexagonal symmetry. First, the anisotropic Christoffel matrix, equation (59) from chapter 6, is altered to reflect the symmetry conditions. The stiffness matrix for hexagonal symmetry, or uni-directional CFRP, is given by equation (139)

$$[C] = \begin{bmatrix} C_{11} & C_{12} & C_{13} & 0 & 0 & 0 \\ C_{12} & C_{11} & C_{13} & 0 & 0 & 0 \\ C_{13} & C_{13} & C_{33} & 0 & 0 & 0 \\ 0 & 0 & 0 & C_{44} & 0 & 0 \\ 0 & 0 & 0 & 0 & C_{44} & 0 \\ 0 & 0 & 0 & 0 & 0 & C_{66} \end{bmatrix} \; with\; C_{66} = \frac{C_{11} - C_{12}}{2} \quad (139)$$

Inserting the 0 values into equation (59) from chapter 6, gives the Christoffel matrix for hexagonal symmetry, which is given as equation (140).

$$\begin{bmatrix} C_{11}{k_x}^2 + C_{66}{k_y}^2 + C_{44}{k_z}^2 & (C_{12} + C_{66})k_x k_y & (C_{13} + C_{44})k_z k_x \\ (C_{12} + C_{66})k_x k_y & C_{66}{k_x}^2 + C_{11}{k_y}^2 + C_{44}{k_z}^2 & (C_{44} + C_{13})k_y k_z \\ (C_{13} + C_{44})k_z k_x & (C_{44} + C_{13})k_y k_z & C_{44}{k_x}^2 + C_{44}{k_y}^2 + C_{33}{k_z}^2 \end{bmatrix} (140)$$

For a wave propagating in the [1,1,0] direction, with the fibre direction in the z direction, a wave vector which is equal in both the x and y direction will result in in a unit vector of

$$\hat{k} = \left[\frac{1}{\sqrt{2}}, \frac{1}{\sqrt{2}}, 0\right] \quad \rightarrow \quad k_x = k_y = \frac{1}{\sqrt{2}}, \qquad k_z = 0$$

Noting that for clarity this direction may be represented graphically, given as Figure 66.

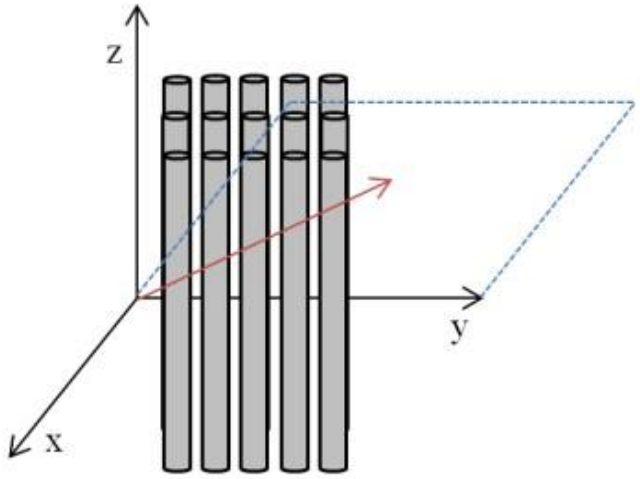

Figure 66 – Unidirectional fibre arrangement which may be modelled using Hexagonal symmetry. For a fibre in the z directional the material may be regarded as transversely isotropic to this axis

The Christoffel matrix for this direction of propagation is equal to,

$$\begin{bmatrix} C_{11}{k_x}^2 + C_{66}{k_y}^2 & (C_{12} + C_{66})k_x k_y & 0 \\ (C_{12} + C_{66})k_x k_y & C_{66}{k_x}^2 + C_{11}{k_y}^2 & 0 \\ 0 & 0 & C_{44}{k_x}^2 + C_{44}{k_y}^2 \end{bmatrix}$$

Thus, upon substituting for the unit wave vector elements and inserting these matrix elements into equation (12), then the Christoffel equation for hexagonal symmetry takes the form,

$$\begin{bmatrix} \frac{1}{2}(C_{11} + C_{66}) - pv^2 & \frac{1}{2}(C_{12} + C_{66}) & 0 \\ \frac{1}{2}(C_{12} + C_{66}) & \frac{1}{2}(C_{11} + C_{66}) - pv^2 & 0 \\ 0 & 0 & C_{44} - pv^2 \end{bmatrix} \begin{bmatrix} v_x \\ v_y \\ v_z \end{bmatrix} = 0 \quad (141)$$

As previously outlined in equation (138), to determine the three velocities, or the eigenvalues, associated with this particle direction, the determinant of equation (142) should equal 0 i.e.

$$DET\begin{vmatrix} \frac{1}{2}(C_{11}+C_{66})-pv^2 & \frac{1}{2}(C_{12}+C_{66}) & 0 \\ \frac{1}{2}(C_{12}+C_{66}) & \frac{1}{2}(C_{11}+C_{66})-pv^2 & 0 \\ 0 & 0 & C_{44}-pv^2 \end{vmatrix}=0 \quad (142)$$

For a matrix determinant given by

$$A(EI-FH)-B(DI-FG)+C(DH-EG) \quad with \begin{vmatrix} A & B & C \\ D & E & F \\ G & H & I \end{vmatrix}$$

After determining the three eigenvalues which allow the determinant to equal to zero, the eigenvectors, the polarization directions, may be calculated. Typically, this analysis is performed using electronic software programmes such as Mathematica or Matlab given the likelihood of introducing error owing to the very large algebraic manipulations required. Additionally, performing such tasks on software allows for multiple directions within different symmetry groups to be examined with ease and so is a far quicker option. In this thesis, a bespoke piece of Matlab software has been designed to facilitate this task. The details of this bespoke programme may be found in appendix 4.

Using the Matlab programme designed for this thesis, the three velocities and the resulting polarization directions associated with plane wave propagation in the [1, 1, 0] direction are given in Table 48.

Velocity and resulting Polarization table			
Velocity	Vector	Dot product with direction $(1 \quad 1 \quad 0)$	Wave type
$\sqrt{\qquad}$	$(-1 \quad 1 \quad 0)$	0	Transverse wave
$v=\sqrt{\frac{C_{44}}{\rho}}$,	$(0 \quad 0 \quad 1)$	0	Transverse wave
$\sqrt{\qquad\qquad}$	$(1 \quad 1 \quad 0)$	2	Longitudinal wave

Table 48 – plane wave velocities and associated polarization directions for a plane wave propagation in the [1, 1, 0] direction

Thus, it is shown that for a plane wave propagating in direction [1,1,0] for fibre direction of z, in an x, y, z coordinate plane, that three unique velocities with three pure modes polarizations are obtained, two transverse waves and a longitudinal wave.

Appendix 2: Elastic constant determination of CFRP via the ultrasonic immersion based through transmission technique: A review

2.1 Introduction

This literature review covers the same subject and papers as what was described in chapter 7. However substantial more depth is presented, in that each publication is reviewed on its merits, with benefits and drawback identified. This appendix is an initial version of a journal publication able to be found using the link https://doi.org/10.1016/j.pmatsci.2018.04.001. This was under review at time of thesis examination.

2.2 Review Methodology

When conducting a review, the typical theme within literature is to report the results of a publication and refrain from giving each publication a detailed and rigorous review. Adopting this reporting of results strategy allows for very effective wide ranging reviews; findings from a large volume of literature in multiple areas can be presented efficiently within literature. This paper however limits the scope of the review to allow for a more in depth analysis of the literature. Adopting this approach has three benefits, 1) drawbacks or concerns within literature are clearly identified, 2) not only a recap of findings but a full contribution to knowledge is able to be presented and 3) seminal works within the field are collated, organized and reviewed in a single document which may be used as a future reference text. Thus, this review goes deeper than a reporting of the results and presents a more in depth analysis of the available seminal works. Existing substantial reviews of ultrasonic based analysis of composite material, such as (Hosten, 2001; Rokhlin et al., 2011), present a comprehensive discussion of the methods to ultrasonically determine the elastic constants of unidirectional composites. However, a clear distinction between those works and this

work can be made. Important works such as, (Hosten, 2001; Rokhlin et al., 2011), focus more on the techniques used within industry and academia, with practitioners cited as references, and less on the contributions from individual authors (although in the case of (Rokhlin et al., 2011) the authors of this text at times directly discuss their previous publications on the subject). This paper is more aligned with (Summerscales, 1990), in that, there is less focus on the theoretical and more on the practical findings arising from individual texts. Thus it is envisaged that this review may be used in conjunction with or to complement the existing literature reviews (Hosten, 2001; Rokhlin et al., 2011).

Regards the boundaries of the research, Table 49 identifies the scope of literature reviewed.

Boundaries on the literature reviewed	Examples of research areas falling outside boundaries (excluded research areas)
Bulk waves (waves treated as acting in an infinite medium)	Lamb waves, Rayleigh waves, guided waves
Unidirectional composite (with where possible polymer matrix)	Cross ply composite, multidirectional laminates, thick composites, woven composites
Carbon fibre or graphite fibre (where possible)	Kevlar or Boron based fibres
Non gas coupled ultrasound through transmission (velocity based measurement)	Wave attenuation measurements, pulse echo techniques, point source point receiver technique, A-scans, B-scans, C-scans, Air coupled ultrasound, transmission – reflection coefficients
Elastic constant determination (mechanical properties) through experiment	Defect detection, porosity, fibre content, attenuation factor, theoretical modelling based on composite properties, mechanical tests, viscoelastic properties

Table 49 - Identifies the boundaries and scope of the literature review

Note that on occasion, one or more of the excluded research areas is discussed in the literature review. The rationale for discussing areas outside of the scope is made apparent from the context at that point.

The literature selected for this review was journal articles, conference papers and book publications. This literature was identified in part by searching through databases and also by reviewing the references cited in almost all published journal articles. Lastly, book reviews such as (Hosten, 2001; Rokhlin et al., 2011; Summerscales, 1990) also helped to identify further relevant literature.

It is important to emphasize that the decision to review a particular publication was at times taken of the opinion of the author. For instance, (Stijnman, 1995), employed an already existing method (at that point) to determine the elastic constants of a composite that was not in general either graphite composite or carbon fibre reinforced plastic (CFRP). As Stijnman used an existing technique to determine these elastic constants, reviewing this work served no real purpose and so the decision was taken not to review. Similar decisions taken on reviewable literature were at the discretion of the author and as such, the reviewed literature presented in this work, while including most all seminal works, does not include every feasible publication associated with immersion based through transmission technique.

In terms of review structure and to ensure efficiency, the early works (1970‟s -1980‟s) are often given more attention in certain areas than later works. The main reasons for this approach are a) this period was a significant period for the development of the through transmission technique and b) many of the techniques developed in this period are still used today and so there is no need to repeat discussion in later papers. As such, from 1980‟s onward if no new knowledge was presented within literature relating to sample size, propagation direction etc. then these areas did not always necessarily require discussion. It should be stated that this decision did not prevent any work from being reviewed nor did it prevent specific works from receiving more attention than others. For instance, works that broach new measurement techniques may warrant more depth than publications that use existing measurement techniques.

Further, section 5.4 documents information tables which outline various contributions to knowledge from the authors in this review. However, owing to the large amount of findings documented within the review, a few points are first required to be addressed. The first point of merit is that more than one table exists. That is, findings are not all contained within the one table. Table 58 documents the

1970‟s - 1980‟s, with Table 59 documenting the 1980‟s – modern era. This decision has two clear benefits 1) findings are able to be presented in a more manageable format and 2) a quick way to access the contributions from both time periods is presented. The second point of merit is that not all information presented in the literature review is documented within the tables, that is, tables 58 and 59 are not meant to be used as a substitute for the literature reviewed in this chapter. Thus, the tables present only a recap of the contributions to knowledge from a respective publication. A third point of merit building on both points 1 and 2 is that not all findings from the literature review

are documented within the tables. For instance, Table 59 does not acknowledge whether publications from the period 1980 onward determined the full set of elastic constants. Table 58 demonstrates that determining elastic constants is achievable and so including this information in Table 59 was considered to be of no merit.

2.3 Literature review

One of the earliest recorded events of where ultrasonic wave velocity measurements are used to determine all the elastic constants of a fibre composite was by (Zimmer and Cost, 1970). Alongside determining the complete set of elastic constants for a unidirectional composite the authors also sought to validate earlier theoretical predictions developed by previous authors. The type of sample used in this study was Scotchply 1002, a glass reinforced epoxy („E" glass fibres with a 1002 epoxy resin). The density, average fibre diameter and fibre volume fraction of this material was recorded as 1.9 g cm^{-3}, 0.011 mm and 0.49 respectively. It is also recorded that while the unidirectional composite had a random fibre array (fibres were somewhat randomly orientated per volume area), large areas were recorded as tending towards hexagonal symmetry and so the material was considered transversely isotropic, thus only 5 elastic constants were required to determine the mechanical properties. The method used by the authors to determine the elastic constants was the ultrasonic pulsed through transmission technique. In this arrangement the test piece is placed between two transducers and the length of time taken for a pulse to leave one transducer and arrive at the second transducer was recorded. The system used by the authors is given in Figure 67.

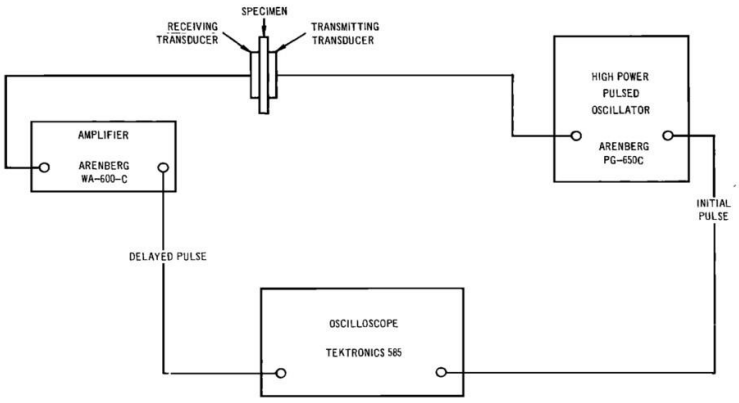

Figure 67 - Pulsed through transmission set up used by (Zimmer and Cost, 1970). *Reprinted with permission from Zimmer JE, Cost JR. Determination of the elastic constants of a unidirectional fibre composite using ultrasonic velocity measurements. Acoust Soc Am; 47: 795–803.Copyright 1970, Acoustic Society of America*

To determine the five elastic constants both longitudinal and transverse waves were propagated through the test piece in different directions and polarizations relative to the fibre direction. To facilitate this requirement, the authors used various samples which were cut from a larger piece of composite (larger size stated as 0.31 inches thick); the samples used in the study had fibre direction angles of 0º, 15º, 30º, 45º, 60º, 75º and 90º to the sides of the test piece. It is of merit to note that although 7 samples were created, only 3 were required to allow for the determination of elastic constants. The four remaining samples, 15º, 30º, 60º and 75º were used by Zimmer and Cost to validate the ultrasonic velocity method. The transducers used were stated as being quartz, and were bonded to each end of the test piece using Salol (phenyl salicylate). The frequency used for these tests was noted as 5MHz with the authors stating that this frequency was chosen to reduce interactions between the wave and the fibre (for a wavelength approximately equal to fibre diameter unwanted interactions can occur) and also because attenuation increases with frequency – although quite high attenuation was still recorded in each sample. The samples were of various thicknesses and this was shown not to have a large effect on the velocity measurements.

To determine C_{33} and C_{11} the authors state that longitudinal waves are propagated in the fibre direction and at right angles to the fibre direction respectively. To determine C_{44} and C_{66} (noting that C_{66} is not independent but instead relies on C_{33} and C_{23}) transverse waves were propagated perpendicular to fibre direction and polarized in and normal to the plane of the fibre respectively.

Additionally C_{44} was determined by propagating a transverse wave in the direction of the fibres. However, this proved to be an inaccurate method for measuring C_{44} and so the value for C_{44} was taken from the perpendicular measurement. The last elastic constant, C_{12} was quoted as being determined through propagating a longitudinal or transverse wave at 45º to fibre direction. This process resulted in quasi-wave propagation (particle deviation from equilibrium is not parallel or perpendicular with propagation direction for a quasi-wave) with wave polarization for quasi-transverse waves recorded in the plane of the fibre and propagation direction.

The authors documented results from theoretical models (outside the scope of this review) and found close agreement with the theoretical values and ultrasonically measured values. In relation to elastic constant error, which resulted from a 2.5% and 1% error in velocity and density measurements, the elastic constants accuracy varied. These results are recorded in Table 50.

Elastic constant	Experimental error (%)
C_{11}	6%
C_{12}	100%
C_{23}	15%
C_{33}	6%
C_{44}	6%

Table 50 - The elastic constants and associated experimental error derived from using ultrasonic velocity measurements on Scotchply 1002 (Glass fibre composite) adapted from (Zimmer and Cost, 1970)

It is also the case that Zimmer and Cost recorded both a positive and negative value C_{12}; the explanation provided by the authors was that the equation for C_{12} contained a square term, thus from the experiments conducted, there was no way in knowing which value to select. Ultimately, the authors opted for the positive value, noting that this value provides a more accurate result in relation to the theoretical predictions for material of hexagonal symmetry.

The penultimate area investigated by Zimmer and Cost was dispersion effects, noting that the additional samples which recorded angles of fibre direction to the side of test piece of 15º, 30º, 60º and 75º were used. When discussing shear waves polarised at right angles to the plane of the fibre, the authors state that a straight line will be produced if the stiffness associated with propagating a shear wave from 0º - 90º, with respect to fibre direction is plotted against the squared sine of the angle of propagation, with respect to fibre direction. Zimmer and Cost outline that the straight line

relationship is not recorded by experiment and deviates owing to dispersion effects - they state that from 0º the dispersion effects increase until a maximum, at about 15º from fibre direction is reached. After 15º, a decrease in dispersion effects was recorded until the angle of 90º was reached. The authors also demonstrate that when the angle of propagation to fibre reaches 45º, dispersion effects are approximately 30% (noting that C_{12} is determined using wave propagating at 45º) and for the samples of 60º and 75º dispersion caused the phase velocity to be increased by less than 15º. These results are documented in Figure 68.

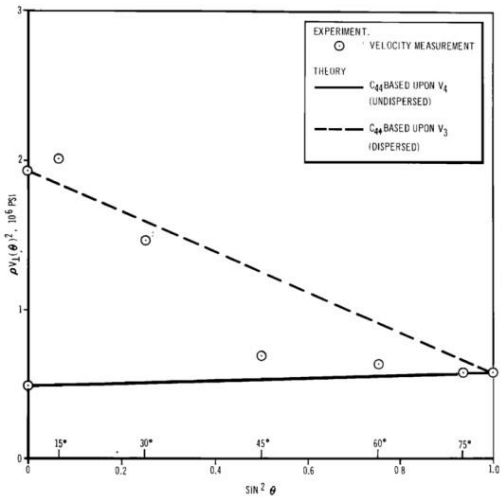

Figure 68 - Dispersion effects recorded by Zimmer and Cost when propagating shear waves polarized at right angles to the fibre. At angles of propagation to fibre direction of less than 45º (excluding 0º) noticeable dispersion was recorded. *Reprinted with permission from Zimmer JE, Cost JR. Determination of the elastic constants of a unidirectional fibre composite using ultrasonic velocity measurements. Acoust Soc Am; 47: 795–803.Copyright 1970, Acoustic Society of America*

The authors record a similar analysis when examining dispersion effects associated with longitudinal waves and found that dispersion was less severe (around 5% for velocity), noting that generally velocity increased for angles < 20º and decreased for angles >20º. Note also, that when quantifying dispersion effects for shear and longitudinal waves, the two values of C_{44} (the accurate one obtained from 90º to fibre axis propagation and the one obtained from 0º to fibre axis propagation) was used by the authors.

Lastly, Young‟s modulus as a function of fibre angle was also studied noting that the theory discussed was based on a single crystal material. Zimmer and Cost found that Young‟s modulus, derived from experimental elastic stiffness constants and equations found in single crystal theory, was within 15% of theoretical values calculated using

existing models thus further verifying ultrasonic velocity as a viable method to determine the elastic constants of glass fibre composite. It was for the first time demonstrated by Zimmer and Cost that using an existing ultrasonic velocity technique (previously used to investigate single crystal materials), the full set of elastic constants for a transversely isotropic glass fibre composite could be determined. Further, the authors also documented the associated stiffness when propagating both shear waves and longitudinal waves through material with fibre angles of 0º, 15º, 30º, 45º, 60º, 75º and 90º and that Young‟s Modulus could be determined using the experimentally derived elastic constants. Thus, ultrasonic velocity measurements were presented as an effective way to determine the elastic properties of a material. While this work is held in high regard and precedent setting, there were issues with the publication. Problems such as a) glass fibres (opposed to carbon fibres) were used b) the accuracy of result was good but could be better (C_{12} was recorded as has having uncertainty of 100%) and c) multiple samples of composite were required to conduct these tests. Looking specifically at the last concern, it can be said that even though the test is nondestructive (test piece not destroyed) the original larger section of composite was required to be cut into smaller sections to create multiple test pieces, ergo there was still a large degree of destructive testing in this system.

Developed at approximately the same time, circa 1970, was an alternative system devised by (Markham, 1970). Published in the same month, Markham presented a system in which the elastic constants of a fibre composite were able to be determined without any initial destructive operations required to be conducted on a test piece, i.e. only 1 sample is required. Similar to (Zimmer and Cost, 1970), the sample used in this study was unidirectional composite exhibiting transverse isotropy and so therefore again only 5 elastic constants were sought. Markham‟s study uses carbon fibres, as opposed to glass fibres, regarding the sample specifics, other than a density quote of 1671 kg m^{-3} Markham simply refers to the sample as a „typical carbon fibre-epoxy resin composite‟.

Looking now at Markham‟s method, similar to (Zimmer and Cost, 1970), the ultrasonic velocity principle is again adopted as the basis for determining the elastic constants. The novelty in Markham‟s work is that a single sample is rotated on an axis to allow for an incident beam to strike the surface at a given angle and therefore producing a refracted wave at a given angle through the material. That is, the pulse transmission system is again deployed but critically the sample is not held rigid but

instead mounted on a turntable with both transducers and turntable immersed in a coupling medium, typically water.

An additional level of complexity is thus introduced; in terms of wave propagation, water only generally permits longitudinal waves and so to propagate transverse waves in the sample, mode conversion (dictated by Snell‟s law and created by turntable movement) is required. The apparatus used by Markham is documented in Figure 69 with Figure 70 documenting a simplified version of the rotatable turntable system.

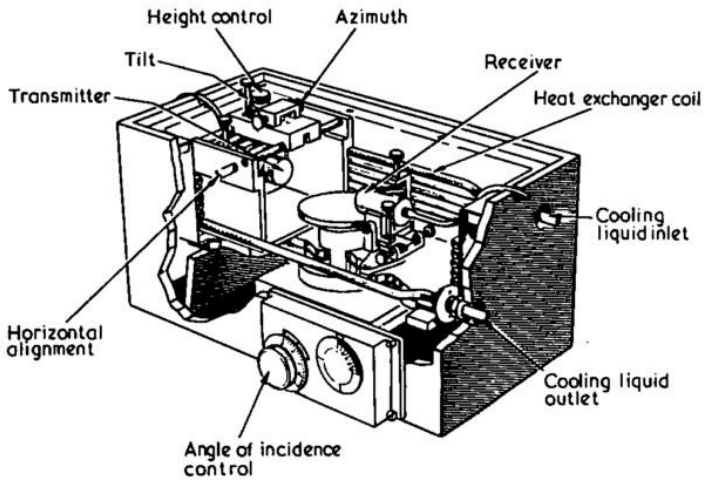

Figure 69 - General representation of the immersion based through transmission system. *Reprinted from Composites, Vol 1 / edition number 3, Markham, M. F., Measurement of the elastic constants of fibre composites by ultrasonics, Pages No 145-149., Copyright (1970), with permission from Elsevier*

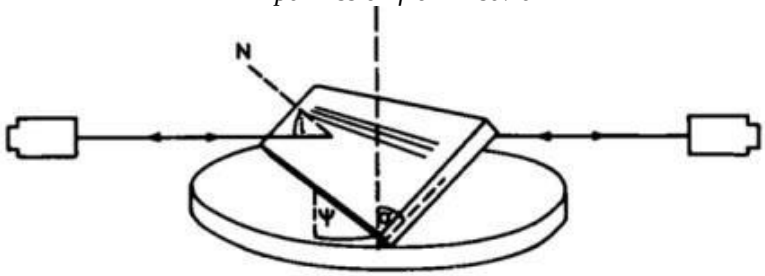

Figure 70 - General representation of transducer placement and of the rotatable turntable. *Reprinted from Composites, Vol 1 / edition number 3, Markham, M. F., Measurement of the elastic constants of fibre composites by ultrasonics, Pages No 145-149., Copyright (1970), with permission from Elsevier*

The transducers in this work were not identified however the transducer frequency was stated and discussed. To avoid (as much as possible) aforementioned interactions between the wave and the fibre and to allow for the assumption of an infinite medium, Markham states, similar to (Zimmer and Cost, 1970), that the wavelength should be larger than the fibre diameter but smaller than thickness of the sample. He develops this argument further than (Zimmer and Cost, 1970) and states that owing to transverse and longitudinal waves having the potential to travel at different speeds (Markham quotes that the potential exists for speeds to range from 1600 m s^{-1} to 12000 m s^{-1}), then to satisfy bulk wave conditions, transverse and longitudinal waves may need to be used at different frequencies. Thus, the frequency spectrum for operation ranged from 1.25 MHz to 5 MHz.

A pulse of 1 μs with a repetition rate of 1 kHz was selected along with a digital delay timing system, accurate to $\pm 1x10^{-9}\, ns$, to record time of flight measurements between transmitter and receiver (both with and without a sample in between). Similar to (Zimmer and Cost, 1970), the nature of the waves required in this study were a) two longitudinal waves propagating along fibre direction axis and a direction perpendicular to this axis, b) two different transverse waves propagating perpendicular to the fibre axis and c) a longitudinal or transverse wave propagating at 45º to fibre axis with polarization in the plane of the fibre.

Markham also puts forward an additional technique to allow for transverse waves to propagate through a composite at normal incidence. A prism with a 90º angle is situated on the turntable with the sample bonded to one of the sides of the prism, Markham calls this side AB. When a longitudinal wave is incident at around 18º from the normal at the opposite side, Markham denotes this as BC, a transverse wave will propagate in the direction towards the bonded sample at AB. When the wave reaches the sample/prism interface, it continues (approximately) and thus a transverse wave is propagated within the sample. Under this system, the generating transducer also must act as a receiving transducer due to a liquid boundary being completely reflective of transverses waves. This system is shown as Figure 71.

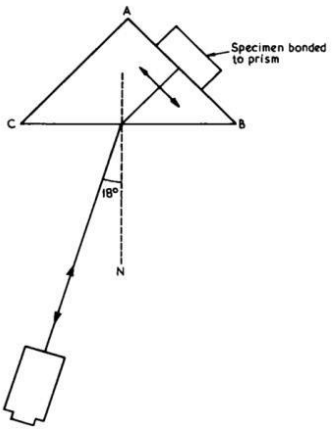

Figure 71 - Generating transverse waves normal to the sample surface using a bonded prism. *Reprinted from Composites, Vol 1 / edition number 3, Markham, M. F., Measurement of the elastic constants of fibre composites by ultrasonics, Pages No 145-149., Copyright (1970), with permission from Elsevier*

Through employing Snell‟s laws and using the equipment in Figure 69, Markham was able to propagate all the required waves and thus obtain the 5 elastic constants for the CFRP sample. Additionally, Markham also investigated the variation in velocity of both transverse and longitudinal waves propagating at varying angles to the fibre axis and found that maximum transverse and longitudinal velocity occur at about 75º and 0º to the fibre axis respectively. Note however, that further analysis following in the same vein as that considered by (Zimmer and Cost, 1970) was not conducted.

In this work, Markham demonstrated that for a single piece of unidirectional CFRP exhibiting transverse isotropic symmetry that the full set of elastic constants could be determined using ultrasound velocity measurements. Using the pulse transmission technique, the novelty in this work was through immersing both the transducers and sample in a water tank while rotating the sample. Further, Markham also presented a method to generate transverse waves at normal incidence to the test piece using a prism.

Despite this work being trend setting, widely accessible and providing an excellent contribution to knowledge, there were however drawbacks with it. These include a) the specifics of the sample are not stated b) the specifics of angle rotation to create transverse waves are not presented (although the required equations for calculations are), c) the equation for C_{13} is not included (the reader is left to calculate it), d) dispersion effects are generally not considered and thus the margin for error is also not generally discussed e) the equipment or apparatus used is generally not discussed and

f) the values for elastic constants obtained have not been cross referenced with mechanical based testing or theoretical modelling. As such, while trend setting, areas to build upon were evident. Both (Zimmer and Cost, 1970), and (Markham, 1970), demonstrate the applicability of the pulse based transmission approach in determining the elastic constants of unidirectional CFRP with the techniques still used today. Thus, the remainder of this review predominately charts the chronological progression within literature of how these methods have assisted in both improving the accuracy of result when determining the elastic constants and when investigating factors relating to the elastic constants of CFRP. Moving forward, this review refers to these methods as the Zimmer and Cost approach, and the Markham method (or the immersion technique).

Expansion of the previous works was by (Smith, 1972), who used the pulse transmission technique to investigate transversely isotropic fibre reinforced plastic (documenting both carbon fibre and graphite fibre based samples). The composite properties sought in this study include the five independent elastic constants C_{11}, C_{12}, C_{13}, C_{33}, C_{44}, the variance in elastic constants of both graphite based fibre composite and carbon based fibre composite (noting that graphite fibres are isotropic but carbon fibre are only isotropic in direction of the fibre), the variance of elastic constants with regard to strength of fibre-matrix bond, Poisson ratio of fibres and the variance of elastic constants with fibre density and thus composite density. Table 51 outlines some general characteristics of the 13 different samples used by Smith.

Sample Property	Information
Fibre origin	Rayon or Polyacrylonitrile (PAN)
Brands of fibre (Yarn)	„WYB‟, „Thornel 25,40,50,50s, 75s and 400‟, „VYB‟, „Courtaulds HTS‟ and experimental based
Sample symmetry	Samples are unidirectional transversely isotropic
Young‟s Modulus (Fibre)	Varies from 6 – 80x10^6 psi
Composite density	Varies from 1.28 – 1.61 g cm^{-3}
Torsional shear strength	Varies from 4.5 – 13.8x10^3 psi
Fibre volume fraction (uncertainty recorded at 2%)	Varies from 0.53 – 0.64
Sample geometry	Face 10 cm^2 , thickness 3-5 mm (0.5% accurate)

Table 51 - Adapted general characteristics of the fibre composite samples used by (Smith, 1972)

Reviewing both the Zimmer and Cost approach and the Markham method, Smith opts for the Markham method to conduct this study. Smith found that although the number of modes able to be generated using the immersion technique is limited, this is still preferable to the lack of accuracy with regards to the alignment of the faces in relation to the fibre and the assumption of sample uniformity present in the multiple sample method.

The immersion technique presented is almost identical to the Markham method with the main difference being that additional transmitting and receiving transducers are arranged in parallel with the standard set up and which were used to trigger the oscilloscope just prior to arrival of wave propagating through the sample. The arrangement used by Smith alongside a representation of waves propagating through CFRP is shown in Figure 72 a) and b)

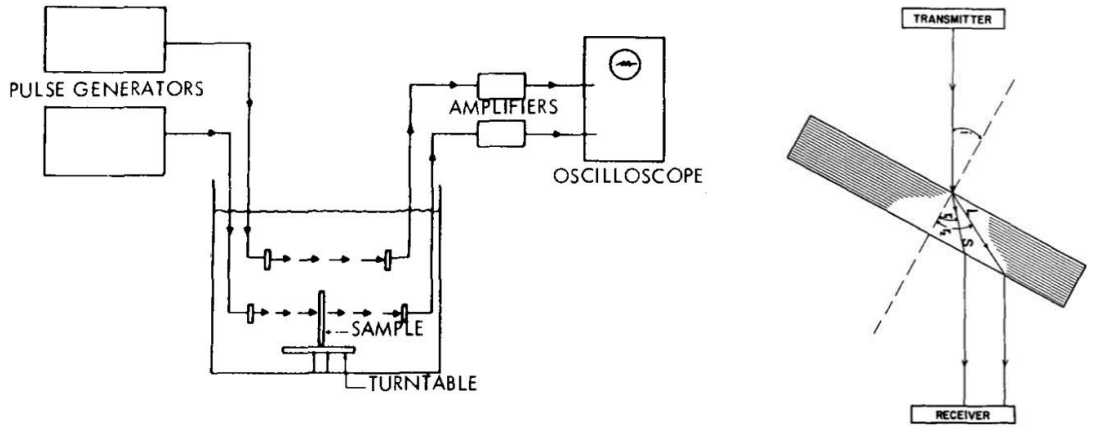

(a) (b)

Figure 72 – Figure (a) documents the experimental arrangement as used by Smith, figure (b) documents the mode conversion process allowing both a longitudinal and shear wave to propagate through the sample when incident waves strike the surface at oblique angles.
Reprinted from Smith RE. Ultrasonic elastic constants of carbon fibres and their composites. J Appl Phys; 43: 2555–2561with the permission of AIP Publishing

The turntable rotates on an axis perpendicular to the ultrasonic beam thus allowing the angle of incidence to be varied with a resolution of 0.1º. For the immersion medium,

Smith opts for distilled water, noting that a large body was used to promote thermal inertia - temperature was recorded constant to about 0.1º over several hours. Similar to previous works the frequency used in this study was in the region of 5 MHz and a Tektronix 555 oscilloscope was also used. Unlike in previous works, when selecting a transducer to act as the receiver, Smith states that compared to the transmitting transducer, a higher frequency transducer was chosen to combat fringe or resonant effects - the transmitting transducer was ¾" in diameter and the receiving transducer was 10 MHz and ½" in diameter.

Similar to previous work the waves used to determine C_{11} and C_{33} were both longitudinal and propagated with the ultrasonic beam both normal to and parallel to the fibre direction. The wave required to determine C_{66} was a transverse wave created in part by placing a principle axis (in this case the 3 axis, the axis parallel with fibre direction) perpendicular to the ultrasonic beam direction and then rotating the sample on this axis. The propagation direction and polarization direction is not explicitly stated by Smith, however, it can be said that principle axis propagation is mentioned (angle to fibre direction stated as being 90º) and that judging by previous work and geometry of the samples, this will be in the 1-2 plane with polarization at a right angle. The two remaining constants, C_{44} and $C_{13,}$ are said to have been created from rotating the 2 axis. Smith does not explicitly state what angle of propagation to fibre direction is used, however, it can be said that the equations do not allow for this angle to 90º; in the case of 90º the equations cited in text force C_{44} and C_{13} to equal 0. None the less, the full set of elastic constants was able to be determined with the equations required to do so presented in the text.

Key findings recorded by Smith are presented in Table 52.

Key Findings (Composite level)	
Accuracy of result	C_{11}, C_{33}, C_{44} and C_{66} recorded as ±3%, C_{13} recorded as ±20%
Impact of fibre Young‟s modulus	$C_{11,}$ C_{33} and C_{66} dependent on Young‟s modulus. C_{13} and C_{44} independent of fibre modulus but varied with fibre type for graphite fibres and were unclear for carbon fibres.
Impact of shear strength (used to evaluate fibre-matrix bond)	Constants do not greatly depend on shear strength
Differences between constants of graphite fibres and carbon fibres*	C_{11} and C_{66} differ greatly for graphite and carbon fibres. Carbon fibres being 10‟s of percent higher than graphite counterparts

*When elastic constants normalised to the same fibre loading, the difference between elastic constants was found to be as a result of the difference in properties of fibres and not through loading effects

Table 52 - Key findings on the composite level, adapted from results by (Smith, 1972)

Additionally, using the composite ultrasonic velocity measurements and modelling techniques Smith studied individual fibres and was able to determine the Poisson ratio and Young‟s modulus of the fibres. Smith also used small scale X-ray analysis to average porosity for certain carbon fibre samples and sought to correct the fibre properties accordingly. Attention can be turned to text for the various findings regarding the specific differences between carbon fibres and graphite fibre elastic constants.

Further, Smith also investigated the validity of theory and essentially repeated the same experiment as conducted by Zimmer and Cost (Zimmer and Cost, 1970), to determine the curve associated with propagating transverse waves at angles of 0º to 90º to fibre direction. Note, that in reality propagation excluded 0º and 90º and only covered the angles of approximately 15º - 75º; it is presumably the case that accurate measurements of below 15º and above 75º were not able to be made using the immersion technique, however the author does not generally elaborate on this point. Smith confirmed the observations from (Zimmer and Cost, 1970), that C_{44} obtained from propagating a transverse wave at 90º to the fibre direction allows for better agreement between the experimental and the theoretical. Smith‟s experimental and theoretical result for C'_{55} (a variable presented in the text), is given as Figure 73.

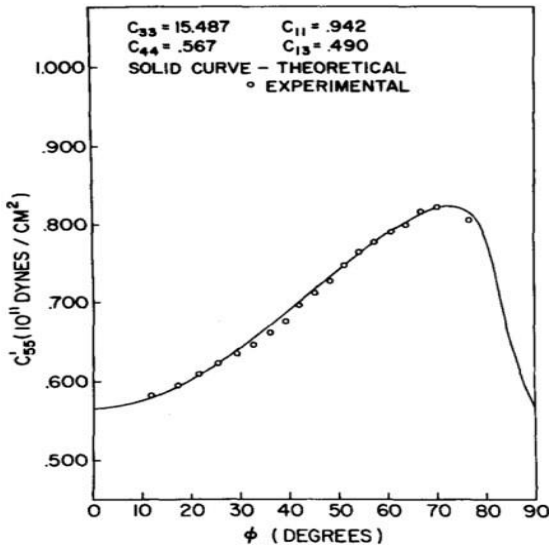

Figure 73 – Documenting the findings from Smith that a close relationship to the theoretical is recorded using the C_{44} value obtained from propagating a transverse wave at ^{0} 90 to fibre direction. Note that the variable C"$_{55}$ used by Smith was dependent C_{11}, C_{13}, C_{33} and C_{44}.

Reprinted from Smith RE. Ultrasonic elastic constants of carbon fibres and their composites. J Appl Phys; 43: 2555–2561 with the permission of AIP Publishing

It is of merit to note however that Smith uses either a carbon fibre or graphite fibre composite (Smith does not clarify) to investigate C_{44} while Zimmer and Cost used a glass fibre composite.

With regards to the values of C_{44} not arising from 90º wave propagation, Smith, in the opinion of the author, is slightly ambiguous. When describing the theoretical predictions associated with using the other values of C_{44}, he states that the good agreement between the theoretical and the experimental would not have resulted if the angle of deviation changed by as much as 5º between 0º and 90º. To understand this statement, two questions are required to be answered, 1) is the value of C_{44} determined from the 90º measurement the same as the one recorded from measurement at 0º? And 2) is the value of C_{44} calculated from wave propagation at 90º successively altered by introducing progressive steps of 5º all the way from 90º to 0º, thus forcing the most accurate and inaccurate method of determining C_{44} to be 90º and 0º respectively? Going by the work of both (Zimmer and Cost, 1970) and (Markham, 1970) , for the large part the probable answer to question 1) is no and the probable answer to question 2) is in general yes (note, that the most inaccurate measurement may actually result from 15º to fibre axis and that at 0º and 90º the velocities may be far more closely related). Further, although C_{44} was calculated at 90º for the theoretical experiments by Smith, Smith also states that C_{44} was calculated using an equation which does not permit C_{44} to be calculated at 90º. To help in this regard, adopting a similar approach to that of (Zimmer and Cost, 1970), i.e. documenting more than one value of C_{44}, or indeed taking a new approach and presenting the determination of C_{44} as a function of propagation angle to fibre axis would have been of considerable merit.

Similar to previous authors Smith obtained the full set of elastic constants for transversely isotropic material. Smith took the previous work further, in that he found that ultrasonic velocity measurements could be used to determine not only the elastic constants outright but also their dependence on a) the fibre Young"s modulus and b) the fibre matrix bond, while at the same time comparing both graphite fibre and carbon fibre based composite. Further, Smith demonstrated that modelling could be used to

theoretically predict the fibre engineering constants such as Poisson ration and fibre modulus. Additionally, the elastic constants were shown that they could be corrected for porosity.

Smith comprises a solid and comprehensive body of work that clearly outlines the applications of velocity measurements. It is also the case that improvements could have been made to this paper; quasi-wave analysis was not generally discussed, certain propagation directions for waves (waves corresponding to C_{44} and C_{13}) were ambiguous and the method of determining C_{44} could have been presented better to provide more clarity on the issue. Lastly, Smith mentions that a higher frequency transducer was used as the receiver to combat any fringe or resonant effects but does not quantify or discuss the implications of these effects in the text.

In 1973, a further investigation into the applicability of ultrasonic velocity measurements with regards to CFRP was by (Dean and Lockett, 1973). The authors demonstrated that not only could the full set of elastic constants be determined, but also discuss the applicability of using ultrasound to identify and quantify specimen homogeneity, symmetry, degree of fibre misorientation, viscoelastic properties and associated theoretical problems (note defect detection is also discussed but this generally does not concern velocity measurements in this context). The samples used by the authors were quoted as being transversely isotropic high modulus carbon fibre reinforced epoxy with a front surface of 18 by 11 mm and a variable thickness of 12 mm, 5 mm, 2,6 mm, 2 mm and 1.6 mm. The density was quoted as being 1.668 g cm^{-3} for sample thickness of 12 mm and 1.670 g cm^{-3} for the remaining four samples.

The approach taken by Dean and Lockett was the Markham method using in fact, the same type of equipment as used by Markham. That is, at the time of respective publications Dean and Lockett and Markham both worked and conducted experiments at the National Physics Laboratory (NPL) in Middlesex, England; Figures 69 and 70 outline the measurement apparatus. Additional experimental information not supplied by Markham but supplied by Dean and Lockett is that the angle of incidence may be varied by ±0.1º precision and that the initial alignment of the specimen, relative to the turntable, has ±0.5º and ±0.1º precision for the 1.25 MHz and 5 MHz transducers respectively. Additionally, the speed of longitudinal waves in the immersion liquid (presumably water, not explicitly stated) was taken from tables and not verified through experiment, density was taken from measurements conducted in both air and

in water and that the total experimental time per sample was approximately 30 minutes (with the data analysis performed on a computer).

Similar to Markham, Dean and Lockett documented the variation in velocity changes with respect to angle of propagation in the plane containing fibre direction, given here as Figure 74.

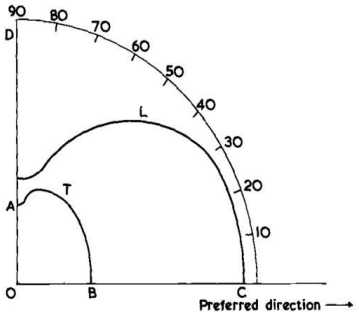

Figure 74 - Variation in velocity of transverse waves and longitudinal waves propagating in the plane containing fibre direction. *Reproduced with permission from Dean GD, Lockett FJ., Determination of the Mechanical Properties of Fibre Composites by Ultrasonic Techniques. Anal Test Methods High Modul Fibres Compoistes ASTM STP 521, Am Soc Test Mater; 326–346., Copyright ASTM International 100 Barr Harbor Drive, West Conshohocken, PA 19428*.

Additionally, the authors offer further discussion on C_{44}. They state that C_{44} is not able to be measured directly from experiment (90º velocity is different than 0º velocity) and in a similar but not identical way to (Zimmer and Cost, 1970), Dean and Lockett, further provide discussion on extrapolating C_{44} from experimental results.

The authors recorded the elastic constant accuracy as a standard deviation; C_{11} and C_{22} recorded as less than ½ %, C_{44} and C_{66} recorded less than 1% with C_{12} being recorded as uncertain. These results provide an improvement on those outlined by (Zimmer and Cost, 1970), however the previous authors did not use CFRP. The omission of an uncertainty value for C_{12}, by Dean and Lockett was based on the premise that a quasi-transverse wave, polarised in the plane of the fibre, has no direction of propagation in which the velocity dependence on C_{12} is significant.

Thus, to gauge the accuracy of C_{12} then extremely accurate measurements of the other required constants (noting that quasi-waves are typically dependent on multiple constants) would be required. This is similar to findings that one draws from (Markham, 1970) who also allude to this fact.

Building on the concept of accuracy, it was highlighted by the authors, that while accuracy of result typically relies on the angle of incidence or the measuring

equipment, in reality the accuracy is often limited by the quality of the sample, (localized areas of voids, dissimilar fibre alignment and packing sequence all playing a role). It was also reported by the authors, as verified through experiment and similar to (Zimmer and Cost, 1970), that the thickness of sample did not generally play a significant role in velocity measurements; very little changes in C_{11}, C_{22}, C_{33} and C_{44} were observed when reducing the sample thickness - plane body wave behaviour was assumed, i.e. specimen dimensions were kept above two wavelengths. Further, the authors also found that when propagating waves in the fibre direction that even if the thickness was comparable or perhaps less than pulse wavelength, no significant pulse distortion occurred. Coupling this with the fact that the velocity difference between body waves and waves in proximity to a free surface was found to be around 1%, Dean and Lockett found that data relating to mode changing as the sample thickness was reduced was inconclusive. Additionally, Dean and Lockett discussed areas only inferred by preceding authors. While (Smith, 1972), presented findings on the relationship between fibre content and elastic constants, but focused more on gauging Young‟s modulus, Dean and Lockett investigated the variation in elastic constant with fibre volume content – noting that significant scatter (inferring void content) was present in some results.

Further, the authors also reported a method of determining homogeneity by conducting measurements along the same axis but at different points of the sample while also reducing the beam size. The authors state that when propagating a wave along the fibre axis in unidirectional fibre, variations in velocity would be indicative of localized variations of fibre content and alignment. Expanding on this, the authors cite earlier work, (Dean, 1971), that sought to determine the elastic moduli of disorientated fibres in composite. The authors also put forward a strategy for gauging the material symmetry through the use of velocity surfaces and crystallographic theory and they also conducted a brief analysis of the viscoelastic properties of composites – both areas not touched upon by preceding authors reviewed at this point.

Dean and Lockett, conducted similar tests to those of Markham and presented additional information relating to the test apparatus. The full set of elastic constants were able to be determined with good degree of accuracy, however, unlike previous published works, the authors failed to present accuracy statistics for C_{12}. Also, in addition to earlier work the authors documented that C_{44} was only able to be inferred from velocity measurements; however, based on collective finding between

publications it can be said that the correct value of C_{44} is the value associated with waves at 90º. Dean and Lockett also discussed the applicability of using ultrasound to investigate fibre orientation, viscoelastic effects and symmetry, aspects which are only inferred by other authors. There is however, generally no significant investigation or findings presented in this work regarding these concepts (excluding the references cited), but applicability was stated none the less. At this point, a sidestep back to 1971 to review (Dean, 1971), is appropriate. This work covered both the immersion technique and the development of a model to investigate disorientated fibres. As Dean only presents a general overview of the immersion technique as used by, (Markham, 1970) and not generally any significant findings such as the mathematical framework, the decision was taken to first establish the velocity based elastic constant determination techniques from literature prior to evaluating the disorientation model in this work. Also, while the disorientation model falls outside the scope of this review, determining the elastic constants of a composite rely on correct fibre orientation and so the decision was taken to review this work.

Taking into account that on occasion composite may be designed to deviate from a uniaxial and instead be designed to meet the requirements of a particular load; Dean investigated the applicability of using velocity measurements to determine the degree of fibre orientation for a given CFRP test piece. The fundamental premise presented in this study was to develop a so called orientation function, that is, if the standard method to determine elastic constants is performed on a uniaxial test piece (aligned and misaligned), the constants could then be compared and be related through fibre orientation functions.

To establish the orientation function, Dean documents a simple model of a short chopped transversely isotropic composite fibre in which the composite is broken down into individual elements - noting that each element contained a single fibre surrounded by an irregular prism of matrix. Each element was perfectly bonded together (no voids) and thus a model composite was visualized as comprising individual elements – noting that each element recorded identical elasticity around the fibre axis. On a composite level Dean selected the 3 axis as the axis of preferred direction and on an individual cell basis the 3 axis was also the axis of fibre direction.

Having established the specimen geometry, to define the elastic constants, in terms of the coordinates used to define a particular cell, the constants of a cell were rotated through angle θ. Thus a new constant, which is generally dependent on more than one

original constant, was provided and so the elastic constants of a cell were able to be expressed in terms of the elastic constants of the specimen via a directional cosine relationship. It is of merit to note that in this model disorientation is recorded in only in one plane (1-3), hence only one elastic constant rotation was required in this instance. Having shown that a single cell was able to be expressed in terms of the elastic constants of the specimen, the next stage was to present the complete set of elastic constants for the specimen in terms of the total contribution from all cells.

To achieve this, the elastic components of the specimen were taken as an average with an assumption that for a given stress, each unit will experience identical strain. Obtaining the average elastic constant value (mathematically) was done by expressing a single cell in terms of the elastic constants of the specimen and then using the average value for angle of deviation to provide the average value of specimen elastic constant. Dean expresses θ in terms of a normalised probability distribution (noting the probability between 0 and π was equal to 1) and so was able to present the complete equation set required to determine the average elastic constants of the specimen in terms of an individual cells elastic constants and the average value of the directional cosines.

Further, if the elastic constants of an individual cell are equal to those of a continuous homogeneous transversely isotropic fibre sample with no voids, then the equations presented by Dean, relate the elastic constant of disorientated fibre to the elastic constants of uniaxial fibre multiplied by the average directional cosines, noting that these cosines are now referred to as orientation functions. It is also of merit to note that although 5 orientation functions exist, only two are required (the law of cosines allows the remainder to be determined).

Testing the hypothesis, the technique adopted by Dean was the Markham method, noting that both the standard rotation technique and the prism technique were adopted. The chopped fibre specimens were rectangular samples with the long axis being either perpendicular or parallel to preferred fibre direction. The dimensions (length, width, breadth) of the samples were recorded as being approximately 5 by 1 by 0.08 cm or 8 cm by 1.3 by 0.15 cm. Fibre volume fraction for the chopped fibre samples was recorded as approximately 40%, however, a similar continuous composite (required to determine unidirectional elastic constants) was not able to be located and so various samples with degrees of fibre volume fraction were selected and extrapolated to 40% fibre fraction. The results obtained by Dean infer that the samples used in this study

were highly orientated (values approaching 1 were recorded for orientation function) principally because C_{33} was recorded as being almost equal to that of continuous fibre, and that the main factors affecting C_{33} are fibre volume and orientation.

(Dean, 1971), documents an interesting body of work with the average elastic constants for a disorientated transversely isotropic CFRP, with disorientation in one plane only, able to be determined. Areas of improvement however, can be found - samples used in this study were of particular dimensions and quality and so when determining the elastic constants of the thinner samples of chopped fibre, it was not possible to successfully propagate a bulk wave in the 1 direction thus C_{11} could not be determined. Also, for certain chopped fibre samples only C_{33} from longitudinal wave propagation was able to be recorded. Continuous fibre samples were also recorded as being poor quality such that, C_{44}, C_{22}, C_{55} and C_{66} were not able to be accurately reported, with C_{44} being determined through a theoretical model. Additionally, C_{66} in some cases was not reported at all and in other cases was determined using the lower accuracy prism technique.

It is also noteworthy, to highlight the subtle difference between findings from this text and that from (Zimmer and Cost, 1970), who reported findings on Young‟s modulus in terms of fibre orientation. The key difference is that Zimmer and Cost used uniform crystal disorientation as a function of Young‟s modulus but Dean presented the average elastic constants (elastic constants may be used to determine Young‟s modulus) as a function of the average disorientation of an individual cell. The system presented by Dean is probably more realistic in that all fibres would likely not be disorientated in the same direction, but is no means the finished article. For instance, disorientation in only one plane is considered, the chopped fibres samples considered were highly orientated and only the average elastic constant (as opposed to a say a standard deviation from true value) of the specimen is presented. Moving forward to 1974, (Wilkinson and Reynolds, 1974), sought to further investigate the propagation of shear and longitudinal waves over multiple directions in a unidirectional composite. Although previous work, (Zimmer and Cost, 1970), – noting that this text is not discussed by the authors - had previously shown that dispersion phenomenon effects shear and longitudinal wave propagation to different degrees depending on angle of propagation to fibre direction in glass fibre based composite, Wilkinson and Reynolds sought to better understand this process on CFRP. The authors state that previous work, (Reynolds, 1971), suggested that internal reflections may interfere with longitudinal

wave propagation and alter velocity, thus in this text, shear and compression waves were propagated in various directions with action taken to reduce internal reflections as best possible.

The sample used by Wilkinson and Reynolds was a high modulus unidirectional fibre based composite in the shape of a disk. The sample was machined from a larger rectangular composite and measured 140mm in diameter and 23mm in thickness. 57% fibre volume and a density of 1.62 $x10^3$ kg m^{-3} were also recorded. Two cylindrical piezoceramic probes with frequencies of 0.5, 1.25 and 2.5 MHz were also used. For shear waves, propagation was achieved through the immersion technique and also a slight variation on the prism technique as demonstrated by (Markham, 1970) - noting that Wilkinson and Reynolds denote this prism techniques as the angled probe approach - and also by adopting the Zimmer and Cost approach. Thus, shear waves were able to be propagated at various angles to fibre direction and polarized in the plane of the disk and normal to the plane of the disk. In the case of longitudinal waves, these were propagated using the angled probe approach; namely, a shoe prism (concave) bound to the disk and transducer using glycerine. Figure 75 outlines the general composite and typical wave propagation direction to fibre axis arrangement in this work.

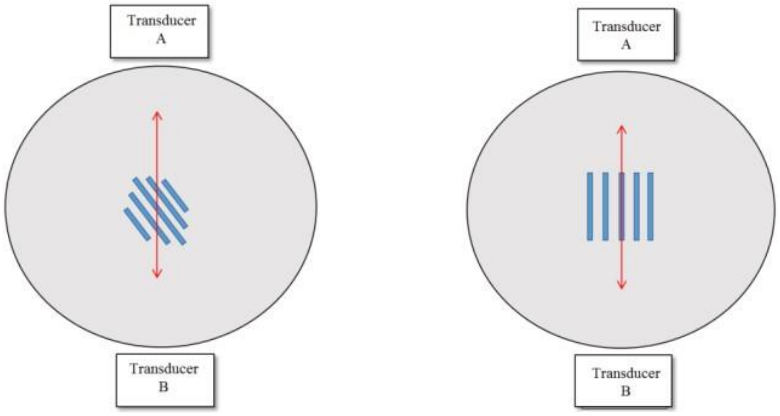

Figure 75 - The sample and fibre direction for a stationary and rotated case is shown. The arrow indicates direction of wave propagation. Smaller non diameter (chord) paths were also used and compared with longer paths to eliminate effects of internal reflection.

As expected, a full set of elastic constants was recorded by the authors. C_{11} and C_{33} were recorded through longitudinal waves while C_{44}, C_{66} and C_{13} were recorded

through transverse waves – noting also, similar to previous work the authors encountered a degree of difficulty in accurately measuring the known problematic elastic constant, C_{13}. Similar to (Smith, 1972), the expected curve outlining the variance in elastic stiffness in relation to the angle of fibre direction to propagation (i.e. 0º - 90º) was also produced. Similar to what was demonstrated by (Smith, 1972), out with 0º and 90º only the angles of approximately 15º - 75º were able to be recorded accurately.

In this instance, the authors provide no discussion on the potential error in C_{44} with regards to which angle of propagation to fibre direction is selected; going by previous works however, the value of C_{44} used by the Wilkinson and Reynolds was most likely the more accurate value derived from propagating the transverse wave perpendicular to the fibre axis.

Also, the theoretical prediction of the other transverse wave (polarized at a right angle to the plane of the fibre) was also produced in this work. The authors found good agreement with the expected behaviour based on theoretical predictions from (Musgrave, 1954b), thus confirming a tacit implication from the work of Smith (Smith, 1972); the predictions from Musgrave are able to accurately describe the associated elastic stiffness recorded when propagating a transverse wave polarized in the plane of the fibre at an angle between 0 and 90 degrees.

Looking now at longitudinal waves, typically used to determine C_{11} (propagated at 0 degrees to fibre direction) and C_{33} (propagated at 90 degrees to fibre direction), Wilkinson and Reynolds documented that the theoretical predictions by Musgrave are insufficient to accurate describe the elastic stiffness associated with longitudinal wave propagation between 0º and 90º. They found, that out with 5º of principal axis (i.e. between 5º and 85º) the associated elastic constants lie between the rotated Young‟s Modulus (values calculated from using the elastic constants presented in text) and the Musgrave theoretical values for the expected curve (again calculated using the elastic constants presented in text). The authors also documented that the experimental elastic stiffness followed a pattern similar to the rotated Young‟s modulus and not the curve predicted by Musgrave. Figure 76 documents the findings from Wilkinson and Reynolds for both the transverse and longitudinal wave propagation at various angles to fibre axis.

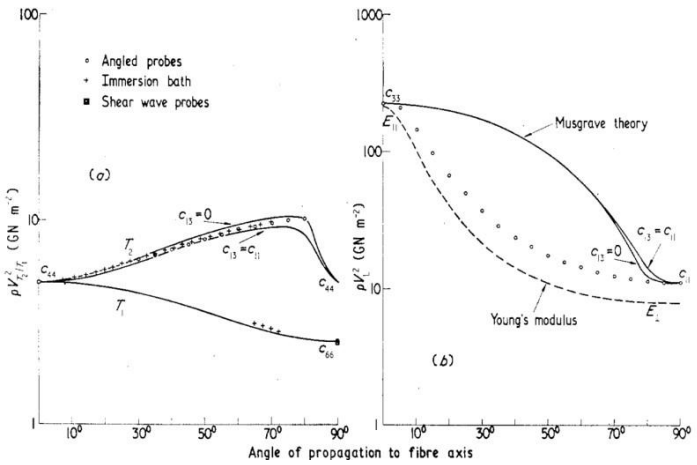

Figure 76 - Figure (a) documents the tranverse wave, figure (b) documents the longitudinal wave. *Wilkinson SJ, Reynolds WN. The propagation of ultrasonic waves in carbon-fibrereinforced plastics. J Phys D Appl Phys; 7: 50–57, © IOP Publishing, Reproduced with permission. All rights reserved*

Regarding the longitudinal wave analysis, the conjecture put forward by Wilkinson and Reynolds was that while Elliot (Elliot, 1973) demonstrated via a goniometer technique that the existence of a quasi-longitudinal wave, predicted by Musgrave, is present within the material, the wave recorded in their experiments was not the same quasi-longitudinal wave. That is, the wave recorded when conducting through transmission experiment is not the Musgrave wave, which quickly attenuates, but instead is another slower wave manufactured within the CFRP sample as a result of the shear bonding of matrix to the fibres; this is denoted by Wilkinson and Reynolds as a pseudo-L wave (noting, that L is previously used by the authors to denote quasilongitudinal).

The explanation of how this wave originates was put forward as follows. Any disturbance at a fibre end causes waves (longitudinal) to propagate along the fibre direction with little attenuation (assuming no changes in fibres structure) occurring. As a result of the high shear bonding of the fibre to the matrix however, the fibres act in this instance as a source of transverse waves - propagated typically at around 80º (this angle recorded in text as producing the fastest velocity of shear waves). These new transverse wave fronts cause adjacent fibres to experience longitudinal waves by reconversion and so the pattern continues producing a somewhat „zigzag“ propagation pattern. Figure 77 is given to assist in demonstrating this type of wave.

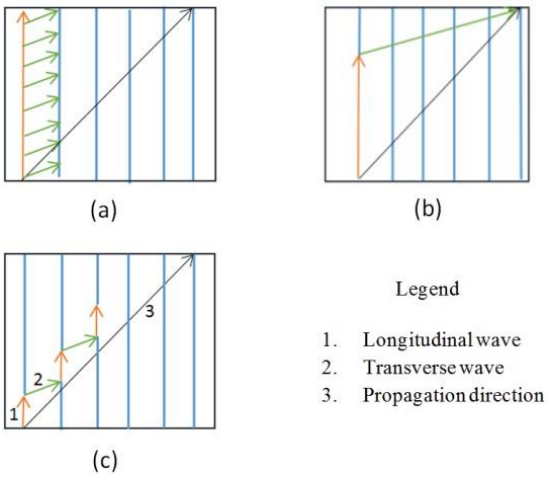

Figure 77 - Figure (a) documents longitudinal waves in fibre direction causing transverse waves at 80º which in turn cause new longitudinal waves in adjacent fibres. Figure (b) documents overall propagation path consisting of both longitudinal and transverse waves. Figure (c) demonstrates that shows that wave conversion as given by (a) is a continuous process.

To demonstrate the pseudo-L wave effect, the authors conducted two experiments; the first experiment incorporated similar samples in the shape of disks with and without a hole excised from the middle and the second experiment involved the transmission of shear waves, converted from longitudinal using CFRP as a mode convertor, into a sheet of metal.

The first experiment found, that for angles of propagation to fibre direction of approximately 25-65º the theoretical prediction (presented in text by the authors) is in keeping with experimental measurements. The study also found that for angles outside this range, the experiments deviated more from the theoretical predictions owing to the hole excised from the sample, thus confirming the hypothesis presented.

Figure 78 documents the results.

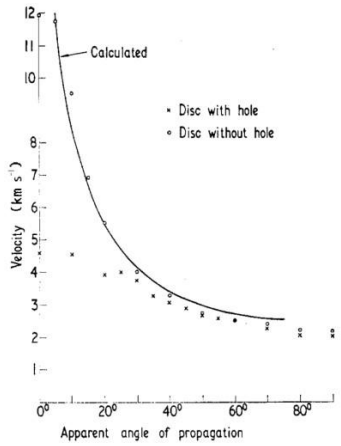

Figure 78 – Variation from theoretical for longitudinal waves in composite disk with hole excised is notable for propagation to fibre direction angles outisde of around 25º - 65º. *Wilkinson SJ, Reynolds WN. The propagation of ultrasonic waves in carbon-fibre-reinforced plastics. J Phys D Appl Phys; 7: 50–57, © IOP Publishing, Reproduced with permission. All rights reserved*

The second experiment demonstrated that CFRP could be used as a reliable converter of longitudinal to shear waves and thus the shear modulus of the metal could be determined. That is, a longitudinal and shear wave could both be propagated within the metal provided (only in the case of the shear wave) the CFRP acted as a convertor.

Multiple contributions to knowledge were recorded by Wilkinson and Reynolds. In the case of shear wave propagation, the theoretical predictions from (Musgrave, 1954b) were found to be an accurate way to predict the associated stiffness when propagating waves in directions ranging from 0º-90º within CFRP. In the case of the through transmission based generation of longitudinal waves, the Musgrave prediction was found not to hold (the quasi-wave attenuates rapidly) and the hypothesis of a pseudo-L wave, comprised of both longitudinal and transverse elements, was put forward. This wave was experimentally verified with the authors also noting that CFRP could act as a reliable convertor of longitudinal to shear waves. This work is also the first recorded to state that the known problematic constant of C_{13} is best recorded using the angled probe, noting that rotation system and direct wave analysis were also both used.

However, limitations are also present within this text. For instance, previous works such as (Zimmer and Cost, 1970), are not referenced or discussed, thus no acknowledgement or comparison of the work shown in (Zimmer and Cost, 1970), which demonstrates that in the case of longitudinal propagation in glass fibre

composite, experimental results are much more closer aligned to the theoretical predications put forward by (Musgrave, 1954b) or (Gold, 1950). It is also the case that Wilkinson and Reynolds could have been clearer on problems associated with determining C_{44} (text documented the value at 0º was the same as the value at 90º, which presumably indicates the 0º measurement is fitted or is extremely close to the 90º measurement).

Wilkinson and Reynolds present a good body of work but also missed out an opportunity to seriously build on previous works. It was not at all mentioned by Wilkinson and Reynolds that previous studies, texts cited in this review, all used transverse (and not longitudinal waves) to determine off axis constants. However, Wilkinson and Reynolds did present the issues concerned with longitudinal propagation in off axis directions within CFRP, ultimately developing more knowledge on the subject matter.

The next publication touches on the, hitherto largely ignored by this review, issue of composite porosity and fibre content; more specifically, an investigation on how to obtain reliable information on the degree of porosity and fibre volume using existing techniques is reviewed. As stated in Table 49, these areas generally fall outside the scope of this review, however it has at this point been documented that elastic constants are directly related to velocity measurements and so relating fibre content and porosity to velocity measurements is thus of interest and therefor this area is briefly discussed - the particular publication of interest being (Reynolds and Wilkinson, 1978).

Consideration was given to discussing previous works on ultrasonic voids and fibre fraction in CFRP, namely (Dean and Turner, 1973; Jones and Stone, 1976; Reynolds and Wilkinson, 1974; Stone and Clarke, 1975) however the decision was taken to review (Reynolds and Wilkinson, 1978) only; principally because (Reynolds and Wilkinson, 1978) builds on these previous works and that ultrasonic void content and fibre fraction, while important for the role it plays on elastic constant quantification, is not strictly the object of this review.

Reynolds and Wilkinson highlight that effective ultrasonic attenuation measurements such as C-Scan have been put forward as a means to identify voids within a composite; however, the authors further state that while these methods are able to identify porous regions, they are not really suited for quantifying void effects - for instance the size, shape and distribution of voids can affect the shear strength in various ways. In this

work, Reynolds and Wilkinson build on the works of (Boucher, 1976, 1975), who presented equations to determine the elastic constants of an isotropic matrix which contains voids – by applying the existing theoretical predictions to analyse CFRP which may contain voids.

The sample used by the authors was quoted as uniaxial orthotropic sections - the idea being that more complicated composites could be created from these sections, should one wish to expand on this work. Transverse isotropy can be considered a special case of orthotropic material in that a plane of symmetry exists which is perpendicular to fibre direction; for orthotropic material this does not exist and so orthotropic material has 9 elastic constants and not 5. Both glass fibres and carbon fibres were used, owing to the scope of this review, the results from the glass fibre analysis will be largely overlooked.

Two varieties of both carbon fibres and epoxy resin were quoted by the authors, thus four different CFRP composites were documented, each having up to 25% of its matrix presenting as randomly distributed spherical voids.

The elastic constants and densities of the fibre and matrix alongside fibre volume fraction of the composite were used by the authors to form theoretical predictions of the velocity. In the fibre direction the predictions indicated that a) velocity varies noticeably for a change in volume fraction (0-70%) b) the effect of matrix porosity is not considered to impact the velocity greatly and c) the velocity has only a small dependence on the type of resin used. When studying wave propagation perpendicular to the fibres, the authors recorded a not so straight forward relationship - wave propagation in this direction is generally dependent on both porosity of the matrix and the fibre concentration. Using the matrix shear and bulk modulus along with the composite density the authors demonstrate that in the case of longitudinal and transverse waves, polarized in the plane of the fibre, the porosity had more effect on the velocity than did the fibre volume. The opposite relationship (not directly polar) was found for transverse waves polarised perpendicular to the plane of fibre in that the fibre volume had more of an effect than did the porosity content. It was also found that the relationship between longitudinal waves and transverse waves (polarized in the plane of the fibre) for type 1 and 2 fibre was not identical, thus, a generalised relationship between two sets of waves was not really able to be established, indicating that effects were to some degree fibre specific. Figures 79 (a) and 79 (b) document these findings from (Reynolds and Wilkinson, 1978).

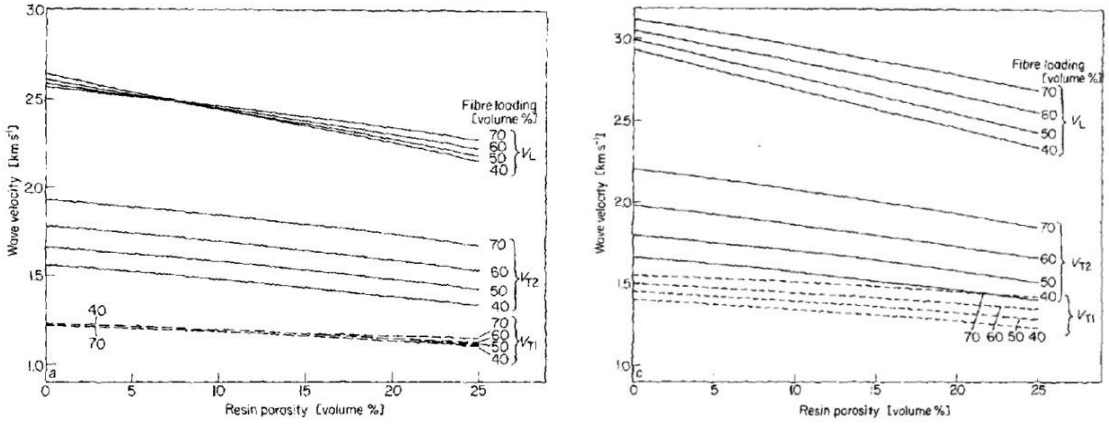

(a) (b)

Figure 79 – Figure (a) documents the variance of velocity with regards porosity content and fibre volume fraction for type 1 fibre using ERLA 4617 resin. Figure (b) documents the variance in velocity with regards porosity content and fibre volume fraction for type 2 fibre using ERLA 4671 resin. *Reprinted from Ultrasonics, Vol 16 / edition number 4, Reynolds WN, Wilkinson SJ The analysis of fibre-reinforced porous composite materials by the measurement of ultrasonic wave velocities, 159-163., Copyright (1978), with permission from Elsevier.*

Reynolds and Wilkinson also conducted similar experiments to those conducted previously on CFRP; waves were propagated in off axis directions through glass fibre composite. For transverse waves the results produced a better fit to the theoretical, for longitudinal waves, the results provided not such a good fit to the theoretical – some direct contact measurements were recorded far exceeding the boundary limit of C13 = 0. These results are similar to what was recorded in (Wilkinson and Reynolds, 1974) in that the Musgrave wave was attenuated strongly and wave propagation resulted due to both longitudinal and transverse motion. It should be mentioned that although similar results to that of CFRP were recorded in this study, the variance of the experimental from the theoretical appears to be smaller for glass fibre based composite. These results are given as Figure 80.

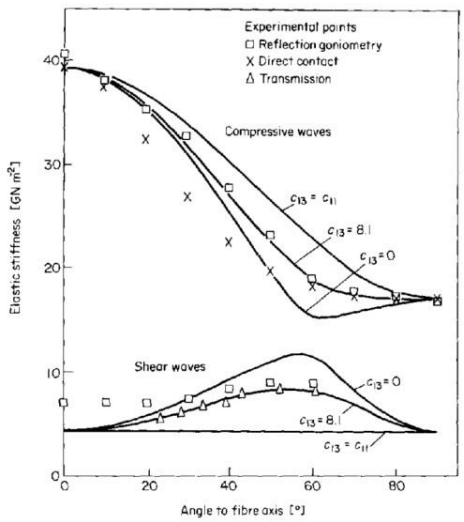

Figure 80 – Variation of stiffness with reference to propagation direction to fibre direction for both shear waves and longitudinal waves. *Reprinted from Ultrasonics, Vol 16 / edition number 4, Reynolds WN, Wilkinson SJ The analysis of fibre-reinforced porous composite materials by the measurement of ultrasonic wave velocities, 159-163., Copyright (1978), with permission from Elsevier.*

Reynolds and Wilkinson outlined theoretical predictions which allow for the porosity and the fibre volume content to be evaluated when propagating ultrasonic waves in uniaxial composite material. Thus, a key aspect missing from previous reviewed works was addressed i.e. along with elastic constant determination, velocity measurements may also be used to indirectly monitoring the CFRP production process (for example, poor production processes can potentially result in more porous materials).

Draw backs with this study include a lack of experimental work to a) demonstrate the theoretical predictions are correct (Boucher previously carried out experimental work but not on CFRP) and b) to provide information on the role porosity plays on the composite elastic constant values (granted, that having shown the velocity this could be worked out if the composite density was known). Additionally, in the case of off axis longitudinal wave propagation there is no quantitative analysis between glass fibre composite and that of CFRP. The inclusion of additional information, would have a) presented the differences in longitudinal wave propagation effects for the two materials more clearly and b) built on the work of (Zimmer and Cost, 1970) – who stated that more research should be geared towards dispersion effects associated with off axis propagation of waves.

The next study reviewed, and the last from the 1970‟s, is (Kriz and Stinchcomb, 1979). The text is similar to (Reynolds and Wilkinson, 1978), in that calculations

relating to fibre volume are used to determine properties of composite with an additional novelty being the exploitation of one of the many seminal theoretical works by Hashin, namely (Hashin, 1972).

The authors manipulated the Hashin equations and wrote these in terms of the composite material properties, such as Young‟s modulus, shear modulus and Poisson‟s ratio. Using an already existing ultrasonic data set from (Dean and Turner, 1973) - those authors calculated the elastic constants of transversely isotropic material - and through curve fitting Kriz and Stinchcomb found that all fibre properties, matching those of (Dean and Turner, 1973), were able to be determined - assuming the fibres were transversely isotropic.

The second contribution to knowledge, having shown that the Hashin equations are suitable to allow for extrapolation of fibre properties, is to use them to determine composite properties. Thus Kriz and Stinchcomb perform ultrasonic velocity measurements and compare the results to those as predicted by the standard (non-manipulated) Hashin equations. The nature of the experiment work conducted was closely aligned to that of (Zimmer and Cost, 1970), noting this text is not cited by the authors, in that the sample was bonded to a receiving transducer and a transmitting transducer (through an additional buffer block). This transducer arrangement used by the authors is given as Figure 81.

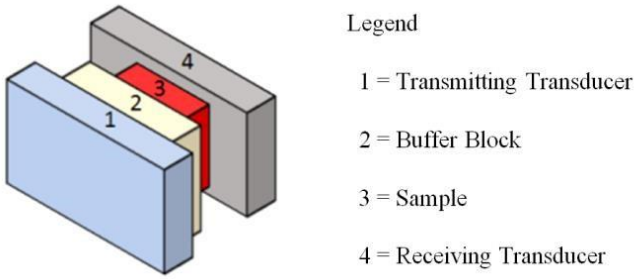

Figure 81 - The transducer and sample arrangement is documented. Note the inclusion of a buffer block, included by the authors to combat any potential pulse transmission reflection cross over issues.

The authors created six samples, with each sample having a different angle between the sides of the composite and fibre axis. The transducers quoted for longitudinal and transverse waves were Panametric M110 and V156 respectively with the frequency recorded being the standard 5 MHz used within academia. By propagating a wave

through the arrangement in Figure 81 and through a buffer block only (sample removed) and comparing the two results, the time taken for the waves to travel through the specimen was determined.

The authors recorded the full set of elastic constants using this technique. Note however, the authors reported that different values of C_{44}, C_{55} and C_{66} were recorded along with documenting accuracy issues for C_{23}, $C_{12,}$ and C_{13}. When presented with different values of $C_{44,}$ $C_{55,}$ and C_{66}, in this case a result of nonidentical density and fibre volume fraction, the values which provided the closest theoretical results were used to calculated constants C_{23}, C_{12} and C_{13} - note however

Kriz and Stinchcomb do not enter discussion as to why differences were recorded in elastic constants to the same depth as earlier authors such as (Zimmer and Cost, 1970). Upon using the standard (non-modified) Hashin equations, the authors found that through knowledge of fibre properties, matrix properties and fibre volume fraction, the Hashin equations were in good agreement with the experimentally determined elastic constants.

At this stage, the relationship between phase velocity and group velocity and how this impacts on the potential thickness of a sample has generally not been considered by the works reviewed thus far. Kriz and Stinchcomb provide discussion on this matter. Kriz and Stinchcomb put forward the argument that potential exists for transversely isotropic material to cause wave energy to deviate from the wave normal to the extent where the receiving transducer would have to be moved in order to accurately record the wave and to avoid receiving a wave as result of a particular material reflection - essentially the group velocity effect. Using an existing equation set from previous work by the author‟s, Kriz and Stinchcomb calculated the wave energy deviation for wave propagation 45^{o} to the fibre direction. The results are demonstrated in Figure 82.

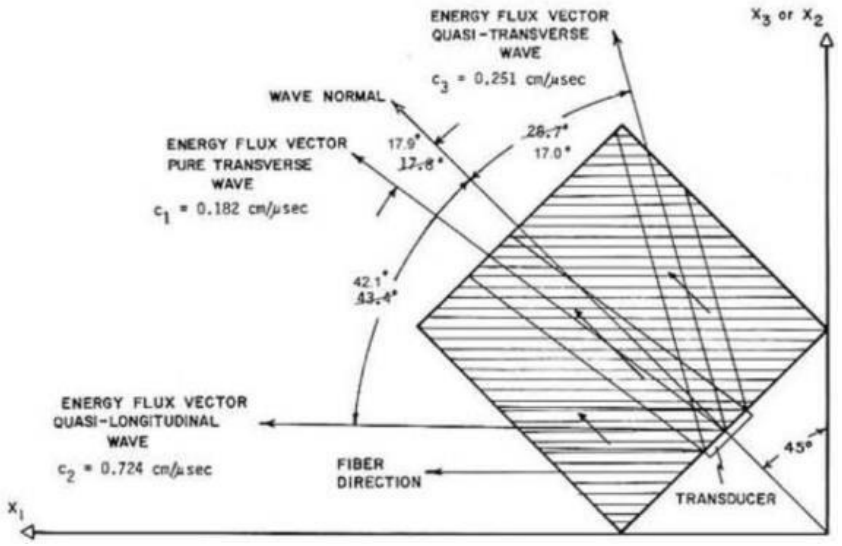

Figure 82 - Group velocity effect for three different types of wave propagating at 45o to fibre axis. Direction of pure transverse records an angle deviation of 17.9o from wave normal. Direction of quasi-transverse wave records angle deviation of 17o from wave normal. Direction of quasi-longitudinal wave records angle deviation of 42.1o from wave normal. *Experimental Mechanics, Elastic moduli of transversely isotropic graphite fibres and their composites, 19, 1979, page 41-49, Kriz RD, Stinchcomb WW, With permission of Springer*

Taking group velocity effects in consideration the thickness of the samples was designed to be within limits such that wave energy deviation effects were kept to a minimum - equations provided by the authors allowed for the maximum and minimum thickness to be calculated. Only 2 out the 6 samples used by the authors showed deviation effects and so 2 samples only were confined in relation to the amount of thickness.

Kriz and Stinchcomb demonstrated that the full set of elastic constants of transversely isotropic graphite fibre could be found from using (potentially in harmony) both ultrasonic velocity measurements and by using both modified and original equations of those by (Hashin, 1972). That is, knowledge of fibre properties, matrix properties and fibre volume fraction has been shown to allow for a good theoretical prediction of composite properties. Kriz and Stinchcomb point out that the known problematic constants, C_{12} or C_{13}, are thus able to theoretical determined – the authors do not validate the accuracy of result however.

Concerning the group velocity effect identified by Kriz and Stinchcomb, it is of interest to note that no preceding author in this review who investigated dispersion

effects when propagating waves in non-axial directions has discussed the group velocity effect. This is because a) none existed, b) the thickness of sample is coincidentally in the correct region to significantly minimize the effect or c) effects were counted under the general term of „dispersion effects". Note in this instance that Kriz and Stinchcomb did not discover group velocity effects in general; when working on aluminium based composites, (Gieske and Allred, 1974), identified that the Markham method was using group velocity and not phase velocity. However, Kriz and Stinchcomb recorded these effects on carbon fibre based composites.

Within literature it has thus far been documented that the pulse transmission technique can be conducted via a) immersing a sample in water b) direct contact between the transducer and sample or c) direct contact between the transducer, a mode changing mechanism (such as a glass prism) and the sample. So established is the pulse transmission technique for conducting ultrasonic velocity measurements that areas such as void content, homogeneity and symmetry, the relationship between fibre and matrix, fibre orientation etc. have all been shown to be approachable areas of study using this technique. Table 58 in section 5.4 presents a summary of some the milestones related to elastic constant determination that the 1970"s provided.

It is also the case that hitherto similarities between certain pulse-echo techniques and the through transmission technique have largely been ignored – pulse echo falls outside the scope of this review. However, it is true that both pulse echo and through transmission can be used to conduct velocity measurements of body waves. Further, it will be shown that the, not yet discussed, double through transmission technique effectively builds on standard pulse echo and so lightly touching on standard pulse echo is appropriate.

Pulse echo is typically used to determine defects or flaws within a particular material but can also be used to determine the elastic constants. In regards to defect detection, pulse echo can be thought of as the following. A wave propagates through a given material and encounters a void which is large compared to the wavelength of wave, the dramatic change in acoustic impedance between the material and void causes a wave to be reflected back to the surface. A time of flight measurement is then taken to gauge the depth of the void.

In regard elastic constant determination, pulse echo can at times be considered the same as through transmission. That is, if the wavelength is large, compared to any potential voids, but small compared to the specimen geometry, then the propagating

wave will treat the material as a continuum (ignore the void) and the back wall of the specimen will reflect some of the wave back to the original transducer. A time of flight measurement can be taken and so the wave velocity may be determined. From a physics standpoint this process is really no different to the through transmission approach; owing to aspects such as waves traveling through the specimen twice, it is not classed as through transmission however. Evidence of where the pulse echo technique has been used to measure the velocity in composite can be found in a report written by (Prosser, 1987) commissioned by the National Aeronautics and Space Administration (NASA). Prosser demonstrated the applicability of the pulse echo techniques to unidirectional graphite composite when he sought to determine the elastic constants of a composite used in a previous publication by (Kriz and Stinchcomb, 1979). Using a pulse overlap system – essentially, the comparison of successive back wall reflections to determine the time difference and subsequently the wave velocity – Prosser demonstrated that the elastic constants of a unidirectional graphite composite (T300/5208) could be determined. As with Zimmer and Cost (Zimmer and Cost, 1970), to obtain the desired velocities, multiple samples were required to allow for propagation at varying angles to fibre axis. Prosser compares the elastic constants determined through pulse echo with those of Kriz and Stinchcomb and found in general good agreement. Note that C_{33} was found to be around only 70% of that calculated in the work by Kriz and Stinchcomb owing to the authors using samples which were not identical to Kriz and Stinchcomb in terms of void content fibre content and dimensions. Additional reading can be found from (Graciet and Hosten, 1994) who present similar analysis when they adopt pulse echo and Fourier analysis to determine attenuation, wave speed, thickness and density simultaneously Moving back to literature concerning the through transmission technique, (Pearson and Murri, 1987), built on the work by (Kriz and Stinchcomb, 1979) and further investigated the issue of the group velocity vector deviating from the phase velocity vector within an anisotropic medium. Noting that the inference from Kriz and Stinchcomb that the group velocity vector points in the same direction as the phase velocity vector for pure wave propagation along principal axis‟s was established by Pearson and Murri , thus to investigate group velocity vector deviation from normal, wave propagation in off-axis directions was required .

For unidirectional graphite composite exhibiting orthotropic symmetry and the assumption that the 1 direction is the fibre direction, Pearson and Murri created

multiple samples with varying fibre axis to sample surface relationships and performed ultrasonic measurements using the Zimmer and Cost approach in the 1-2 plane – only longitudinal waves were propagated. Figure 83 is provided to illustrate both the samples and the group velocity effect.

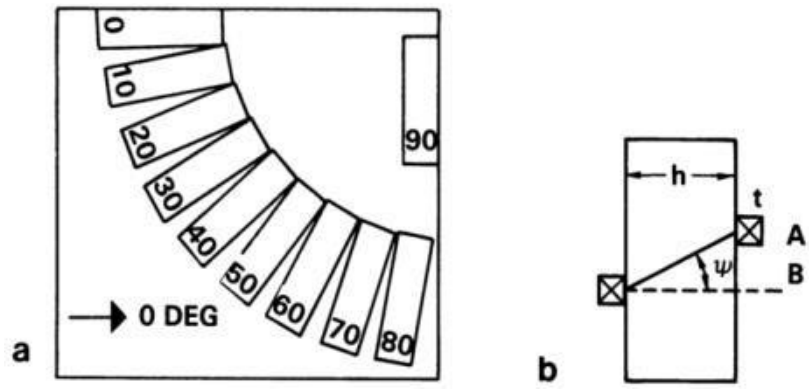

Figure 83 – Figure (a) documents various samples with degrees being reference to the fibre axis, figure (b) documents transducer placement and group velocity effect; transducer is moved to position A from position B, to compensate for group velocity effect as given by angle Ψ.
Review of Progress in Quantitative Nondestructive Evaluation, Chapter 6, Measurement of ultrasonic wavespeeds in off-axis directions of composite materials, Vol. 6A, 1987, page 1093–1101, Pearson LH, Murri WJ, Copyright Springer Science+Business Media New York *US, With permission of Springer*

The authors found that the time taken for a pulse to propagate through the sample using the group velocity at angle of 0º deviation was the same as the phase velocity. That is, the only difference recorded between the group velocity and phase velocity calculations was that the time taken in the case of group velocity was multiplied by the cosine of the angle of deviation, Ψ. Thus the authors state that if the receiving transducer is positioned to correctly receive the transmitted pulse (in this case point A), the calculated group velocity can be related quite easily to the phase velocity (assuming the refraction angle of phase velocity is 0º, i.e. wave strikes composite at normal incidence) that would be recorded at point B.

Using the phase velocity determined in this plane, the authors conducted a least squares fit procedure to determine all available elastic constants (remembering that transverse waves in various directions are required to determine the full set of constants). The determined constants were found to be in good agreement (accuracy Figure not provided) with those obtained through theoretical predictions. It is of merit to note in this instance, that previous authors have not adopted the least squares fit

procedure, but it is also true that Pearson and Murri provide very little information on how this was performed. With later works documenting this procedure(s) in varying degrees of depth, discussion of least squares fit is held off until these works are discussed. Figure 84 (a) documents the relationship between the experimental and theoretical phase velocity to angle propagation relationship. Regarding the size of deviation angle arising via the group velocity effect, caused by the anisotropy of the sample, the authors found that theory matched experiment and that in the most extreme cases angles of up to around 55º were recorded. Figure 84 (b) documents the deviation angles recorded by the authors.

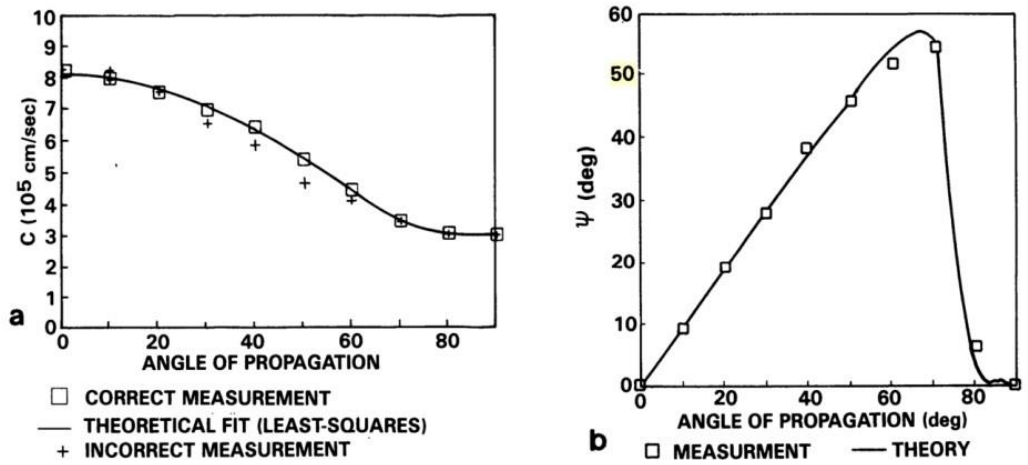

Figure 84 – Figure (a) documents experimental and theoretical agreement for quasi-longitudinal phase velocity, calculated from group velocity, for the samples outlined in figure 83 (a). Figure (b) documents the group velocity effect causing maximum wave deviation of around 55o for propagation to fibre axis of around 75o. *Review of Progress in Quantitative Nondestructive Evaluation, Chapter 6, Measurement of ultrasonic wavespeeds in off-axis directions of composite materials, Vol. 6A, 1987, page 1093–1101, Pearson LH, Murri WJ, Copyright* Springer Science+Business Media New York, *With permission of Springer*

Turning attention to quasi-transverse waves, Pearson and Murri documented an interesting set of results. For quasi-waves propagating in the 1-3 plane with propagation angle to fibre axis of 0º to around 65º the angle deviation was recorded as being negative. The negative value of angle deviation infers that the group velocity effects oppose the initial refraction that arises from Snell‟s laws, thus, bolstering the case that correct placement of transducer is vital to accurately measure the time taken for waves to propagate through a sample. Further, for propagation to fibre axis angles

of angles between 65º and 80º the wave deviation was recorded as being around 55º in some instances. Owing to inspection technique used, angles of fibre propagation outside 80º were not able to be studied. Figure 85 (a) and (b) documents the findings from Pearson and Murri. Note that the theoretical and experimental did not provide as good a relationship as it did for quasi-longitudinal waves.

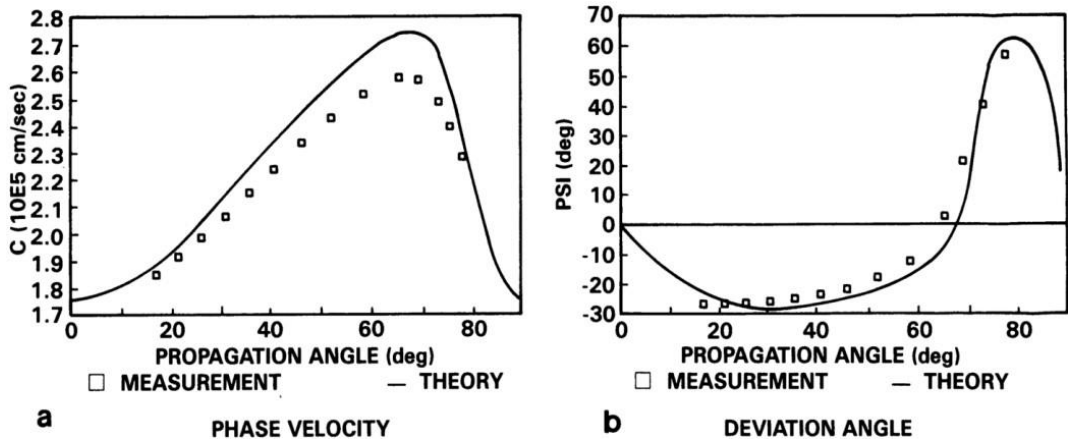

Figure 85 – Figure (a) documents experimental and theoretical agreement for quasi-transverse phase velocity, calculated from group velocity, determined using the Markham method. Figure (b) documents the group velocity effect causing negative angle deviation of around 30^0 maximum and positive angle deviation of around 55^0 maximum. *Review of Progress in Quantitative Nondestructive Evaluation, Chapter 6, Measurement of ultrasonic wavespeeds in off-axis directions of composite materials, Vol. 6A, 1987, page 1093–1101, Pearson LH, Murri WJ, Copyright* Springer

Science+Business Media New York, *With permission of Springer*

As mode changing was required by the authors to generate quasi-transverse waves the refraction angle therefore cannot equal 0º. Thus, the authors highlight that the previous relationship (proportionality to cosine of wave deviation angle) is no longer viable. Pearson and Murri provide the solution however and document the relation between group and phase velocity using the Markham method. While not as simplistic as just multiplying the time by the cosine of deviation angle as with the quasi-longitudinal case, the authors do provide an equation set to calculate phase velocity from group velocity for quasi-transverse waves propagating via the Markham method.

The two main contributions to knowledge from Pearson and Murri were a) when quasi-waves propagate in off-axis directions then particular care should be taken when

deciding the correct location of the receiving transducer when employing the through transmission technique and b) presentations of equations which can be used to relate the phase velocity to group velocity for both longitudinal and transverse waves. Looking closer at point 1) while there is of course no definitive answer to where the transducer should be placed and although authors put forward the deviation angle as a function of propagation angle, further investigation on the correct placement of transducer would have been of considerable interest. Further, although not discussed by the authors, a potential implication of this work is that shear waves may be the most accommodating option for studying wave propagation in off axis directions in unidirectional CFRP. More accommodating in the sense that due to refraction and group velocity wave deviation effects being both potentially positive and negative and thus fighting against each other, the transducers may potentially be able to stay directly in line with each other under certain circumstances; this claim is not verified in the work however. In 1989, two publications, (Rokhlin and Wang, 1989a, 1989b), introduced what is known as the double through transmission technique. The double through transmission technique is essentially the through transmission technique with an arguably slight combination of the pulse echo technique. It is used in many modern publications and so is considered a very important technique. Looking first at (Rokhlin and Wang, 1989a), the experimental apparatus involved in the double through transmission technique is shown in Figure 86.

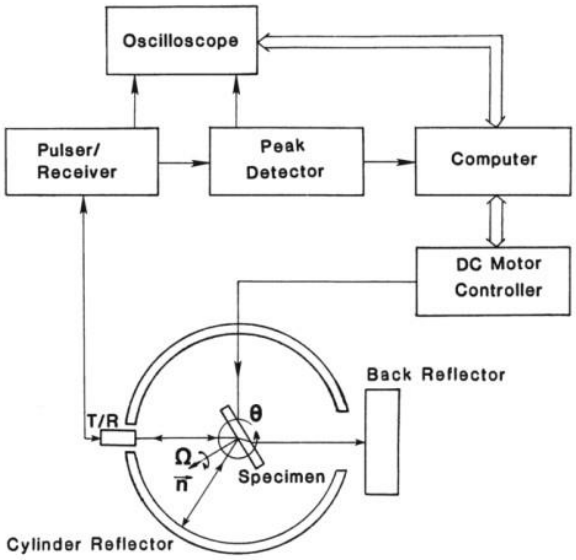

Figure 86- Experimental apparatus of the double through transmission technique. A single transducer operates as both transmitter and receiver, both surface reflections and through transmission signals are able to be measured and note that the sample, transducer, cylinder and reflector are immersed in water (accurate to temp – 0.1)^{o} *Review of Progress in Quantitative Nondestructive Evaluation, Chapter 8, Ultrasonic evaluation of in-plane and out-of-plane elastic properties of composite materials, Vol. 8, 1989, page 1489–1496, Rokhlin SI, Wang W, Copyright Springer Science+Business Media New York, With permission of Springer*

The double through transmission technique operates as follows; an ultrasonic wave is transmitted towards the sample, noting that the sample is able to be rotated around a central axis (recorded at 0.01º precision). Upon striking the sample, and depending on the angle of incidence, the wave is both reflected and transmitted through the sample. Looking first at transmission, the wave propagates through the sample in the direction of the group velocity, that is, in the direction of wave energy (not necessarily the refraction angle as dictated by Snell‟s laws). Upon reaching the reflecting block, the transmitted wave is reflected back towards the transmitting transducer, now acting as a receiving transducer, in exactly the same path taken up to that point. Thus, the problem of wave vector deviation is removed owing to the reflecting path taking exactly the same route as the transmitting path. Rokhlin and Wang elegantly depict this process, given as Figure 87.

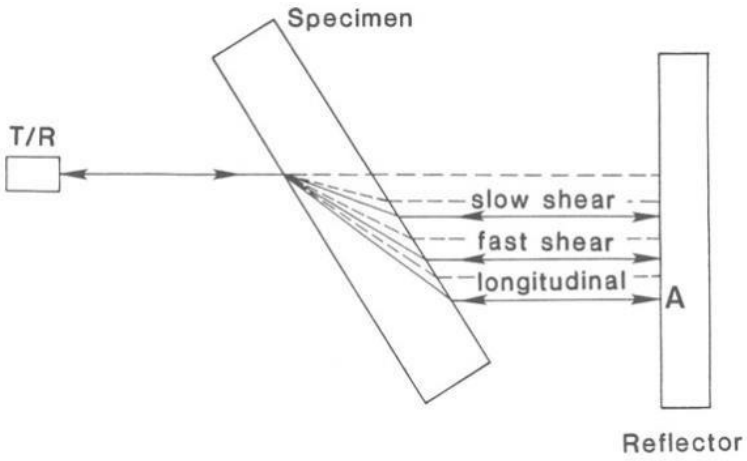

Figure 87 – Showing the transmitted waves and reflected waves travelling along the same path, thus eliminating the need to alter transducer placement in this approach. The dotted lines indicate phase velocity direction; solid lines indicated group velocity direction. *Review of Progress in Quantitative Nondestructive Evaluation, Chapter 8, Ultrasonic evaluation of in plane and out-of-plane elastic properties of composite materials, Vol. 8, 1989, page 1489–1496, Rokhlin SI, Wang W, Copyright Springer Science+Business Media New York, With permission of Springer*

Looking now at surface reflections, the initial incident wave is reflected and heads towards the aluminium cylinder. It is subsequently reflected again and, similar to the through transmission approach, takes exactly the same path back towards the receiving transducer. Rokhlin and Wang propagated waves, more than once, for each type of wave (number not specified) and the average amplitudes of reflected signals (both from surface reflections and from through transmission reflection) were recorded. Looking first at surface reflection technique the authors quote earlier work, which demonstrated that when the critical angle is reached for both quasilongitudinal and quasi-transverse waves a maximum reflection coefficient was generally recorded. The critical angle is defined in this instance as the point of incidence which causes the refracted energy of the wave to propagate parallel to the plane of incidence - noting that energy (group velocity direction) is used instead of phase velocity direction. It was also recorded by the authors that when the fibre axis to propagation direction changed the critical angle was also changed.

Thus, the authors used the double through transmission technique to record the amplitude of the surface reflection and therefor the critical angle was also able to be determined. Knowing the critical angle and velocity of incident wave, allowed the authors to calculate the refracted wave velocity using Snell‟s laws. Thus, elastic constants may be realised in this instance if the propagation angle to fibre axis and wave type is known. The authors‟ state however that due to group velocity effects the only available plane in which the above contention is valid, was for propagation in the plane of incidence, or as the authors put it, in-plane phase velocity measurements only.

Looking now at the through transmission arrangement, outside of the contention that that this system improves on the Markham technique, which has the potential to provide errors if one is not careful with transducer placement and composite width, there is little to be discussed. The authors effectively conducted exactly the same measurements as conducted by preceding authors, that is, time of flight measurements of different waves at different angles to fibre axis to determine the phase velocity. Note here that the phase velocity is determined through a relationship with the group velocity, which the authors effectively calculate in the same way as was previously outlined by (Pearson and Murri, 1987).

The final area of interest from Rokhlin and Wang is the technique used to determine the elastic constants of the sample. Up to this point, excluding Pearson and Murri, to determine the elastic constants of the composite, literature presented in this review has

used the Musgrave equations, (Musgrave, 1954a, 1954b), which effectively force specific waves at specific angles to fibre axis to be measured. This technique was not adopted in this text, the technique adopted was to evaluate a slowness profile and perform a statistical process to find the best values of constant to create such a curve. The process is stated by the authors as being called the „least squares fit" or „least squares optimization". A slowness profile is a particular type of wave surface profile in that what is charted is simply the inverse of the phase velocity against either the angle of wave vector direction or the angle of propagation to fibre axis. (Ledbetter and Kriz, 1982), can be sighted for additional examples of such surfaces. The least squares method is discussed further in another not yet discussed publication by (Rokhlin and Wang, 1992).

The authors calculated the phase velocity experimentally using the double through transmission approach and compared these results to the phase velocity derived through the reconstruction of elastic constants from a critical angle measurement and found good agreement, thus verifying both the double through transmission approach, critical angle approach and least squares mechanism. Figure 88 is given to exemplify the results.

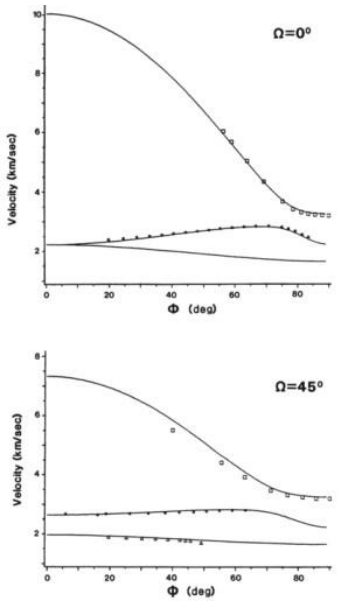

Figure 88 – The solid line is reconstructed phase velocity from elastic constants determined via critical angle technique. The experimental points are phase velocity as recorded via double through transmission technique for two quasi – transverse and one quasi-longitudinal wave for surfaces of 0o and 45 to fibre axis. Φ is 90- angle of refraction. *Review of Progress in Quantitative*

In this work, Rokhlin and Wang demonstrated a novel way to determine the elastic constants of CFRP. The double through transmission technique removes the possible errors that group velocity wave deviation may bring in other techniques such as the Markham method. Also, the experimental arrangement allows for phase velocity to be determined through critical angle measurements. However, this work does not examine the work of (Wilkinson and Reynolds, 1974), who stated that longitudinal wave propagation is a result of a pseudo-L wave. Additionally, this work and equally the work of Pearson and Murri do not examine just how much inaccuracy there is in the existing Markham approach, the authors only state that this method is inaccurate. It was not shown to be the case that wave deviation always introduces significant accuracy concerns for samples of CFRP of certain dimensions. The other 1989 publication by Rokhlin and Wang, (Rokhlin and Wang, 1989b), discusses using the double through transmission arrangement in the critical angle mode of operation further. As this technique is outside the scope of this literature review, this paper is not reviewed. However, attention can be turned here for additional reading on the critical angle technique.

In 1990, (Castagnede et al., 1990), similar to (Dean, 1971), investigated the applicability of using ultrasound velocity measurements to investigate symmetry within CFRP, more specifically to determine the orientation of principal axis of symmetry. In a not too dissimilar way to Dean, the authors produced an algorithm, based on the standard Musgrave equations, to relate the angular parallax (angular parallax being angle between the geometric axis and crystal axis) along with the elastic constants to standard velocity measurements determined using the standard Markham approach. Not discussed in this text however, are the effects brought on by wave deviation (group velocity effects).

A work which does discuss the fact that hitherto the Musgrave equations were determined using the group velocity and not the phase velocity was (Rokhlin and Wang, 1992). Building on previous works (Pearson and Murri, 1987; Rokhlin and Wang, 1989a), the authors outlined three clear goals, 1) demonstrate – in a different way to (Pearson and Murri, 1987) - the relationship between phase velocity and group velocity in a unidirectional CFRP sample, 2) discuss the already outlined, (Rokhlin and Wang, 1989a), double through transmission method and present experimental

results and 3) demonstrate the robustness of a non-linear least squares methodology for elastic constant determination – noting that point 3 is the main contribution to knowledge.

Looking at point 1), Rokhlin and Wang demonstrated through an geometric presentation that the phase velocity can be related to the group velocity and similar to (Rokhlin and Wang, 1989a), the authors determined effectively the same equation as previously outlined by (Pearson and Murri, 1987). Further, similar to observations from (Kriz and Stinchcomb, 1979), if the initial wave is not refracted, i.e. it strikes with normal incidence, the group velocity will equal phase velocity. Moving on to discuss point 2), additional information not discussed in (Rokhlin and Wang, 1989a), was that the water tank was kept at 29.8º accurate to (+/-) 0.05 ºC, the transducers used were 15 MHz and the sample was unidirectional graphite epoxy with a thickness of 2.1mm. The authors propagated both quasi– longitudinal and quasi-transverse waves in various directions in which the plane of incidence was at angles of 0º, 45º, and 90º to the fibre direction. For all available angles of refraction the phase velocity as a function of 90º minus refraction angle was recorded by the authors. Note also, that to determine the degree of result accuracy, theoretical realisations of the phase velocity, obtained using the aforementioned critical angle technique, were produced and superimposed onto these plots by the authors. Similar to the findings from (Rokhlin and Wang, 1989a), Figure 88, the authors found a very accurate relationship between the phase velocity as determined through using the critical angle technique and the double through transmission technique.

Looking now at point 3), a non-linear least squares minimizing technique was used by the authors to evaluate the elastic constants. The method adopted by the authors was to initially guess the elastic constants and then to calculate the expected phase velocity with the sum (over a series of propagation angles) of the squared difference between the experimental velocity and the calculated phase velocity being evaluated. Continually minimizing this difference, by altering the initially guessed elastic constants, will eventually lead to the correct elastic constant values. In this instance, the determined constants were found to be in good agreement with the original value and independent of the initial guess (up to a point of 20% difference) thus, reinforcing the determination technique.

Regarding the determination of elastic constants using the Musgrave equations, the authors state this method of determining the constants (specific waves along specific

directions within the material) is somewhat sensitive to error; however, there is no general development of this issue within the text, nor does the text cite any major works which discuss it.

Having established the least squares optimization technique, Rokhlin and Wang investigated the robustness of the algorithm. Firstly, the phase velocity was calculated using a set of elastic constants which define an orthotropic material; noting here that angles of fibre axis to plane of incidence of 0º, 30º, 45º, 60º and 90º were used. Then, a computer simulation was performed which allowed 0.1%, 1% and 5% noise to be superimposed on the phase velocity results. With each new value of phase velocity, the elastic constants were then determined again. The authors documented that even at 5% noise level the elastic constants determined were adequate. Also, it was recorded that reconstructing the elastic constants using the phase velocities in the plane of symmetry produces slightly better results than doing so using the phase velocities from non-symmetry planes (noting that a symmetry plane contains two principal axes).

Rokhlin and Wang constitute a good body of work. Building on (Rokhlin and Wang, 1989a), the authors documented more thoroughly the relationship between the group velocity and phase velocity and also identify that phase velocity is required for elastic constant determination. Further, the authors document a least squares algorithm that allows for the elastic constant to be determined with a good degree of accuracy, even in the face of up to 5% scatter in the phase velocity results.

However, while the authors touch on the subject of why one should use the least squares algorithm, a comprehensive case was not, in the opinion of the author, put forward as to why one should always perform a least squares algorithm. For instance, the authors state that only propagation in non-symmetry planes is required and infer that only one type of wave is needed, while at the same time also stating that the older system using both waves in specific directions is prone to error. However, the text documents no quantitative data which compares these methods of elastic constant determination. Further, for a transversely isotropic material, only five elastic constants are required and only one of these is off axis, thus a comparison would be required in literature to determine if the least squares method (which can potentially require more time spent to perform) is required in every instance.

An upgrade to the double through transmission technique was recorded in a series of publications by Chu Rokhlin, (Chu and Rokhlin, 1994a, 1994b, 1992), via a slight variation of the original technique; with the upgraded technique being known as the

self-reference model (SRM). The (Chu and Rokhlin, 1994a) study, examines a comparison between the double through transmission system and the self-reference system, thus, out of the three this is the paper discussed. When using the double through transmission system for oblique incidence it is the group velocity that propagates through the sample, thus, in order to relate the recorded group velocity to the required phase velocity, a reference acoustic path (amongst other parameters) is required. This takes the form a standard velocity measurement from transducer to reflector with no sample in between. The selfreference model upgrades this system and measures the required acoustic path with the sample inserted (waves striking at normal incidence) between the transmitter and reflector block. This distinction is shown in Figure 89.

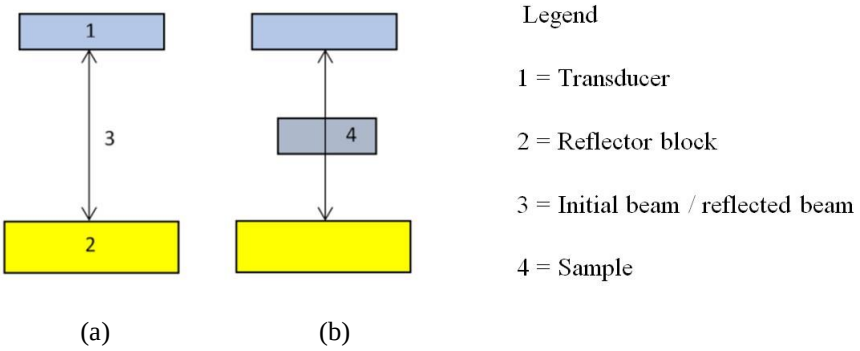

Figure 89 - Documenting the distinction between the standard double through transmission method and the SRM. Fig a) documents that the acoustic reference signal (water coupling medium not shown) measurement is made without the sample, fig b) documents for the SRM treference measurement is made with sample at normal incidence. hat acoustic

The improvement the self reference system has over the double through transmission system is that parallelism of the sample (opposite faces of the sample being flat but not parallel) and surface curvature, both of which have the potential to introduce slight errors into phase velocity calculations, are taken into account.

Gauging the contribution of this novel measurement system, the authors experimentally measured the phase velocity using both the double through transmission system and the self-reference system. In this instance, a unidirectional graphite epoxy composite along with a 5 MHz transducer was used. The incident plane was chosen to be parallel to the fibres (strong angular dependence recorded in this

direction) with angular repeatability and resolution (referring to sample rotation parameters) recorded better than 0.01º.

For the double through transmission system the authors found that maximum error due to parallelism was at normal incidence and then reduced as the angle of refraction increased. Via the SRM, a contrasting relationship was found; the most accurate results were obtained at normal incidence with slight increases in error being recorded as the refraction angle increased. Conducting similar tests on isotropic steel with curved sides, the authors recorded up to 7% error in velocity measurements, however for strongly parallel surfaces, these errors significantly reduce. The authors point to these experiments to give basis to the reporting that the self-reference method is more tolerable to surface imperfections than the standard double through transmission approach. Thus it was demonstrated by Chu and Rokhlin that by inserting the sample between the transmitter and reflector to gauge the acoustic reference path then the accuracy of phase velocity result can be improved.

In relation to temperature effects, the authors went further than previous authors and investigated quantitatively the effects of temperature variation. Unlike previous authors who state the temperature of the coupling medium should remain at a constant, the authors in this instance recorded that for a temperature change of 1ºC, error of up to 15% can potentially be present. Chu and Rokhlin also outline further techniques that can be used if no temperature regulation equipment is available for experimental use while also noting that temperature should be measured to an accuracy of 0.01 ºC.

Two additional publications from 1994 which sought to determine the elastic constants of unidirectional CFRP from limited ultrasonic velocity measurements are (Chu et al., 1994; Chu and Rokhlin, 1994c). These works investigate the robustness of determining the elastic constants from measurements in a) symmetry planes only and b) non-symmetry planes only. While it may be argued that this in itself is not new knowledge, it was previously demonstrated that for ultrasonic measurements with up to 5% noise the determination of elastic constants through symmetry plane measurements at various refraction angles was more accurate than through nonsymmetry measurements (Rokhlin and Wang, 1992), the authors put forward an analysis of the optimal refraction angles for elastic constant determination along with an investigation in to which elastic constants are able to be determined from the symmetry plane only and non-symmetry planes only.

Looking initially at (Chu and Rokhlin, 1994c), which investigates planes of symmetry; the authors expressed the phase velocities in terms of a polarization factor. Noting here, that the polarization factor is a measure of the polarization difference between a pure mode and a quasi-mode - for a pure mode the value is denoted as 0, which increases in value for deviation away from pure mode. For a value of polarization factor squared of less than 0.4 the authors denote the material as weakly anisotropic and for larger values the authors denote the material as strongly anisotropic. In this work, the authors recorded that in the case of a weakly anisotropic material, the longitudinal phase velocity in the 1-3 plane (1 direction being the fibre direction) was dependent mostly on the constants C_{11}, C_{33} and the combination (C_{13} + 2C_{55}), and in the 2-3 plane was dependent on C_{22}, C_{33} and the combination (C_{23} + 2C_{44}). Thus, the authors found agreement with a previous study, (Every and Sachse, 1992), and reported that for a weakly anisotropic composite the constants C_{44} and C_{55} cannot be determined directly from longitudinal data in symmetry planes. Therefore, to determine the seven constants available from symmetry plane analysis, transverse wave propagation is also required. The transverse phase velocity in the 1-3 plane was found to depend on C_{55} along with the combination of (C_{11} + C_{33} + 2C_{13}) and in the 2-3 plane on C_{44} and the combination of (C_{22} + C_{33} – 2C_{13}). Figure 90 documents the fibre direction to plane relationship.

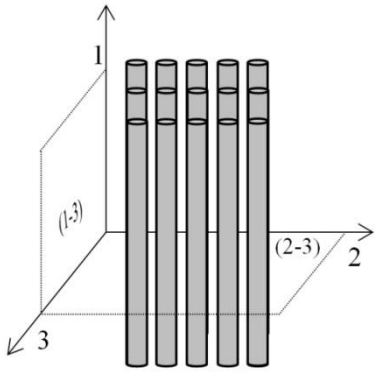

Figure 90 – Documents fibre direction along with the (1-3) plane and the (2-3) plane. The (1-3) allows for propagation in the direction of fibre and through the fibres, the (2-3) plane allows for propagation across the fibres and through the fibres.

The authors went further and investigated the sensitivity of phase velocity by performing a partial differentiation of the phase velocity with respect to the specific elastic constants. They found that the phase velocity change was in all cases a function

only of refraction angle, thus, the optimal refraction angle for the determination of seven out of a possible nine elastic constants of an orthotropic material were able to be determined. These findings are summarized in Table 53.

Optimal refraction angle for elastic constant determination		
Elastic constant	Refraction angle (quasilongitudinal velocity)	Refraction angle (quasitransverse velocity)
C_{11}	90º	45º
C_{22}	90º	45º
C_{33}	0º	45º
C_{13}	45º	45º
C_{23}	45º	45º
C_{44}	45º	0º
C_{55}	45º	90º

Table 53 – Optimal refraction angles in planes 1-3 and 2-3 for elastic constant determination as adapted from (Chu and Rokhlin, 1994c)

Although not stated by the authors, it can be said that the results outlined in Table 53 are not entirely surprising noting that as early as 1970 Zimmer and Cost, and Markham, (Markham, 1970; Zimmer and Cost, 1970) put forward a similar view point (which is a fall out from the Musgrave equations). For instance to determine C_{11}, C_{33}, and C_{44} for example, propagation should be at 0º (longitudinal), 90º (longitudinal) and 90º (transverse). Noting here that refraction angle and propagation direction are in the same direction in terms of wave vector (i.e. propagation in 1-3 plane at 0 degrees to fibre axis is in same direction as a 90º refraction of an incident wave in this plane).

The authors performed a similar sensitivity analysis on strongly anisotropic materials and recorded not so straight forward relationships (in the sense that sensitivity was not strictly dependent on the angle of refraction alone). For longitudinal wave propagation in the 1-3 plane, unlike weakly anisotropic materials where phase velocity was largely independent of C_{55}, the authors found that for strongly isotropic material C_{55} impacted upon the sensitivity, i.e. C_{55} plays a role of noticeably increasing or reducing the phase velocity. Thus, the authors concluded that C_{55} was able to be determined from longitudinal waves in this plane. C_{44} however was still required to be found using a transverse wave. It was also recorded by Chu and Rokhlin that the elastic constants C_{11} and C_{33} played a more prominent role in sensitivity analysis of transverse waves.

Lastly, as experimental apparatus may not allow the phase velocity at all angles of refraction to be calculated, Chu and Rokhlin also examined the elastic constant accuracy as determined using the non-linear least squares technique with only limited

phase velocity data (i.e. angle range 0-90º not fully covered). Using phase velocity data at scatter level of 2%, the authors found that for satisfactory results of elastic constants (0-3% from nominal value), in the case of longitudinal waves the phase velocity data range should extend from 0º- 45º (or above) and for transverse waves the range 35º-75º (or above).

Looking now at a similar analysis with wave propagation in non-symmetry planes, (Chu et al., 1994). While previous authors (Chu and Rokhlin, 1994c), documented that a non-linear least squares recovery algorithm is robust in terms of 5% scatter and independent of the initial guess of elastic constant in planes of symmetry, for non-symmetry planes (Chu et al., 1994) recorded a mixed set of results. For an incidence plane rotated 45º around the fibre direction of an orthotropic material, the authors recorded that only C_{33}, C_{44} and C_{55} were independent of both the initial guess (up to 20% difference) and scatter (up to 2%); noting that the remaining elastic constants were influenced by the initial guess and scatter level in varying ways. Using this plane to determine the elastic constants, the authors found that an initial guess of within 2% nominal value with 0.5% scatter produces fairly accurate results (largest deviation from the determined true elastic constant values was shown to be 1.3%), noting that additional scatter or more inaccurate initial guesses, drastically causes these results to change.

It was also documented by the authors that if the independent elastic constants C_{12} and C_{66} are calculated using the least mean squares method (note that these constants are not able to be determined from measurements in symmetry planes) and all other constants are known and held constant during the process, then the least squares method is both robust to at least 2% scatter and up to +/- 20% inaccuracy of initial guess. Thus, building on (Chu and Rokhlin, 1994c), Chu et al, put forward the conjecture that when investigating orthotropic materials, one should determine seven out of the nine elastic constants from symmetry planes, using only non-symmetry planes for the remaining constants (unable to be determined from symmetry planes).

The optimum method for determination of constants C_{12} and C_{66} was also put forward by the authors. Similar to (Chu and Rokhlin, 1994c), this analysis was by way of a sensitivity analysis. Using a very good approximation of the phase velocity for arbitrary angles of refraction, the optimum angles of refraction in non-symmetry plane of 45º to the fibre axis were recorded. Results found by the authors are given in Table 54.

Optimal refraction angle for elastic constant determination			
Elastic constant	Refraction angle (quasilongitudinal velocity)	Refraction angle (fast quasitransverse velocity)	Refraction angle (slow quasitransverse velocity)
C_{12}	90º	90º	Not dependent on C_{12}
C_{66}	90º	45º	Not in general dependent on C_{66}

Table 54 – Optimal refraction angles for non-symmetry plane 45º to fibre axis for elastic constant determination adapted from (Chu et al., 1994)

Both (Chu and Rokhlin, 1994c) and (Chu et al., 1994) documented phase velocity sensitivity to changes in specific elastic constants and the optimum set of phase velocity measurements (in terms of propagation angle) for determining the most accurate set of elastic constants by way of a least squares optimization procedure. It is also the case that (Chu and Rokhlin, 1994a, 1994b, 1992; Pearson and Murri, 1987; Rokhlin and Wang, 1992, 1989a, 1989b) demonstrated that group velocity was able to be related to the phase velocity when conducting the Zimmer and cost approach, the Markham method and the double through transmission approach. Thus circa 1994 the methods to determine the elastic constants of unidirectional composite materials were strongly established within literature. It noteworthy to mention however that not all measurement techniques are based on the Zimmer and Cost approach, the Markham method or the double through transmission approach however, and through the 1990‟s investigations into how to relate phase velocity to group velocity measurements within CFRP was a field ongoing research. As such, indirect relationships between the group velocity and elastic constants were established within literature. Noting that indirect in this instance means that the group velocity is not able to be related directly to elastic constants (unlike the phase velocity in the Musgrave equations) and must rely on aspects such as wave vector deviation and phase velocity refraction angles. Additionally, innovative reconstruction algorithms based on aspects such as ray surfaces (group velocity version of the inverse of a slowness profile) and the wave normals to this surface were developed to help determine the elastic constants from group velocity measurements.

As this review is concerned primarily with through transmission (of which it has already been documented how to determine elastic constants from group and phase

velocity measurements), these additional reconstruction algorithms along with group and phase velocity relations are generally outside the scope of this review. However, seminal works in this period are cited as a matter of completeness,
(Arist gui and Baste, 1997; Balasubramaniam and Rao, 1998; Castagnede et al., 1989; Degtyar and Rokhlin, 1997; Deschamps and Bescond, 1995; Every and Sachse, 1992, 1990; K. Y. Kim et al., 1995; Kim, 1994; Kwang Yul Kim et al., 1995;
Seiner and Landa, 2004).

Additionally, around the same time, circa late 1980‟s – late 1990‟s various works, including significant contributions from a Bordeaux group led by Professor Bernard Hosten, documented a lot of work concerning the viscoelastic properties of unidirectional composite materials, (Baudouin and Hosten, 1997, 1996; Cawley and Hosten, 1997; M Deschamps and Hosten, 1992; M. Deschamps and Hosten, 1992; Hosten, 1991; Hosten et al., 1987; Hosten and Baudouin, 1995; Hosten and Castaings, 1993a, 1993b; Roux, 1990). Investigating viscoelastic properties of composites, while interesting in its own merit and with literature documenting analysis of reflection and transmission coefficient amplitudes along with general attenuation measurements to investigate these properties, it is the case that viscoelastic properties are outside the scope of this review. However, it is indeed the case that when determining the complex stiffness matrix (viscoelastic material), an understanding of the real part of the complex stiffness matrix (the standard elastic constants) is demonstrated within literature; and so, while the literature is more primarily concerned with viscoelastic analysis, the real constants are also determined in these works.

Further, although the elastic constants may be determined through both theoretical predictions and using transmission coefficient measurements and also by virtue of velocity measurements, for instance, (Cawley and Hosten, 1997) state that obtaining the complete viscoelastic properties of a particular glass fibre composite were not obtainable using the transit time method owing to difficulties in measuring the reduction in amplitude from successive echoes and thus used a theoretical prediction and fitted the results, the majority of the literature identified, i.e. (Baudouin and Hosten, 1997, 1996; Cawley and Hosten, 1997; M Deschamps and Hosten, 1992; M. Deschamps and Hosten, 1992; Hosten, 1991; Hosten et al., 1987; Hosten and Baudouin, 1995; Hosten and Castaings, 1993a, 1993b; Roux, 1990) performed the Markham method and least squares fit algorithm to determine the real elastic constants required.

Further still, an area not discussed in this review thus far is the determination of elastic constants via air born ultrasound, i.e. only wave propagation via a gel, or fluid has been considered thus far. While air born wave propagation is outside of the scope of this review, it is of merit to briefly discuss why and identify relevant literature.

Ultrasonic waves have a difficult time propagating efficiently through air owing to a typical large impedance mismatch between the transducer and the naturally compliant air (noting that opposite relationship is found in solids and fluids). Additional problems associated with propagating ultrasonic waves through air as highlighted by (Rokhlin et al., 2011), include the much slower wave speed recorded in air than for solids and fluids and so the refraction upon entering a sample is often times extreme (owing the mismatched wave speeds). Also, coupling between mediums work best when the densities and wave speeds for the medium are approximately the same, and therefor air born ultrasound coupling to a solid is very likely be poor with the wave highly attenuated.

As this review has focused on literature which uses very efficient coupling mediums, and the fact that the laws of physics governing the elastic constant relationship to phase velocity do not change with respect to the coupling medium, the decision was made not to include air born ultrasound in this review. Even with the double through transmission system having been documented in this field (Hosten et al., 1996), with aspects such as transducer selection, experimental arrangement, counter acting attenuation, counter acting the impedance mismatching all being required to be discussed before the wave actually propagates through the sample, it was felt that air born ultrasound would be best suited to having its own literature review. A recent literature review by Professor Chimenti of Iowa State University, (Chimenti, 2014), identifies both pertinent literature and also gives particular focus to the many seminal works conducted as part of the French group led by Professor
Hosten at Bordeaux University.

Moving back to the immersion based approach, additional improvements (in terms of accuracy) to the Markham method and double through transmission approach are still able to be found within literature. These improvements were developed through noticing that on a water/solid interface, a transverse wave records a phase shift when the critical angle for longitudinal waves is exceeded. In 1997 (Lavrentyev and Rokhlin, 1997), identified that when a longitudinal wave strikes a water/solid (in this case

graphite epoxy composite) interface at angles above the critical angle, a longitudinal evanescent wave (exponentially decreasing disturbance created when critical angle is exceeded) is produced which then forces the refracted shears waves to undergo a phase shift.

Thus, to correct for the very slight phase shift the authors put a slight modification (in mathematical terms) to the self-reference double through transmission method. To realise this, the authors initially calculated the elastic constants using the standard procedure and pay no attention to the potential phase shift. Using this data, the phase error shift was calculated, note here that the authors are not very explicit about how this calculation should be performed, however this information is presented in a different publication, (Hollman and Fortunko, 1998). Once the phase shift (degrees) is known, the authors put forward a very slight change to the theory previously outlined in (Chu and Rokhlin, 1994a), in that for a given

incidence angle the phase velocity (a function of refraction angle) now also has a dependence on phase shift. Also, the frequency of operation is required in this relation and so the authors advise that a narrowband signal should be used when measuring the phase velocity. Iterations of this procedure can be performed to continually increase the accuracy of result.

Using the updated phase velocity relation the authors recorded a difference of 0.2%, 0.3%, 1.2%, and 0.4% in the elastic constants of C_{11}, C_{33}, C_{13} and C_{55} respectively for graphite epoxy composite. The authors recorded differing percentage effects using other materials in this study and further found that the area of stress determination reliant on accurate phase velocity, however both areas are outside the scope of this review.

While this work is of interest (it technically improves the accuracy of elastic constant) the differences recorded in the paper are small in value and so adopting this approach to determine the elastic constants may not be required in every instance, however further work is required to verify this claim. Additionally, the authors present only four elastic constants and do not discuss a typical number of iterations
(if any).

Approaching the same issue from a different perspective was (Hollman and Fortunko, 1998). It is the case however that this text does not discuss unidirectional composite, with the authors stating additional work would be required as the findings are not

directly translatable to strongly anisotropic material, noting that unlike (Chu et al., 1994; Chu and Rokhlin, 1994c) strongly anisotropic material is not defined, and so it is not discussed in this review. Note however this different method, which relies on Fourier series analysis to measure the phase velocity, and has been verified on isotropic steel, improves on the previous method in that broadband transducers are able to be used.

(Wang et al., 2003), built upon (Lavrentyev and Rokhlin, 1997) by expanding on the phase correction issue caused by oblique incident angles greater than the critical angle and also investigated possible diffraction effects. Looking first at the phase effects, when investigating the phase shift for unidirectional graphite composite in three different planes, 0º, 90º and 45º to the surface normal, the authors found the most dramatic phase shift was in the 45º plane. At the first critical angle in this plane (longitudinal wave) the authors found phase shift rising to 90º then falling suddenly to 0º as the angle of incidence to fibre axis was increased. Between the first and second critical angle (fast transverse wave) the phase shift increased by less than 2º. Between the second and third critical angle (slow transverse wave) the phase shift fell to around - 90º. Further, the authors present relationships which allow for the realisation of a given materials phase shift, which incorporates such aspects as Young‟s modulus, density and Poisson‟s ratio and also identify that phase shift is more stabilized and less severe in the other planes, i.e. planes of 0º, 90º. Additionally, the authors put forward a means to estimate the error introduced into the experiment. Regarding the effects of this calculable error, the authors state that while phase shift is significant around the critical angle regions, phase error for a small number of angles is not sufficient to account for a drastic change in elastic constants when using the least squares algorithm over a large data set (multiple angles of incidence).

Looking now at diffraction effects caused by finite sized transducers; note that an ultrasonic beam spreads out as it propagates and so it is possible that owing to a fixed sized transducer facing (not covering the whole beam), that waves are picked up at the rear and sides of the transducer thus causing possible interference with the transmitted signal on the front face of the transducer.

Presenting a theoretical model (noting that diffraction transducer analysis can be cited as far back as 1940), for a recorded beam width of 5 mm and a distance between the transducer and the reflecting block of 80 mm, the authors demonstrated that diffraction effects, when the transducer is in the far field, accounted for less than 0.2% difference

in phase velocity. That is, the phase shift was virtually non-existent, thus diffraction effects are such that the recorded time difference is extremely small. Thus, the authors put forward the conjecture that in general, diffraction effects can be ignored. Judging by earlier works which do not consider diffraction effects while still recording fairly accurate results – in 1970 (Smith, 1972) recorded elastic constants accurate to 3%, in the 1990‟s, (Chu et al., 1994) recorded constants accurate to ≤
1.3% - this argument has solid basis.

Note a caveat however, similar to phase effects, the authors recorded that for measurements at the critical angles, the diffraction effects caused the plane wave approximation to be recoded as invalid and so could not be ignored. The authors further document that diffraction effects also in the general sense cause a reduction in amplitude of the signal. While not strictly a concern when conducting elastic moduli evaluation this finding is of course important when determining aspects relating to sample attenuation.

Hitherto 2005, as a means of determining the elastic constants of transversely isotropic unidirectional composite, the double through transmission system had not generally been thoroughly compared with the standard Markham method i.e. the standard through transmission system. (Reddy et al., 2005), investigated this gap in knowledge.

Using isotropic glass epoxy composite, graphite epoxy composite and isotropic aluminium, Reddy et al. performed 100 different iterations, with the average value taken to offset noise effects, using both the double through transmission system and the Markham method. The double trough transmission system used by the authors is given as Figure 91.

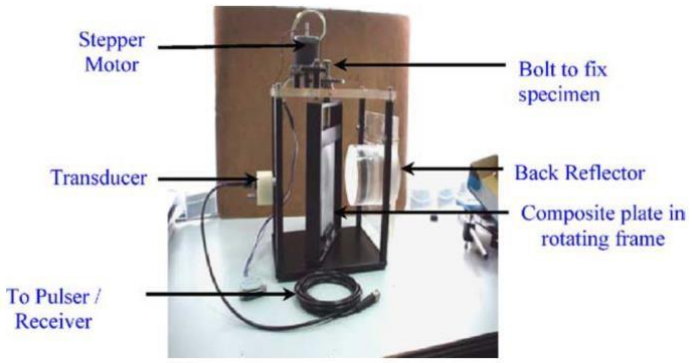

Figure 91 – Experimental arrangement of the double through transmission system as used by (Reddy et al., 2005) *Reprinted from Composites structures, Vol 67 / Edition number 1, Reddy, S. Siva Shashidhara, Reddy; Balasubramaniam, Krishnan; Krishnamurthy, C. V; Shankar, M; Ultrasonic goniometry immersion techniques for the measurement of elastic moduli, Pages 3-17., Copyright (2005), with permission from Elsevier*

The authors recorded that the double through transmission system was more accurate in relation to the elastic constants and more precise (repeatability) than the through transmission technique - noting that reference elastic constant values were taken from contact testing (Zimmer and Cost approach) and from the manufactures data. Note additionally, as the thickness of the sample grew the more the through transmission method differed from the contact based analysis. Tables 55 and 56 document the elastic constants for two samples of glass epoxy measured using the double through transmission technique.

Elastic constants (in GPa)	Immersion testing	Contact testing
C_{11}	15.42 ± 0.78	15.30 ± 0.33
C_{13}	12.10 ± 1.04	Not measurable
C_{33}	50.15 ± 1.14	Not measurable
C_{44}	3.8 ± 0.42	Not measurable
C_{66}	4.76 ± 0.03	4.77 ± 0.17

Table 55 - Elastic constants as determined using the double trough transmission technique and Zimmer and Cost approach for glass epoxy 10.88 mm thick. *Reprinted from Composites structures, Vol 67 / Edition number 1, Reddy, S. Siva Shashidhara, Reddy; Balasubramaniam, Krishnan; Krishnamurthy, C. V; Shankar, M; Ultrasonic goniometry immersion techniques for the measurement of elastic moduli, Pages 3-17., Copyright (2005), with permission from Elsevier*

Elastic constants (in GPa)	Immersion testing	Contact testing
C_{11}	14.54 ± 0.11	13.65 ± 0.68
C_{13}	11.40 ± 0.42	Not measurable
C_{33}	47.5 ± 0.15	Not measurable
C_{44}	2.9 ± 0.38	Not measurable
C_{66}	4.58 ± 0.36	4.15 ± 0.16

Table 56 – Elastic constants as determined using the double trough transmission technique and Zimmer and Cost approach for glass epoxy 4 mm thick. *Reprinted from Composites structures, Vol 67 / Edition number 1, Reddy, S. Siva Shashidhara, Reddy; Balasubramaniam, Krishnan; Krishnamurthy, C. V; Shankar, M; Ultrasonic goniometry immersion techniques for the measurement of elastic moduli, Pages 3-17., Copyright (2005), with permission from Elsevier*

Comparing the elastic constants as recorded by the double through transmissions and through the Markham method, with regards to glass epoxy composite and aluminium, the authors put forward the conjecture that the double through transmission system was the best option for conducting through transmission type ultrasonic wave measurements to determine the elastic constants. There is however problems

associated with this publication and also areas in which, in the opinion of the current author, warrant more rigorous investigation. The first concern is that, in terms of the subject of this review, the elastic constants from the graphite epoxy sample was only determined using the double through transmission technique, i.e. the authors did not record figures using the Markham technique. So, while the authors quote graphite epoxy precision and accuracy figures for the double through transmission system, they do not exist for the through transmission technique. As such, we must take the author on good faith that the precision and accuracy is lower; note the authors cite an earlier master‟s thesis to establish this claim.

Another concern is that the authors state the receiving transducer is held fixed during the through transmission technique. As group velocity effects have been well documented up to this point in literature, it is clear that holding the receiving transducer in a fixed position has the potential (depending on sample width) to increase the inaccuracy of elastic constant determined. Thus, it may unfair to point blankly state the double through transmission method produces more accurate results if no measures have been taken to ensure optimal receiving transducer placement.

Lastly, the accuracy of the through transmission and double through transmission method is measured against the elastic constants, and so these results can be said to be dependent on the measurements equipment / technique. Returning to the issue of possible experimental error caused by diffraction, a series of publications by Adamowski et al, (Adamowski et al., 2010, 2009, 2008, 2007), expanded on (Wang et al., 2003). Unlike (Wang et al., 2003) who conducted only a simulation of the diffraction effects, the aforementioned authors conducted physical experiments and so these texts are worthy of discussion. Employing video scan 19mm (diameter) transducers of 1, 2.5, 5 and 10 MHz and focused 10 mm transducers of 5 MHz, (Adamowski et al., 2007) investigated diffraction effects via the through transmission approach. They found for the 19 mm transducers with frequencies lower than 2MHz and for 10 mm for frequencies as high as 5 MHz, that diffraction effects caused around 1% error in velocity measurements (note that in both cases diffraction effects were found to reduce as the frequency increased). To counter these effects, the authors replaced the receiving transducer with an 80mm diameter polyvinylidene fluoride (PVDF) receiver. The authors recorded that the diffraction effects caused a negligible effect on phase velocity measurements, thus the effects were eliminated. Using a 10 mm 5 MHz transducer along with the PVDF receiver, the full set of transversely

isotropic CFRP constants were able to be determined. Additionally, the authors also recorded that as the operational frequency increased so did dispersion effects. A similar analysis was presented by (Adamowski et al., 2009, 2008), who developed the dispersion aspect slightly further. Using a 19 mm transducer and PVDF receiver, it was documented that between 1 MHz and 10 MHz, the velocity increased by approximately 1% owing to dispersion effects. Similar reconstruction of elastic constants was also recorded with a 5 MHz and 2.25 MHz transducer being used in the respective publications. Thus, the authors allude to (this aspect is not explicitly investigated) the idea that using a PVDF receiver is a better option when seeking to obtain the phase velocity effects with a high deal of accuracy. Additionally, it can also be stated that although (Adamowski et al., 2009, 2008, 2007) demonstrate the elimination of diffraction effects, in terms of unidirectional composite the diffraction effects were not recorded - aluminium was used to record these. Thus these text‟s cannot be exactly compared with the findings of (Wang et al., 2003).

An additional publication, extending the diffraction effect further again is (Adamowski et al., 2010). Closely paralleling the previous works (note however, this paper also includes density measurements of liquids outside the scope of this review), using the through transmission technique the authors determined the elastic constants via a PVDF based receiver. As before, the changes in velocity caused by diffraction effects in aluminium were found and the authors also report that the separation of the transducers was 100mm. As such, the changes in velocity owing to diffraction effects were again recorded at 1% and changes to velocity owing to dispersion effects within CFRP were found to be 1%. Filling, somewhat, a gap of the previous works, the authors found that if the elastic constants were reconstructed using velocity data that was 1% inaccurate, the resultant constants were within 4% of their correct value.

Concluding this review is (Castellano et al., 2014). At this point some 45 years of literature documenting bulk ultrasonic wave through transmission (in one form or another) of unidirectional composite has provided much information. Thus, (Castellano et al., 2014) document not a new experimental approach designed to increase the accuracy of measurement but instead document a bespoke computer programme to handle an existing measurement technique.

Using the double through transmission approach as pioneered by (Rokhlin and Wang, 1989a, 1989b) the authors determined the full five elastic constants of transversely isotropic CFRP. It should be mentioned that the authors designed their own apparatus

in this instance, that is, the system allowed for both the Markham method and the double through transmission approach to be used. Figure 92 documents how a custom mechanical grip allowing for both system to be used.

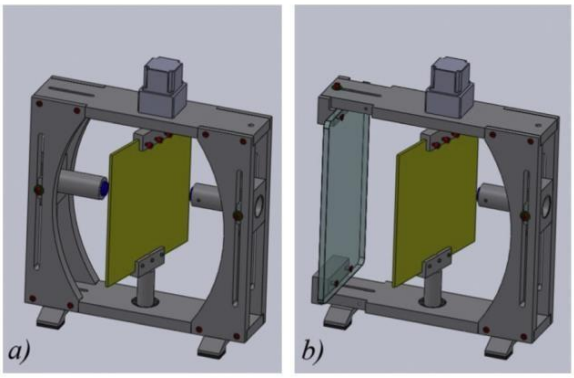

Figure fig (a) and the double through transmission method fig (b) to be used. **92** – Equipment used by (Castellano et al., 2014) that allows for both the Markham method *Reprinted from Composites part B: Engineering, Vol 66, Castellano, A; Foti, P; Fraddosio, A; Marzano, Salvatore; Piccioni, Mario Daniele; Mechanical characterization of CFRP composites by ultrasonic immersion tests: Experimental and numerical approaches, Pages 299-310, Copyright (2014), with permission from Elsevier*

The main novelty herein was the use of bespoke LabVIEW software. The software, deployed on a commercial PC, was used to control the oscilloscope, the rotation of stepper motor and the acquisition and reprocessing of experimental data to allow for a fully automated experimental process.

Figure 93 documents the graphic interface developed by the authors.

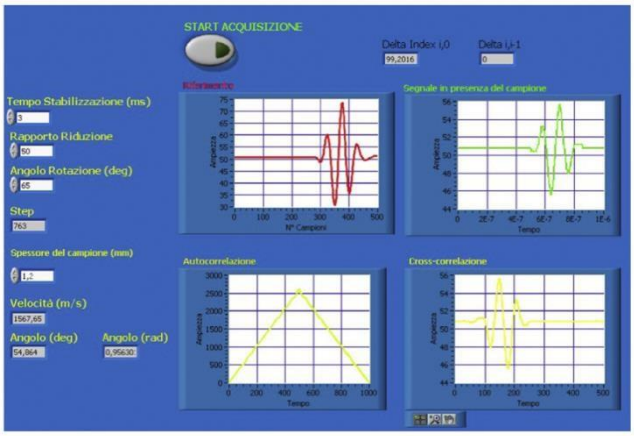

Figure 93 - Graphical interface as used by the authors. Reprinted from Composites part B: Engineering,

Such is the precision of the bespoke experimental arrangement, through Snell‟s laws the three the three waves which propagate in both the isotropic and anisotropic plane were picked out with good deal of accuracy. Figure 94, is given to demonstrate the results obtainable.

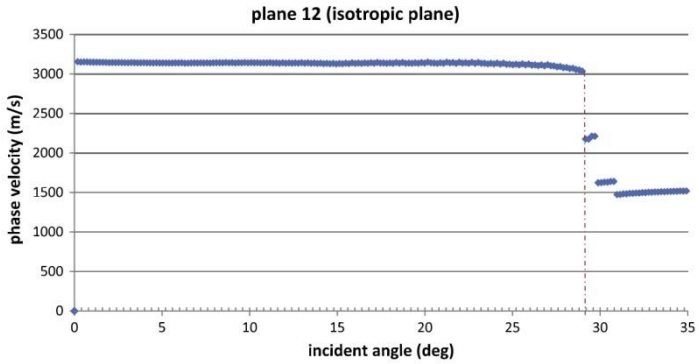

Figure 94 - The longitudinal, fast transverse and slow transverse waves recorded in the isotropic plane. Data between the longitudinal wave and the fast transverse wave is thought to be experimental error. *Reprinted from Composites part B: Engineering, Vol 66, Castellano, A; Foti, P; Fraddosio, A; Marzano, Salvatore; Piccioni, Mario Daniele; Mechanical characterization of CFRP composites by ultrasonic immersion tests: Experimental and numerical approaches, Pages 299-310, Copyright (2014), with permission from Elsevier*

2.4 Information Tables

This review has identified multiple contributions to knowledge concerning the determination of elastic constants of uni-directional CFRP. These findings are now recorded in two unique information tables. Notable findings documented within literature within the period 1970 – 1980 are documented in Table 57 and notable findings for the period 1980 – present day are documented in Table 58.

2.5 Conclusion

This review has documented the progression of how the elastic constants of unidirectional composite were experimentally determined using ultrasonic bulk wave

velocity measurements as outlined in publications spanning 1970 – 2014. Additionally, it outlines which experimental techniques are used by which authors and documents the most accurate technique of modern times, the double through transmission technique.

This review differs from previous review works in that the scope was limited in order to enable a deeper analysis (in terms of experimental findings) of the individual publications to be carried out. Performing such an analysis allowed for a) the contribution to knowledge from a particular publication to be presented in its own right, with significant findings being presented in Table 57 and 58 (documenting some 40 different contributions to knowledge), b) any issues with a publication were identified and c) seminal works during this period were able to be collated and organized in one document, resulting in a review which is chronological in structure and has arguably more depth than current existing reviews.

It was also recorded that there is a paucity of literature on the determination of elastic constants of CFRP manufactured using recycle material via an immersion based ultrasonic through transmission technique. With over 45 years of recorded knowledge and experimentation conducted on uni-directional v-CFRP, this review has given insight into the type of research that has yet to be conducted on these relatively new materials. Given that composite recycling may result in materials with wide ranging properties, areas outlined in this review such as elastic constant determination, critical angle measurements, phase shifts, group velocity effects, robustness of reconstruction algorithms in terms of scatter and plane of determination, etc. are all potential areas for future investigation.

Key Findings:1970 – 1980	Authors
Standard transmitting frequency used in measurements is 5 MHz but some authors also reported lower frequency at around 1 MHz	All
Sample specimen is limited to ensure body wave behaviour (in general thickness kept above two wavelengths and wavelength kept above fibre diameter).	All
When propagating in fibre direction, if pulse width equal to sample width, data on mode changing in inconclusive	(Dean and Lockett, 1973)
Unidirectional composite causes the wave energy direction to skew at angle, θ, from the phase wave front normal when waves strike surface obliquely	(Kriz and Stinchcomb, 1979)
Velocity able to be measured using direct contact through transmission technique	(Kriz and Stinchcomb, 1979; Reynolds and Wilkinson, 1978; Wilkinson and Reynolds, 1974; Zimmer and Cost, 1970)
Velocity able to be measured via immersing transducers in water and rotating sample and using through transmission technique	(Dean, 1971; Dean and Lockett, 1973; Markham, 1970; Reynolds and Wilkinson, 1978; Smith, 1972; Wilkinson and Reynolds, 1974)
Velocity able to measured using prism technique	(Dean, 1971; Dean and Lockett, 1973; Markham, 1970; Reynolds and Wilkinson, 1978; Wilkinson and Reynolds, 1974)
All elastic constants determined	(Dean and Lockett, 1973; Kriz and Stinchcomb, 1979; Markham, 1970; Reynolds and Wilkinson, 1978; Smith, 1972; Wilkinson and Reynolds, 1974; Zimmer and Cost, 1970)
Composite Young‟s Modulus (at varying angles to fibre axis) can be determined from velocity measurements	(Dean, 1971; Dean and Lockett, 1973; Zimmer and Cost, 1970)
C_{44} changes value depending whether the fibre axis is perpendicular or parallel to wave direction	(Dean, 1971; Dean and Lockett, 1973; Kriz and Stinchcomb, 1979; Markham, 1970; Smith, 1972; Zimmer and Cost, 1970)
Theoretical predictions for stiffness are in general in close agreement with experiment when propagating shear waves polarised in plane of the fibre from 0º - 90º in CFRP (using C_{44} measured perpendicular to fibre axis)	(Reynolds and Wilkinson, 1978; Smith, 1972; Wilkinson and Reynolds, 1974)

When propagating longitudinal waves for angles greater than 0º and less than 90º to the fibre direction in CFRP (in the plane of the fibre), the experimental values for stiffness do not follow the expect theoretical curve, thus, through attenuation, refraction and reflection (a pseudo-L wave is actually being propagated throughout the sample)	(Reynolds and Wilkinson, 1978; Wilkinson and Reynolds, 1974)
Theoretical predictions for stiffness are in general closer to experimental values when angle of propagation direction to fibre axis is >65º when propagating shear waves polarized perpendicular to plane of the fibre from 0º - 90º in glass composite or CFRP	(Wilkinson and Reynolds, 1974; Zimmer and Cost, 1970)
Theoretical predictions for stiffness are not in as good agreement with experiment to those of shear waves when propagating longitudinal waves from 0º - 90º in glass composite	(Zimmer and Cost, 1970),
The elastic constants determined through ultrasound velocity technique may be used with theoretical predictions to calculate individual fibre properties	(Kriz and Stinchcomb, 1979; Reynolds and Wilkinson, 1978; Smith, 1972)
Composite elastic constants $C_{11,}$ C_{33} and C_{66} are dependent on the fibre Young‟s modulus, while C_{13} and C_{44} are independent of fibre modulus but vary with fibre type (graphite fibres) and have a slightly unclear relationship in carbon fibres. Also, elastic constants do not greatly depend on shear strength of composite	(Smith, 1972)
Average elastic constants of disorientated CFRP (in one plane only) can be calculated	(Dean, 1971)
Velocity in fibre direction is not greatly impacted by void content and only a small dependency on type of resin used	(Dean, 1971; Reynolds and Wilkinson, 1978)
Velocity perpendicular to fibres dependent on both void content and type of fibre concentration	(Dean, 1971; Reynolds and Wilkinson, 1978)
Elastic constant determination through velocity measurements may be used to determine degree of porosity and fibre content	(Reynolds and Wilkinson, 1978)

Table 57 - Key findings from the reviewed text. Findings demonstrate the ultrasonic velocity measurements are a legitimate and able practice to determine the elastic constants of transversely isotropic CFRP and what the constants are dependent upon. Findings also indicate the applicability of ultrasonic velocity measurements to gauge the porosity, fibre concentration and degree of disorientation of transversely isotropic CFRP.

Key Findings from 1980 – 2014	Authors
Establishment of group velocity relationship to phase velocity using time of flight data	All
Identification of possible error arising from incorrect placement of receiving transducers in Markham Method	(Pearson and Murri, 1987; Rokhlin and Wang, 1992, 1989a)

Group velocity effects cause different degrees of deviation for different wave types	(Castellano et al., 2014; Pearson and Murri, 1987; Rokhlin and Wang, 1992, 1989a)
A least squares minimization technique used (wholly or in part) to determine the set of elastic constants	(Adamowski et al., 2010, 2009, 2008, 2007; Castellano et al., 2014; Chu et al., 1994; Chu and Rokhlin, 1994c; Lavrentyev and Rokhlin, 1997; Pearson and Murri, 1987; Reddy et al., 2005; Rokhlin and Wang, 1992, 1989a; Wang et al., 2003)
Investigated robustness of least squares algorithm in relation to the choice of initial guess of elastic constant and noise inserted onto phase velocity measurements	(Chu et al., 1994; Chu and Rokhlin, 1994c; Rokhlin and Wang, 1992)
Identification that when using least squares algorithm for limited velocity data on orthotropic unidirectional graphite composite that ideally longitudinal waves should cover the region 0- 45º (or above) and transverse waves should cover the region 35 - 75º (or above) to the fibre axis	(Chu and Rokhlin, 1994c)
Double through transmission method used to determine phase velocity / elastic constants	(Castellano et al., 2014; Reddy et al., 2005; Rokhlin and Wang, 1992, 1989a)
Orientation of the principal axis of symmetry determined using the Markham method	(Castagnede et al., 1990)
15 MHz transducer used in double through transmission arrangement	(Rokhlin and Wang, 1992)
Self-reference method used to determine phase velocity / elastic constants	(Chu et al., 1994; Chu and Rokhlin, 1994a, 1994c; Lavrentyev and Rokhlin, 1997; Wang et al., 2003)
Double through transmission system encounters maximum error due to parallelism effects at normal incidence and decreases as angle of refraction increases with the self-reference method having a contrasting relationship for phase velocity measurements in unidirectional graphite fibre composite	(Chu and Rokhlin, 1994a)
Identification of the optimum wave refraction angles, within a plane of symmetry, for determination of seven out of nine elastic constants in a weakly anisotropic composite (orthotropic unidirectional graphite composite)	(Chu and Rokhlin, 1994c)
Identification that for a strongly anisotropic composite (orthotropic unidirectional graphite composite) the sensitivity of elastic constants is not dependently only the refraction angle (i.e. phase velocity is not dependent on angle of refraction only)	(Chu and Rokhlin, 1994c)
Identification that for orthotropic materials that determination of seven, out of nine, elastic constants from symmetry planes and the remaining two, out of nine, from non-symmetry planes will result in more accurate values than would determination of all constants from non-symmetry planes	(Chu et al., 1994)
Identification of optimum refraction angles for determination of two elastic constants in non-symmetry planes of unidirectional orthotropic graphite composite	(Chu et al., 1994)
Identification, including subsequent compensation measures, that at certain angles of incidence a resultant	(Lavrentyev and Rokhlin, 1997; Wang et al., 2003)

Table 58 - Key findings from the reviewed text. Findings demonstrate the double through transmission is used extensively along with elastic constant reconstruction algorithms. These findings also indicate the optimum way to determine constants from orthotropic material along with methods to increase accuracy of results

phase shift can cause erroneous phase velocity measurements	
Diffraction effects cause a reduction in amplitude while having little effect on phase velocity measurements for refraction angles out with critical angle regions on unidirectional graphite fibre composite	(Wang et al., 2003)
Double through transmission verified as producing more precise and repeatable results than Markham method with more inaccuracy being recorded as the thickness of samples grew (transducers fixed)	(Reddy et al., 2005)
Demonstrated that as frequency increased diffraction effects decreased and dispersion effects increased for an aluminium plate and employed a PVDF receiver to reduce possible diffraction effects and measured elastic constants of unidirectional graphite fibre composite	(Adamowski et al., 2010, 2009, 2008, 2007)
Demonstrated that bespoke PC software, created on LabVIEW, was able to facilitate automated double through transmission based experiments	(Castellano et al., 2014)

Appendix 3: Experimental wave velocities

This appendix outlines in full, the recorded experimental wave velocities for both the v-CFRP and the rf-CFRP outlined in chapter 6.

Sample reference velocity and sample weights				
Sample	v-CFRP 1	v-CFRP 2	v-CFRP 3	v-CFRP 4
Reference velocity plane 1-2	660.1 m/s	661.4 m/s	661 m/s	662.8 m/s
Reference velocity plane 1-3	660.1 m/s	661.2 m/s	661 m/s	662.8 m/s
Weight	6.4g	6.4g	6.95g	6.942g
Sample	rf-CFRP 1	rf-CFRP 2	rf-CFRP 3	rf-CFRP 4
Reference velocity plane 1-2	662.1 m/s	661.5 m/s	663.9 m/s	662.7 m/s
Reference velocity plane 1-3	662.6 m/s	661.2 m/s	663.4 m/s	662.4 m/s
Weight	4.765 g	4.504 g	4.476 g	4.6636 g

Table 59 – Reference velocity and sample weights recorded for v-CFRP sample 1, 2, 3 and 4

Experimental Velocities recorded for v-CFRP samples 1, 2, 3, 4. Plane of incidence is the 1-2 plane.				
Angle	Sample 1	Sample 2	Sample 3	Sample 4
0	2158	2115.6	2236.5	2233.5
3	2120	2118.4	2212.2	2218.6
6	2103	2102.1	2206.3	2234.6
9	2122.9	2124.6	2227.2	2254.2
12	2207.3	2232	2278.5	2337.8
14	2336.7	2362.3	2370	2443.6
15	2434	2214	2409.9	LTT
16	1091.5	1134.7	1136.8	1134.6
17	1112.4	1117.2	1130.5	1153.7
18	1127.1	1132.3	1148.5	1166.5
19	1140.8	1140.7	1154.9	1178.1
20	1147.9	1153.7	1165.4	1183.1
21	1153.8	1154.4	1164.6	1181.9

24	1149.3	1165.7	1165.4	1176
27	1136.1	1137.9	1151.8	1166
30	1114.8	1113.5	1135.5	1147.6
33	1108.2	1091.5	1128.4	1142.2
36	1070	1069.8	1087.4	1127
38	1041.1	1039	1073	Correlation difficulty
40	1007.7	Correlation difficulty	Correlation difficulty	Correlation difficulty

Table 60 – Results from ultrasonic velocity measurements on v-CFRP samples 1, 2, 3 and 4 in the 1-2 plane

Experimental Velocities recorded for v-CFRP samples 1, 2, 3, 4. Plane of incidence is the 1-3 plane.				
Angle	Sample 1	Sample 2	Sample 3	Sample 4
0	2231.4	2242	2285.6	2232
2	2220.6	2231.7	2307.8	2336.7
3	2232.4	2192.5	2325.6	2321
4	2289	2087.2	2420.6	2426.3
5	1725.8	2013.4	1983.3	1898.2
6	1822.1	1968.5	1984	1950.6
8	1816.2	1974.6	1983.5	1968.3
10	1769.2	1911.8	1919.7	1921.2
12	1716.4	1828.3	1836.8	1851.2
14	1648.9	1676.4	1765.2	1777.8
16		1615.7	1692.2	1703.2
18	1542	1554.5	1627.8	1629.3
20	1498.4	1507.4	1569.3	1570.9
22		1452.5	1519.8	1516.2
24	1406.9	1403	1456.8	1463.1
26		1388.5	1429.9	1429
28	1344	1347.7	1375.4	1377.6
30	1290.1	1305	1306.5	1310.6
32	1229.9	1239.8	1239.0	1241.9
34	1156.2	1178.1	1182	1184.3

Table 61 – Results from ultrasonic velocity measurements on v-CFRP samples 1, 2, 3 and 4 in the 1-3 plane

Experimental Velocities recorded for rf-CFRP samples 1, 2, 3, 4. Plane of incidence is the 1-2 plane.

Angle	Sample 1	Sample 2	Sample 3	Sample 4
0	2430.2	2029	2489.5	2201.6
3	2398.2	2012.5	2234.3	2085.1
6	2527.1	2054.5	2253	2105.3
9	2299.8	2000.8	2205.2	2144.3
10	2300.2	2047.1	2232.1	2170.2
11	2189.3	2057.5	2412.9	2186.2
12	2226.2	2216	2403.4	2334.5
13	2403.2	2198.5	2188.6	2067.7
14	2530.6	1975.1	1255.6	1223.5
15	1241.4	1178.2	1245.9	1239.6
16	1233.3	1199.4	1261.6	1254.5
17	1273.5	1199.7	1275.9	1268
18	1258.8	1228.3	1263.1	1279.8
19	1277.4	1235.6	1274.2	1265.9
20	1279.8	1232	1283.4	1274.4
21	1280.2	1236.5	1267.3	1281
24	1278.5	1261.7	1299.7	1268.1
27	1295.7	1244.3	1283.6	1241.6
30	1233	1202.4	1223.0	1225.6
33	1191.8	1158.9	1170.5	1171.1
36	Correlation difficulty	1088.6	1098.1	1127.5

Table 62 – Results from ultrasonic velocity measurements on rf-CFRP samples 1, 2, 3 and 4 in the 1-2 plane

Experimental Velocities recorded for rf-CFRP samples 1, 2, 3, 4. Plane of incidence is the 1-3 plane.				
Angle	Sample 1	Sample 2	Sample 3	Sample 4
0	2176.3	2046.5	2421.8	2075.5
2	2134.2	1974	2407.7	2159.8
3	2039.7	1850	2180.4	1981
4	2214	1895	1999.4	1835.4
5	1759.4	1909	1982.9	1885.8
6	1946	1852	1963.2	1865.2
8	1923	1848.8	1915.8	1825
10	1865.7	1799.7	1859.6	1781.1
12	1783.7	1764.2	1850.3	1727.3
14	1735.2	1757.5	1777.3	1712.1
16	1680.6	1751.5	1784.4	1684.6
18	1634	1725.5	1766.1	1678.9
20	1601.3	1714.4	1723.8	1652.6
22	1564.5	1654.3	1661.5	1627.5

24	1531.3	1547.3	1572.8	1533.4
26	1460.3	1453.9	1468	1448
28	1379.1	1367.4	1377.9	1361.7
30	1301.7	1291.8	1299.6	1286.5
32	1233.6	1222.8	1225.5	1214.1
34	1164.8	Correlation difficulty	1166.2	1156.8

Table 63 – Results from ultrasonic velocity measurements on rf-CFRP samples 1, 2, 3 and 4 in the 1-3 plane

Appendix 4: Bespoke Matlab programme for identification of elastic constants of CFRP

Please click on the following links for access to these MATLAB programmes

Christoffel equation via MATLAB:

http://dx.doi.org/10.15129/fefd3fb0-1c13-483c-b7ea-87f1c029d631

Determination of Elastic Constants of transversely isotropic materials using ultrasonic wave velocity and MATLAB http://dx.doi.org/10.15129/355ee84a-c02d-46be-96c2-1f5a67f413d6

Appendix 5: v-CFRP and rf-CFRP force displacement data from mechanical testing

Please click on the following link to access this data

http://dx.doi.org/10.15129/b0e880c0-d109-4724-9e3f-00b3225bc81f

Appendix 6: Ultrasonic bulk wave measurements on composite using fibre from recycled CFRP

This appendix is a conference paper presented at the 2017 Review of Progress of Quantitative Non-Destructive Evaluation (QNDE 2017). This paper is due to be published as part of the conference proceedings by the American Institute of Physics (AIP) in early 2018.

Authors - David Patereson[1, a)], Winifred L Ijomah[1], James FC Windmill[2], Chih-Chuan Kao[1], Grant Smillie[2]

1 Design, Manufacture, and Engineering Management, University of Strathclyde, 75 Montrose St, Glasgow, United Kingdom, G1 1XJ
2 Dept. of Electronic and Electrical Engineering, University of Strathclyde, 204 George Street, Glasgow, United Kingdom, G1 1XW.

6.1 Abstract

This study investigates the velocity profile for both a virgin carbon fibre reinforced plastic (v-CFRP) and a reused fibre CFRP (rf-CFRP) which exhibit quasi-isotropy; all samples have 3 iterations of symmetry type [0, -45, +45, 90]s. An isotropic virgin CFRP (v-CFRP), produced by using a hand layup process, is presented along with a pyrolysis recycling process (at 600oC) designed to extract the carbon fibres. A virgin carbon fibre mat with a similar architecture was also thermally conditioned under the same pyrolysis conditions. Both resultant carbon fibre mats were used to produce the rf-CFRPs. Ultrasonic wave velocities at different angles of incidence for both vCFRP and rf-CFRP were recorded. In the case of v-CFRP, two samples were studied and it was recorded that the velocity for both a longitudinal wave and transverse wave remained relatively constant up until these waves completely attenuated at observed angles, indicating what would be expected from an isotropic sample. A close relationship in terms of waves speed was also recorded for the two v-CFRP samples. In the case of rf-CFRP, the longitudinal wave velocities were generally less closely related when compared to the v-CFRP, with a maximum of approximately 32% difference being recorded. The transverse wave velocity was also found to decrease with incident angle indicating sample anisotropy. The authors suggest that the more severe decreasing velocity with increasing incident angle, when compared to v-CFRP, may be caused by resin impregnation issues and not by changes that occur during the

recycling process. Therefore, a hypothesis that both the rf-CFRP and the V-CFRP will return a similar wave profile given an identical resin fibre content is put forward.

6.2 introduction

The study of bulk wave propagation via immersion based ultrasonic velocity measurements has received significant attention within literature, with areas such as frequency selection, the anisotropy of the sample, sample rotation, wave direction, symmetry plane analysis, critical angle evaluation, group velocity wave deviation all being investigated (Hosten, 2001; Markham, 1970; Pearson and Murri, 1987; Rokhlin et al., 2011; Rokhlin and Wang, 1992; Zimmer and Cost, 1970). However, almost all literature is concerned with v-CFRP only; no literature to the authors‟ knowledge exists which investigates if bulk wave propagation follows the same pattern of wave propagation when propagating in rf-CFRP - CFRP manufactured using fibres from a virgin CFRP that has undergone a recycling process (Paterson et al., 2016). Note this material is also commonly referred to as recycled CFRP in literature (Oliveux et al., 2015; Perry et al., 2012; Pickering, 2006; Pimenta and
Pinho, 2012, 2011).

This work will seek to investigate this area and conduct wave velocity measurements on quasi-isotropic CFRP with 3 iterations of layup $[0, -45, +45, 90]_s$. First, an identification as to why wave velocity measurements are conducted is put forward. Following this, an experimental section outlining the composite creation process for both v-CFRP and rf-CFRP is documented along with like for like ultrasonic wave propagation analysis on both v-CFRP and rf-CFRP. Lastly, a discussion section evaluating the results obtained for rf-CFRP and v-CFRP is presented alongside a conclusion.

6.3 Relationship between velocity and elastic constants

Typically when determining material properties such as ultimate tensile strength, Young‟s modulus, shear Modulus and Poisson ratio the experiments tend to be destructive and often require particular shaped parts (Pimenta et al., 2010; Pimenta and

Pinho, 2012). These material parameters all depend on the elastic constants of a material, which through wave propagation are able to be determined nondestructively. Consequently elastic wave propagation is and has been for some time a common method to determine the elastic constants of materials; the relationship between the phase velocity and the elastic constants is through the Christoffel equation (Auld, 1990; Hosten, 2001; Markham, 1970; Miller and Musgrave, 1956; Musgrave, 1954a, 1954b; Prosser, 1987; Rokhlin et al., 2011; Rokhlin and Wang,
1992; Zimmer and Cost, 1970).

For propagation in an isotropic material, noting that the composite used in this research is quasi-isotropic, equations 143-145 outline phase velocity elastic constant relationships.

$$v_x = \sqrt{C_{44}/\rho} \quad (143)$$ v_y

$$= \sqrt{C_{44}/\rho} \quad (144)$$ $v_z =$

$$\sqrt{C_{11}/\rho} \quad (145)$$

Where, the subscript x, y or z, identifies the direction of wave polarization for waves propagating in given direction. The symbol ρ is the density of the material, and is calculated by dividing the mass by the volume.

6.4 Experimental method

6.4.1 v-CFRP Manufacture

24 square Toray T300 unidirectional carbon fibre samples of 18 cm by 18 cm were excised from a standard 1m by 1m roll. Of these 24 samples, 6 had the fibre direction 0^0, 6 had the fibre direction 90^0, 6 had the fibre direction -45^0 and 6 had the fibre direction $+45^0$. Figure 95 is given to reinforce this concept

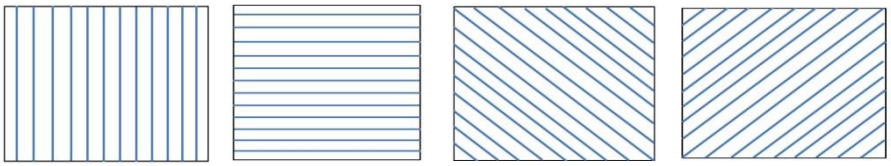

(a) (b) (c) (d)

Figure 95 - Figure (a) documents fibre direction of 0o to the top edge, (b) documents 90o, (c) documents -45 and (d) documents +45 o o

The manufacturing process was by hand layering as follows. First, a flat piece of metal was coated in a polyvinyl alcohol (PVA) mould release agent with the first square fibre mat of 0 placed o upon it. A degassed resin hardener solution mixed to specification of 100:30 was poured over the sample. The second fibre mat of -45 o was then placed up the 0o sample, with baking paper placed over the -45o sample. A 50mm bristled roller was then rolled over the samples to ensure both compactness and an even spread of resin between the two fibre layers. Further resin was poured on the -45 o sample with a similar process being carried out until the composite had 24 layers. At this stage, a large heavier flat piece of metal, coated in release agent was placed onto the top layer. The structure was placed inside a fume extractor hood and left in situ for 48 hours, with a heavier weight placed upon the top metal layer. The resultant composite was 4mm thick. All materials were purchased from Easycomposite.co.uk noting that the resin was EL2 epoxy with slow hardener

At this point the composite was hard and rigid and thus suitable for further mechanical treatment. From this larger section of composite, two samples of approximately 36cm^2 (6cm by 6cm) were machined using a Roland EGX-600 CNC router. These samples are v-CFRP A and v-CFRP B. Note that due to an error occurring during preparation, the 5th layer, which according to the sequence should have been set to 90 was set to 0 instead. o o

6.4.2 Pyrolysis Recycling Process

The pyrolysis process performed was in keeping with that reported in literature, (Meyer et al., 2009; Oliveux et al., 2015; Pickering, 2006; Pimenta and Pinho, 2012, 2011; Shi et al., 2012b) A standard Carbolite oven was preheated for approximately 1 hour until the figure of o 600C was reached. The samples were allowed to dwell for 45 minutes and then were removed and allowed to cool in ambient air.

The temperature was chosen in accordance with Meyer et al.(Meyer et al., 2009) who documented that at 600 oC epoxy resin would have gone through a full pyrolysis process resulting in complete oxidation. Further, Meyer et al. (Meyer et al., 2009) also documented that the carbon fibre is general not affected by oxidation at 600C – note these results document only the epoxy resin and carbon fibres in isolation. The authors also identify that for pyrolysis of CFRP at 600C, oxidization of the carbon fibres will increase with increased dwelling times. Striking a balance to fully remove the resin and leave the fibres largely intact, a time period of 45 minutes was selected, in accordance with results outlined in (Meyer et al., 2009).

The sections of v-CFRP placed inside the oven were not the 6cm by 6cm samples, instead smaller sections of v-CFRP, excised from the larger original (18cm by 18 cm) v-CFRP were used instead.

6.4.3 Simulated Pyrolysis Recycling Process

To simulate the recycling process, smaller hand laid up samples of carbon fibre were heat treated under the same conditions as previously outlined for the recycling of vCFRP. Similar to the v-CFRP, the hand laid up structures used in simulated pyrolysis were 36cm^2 (6cm by 6cm) of similar fibre architecture.

6.4.4 Production of rf-CFRP

After the thermal process and the fibres returned to ambient temperature, the fibres were carefully placed onto a metal plate (coated in PVA mould release agent), to ensure the architecture of the fibre mats originating from the pyrolysis and simulated recycled process was maintained. However, as a result of the thermal process, the fibre layers were not easily manipulated by hand. Therefore, unlike the hand-layup process, the degassed 100:30 mixed resin hardener solution was poured evenly over the top layer of the fibre mat before a second piece of metal was placed on top of the fibres with a weight being placed upon the metal plate. The composite was left in situ again for 48 hours.

A variety of different composites were created at this point. Unlike the vCFRP creation process, an output of the rf-CFRP manufacturing process was that an oval shape of partially impregnated region in the centre of each sample was recorded. Thus, available sections of fully cured and impregnated simulated rf-CFRP were manually excised from around these oval regions. 8 rf-CFRP samples, referenced as A1 – D2, were used in this study. Table 64 outlines the fibre mats used for these rfCFRP samples.

Recycling Process	Samples							
	A1	A2	B1	B2	C1	C2	D1	D2
True Recycling	*	*						
Simulated Recycling			*	*	*	*	*	*

Table 64 - Outlining the rf-samples and the types of fibre mat used to create them. A1 and A2 are created using mats from true pyrolysis with B1-D2 using mats from simulated pyrolysis.

6.5 Ultrasonic Velocity Measurements

The velocity measurements were performed using an immersion based ultrasonic through transmission method (Markham, 1970; Rokhlin et al., 2011). Figure 96 (a) and (b) identify the experimental arrangement used for this study.

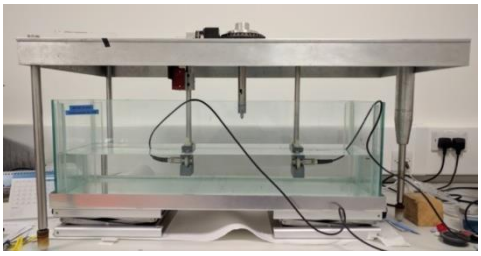

(a)

(b)

Figure 96 - Figure (a) shows both the emitting and receiving transducers, immersed in a body of oil. Figure (b) shows the mechanical rotation device, controlled mechanically from above, upon which the samples were placed. In this research, the samples were not circular and were housed across the slots and not housed within the slots.

An ultrasonic signal was transmitted from transducer A and recorded by transducer B. The transducers frequency was 2.25 MHz with a voltage of 10V peak-to-peak. The

transducer separation distance was 289.55mm (sample placed directly between both transducers) with the coupling medium being Perfluoropolyether oil –PFPE. The longitudinal velocity was recorded by ensonifying the samples at a normal with respect to the emitting transducer. To record the transverse wave velocity, the sample was rotated horizontally (from the transducer‟s perspective) and via mode conversion, a transverse wave was generated and propagated through the sample. To understand the degree of isotropy which existed in the sample, the sample was continually rotated until after the second critical angle (the shear critical angle) was apparent. For an isotropic sample, transverse velocity will remain constant up until the critical angle is reached, at which point, the incident wave is totally reflected.

The velocity was recorded using a correlation method (Trogé et al., 2016), and rearranging equations (143 – 145) allowed for the elastic constants to be determined.

6.6 Experimental Results

6.6.1 v-CFRP

The reference wave velocity (no sample between transducers) was recorded as 662.8 m/s. The samples were weighed using digital scales accurate to one decimal point, with the volume calculated geometrically. Table 65 provides density, weight, volume and % error for the v-CFRP samples.

Data	v-CFRP A	v-CFRP B	% Error
Volume	14.4 cm^3	14.4 cm^3	0%
Weight	19.0 g	18.6 g	2.1%
Density	1319.444 kg/m^{-3}	1291.667 kgm^{-3}	2.1%

Table 65 - Documenting the volume, weight and density values for v-CFRP samples A and B. The % error between samples is also shown.

Initially, both samples were subjected to ultrasonic wave propagation at normal incidence, i.e. ^{0} 0. Both samples at this point were then subsequently rotated to investigate critical angles. Investigating the first critical angle sample A and sample B were rotated towards the theoretical predicted critical angle (calculated using the velocity at 0o) of approximately 16o. At this point the critical angle was not easily observable owing to what was believed to be the early emergence of a transverse wave

o

alongside the decaying longitudinal wave. Moving past the 16 degrees mark, the output signal featured only a transverse element.

The second critical angle was able to be accurately observed and was found to be 32o in both samples, with the estimated critical angle based on velocity at maximum amplitude found to be 29.94 and 30.01 o o degrees respectively.

Investigating this further, from approximately 20o - critical angle velocity, sample A and sample B recorded a % difference in transverse wave velocity of approximately 10.7% and 17.6%. Thus, while quasi-isotropy is assumed, the velocity decrease indicates that the samples are not perfectly quasi-isotropic – particularly as the critical angle was approached. In terms of velocity change with increasing incident angle for the longitudinal waves, the % difference figures were lower and were recorded as 6.57% and 3.5% for sample A and B respectively. In terms of like for like wave velocity measurements, the % error for a

longitudinal wave incident at 0o in samples A and B was approximately 2% which upon taking into account possible inaccuracy arising from experimental error and fibre orientation errors in the hand lay-up process, is very reasonable. A similar measurement was taken at values of maximum amplitude for the transverse waves and found to be even more closely related than the longitudinal waves, with a value of around 0.2% being recorded.

Moving onto the elastic constants, equations 1-3 were used to determine C11 and C44, with small % error being recorded between the samples. These results along with key data recorded for the v-CFRP samples are given in Table 66, with velocity profile and amplitude profile against incident angle for sample A given as Figure 97.

Data	Sample A	Sample B	% difference between samples
Longitudinal wave speed (m/s)	2439	2382.3	2.35%
Transverse wave speed (m/s)	1327.7	1325	0.2%.
First critical angle (**practical**)	N/A	N/A	N/A
First critical angle (**theoretical**)	15.77o	16.15o	2.38%
Second critical angle (**practical**)	32.0o	32.0o	0%
Second critical angle (**theoretical**)	29.94o	30.01o	0.23%
C_{11}	7.85 GPa	7.33 GPa	6.85%

C_{44}	2.32 GPa	2.26 GPa	2.62%

Table 66 - Data recorded for the v-CFRP samples. Small % errors were recorded between the samples, indicating a strong degree of homogeneity in the larger samples used to create both A and B

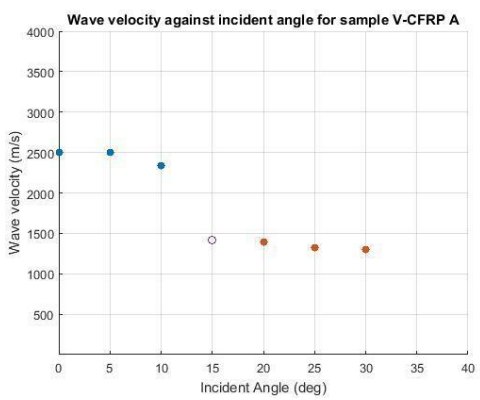

(a)

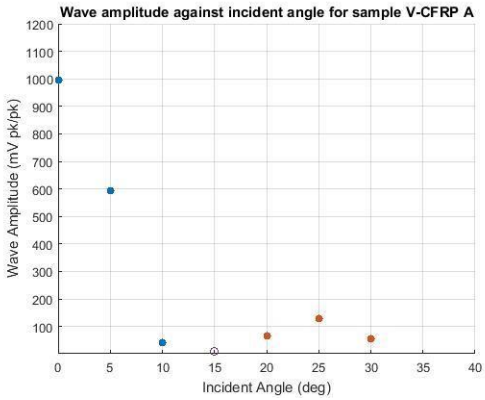

(b)

Figure 97 - Figure a) outlines the longitudinal and transverse wave propagation against incident angle for sample v-CFRP A. Between 0 and 10 there was a 6.3% change in longitudinal velocity recorded, between angles of 20 and 30 there was a 6.6% change in transverse velocity. The hollow point the wave recorded as the longitudinal decays and the transverse builds, the velocity recorded (1413m/s) is more in keeping with the expected transverse velocity, giving rise to the belief that the wave was more transverse than longitudinal. Figure b) documents the amplitude against incident angle showing a decaying longitudinal wave with an emerging transverse wave, with a critical angle in keeping with prediction.

6.6.2 Rf-CFRP

Samples A1 – D2 were all subject to the same ultrasonic testing as outlined for the vCFRP. In this instance, a reference voltage was taken 5 times, once for each class of sample (i.e. once for A, once for B, etc.). The initial reference velocity was recorded as 662.5 m/s and the subsequent reference velocities recorded stayed with 0.5% of this value.

At 0_o incidence % differences of approximately 32%, 30%, 8%, 20% in longitudinal wave velocity was recorded between samples A1 and A2, B1 and B2, C1 and C2, and D1 and D2 respectively. With such differences in velocity, nonidentical resin / CF content between the samples was inferred. Further, the % difference in density between the samples was recorded as 6.35%, 16.45%, 5.32% and 8.53% respectively.

Investigating the first critical angle, with regards to A1 and A2 (the samples created through true recycling), the longitudinal waves was found to quickly attenuate around the 6o incident mark, with the emergence of a transverse wave recorded earlier than that for v-CFRP. For samples B1, B2, C1, C2 and D1, this phenomenon was recorded at around 5, while for sample D2 it was recorded at 8.5. In all cases and similar to the v-CFRP samples, the exact critical angle was difficult to conclusively observe. However, the transverse wave did start to independently emerge in all cases between 10 - 15o, which for the large part is in keeping with theoretical predictions using a longitudinal velocity figure at 0 incidence (see Table 67).

An exceptional case is noted for sample D1 and D2; owing to the relatively large longitudinal velocity figures recorded when compared to samples A1, A2, B1, B2, and C1 and C2, the critical angle was forecast at a lower value of around 5 degrees. Figure 99 a) and b) document the wave amplitude against incident angle for samples A2 and B1

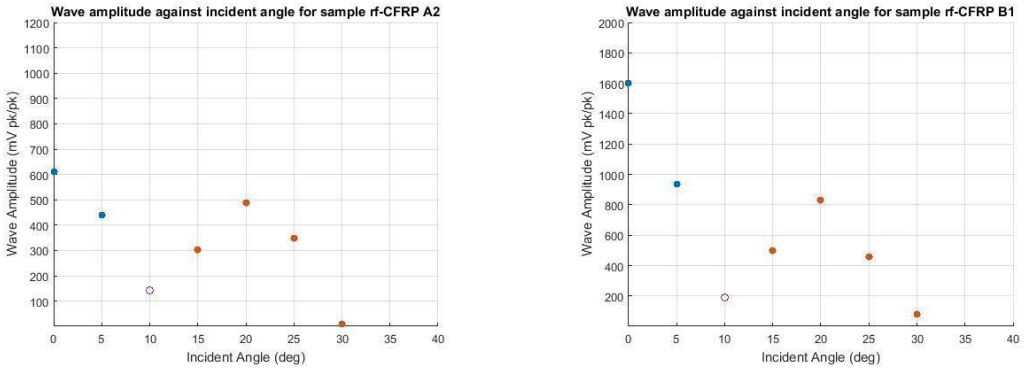

(a) (b)

Figure 98 - Figure a) and b) document the wave amplitude against incident angle for samples rf-CFRP A2 and B1. Close agreement in terms of amplitude profile is found between the figures and with that recorded in figure 97 (b). Similar to figure 96 (b), note the hollow point. The wave profile in this region coincides with an emerging shear wave and decaying longitudinal wave.

Investigating now the second critical angle, the wave profile recorded for all samples differed from that recorded with the v-CFRP. Rotating the rf-CFRP samples towards the second critical angle it was found that the wave velocity steadily decreased as the critical angle was approached, more so than in the case for the v-CFRP. While the % difference between the v-CFRP transverse velocity at 20 and critical angle

velocity was found to be 10.7% and 17.6% for samples v-CFRP A and B, for the rf-CFRP samples the % difference varied between approximately 21 – 33%. The second critical angle for all rf-CFRP samples was observed, with values ranging from approximately 29-32o. This critical angle is in keeping with the vCFRP case, and suggests a fair degree of sample similarity in terms of architecture between both the rf-CFRP samples themselves and between the rf-CFRP samples and the v-CFRP samples. A velocity measurement was taken at maximum signal amplitude for all the samples, and to highlight the decreasing velocity with increasing incident angle another velocity measurement was taken (if applicable i.e. attenuation was not significant) between the maximum amplitude value and the critical angle. These velocities are recorded in Table 67. A full wave profile recorded for rf-CFRP samples A2 and B1, outlining the above wave profile is given in Figures 99 a) and b). Note that owing to correlation problems the wave velocity at 10o was not able to be recorded for B1.

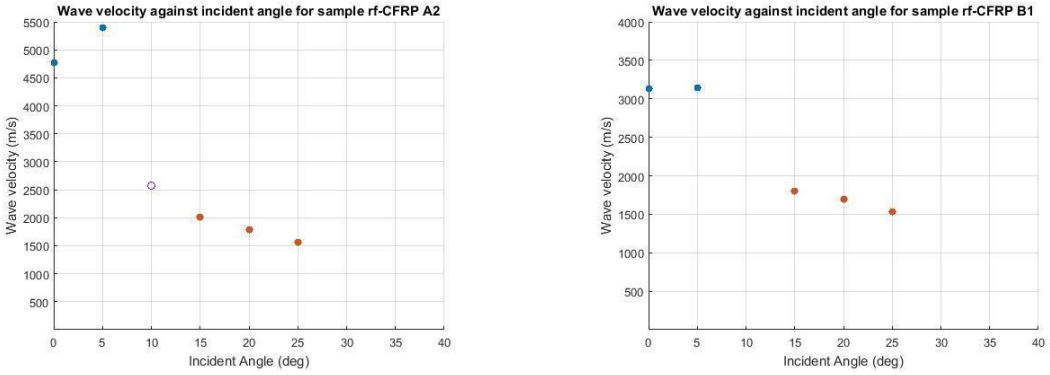

(a) (b)

Figure 99 - Figure a) and b) show the wave velocity against incident angle for rf-CFRP samples A2 and B1. The longitudinal velocity for A1 increases sharply by 11% then decays, noting again the hollow point. B1 longitudinal velocity remains relatively constant. For both samples, the transverse velocity is decreasing with increasing incident angle, between 15 and 25 degrees there is a velocity change of 22% and 15% respectively, which is significant when compared with changes of wave velocity of 6.6% in the case of v-CFRP A (figure 98).

It should be noted that with sample C1 an exception to the above was found. In this sample, a longitudinal wave was found to decay with a transverse wave emerging and then quickly attenuating at around 13.5. At ^{o} this point, a transverse wave emerges again and follows the same propagation pattern as the other samples. It can

also be noted from Figures 99 a) and b) that the wave velocity at the critical angle is not recorded while Table 67 also outlines some velocity values that were not able to be recorded, for instance C1 and D2. The velocity was unable to be recorded in these cases due to a combination of attenuation, sample size and transducer width. Concerning the difficulty in recording the velocity at the critical angles, as the critical angle was approached the sample width was less than beam width and so the receiving transducer recorded not only the transverse wave velocity but also the velocity at which the wave propagated through the coupling medium at either side of the sample. Figure 100 is given to highlight the wave profile recorded when the oil and sample velocities are merged together.

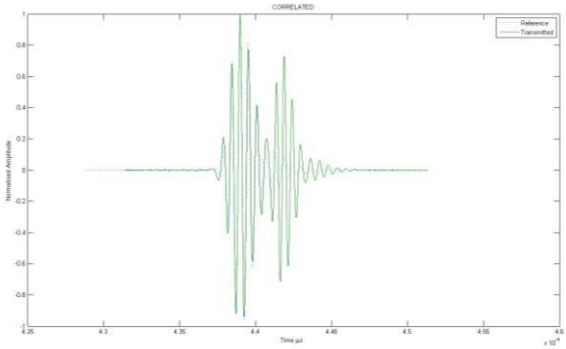

Figure 100 - Correlated image of transverse wave (incident at 26^0) and reference wave for sample A1. The first peak is the transverse wave, the second peak is the reference wave from the oil. If the transverse wave amplitude attenuates below the reference wave, correlation problems start to occur.

With the critical angle able to be visually observed for every sample, a theoretical prediction of the transverse wave velocity at this angle was able to be made. These velocities, along with the relevant information for each sample is again given in Table 67. Note additionally, due to a non-constant wave velocity, equations 143-145 would return inaccurate elastic constants and so these parameters were not determined for the rf-CFRP samples.

Data	A1	A2	% diff	B1	B2	% diff	C1	C2	% diff	D1	D1	% diff
L wave speed (m/s)	3073.3	4245	32.02	3103.9	4228.6	30.69	3459.2	3189.3	8.12	7437.2	6031.2	20.88

Max-amp T wave speed (m/s) (incident angle)	1679.1 (21^{o})	1667.8 (23^{o})	0.67	1765.5 (20^{o})	1778.3 (21^{o})	0.72	N/A	1736.9 (21^{o})	N/A	1623 (24^{o})	N/A	N/A
T wave speed (m/s) between (Max-amp) transverse and critical angle (incident angle)	1495.4 (26^{o})	1458.2 (27^{o})	2.52	1633.4 (23^{o})	N/A (25^{o})	N/A	N/A	N/A	N/A	1454.5 (27^{o})	N/A	N/A
1st critical angle (**practical**)	N/A	N/A	N/A	N/A	N/A	N/A	N/A	N/A	N/A	N/A	N/A	N/A
1st critical angle (**theoretical**)	12.44^{o}	8.97^{o}	32.41	12.3^{o}	9.0^{o}	30.98	11.02^{o}	11.96^{o}	8.18	5.09^{o}	5.71^{o}	11.48
2nd critical angle (**practical**)	30.59^{o}	29.5^{o}	3.63	30^{o}	31.5^{o}	4.88	28.7^{o}	30^{o}	4.43	32^{o}	31.5^{o}	1.57
2nd critical angle (**theoretical**)	N/A	N/A	N/A	N/A	N/A	N/A	N/A	N/A	N/A	N/A	N/A	N/A
Critical angle velocity prediction	1301.9	1344. 4	3.21	1322. 6	1266	4.37	1376. 2	1321. 4	4.06	1246	1263. 54	1.39

Table 67 - Wave phenomenon recorded for the rf-CFRP samples. L: and T indicate longitudinal and transverse wave respectively and N/A identifies that a measurement was not able to take place.

6.6 Discussion

Small % errors in wave velocity were found for both v-CFRP sample A and B, indicating a good degree of homogeneity between the samples. Further, the wave profile recorded for the samples was largely independent of incident angle and was indicative with that expected for an isotropic plane (Auld, 1990; Musgrave, 1954a). Thus, as verified via ultrasonic wave propagation the lay-up presented in this work provides a reasonable approximation for in plane isotropy.

The wave profile recorded for the rf-samples differed from that recorded for the v-CFRP in that the wave velocities were much more susceptible to incident angle. This was particularly true for transverse wave velocity, which decreased as the incident

angle was approached. All rf-samples recorded a relatively similar pattern of wave propagation except from C1, this sample recorded two transverse waves, with one quickly attenuating at around 13.5°. In this case a larger deviation, when compared to the other samples, away from isotropic symmetry was inferred with possible error arising from the rf-CFRP manufacturing process. Further, the degree of homogeneity between the samples was inferred via wave velocity; higher % errors than what was recorded in the case of v-CFRP for longitudinal waves at 0° were found. Additionally, both the recycled and simulated recycled recorded the same wave profiles, indicating that on a macroscopic level the materials behaved very similar in terms of wave propagation. Table 68 provides a general comparison of findings between v-CFRP and rf-CFRP.

The focus of this work was to investigate if wave propagation for rf-CFRP differed in profile from that recorded from v-CFRP, given similar fibre architecture. The close relationship found in terms of critical angles, and wave profile suggests that both v-CFRP and rf-CFRP shared a good degree of similarity. Taking this into account and acknowledging varying velocity and amplitude values observed for the rf-CFRP samples, which underwent identical pyrolysis and manufacturing processes, we suggest that more severe changes in velocity with increasing incident angle for the rf-CFRP were most likely caused by a non-ideal resin impregnation process and that given identical resin fibre content for both v-CFRP and rf-CFRP a more closely related wave profile, in terms of velocity will be returned. This is no way infers that similar sample properties will be recorded; it is overwhelming the case that the elastic constants will differ for the rf-CFRP.

This hypothesis is limited to the composite under investigation in this research and has still to be verified and expanded upon by developing a more robust resin impregnation process. Moving forward, to develop a wider ranging and more fundamental understanding of wave propagation in rf-CFRP, when compared to similar v-CFRP, further investigation into areas such as group velocity effects, different fibre architectures, different types of fibres, different types of wave, residual resin, amplitude profile, attenuation profile, dwell times, fibre/resin adhesion problems, accuracy of elastic constant determination, sample geometry, recycling methods, manufacturing methods etc. is required.

Data	V-CFRP	rf-CFRP (A1-D2)
Longitudinal wave speed	Remained largely constant	Mixed results
Transverse wave speed	decrease with increasing incident angle (% difference of 10-17)	decrease with increasing incident angle (% difference of 21-33)
Velocity variation between samples	Very small changes for both longitudinal and transverse waves	Large changes in longitudinal velocity but very small changes recorded for transverse waves
Amplitude variation between samples	Very small changes in wave amplitude	Mixed results with some cases of large change in wave amplitude
Amplitude profile	As expected from theory	Largely matched v-CFRP in every case bar C1
First critical angle	Not observable	Not observable
Second critical angle	32º	29-32º
Transverse critical angle velocity prediction (average)	1250 m/s	1305.18 m/s

Table 68 - Comparison of experimental findings from application of ultrasound through transmission to v-CFRP and rf-CFRP

6.7 Conclusion

A simple way to create relatively accurate quasi-isotropic CFRP was identified with the in-plane elastic constants identified via ultrasonic wave velocity measurements.

Further, v-CFRP was recycled, with the resulting fibres used to manufacture rfCFRP. The rf-CFRP samples recorded more anisotropy than the v-CFRP samples in that wave velocity decreased more severely with incident angle. Owing to the varying velocity, the elastic constants of the rf-CFRP were not able to be determined using the same equations as for the v-CFRP. The authors suggest that a more closely related wave profile for v-CFRP and rf-CFRP will be produced for the architecture outlined in this research, given similar resin fibre content. However, further investigation using a more robust resin impregnation process is required to verify this claim. Additional research areas were also identified to develop to allow for a better understanding of potential subtle differences recorded when investigating bulk wave propagation in rf-CFRP, when compared to v-CFRP.